UNIVERSITY OF BIRMINGHAM

EXPLORING THE ABERRANT PHENOTYPE OF NEUTROPHILS IN PERIODONTITIS

by

Nurul Iman Binti Badlishah Sham

A thesis submitted to
The University of Birmingham
For the degree of
DOCTOR OF PHILOSOPHY

School of Dentistry
Institute of Clinical Sciences
College of Medical and Dental Sciences
The University of Birmingham
July 2019

i Abstract

Neutrophils, the most abundant leukocyte arrive at the site of infections to eliminate pathogens, particularly by using reactive oxygen species (ROS). They contain the antioxidant glutathione (GSH) to maintain homeostasis and combat ROS induced intracellular damage. Intracellular GSH is essential for a number of homeostatic and cellular processes, including chemotaxis and is the main intracellular redox buffer. During oxidative stress, protein modification by glutathionylation helps defend against oxidative damage.

The aim of this work was to investigate the role of redox balance in the aberrant chemotactic phenotype observed in neutrophils, particularly from periodontitis patients.

In healthy neutrophils, GSH modulating compounds (buthionine sulfoximine, N-acetylcysteine, carmustine and 1-chloro, 2-4 dinitrobenzene) were used to change GSH levels: showing that decreased GSH was associated with a decreased chemotactic ability. In periodontitis patients there was less GSH in neutrophils in comparison to healthy donors, but it increased after successful non-surgical treatment. A similar pattern was observed for neutrophil chemotaxis. This demonstrated a link between these two factors in the same cells for the first time. Proteomic analysis of extracts from patient and control neutrophils demonstrated modulation of glutathione regulation in periodontitis patients.

ii Acknowledgements

I would like to thank my wonderful and beloved supervisor, Dr. Melissa Grant who has been very passionate giving me guidance throughout my PhD years. Not only that, she also helped me with my welfare during my stay in Birmingham, United Kingdom. This encouragement has given me confidence in doing my research work and working with other students and technicians in the laboratory as well as managing my life as a student, wife and mother in Birmingham. I would also like to thank my employer, Universiti Sains Islam Malaysia (USIM) and Ministry of Higher Education, Malaysia for funding my PhD studies. A big thank you to my loving husband, Mohd Noor Mohd Tahir for always being patience giving me support and always being there for me and our kids, nevertheless taking care of the kids while I was doing the research work. To my kids, Ahmad Faris Irsyad, Muhammad Al Fateh and baby Abbas Firnas, thank you for being patience and always being my content of enjoyment. A big appreciation to my parents, Badlishah Sham, father and Saniyah, mother as well as my siblings (Kakak, Mohd, Yayah and Adik) for their endless support and encouragement even though they are far abroad in Malaysia.

To the lab personnel, Dr Helen Wright and Dr Naomi Hubber for their kindness and always giving a hand to help in my blood collection and research work. To the clinical research team of Birmingham Dental Hospital, Dr. Praveen Sharma, Sharon Power, Jacqueline Rees, Ashleigh Smith and Joanne Crumpler for their help during the clinical trial. To fellows in Biosciences School, Dr Sabah Pasha and Dr Jinglei Yu for their kindness and was really helpful throughout my PhD project. To my fellow colleagues in Dentistry and Biosciences School, Dr Siti Aishah, Dr Farha Ariffin, Dr Nina Vyas, Dr Helen Roberts, Dr Ilaria Chicca and Dr Muhammad Dain Yazid, thank you for your kindness and listening ear during my bad days. My big thank you for The Malaysian community in Birmingham (MCIB) and IKRAM friends for the wonderful friendship and knowledge during my stay in Birmingham. They have supported me throughout my PhD study period and have always been my source of motivation. Thank you again to all. I couldn’t have done it without all of you.

This thesis is dedicated to

***My beloved parents**, Badlishah Sham Baharin and Saniyah Abd Wahab,*

***My wonderful husband**, Mohd Noor Mohd Tahir*

and

***My handsome sons**, Ahmad Faris Irsyad, Muhammad Al Fateh and Abbas Firnas*

for their never-ending support and never gave up on me.

Thank you very much.

TABLE OF CONTENTS

LIST OF TABLES

LIST OF FIGURES

ABBREVIATIONS

%	Percentage
°C	Temperature
µg	Microgram
µl	Microlitre
µm	Micrometre
ACN	Acetonitrile
ATP	Adenosine triphosphate
BCA	Bicinchoninic acid
BCNU	Carmustine
bio-GEE	N,N-biotinyl glutathione disulphide
BOP	Bleeding on probing
BSA	Bovine serum albumin
BSO	Buthionine sulfoximine
C18	Reverse phase column
$CaCl_2$	Calcium chloride
CAL	Clinical attachment loss
CDNB	1-chloro-2,4-dinitrobenzene
CID	Collision-induces dissociation
CO_2	Carbon dioxide
CONSORT	Consolidated standards of reporting trials
CRP	C-reactive protein
CXC8	Interleukin-8
CXCL16	Chemokine ligand 16
CXCL8	Interleukin-8
CXCR1	Chemokine receptor 1
CXCR2	Chemokine receptor type 2
Da	Daltons
DAMP	Damage associated molecular patterns
DNA	Deoxyribonucleic acid
DTT	Dithiothreitol
ECD	Electron-capture dissociation
ESI	Electrospray ionization
ESI-MS	Electrospray ionization mass spectrometry
ETD	Electron-transfer dissociation
FBS	Fetal bovine serum
fMLP	N-formylmethionyl-leucyl-phenylalanine
FT-MS	Fourier-transform mass spectrometry
g	Gram
ɣ	Gamma
g/ml	Gram per mililitre
GCF	Gingival crevicular fluid
GIF	Graphics interchange format
gPBS	Glucose supplemented phosphate buffered saline
GPCRs	G protein-coupled receptors
GPx	Glutathione peroxidase
GSH	Glutathione
GSH:GSSH	Ratio total glutathione and oxidized glutathione
GSSG	Oxidized glutathione

h	hour
H_20	Water
H_2O_2	Hydrogen peroxidase
Hb	Haemoglobin
HCD	Higher-energy collisional dissociation
HCl	Acid hydrochloric
HEPES	4-(2-hydroxyethyl)-1-piperazineethanesulfonic acid
HGF	Human gingival fibroblast
HOCI	Hypochlorous acid
HpH	Reversed phase
HPLC	High performance liquid chromatography
Hz	Hertz
ICAM-1	Intercellular adhesion molecule
ICAT	Isotope-coded affinity tag
IL8	Interleukin-8
iTRAQ	Isobaric tags for relative and absolute quantitation
K_2HPO_4	Potassium phosphate dibasic
KCI	Potassium chloride
kDa	Kilodaltons
KH_2PO_4	Potassium phosphate monobasic
$KHCO_3$	Potassium bicarbonate
kV	Kilovolt
LAP	Localized aggressive periodontitis
LC	Liquid chromatography
LC-MS/MS	Liquid chromatography-tandem mass spectrometry
M	Molar
m/z	Mass to charge ratio
MALDI	Matrix assisted laser desorption
mg	Miligram
mg/ml	Miligram/mililitre
$MgCl_2$	Magnesium chloride
min	Minute
ml	Mililitre
mM	Milimolar
mm	Milimetre
MPa	Megapascal
M-PER buffer	Mammalian protein extraction reagent buffer
MPO	Myeloperoxidase
mRNA	Messenger RNA
MS	Mass spectrometry
MS/MS	Tandem mass spectrometry
Na_2 EDTA $2H_2O$	Disodium ethylenediaminetetraacetic acid dihydrate
NAC	N-acetylcysteine
Nacl	Natrium chloride/ Sodium chloride
NADPH	Nicotinamide adenine dinucleotide phosphate
nanoESI MS/MS	Nano electrospray ionization tandem mass spectrometry
NaOH	Sodium hydroxide
NEM	N-ethylmaleimide
NETs	Neutrophil extracellular traps
NH_4Cl	Ammonium chloride

nL	Nanolitre
nL/min	Nanolitre per minute
nm	Nanometre
nM	Nanomolar
NSAIDs	Non-steroidal anti-inflammatory drugs
p	p-value
PAMP	Pathogen associated molecular patterns
PBNs	Peripheral blood neutrophils
PBS	Phosphate buffered saline
PCA	Principal component analysis
PCTE	Polycarbonate track-etch
PI	Plaque index
ppm	Parts per million
PRR	Pathogen recognition receptor
Pr-SSG	Protein-glutathione mixed disulphide adducts
PSI	Pound-force per square inch
PSMs	Peptide spectral matches
PSSG	Glutathionylated
PTMs	Post-translational modification
RA	Rheumatoid Arthritis
RIPA buffer	Radioimmunoprecipitation assay buffer
RNS	Reactive nitrogen species
ROS	Reactive oxygen species
RPMI	Roswell park memorial institute medium
SCX	Strong cation exchange chromatography
SD	Standard deviation
SDS	Sodium dodecyl sulfate
SDS-PAGE	Sodium dodecyl sulfate polyacrylamide gel electrophoresis
SH	Sulfydryl-group
SILAC	Stable isotope labelling with amino acids
SOD	Superoxide dismutase
TBS	Tris-buffered saline
TBST	Tris buffered saline with Tween
TCEP	Tris(2-carboxyethyl) phosphine hydrochloride
TEAB	Triethyammonium bicarbonate
TEM	Transendothelial migration
TFA	Trifluoroacetic acid
TMT	Tandem mass tags
ToF	Time of flight
Uniprot	Human database
V	Volt
v/v	Volume/volume
w/v	Weight/volume
WR	Working reagent
α	Alpha
β	Beta

CHAPTER 1 – INTRODUCTION

CHAPTER 1

INTRODUCTION

1.1 Periodontitis

Chronic periodontitis is a dental disease characterized by non-resolving inflammation which leads to host mediated tissue damage and bone loss around the teeth (Hasturk and Kantarci, 2015). It is initiated by the biofilm but exacerbated by the host response which leads to tissue and bone destruction (Graves and Cochran, 2003). Among the symptoms of periodontitis are redness and bleeding gums, swollen gums, loose gums and teeth, pain on biting as well as bad breath. It is a common infection affecting 11% of the population in its most severe form and over 50% of people over the age of 65 years in any form (Nazir, 2017). The human oral tissues are always exposed to potential and harmful microorganisms and to combat the infections in this area, leucocytes are attracted to and infiltrate into the tissues from the blood stream in response to chemoattractants (Gamonal et al., 2001). A strong neutrophil tissue infiltrate is a characteristic of this disease (Van Dyke, 2007).

Chronic periodontitis can also exert a wide range of systemic effects. A study by Nicu et al., (2009) hypothesized that stimulation by periodontal pathogens has shown platelets and leucocytes to be more sensitive than normal cells. In previous studies, it has been shown that patients with periodontal infection have a higher white blood cell and platelet count compared to healthy controls (Al-Rasheed, 2012). Activated platelets regulate chemokine release by the monocytes in inflammatory lesions (Weyrich et al., 1996). A study found that activated platelets and leucocytes might cause an increase in atherothrombotic activity and eventually leads to atherosclerosis and coronary artery disease (Zeviani et al., 2009), therefore, treatment of periodontitis may be beneficial in control of atherosclerosis because control of periodontitis significantly decreases serum mediators and markers of acute phase response (D'Aiuto et al., 2004).

Periodontal disease is a chronic inflammatory disease and has been associated with other diseases such as rheumatoid arthritis and chronic kidney disease. Rheumatoid arthritis (RA) is a chronic inflammatory joint disease which causes damage to the bone and cartilage (Muller, 2018). There are a number of studies that have suggested an epidemiological, serological and clinical association between RA and periodontitis, where the bi-directionality in that RA affects manifestation of periodontitis and contrary, periodontitis is a risk factor for RA (de Pablo et al., 2009; Potempa et al., 2017). There are suggestions that periodontitis could be the causal factor in the initiation and maintenance of the inflammatory response that occurs in RA (de Pablo et al., 2009). Citrullination has played a role in the development of rheumatoid arthritis and the recognition that oral bacteria and inflammation may play important roles (Bingham and Moni, 2013). There was a discovery that *Porphyromonas gingivalis* which is involved in the development of periodontal disease has a peptidylarginine deiminase enzyme which is capable of citrullination peptide has said to be the mechanistic link between periodontal disease and rheumatoid arthritis (Bingham and Moni, 2013).

Periodontitis has said to be a potential risk for chronic kidney disease. Periodontitis increased the inflammatory burden of this chronic kidney disease where pathogens that cause the destruction of periodontal tissues and entry of this pathogen will go in systemic circulation causing increased systemic inflammation (Wahid et al., 2013). There are also studies mentioned that chronic kidney disease affects teeth, oral mucosa, periodontium and salivary glands which leads to negative effect of the oral hygiene and periodontal status of the patient (Summers et al., 2007).

Periodontitis has been associated with other systemic disease including respiratory diseases, cardiovascular disease and pre-term labour (Ohyama et al., 2009). In addition, periodontitis has been a potential risk for increased morbidity and mortality for diabetes and complications of pregnancy (Fowler et al., 2001). One of the possible mechanisms linking periodontitis with other systemic disease is that the spread of infection from the oral cavity caused by immunological injury induced by oral microorganisms (Taylor, 2001).

Figure 1.1 shows structure of a normal tooth and a tooth that has periodontitis disease. Irreversible destruction of the bone and gum holding the tooth are the causes of periodontitis shown in the figure.

Figure 1.1: Structure of normal tooth and tooth that has periodontitis. Image from shutterstock.com.

1.2 Neutrophils

Neutrophils are the most abundant white blood cells, or leucocytes, they are short-lived, do not divide and cannot easily be genetically modified (Dale et al., 2008),(Bishop et al., 1968)(Cartwright et al., 1964). They are essential for immune defence and contain various antimicrobial proteins and peptides.

Along with other cells, such as basophils and eosinophils, neutrophils are members of the granulocyte family of leucocytes. Neutrophils have the fastest response of towards a site of infection of injury. At the site of infection detect foreign particles such as bacteria and viruses via pathogen associated molecular patterns (PAMP) or signals from damaged tissues, such as adenosine triphosphate (ATP), damaged associated molecular patterns (DAMP), and this causes secretion of inflammatory and activation

of macrophages and endothelial cells after activation of pathogen recognition receptor (PRR) such as Toll-like receptors. Then, these endothelial cells release chemoattractants to attract circulating neutrophils in the blood stream toward the vessel wall. The rolling neutrophils are brought into contact with the endothelial cells, so chemokines can further activate neutrophils and other pro-inflammatory agents on the surface of the endothelial cells (Sadik et al., 2011). Selectin ligand in the neutrophil binds to E-selectin and P-selectin, meanwhile β_2 integrin binds to intercellular adhesion molecule 1 (ICAM-1) as in figure 1.2. Activated neutrophils undergo a cell shape change from round to flat and highly polarized (Filippi, 2016). This shape enables the cell to migrate on the endothelial surface to cross the endothelial cells that lines the blood vessel. This process is called diapedesis. After passing the endothelial barrier, neutrophils must cross the pericyte layer in the basal membrane to enter the inflamed tissues. There are two ways that neutrophils can cross the endothelial cells, by transcellularly, where the cells pass through the endothelial cells themselves (Feng et al., 1998), or paracellularly, where cells travel between endothelial cells in amoeboid fashion (Schmidt et al., 2011). For transendothelial migration (TEM) (Muller, 2013) or diapedesis, the neutrophil forms actin-rich podosomes that indent the endothelium, then, actin-enriched projections are formed by the endothelium which leads to formation of ‘transmigratory cup’ around the neutrophil (Filippi, 2016). For paracellular migration, neutrophil crawls along the endothelial cell surface to the intercellular junctions, which then lamellopodia extends between endothelial cells to disrupt the intercellular junction, followed by translocation of the cell through the inter-endothelial junctions (Schmidt et al., 2011). They then migrate through the interstitial tissue (Ley et al., 2007) to the site they are needed.

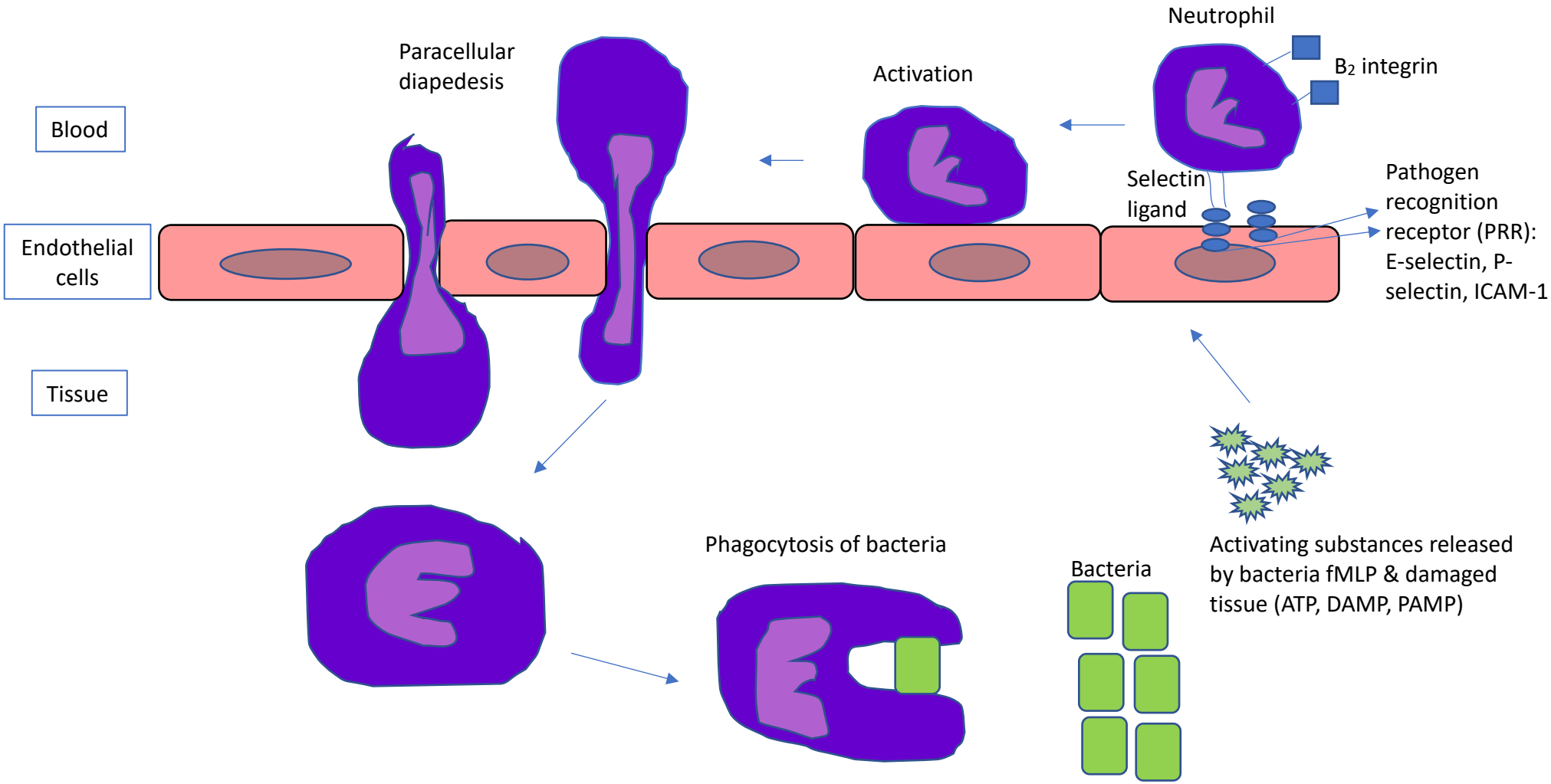

Figure 1.2: Diagram of neutrophils infiltrate the tissues from the blood stream in response to endogenous and exogenous chemoattractant.

1.3 Neutrophil granules

Neutrophils are granulocytes and as such contain high numbers of granules, which contain proteins and reactive substances used in the killing of microbes. The granules are classified by their stage of formation in the bone marrow. There are several types of granules that neutrophils contain which are azurophilic (primary) granules, specific (secondary) granules, gelatinase-rich (tertiary) granules and secretory vesicles. During degranulation, neutrophil granules containing antimicrobial substances are delivered to the phagosome or the exterior of the cell (Faurschou and Borregaard, 2003). Exocytosis is the effect of fusion of granule membrane with the plasma membrane and integration of granule membrane into the plasma membrane. Therefore, membrane proteins in the membrane granules transfer to the surface membrane and provide the neutrophil with new receptors and other functional proteins (Borregaard and Cowland, 1997). When neutrophil is in rolling contact with activated endothelium, secretory vesicles are mobilized which is mediated by selectins and their ligands (Borregaard and Cowland, 1997). Incorporation of the plasma membrane of secretory vesicles causes firm adhesion of the neutrophil to the endothelium. Mobilization of specific granules to the surface membrane could intensify phagocytic capacity of the neutrophils. In the phagosome, the fusion of azurophil and specific granules could bring conditions for independent bacterial activity (Borregaard and Cowland, 1997).

1.4 Neutrophil NETs (neutrophil extracellular traps)

Neutrophils can release neutrophil extracellular traps (NETs) to control microbial infections. NETs are decondensed nuclear chromatin which makes a web-like structure that consist of chromatin backbones, histones and antimicrobial proteins (Manda et al., 2014). NETs are formed in response to a range of pathogens, including bacteria, viruses, fungi, and protozoa as well as host-derived mediators. NETs act to contain and destroy pathogenic organisms. NETs offer fundamental defence strategy to prevent infiltration of bacteria that is important for health and are produced in response to bacteria stimuli including Gram-negative and Gram-positive bacteria (Kaplan and Radic, 2012).

1.5 Production of ROS, NADPH, other mechanisms

One of the roles of the neutrophil is the uptake and killing of invading microbes (Stabel et al., 2002). The physiological function of phagocytes is the killing of microbes. The general aspects of the process of phagocytosis are that the contents of neutrophil granules degrade microbes ingested by the neutrophils (Dale, Boxer and Liles, 2008). A respiratory burst, which is also known as an increment in neutrophil oxygen consumption, occurs during phagocytosis (Dahlgren and Karlsson, 1999). Myeloperoxidase (MPO) released from granules during phagocytosis generates hypochlorous acid (HOCI), a potent antimicrobial substance (Klebanoff, 1968); hydrogen peroxide (H_2O_2) and other reactive oxygen species are produced via nicotinamide adenine dinucleotide phosphate (NADPH) oxidase (Babior et al., 1976). Figure 1.3 shows the diagram of MPO-H_2O_2-chloride antimicrobial system where NADPH oxidase causes the generation of H_2O_2 and other ROS. Then, MPO combines H_2O_2 and chloride to generate HOCI as an antibacterial substance within the phagosome (Klebanoff, 1968). Phagocytosis with generation of reactive oxygen species and hypochlorous acid is still the killing mechanism for most pathogens even though phagocytes have other microbial mechanism such as antimicrobial peptides (Epstein and Weiss, 1989).

In regulation of neutrophil activation and chemotaxis, CXC chemokines play a central role (Doroshenko et al., 2002). Chemotactic cytokines and chemokines cause the migration and movement of neutrophils. Chemokines are small chemotactic proteins, for example interleukin-8 (CXC8). Chemokine receptor 1 (CXCR1) has high affinity for interleukin-8 and low affinity in other chemokines whereas chemokine receptor type 2 (CXCR2) has a high affinity for all CXC chemokines that contains N-terminal Glu-Leu-Arg motif (Schumacher et al., 1992). Exploration of the effect of phagocytic stimuli in human neutrophils on the expression of CXCR1 and CXCR2 of interleukin 8 receptors found that levels of CXCR1 and CXCR2 were constant during phagocytic stimulation of neutrophil. However, after phagocytosis, expression of CXCR1 and CXCR2 was down-regulated and Ca^{++} responses were reduced to ligands, interleukin-8 and neutrophil activating peptide 2. Therefore, this study suggested that down-regulation of CXCR expression may reduce the responsiveness of phagocytosing neutrophils to CXC chemokines (Doroshenko et al., 2002). It is already known that chemotactic responses of neutrophils are impaired after phagocytosis (Bryant et al., 1966).

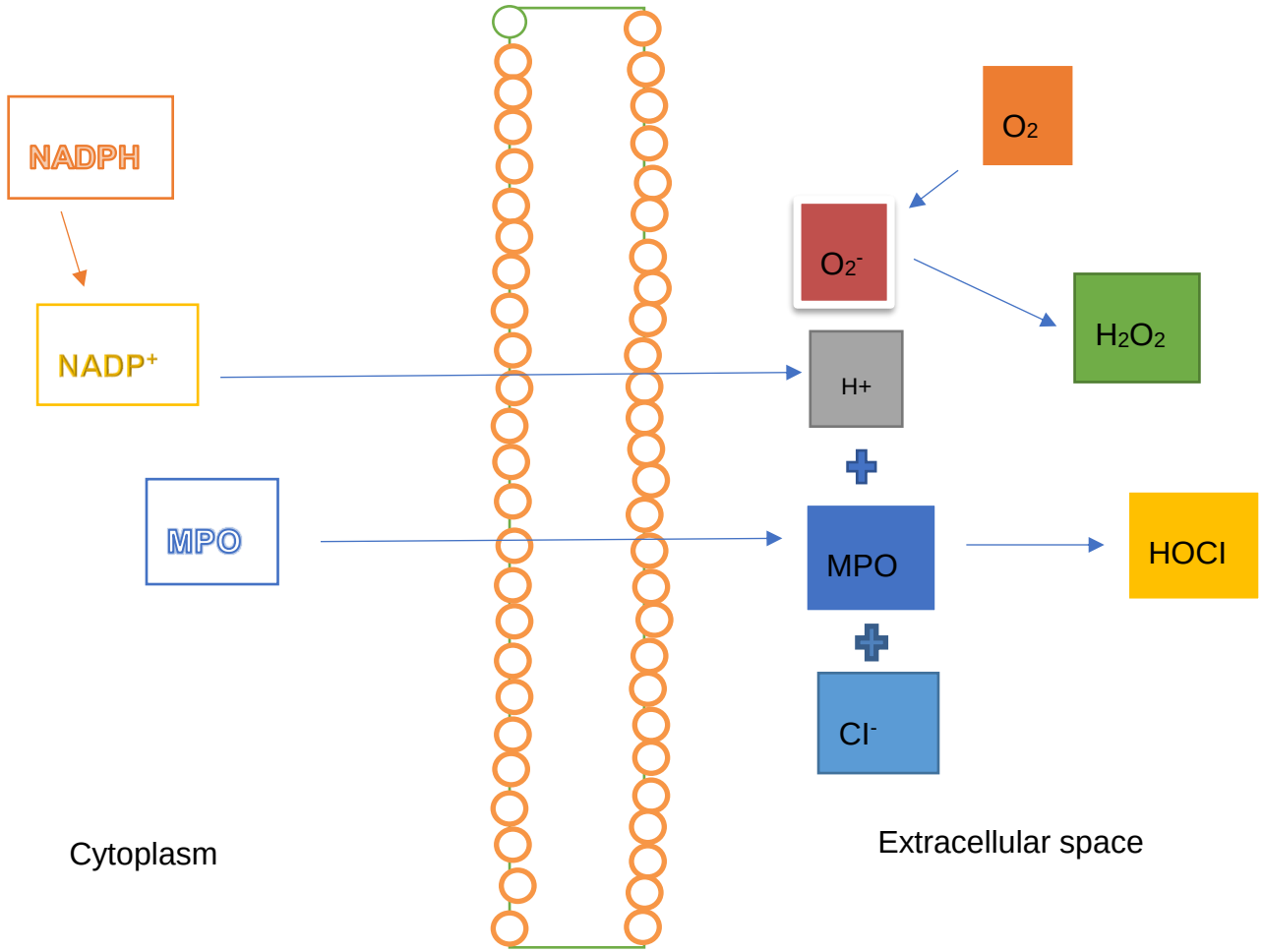

Figure 1.3: The MPO-H_2O_2-chloride antimicrobial system. NADPH represents reduced nicotinamide adenine dinucleotide phosphate; O_2, superoxide anion, MPO, myeloperoxidase and HOCl, hypochlorous acid. Adapted from (Dale et al., 2008).

1.6 Neutrophil ROS and NET production and degranulation in periodontitis

Neutrophil homeostasis is required for periodontal health as they protect the periodontal tissues from damage and they are commonly found in the gingival crevice and epithelium area (Hajishengallis and Hajishengallis, 2014). By killing various pathogenic bacteria either by non-oxidative or oxidative means in an intracellular or extracellular environment, neutrophils are able to protect the host tissue.

It is hypothesized that protease inhibitors present in biological fluids can be inactivated by reactive forms of oxygen that were produced *in vivo* in localized aggressive periodontitis (LAP) patients (Bhansali et al., 2013). Meanwhile, neutrophil-produced matrix metalloproteinases (MMPs) can be activated by reactive oxygen species (Bhansali et al., 2013). It is possible that reactive forms of oxygen produced by neutrophils are particularly important factors causing tissue damage in periodontitis (Bhansali et al., 2013). A phenomenon that is associated with periodontitis is the determinant of oxidative stress which is the rate of reactive oxygen species (ROS) (Dias et al., 2011; Matthews et al., 2007). A study done by Chapple and Matthews, suggested a dual role for neutrophils in the production of oxidative tissue damage, involving a potentially reversible Fcɣ-receptor-mediated hyperactivity and a constitutional hyperactivity relative to baseline oxygen radical release (Matthews et al., 2007).

NETs release is elevated in periodontal pockets of periodontitis (Hirschfeld et al., 2017). The manifestation of periodontitis disease in not merely oral but systemic as peripherally isolated neutrophils display aberrant ROS production, chemotaxis, cytokine production and altered transcription activity (Matthews et al., 2007a; Matthews et al., 2007b; Roberts et al., 2015). From our previous group, a study completed by (Ling et al., 2016) reported that neutrophils from chronic periodontitis patients released more superoxide compared to control group before periodontal treatment and the superoxide release was reduced to control cell levels after treatment. It was also reported that there is a positive relationship between neutrophil superoxide release and plasma C-reactive protein (CRPA) which shows that CRP has a protective role in reducing inflammation. It is hypothesised that defects in the antioxidant defence systems contribute to an imbalance and oxidative stress. A study

by (Van Dyke et al., 1980) indicate that there was impairment of neutrophil chemotactic ability on LAP patients due to cell-associated defect which suggests that neutrophils plays a protective role against periodontal infection.

Periodontal disease is characterized by involvement of chemokines for recruitment of neutrophils. CXC chemokine ligand 16 (CXCL16) is produced by human gingival fibroblast (HGF) and its receptor, CXCR6 are expressed at the messenger RNA (mRNA) and protein levels may be involved in neutrophil migration into periodontal disease inflamed tissues (Hosokawa et al., 2007).

1.7 Neutrophil chemotaxis

Chemotaxis is a process where white blood cells are attracted to chemical factors released at the site of infection by directed cell motility. When an infection occurs, chemical factors are released that attract white blood cells to the site of infection. The attraction of white blood cells is called chemotaxis. The primary white cells attracted are neutrophils and macrophages. Both cells phagocytize the invader. Chemotaxis is a directional movement of cells through a concentrated gradient of a chemoattractant. Chemotaxis is a dynamic process that requires cell polarization, directional sensing, cell adhesion and motility and is a process where cells interact with the chemoattractant, transmit signal across plasma membrane and therefore, localize the response (Janetopoulos and Firtel, 2008).

Factors that cause the directional cell movement are identified as chemoattractants. Chemoattractants such as interleukin-8 (CXCL8) and N-formylmethionyl-leucyl-phenylalanine (fMLP) attract neutrophils to the site of infection. fMLP is a bacteria-derived product, causes the strongest migration and fastest directional movement whereas chemokine CXCL8 is a weak chemoattractant compared to fMLP and causes a lesser amount of migration. fMLP can be detected by G protein-coupled receptors (GPCRs), and chemokines such as CXCR1: these chemoattractants activate signalling cascades via receptor binding to initiate movement. Receptors can be recycled back to the membrane for degradation (Samanta et al., 1990). In chemotaxis, the cells interact with the chemoattractant to localize the response and go through

processes which are cell polarization, directional sensing, cell adhesion and motility (Janetopoulos and Firtel, 2008; Kolaczkowska and Kubes, 2013).

Formation of new pseudopods at the leading edge and retraction at the posterior edge of the cells occurs when chemoattractant is detected (Andrew and Insall, 2007). Reactive oxygen species (ROS) produced by NADPH oxidases are generated by chemoattractant stimulation and play a role in signal transduction of cell movement (Dickinson et al., 2012). ROS derived from NADPH oxidase maintain neutrophil pseudopod formation and chemotactic behaviour through actin glutathionylation and polymerisation (Sakai et al., 2012). It has been shown that when NADPH oxidase is inhibited, chemotaxis inefficiency can occur among neutrophils from healthy donors which are exposed to a chemoattractant (Sakai et al., 2012). Similarly, (Niethammer et al., 2009) showed that hydrogen peroxide (H_20_2) can permeate the plasma membrane and allows directional cell motility towards the chemotactic gradient. Hydrogen peroxide is a secondary messenger that mediates its effects through oxidation of cysteine thiols. Fluorescence imaging microscopy has been used to show that motile cells generate H_20_2 at membranes and cell protrusions (Cameron et al., 2015). H_20_2 inhibits cofilin, part of the cytoskeletal machinery, activity through oxidation of cysteines and helps with cell motility which indicates that H202 contributes to polarized cell motility through cofilin inhibition (Cameron et al., 2015).

1.8 Measuring chemotaxis

Chemotaxis can be analysed by direct or indirect chambers. Direct visualization chambers, for example the Insall Chamber are used for measuring and analysing chemotactic responses as they allow analysis of cell behaviour during the process of chemotaxis by video microscopy. This assay can directly visualize the process of cell motility (Muinonen-Martin et al., 2013), and allows consistent oriented gradients and use of standard thickness coverslips for aberration free microscopy and short working distance objectives.

An indirect chamber example is the Transwell Boyden Chamber assay, where chemoattractant gradients are put in a 96-well plate and neutrophil cells on the filter membrane to examine the up-gradient and down-gradient sides. The Boyden

Chamber assay is based on a chamber of two liquid-filled compartments separated by a microporous membrane (filter). In this assay, cells are placed in the upper compartment and allowed to migrate through the pores of the membrane to the lower compartment where chemoattractant such as fMLP, are present. The number of cells that have migrated to the lower compartment is determined. A potential involvement of an intracellular signalling pathway or cell surface protein in cell motility can also be examined using this assay (Chen, 2005) by manipulating the cells with inhibitors. For example, research done using neutrophil cells incubated with different concentrations of non-steroidal anti-inflammatory drugs (NSAIDs) on chemotaxis found that migration was inhibited in response to interleukin-8 (Bertolotto et al., 2014).

1.9 Neutrophil chemotaxis in periodontitis

In the gingival tissues of dental plaque, an inflammatory infiltrate is usually present with lymphocytes and neutrophils comprising most of the infiltrate. Neutrophil cell migration to the inflammation area maybe in response to chemotactic substances released by the bacteria or complement system activated by bacteria antigens that produce chemotactic factors (Mergenhagen et al., 1970).

Impaired neutrophil chemotaxis seems to be one of the risk factors in the development of periodontal disease. The Insall and Boyden Chamber assays have been used to study neutrophil chemotaxis in chronic periodontitis. A study using the Insall Chamber on chemotaxis reported that speed, velocity and chemotactic accuracy was significantly reduced in chronic periodontitis patients compared to healthy controls for Interleukin-8 and fMLP chemoattractant (Roberts et al., 2015). A study done by (Van Dyke et al., 1980) showed that localized aggressive periodontitis (LAP) patients have been shown to exhibit defective neutrophil chemotaxis.

1.10 Introduction to antioxidants in the body

Reactive oxygen species (ROS) can be beneficial when in controlled situations but when rampant will cause damage to the body. Low levels of ROS refer to redox biology that activates signalling pathways while high levels of ROS refer to oxidative stress which can incur damage to lipids, protein and deoxyribonucleic acid (DNA) (Schieber et al., 2014). Oxidative stress is an imbalance between oxidants and antioxidants within a cell, tissue or organism. Cell damage can result if the imbalance is severe enough. This imbalance can be an effect of increased production of ROS and/or depletion of antioxidants. Free radicals found in living organisms, originate from reactive oxygen species (ROS) or reactive nitrogen species (RNS) (Cooper et al., 2002; Fisher-Wellman & Bloomer, 2009). Overproduction of free radicals may cause oxidative damage to biomolecules, which, if severe, can cause toxic and may lead to cell death. Free radicals can attack lipids, proteins and nucleic acids (Beckman and Ames, 1998). Oxidative stress due to imbalance between antioxidants and oxidants may lead to disruption of redox signalling and/or molecular damage. There is a physiological system to balance this potential for damage via antioxidants. Therefore, an antioxidant system needs to be in place to maintain a well-balanced production and elimination of ROS. There are enzymatic ways of removing oxidants such as catalase, superoxide dismutase (SOD) and also non-enzymatic ways of balancing ROS which are small molecule antioxidants such as vitamins and glutathione. They can be hydrophilic and hydrophobic to allow for control of different compartments, for example, lipid membranes and cytosol or aqueous compartments. Many antioxidants in circulation are found intracellularly. Antioxidants are important as they can eliminate reactive oxygen species (ROS) from the body. In many human diseases, a higher amount of ROS plays a pivotal role, and this may damage the body's cells. In a previous study, it was found that there is overproduction of ROS and lower levels of glutathione in periodontitis patients (Dias et al., 2013). This caused oxidative stress because of imbalance of ROS and antioxidants in periodontitis patients.

An ideal antioxidant is the one that can absorb and quench free radicals at physiologically relevant levels. Glutathione peroxidase, catalase and superoxide dismutase are considered the most efficient enzymatic antioxidants (Matés et al., 1999). For non-enzymatic antioxidants there are vitamin E and C, thiol antioxidants,

natural flavonoids and other compounds (McCall and Frei, 1999). Thiols and vitamins like E and C are example of antioxidants that can inhibit the oxidation process. It is important to have antioxidants as it prevents or slows down the oxidative damage throughout the body.

1.11 Glutathione

Glutathione (GSH) acts as the primary antioxidant against free radicals produced by toxic chemicals (Masella et al., 2005). It is considered the most important of our body's antioxidant, especially since it is found in every cell of the body. It is also essential for a number of homeostatic and cellular processes including chemotaxis and is the main intracellular redox buffer. Glutathione is an antioxidant that neutralizes free radicals due to the high electron-donating capacity of its sulfhydryl-group (-SH) group and prevents damage to important cellular components. GSH is also involved in a multitude of cellular functions such as protein synthesis.

GSH exists in the form of thiol-reduced and disulphide-oxidized (GSSG) (Kaplowitz et al., 1985). The structure of GSH in figure 1.4. Glutathione (ɤ-l-glutamyl-l-cysteinylglycine, GSH) is a ubiquitous tripeptide in mammalian systems, where its intracellular concentration can be as high as 10mM (Appenzeller-Herzog, 2011). Amino acid homocysteine is produced in the body through the metabolism of amino acid methionine. For GSH creation homocysteine is the broken down into amino acid cysteine. Cysteine is needed by cells to make intracellular glutathione where it is combined with glutamate by gamma- glutamyl cysteine synthase, this product is then combined with glycine by glutamate synthetase to form the tripeptide. Glutathione is the most abundant low molecular weight peptide in eukaryotic cells (Johansson et al., 2014), acts as a nucleophilic scavenger, protecting the cells by functioning as an antioxidant and by detoxifying electrophilic species (Johansson et al., 2014). It acts as an antioxidant by interacting with ROS and electrophiles. GSH acts with other redox-active compounds such as nicotinamide adenine dinucleotide phosphate (NADPH) to regulate and maintain cellular redox status (Jones et al., 2011). Glutathione also functions as reserve form of cysteine, stores and transports nitric acid, participates in the metabolism of oestrogen, leukotrienes and prostaglandins, involvement in certain

transcription factors such as in redox signalling and detoxification of endogenous compounds and xenobiotics (Lushchak, 2012).

Cellular GSH can be found in amount of 80-85% in cytosol, about 10-15% in the mitochondria and in the endoplasmic reticulum, there is small percentage of GSH (Hwang et al., 1992; Meredith and Reed, 1982). The liver plays a role in the homeostasis of GSH where most of the plasma GSH originates (Ookhtens and Kaplowitz, 1998).

In figure 1.5, is a diagram of GSH redox cycle. The primary function of glutathione is maintenance of intracellular redox homeostasis as this redox cycle can protect endothelial cells against oxidative stress. Through the action of GSH peroxidase (GPx)-catalysed reactions, the antioxidant function of GSH is achieved: the reduction of hydrogen peroxide and lipid peroxide while GSH is oxidized to GSSG. The GSSG is then reduced back to GSH by GSSG reductase forming a redox cycle. GSSG accumulates inside the cell and the ratio of GSH/GSSG is a good measure of oxidative stress (Dro, 2002). GSH also plays a key role in protein redox signalling. GSH are able to modify oxidation state of protein cysteine residues (Forman et al., 2009).

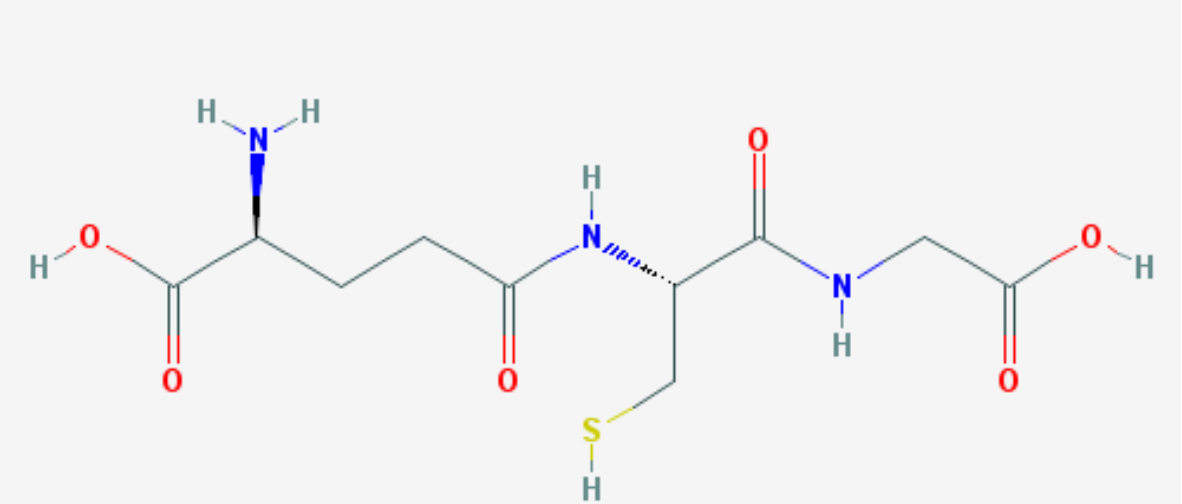

Figure 1.4: Structure of the tripeptide reduced glutathione (GSH: L-g-glutamyl-L-cysteinyl-glycine).

Structure from Pubchem Open Chemistry database

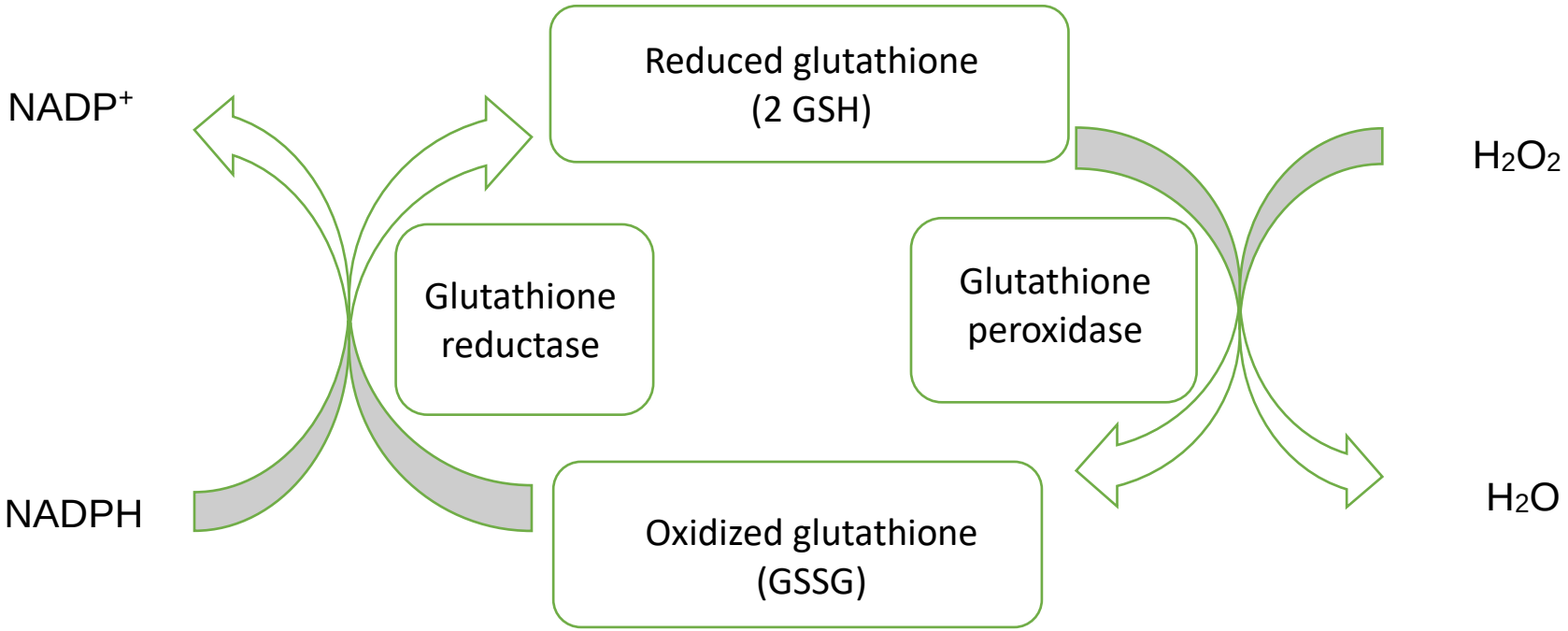

Figure 1.5: Glutathione redox cycle is an important defence system of endothelial cells against oxidative stress.

Glutathione is responsible to maintain redox balance by directly or indirectly reacting with ROS and is involved in detoxification of electrophiles. Certain phytochemicals may effect GSH action on ROS and electrophiles by directly interacting with ROS and electrophiles or by upregulating defensive enzymes. Level of intra and extracellular GSH is determined by balance between its production, consumption and transportation. Efforts have been done to decrease or increase GSH levels in organisms. In the redox cycle, cellular GSH can be depleted by increasing GSH oxidation to oxidized glutathione (GSSG), by inhibition of biosynthesis, or by inactivation of genes encoding the enzymes of GSH synthesis. GSH levels can also be inhibited by key enzyme of GSH biosynthesis and by externally added electrophiles. Increment of GSH levels could be done by cysteine in the form of different esters. Any modification of a parameter may give different results in diverse processes. For example, the increment of GSH level through supplementation of its esters can increase defence mechanisms.

Catalase, or the glutathione peroxidase-glutathione reductase system may detoxify hydrogen peroxide (H_2O_2) in cells (figure 1.2). In this glutathione redox cycle, oxidation of reduced glutathione by H_2O_2 is catalysed by glutathione peroxidase. It is then reconverted by glutathione reductase to form reduced glutathione. At several points *in vitro*, this glutathione redox cycle will be disrupted (Alton, 1983). Carmustine (BCNU) is a selective inhibitor for glutathione reductase (Kehrer, 1983). Reduced glutathione can be depleted by formation of a thioether conjugate such as 1-chloro-2,4-dinitrobenzene (CDNB) which is catalysed by endogenous glutathione-s-transferase (Sherratt and Hayes, 2002). Buthionine sulfoximine (BSO) is a selective inhibitor of ɣ-glutamyl-cysteine synthetase and may inhibit glutathione biosynthesis (Alton, 1983, Griffith, 1982). The glutathione redox cycle is disrupted at several points to modulate oxidant injury to endothelial cells in culture. Carmustine (BCNU) is a selective inhibitor of glutathione reductase and CDNB depleted cellular stores of reduced glutathione and BSO inhibits glutathione synthesis (Harlan at al., 1984).

Post-translational modification (PTMs) is a chemical modification in which properties of protein are altered after its translation, for example by addition of a modifying group to one or more amino acids or by proteolytic cleavage. Besides that, PTMs are also able to alter physical and chemical properties of protein such as its folding, distribution,

stability, activity and functions of the proteins. Oxidative modification is an exposure of some protein thiols to oxidising reagents through variety of mechanisms that involves ROS, nitric oxide or glutathione (Birben et al., 2012). Protein glutathionylation is a modification that can modify protein characteristics and functions. Many proteins contain free thiols that could be modified by the reversible formation of mixed disulphides with glutathione. This modification occurs when the protein thiol group goes through oxidation in response to ROS and reaction with GSH to form protein-glutathione mixed disulphide adducts (PSSG). At cellular signalling, this modification may serve to transduce oxidative stimuli into functional response and as an adaptive response to protect thiol groups in protein (Shao et al., 2012) as thiol groups in reactive sites may be modified thereby inhibiting enzymatic activity and influencing signalling cascades.

1.12 Glutathione in periodontitis

Glutathione is considered an important redox regulator that controls inflammatory process and damage to the periodontium. There are therapeutic considerations for the use of glutathione in management of periodontitis for limiting the tissue damaged caused by oxidative stress (Bains and Bains, 2015). Oxidative stress is involved in many chronic inflammatory disease, such as periodontitis (Kumar et al., 2017), diabetes mellitus (Asmat et al., 2016) and atherosclerosis (Vogiatzi et al., 2009), and it is key to understanding underlying mechanisms that new therapies might be developed.

Intracellular glutathione is essential for a number of homeostatic and cellular processes, including chemotaxis (Sakai et al., 2012). Neutrophils from periodontitis patients have decreased intracellular glutathione (Dias et al., 2013). Previously (Dias et al., 2013) have demonstrated that incubation of neutrophils, isolated from periodontitis patients, with sulforaphane increases intracellular glutathione.

In gingival crevicular fluid (GCF), neutrophils are considered significant contributors for the high concentrations of glutathione. This maybe the result of increased synthesis by cells of the periodontal tissues, or of active release mechanisms or of passive release secondary to protease activity on gingival epithelial cells (Chapple and

Matthews, 2007). A study by (Chapple et al., 2002) observed that glutathione concentrations are reduced in chronic periodontal diseases compared to control in GCF. These lower concentrations of glutathione could be due to several factors resulting in decreased synthesis and/or enhanced local degradation which may involve defect in ɣ-glutamyl pathway of glutathione synthesis. Then, a study (Grant et al., 2010) showed improvement in glutathione concentrations in GCF following periodontal therapy.

1.13 Mass spectrometry

Mass spectrometry is a powerful technique that has transformed the detection of proteins in biology (Haag, 2016): through development of methods and instrumentation. Mass spectrometers consist of the ionisation source and the mass analyser.

The ionization source of a mass spectrometer introduces charges to the molecules of interest in the sample. Types of ionisation are electrospray ionisation (ESI) and matrix assisted laser desorption (MALDI). For ESI, protein sample flows through a capillary where voltage is applied and generates ionised droplets. These ionised droplets are vaporised, and ions are drawn into the mass spectrometry source. MALDI converts non-volatile macromolecules into ionized molecules by using short intense pulses of laser light to induce the formation of intact gaseous ions. After ionization, ions are accelerated in the ion source to a fixed kinetic energy.

In mass spectrometry, a mass analyser is used for the determination of mass-to-charge ratio (m/z) of the ions. There are various kinds of mass analysers used in mass spectrometry such as quadrupole, time of flight (ToF) and orbitrap. A quadrupole mass analyser is a bundle of parallel rods that enables ions to move between the rods, allowing for selection of ions. Meanwhile, ToF measures time taken for ion to reach the detector where lighter and more charged ions will reach the detector faster. The orbitrap detects ions in a circular motion. In figure 1.6, C-trap is used to inject ions into orbitrap and they spread into oscillating rings that induce current detected by the amplifier (Zubarev and Makarov, 2013). Oscillations from detected signal used to calculate mass-to-charge ratio (m/z) formula.

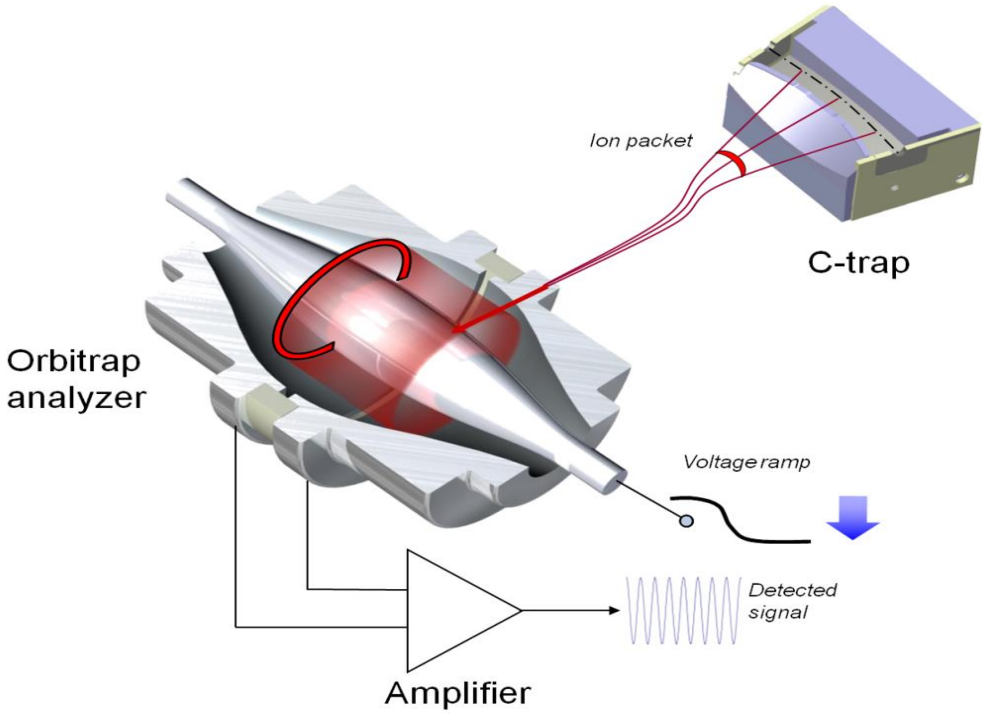

Figure 1.6: Cross-section of the C-trap and orbitrap analyser. In the orbitrap analyser, ions enter during the voltage ramp and form rings that induce current detected by the amplifier. Image taken from Thermo Fisher Scientific.

There are various types of fragmentation in mass spectrometry for protein detection, for example: collision-induces dissociation (CID) and electron-transfer dissociation (ETD). CID results in kinetic energy converting into internal energy from collision of the peptide with a neutral gas to cause fragmentation along the backbone of the peptide (Brodbelt, 2016). Fragment ions generated are recorded along with the parent ion mass and computationally these can be reconciled for sequencing of the peptide amino acid constituents. In ETD, generation of a radical occurs (Hauser et al., 2008) because of rapid neutralization of the charged site by an electron due to electron reacts with positively charged peptides (Kim and Pandey, 2012). The fragmentation is more likely to remove side groups and thus it is a useful technique to gather data on peptide modifications.

High performance of liquid chromatography (HPLC) is molecular fractionation of small and large molecules of various polarities (Ho et al., 2003). Electrospray ionization is able to couple liquid chromatography (LC) with mass spectrometry. The LC column directly feeds into the electrospray. Reverse phase high performance liquid

chromatography is used because of availabilities of various mobile and stationary phases where there is coupling of this technique with sample preparation and detection units (Singh et al., 2011).

Quantitative protein measurements by mass spectrometry have been widely used in research settings, thus, have evolved dramatically over the last decade (Hale 2013). There are different techniques that are carried out which can be divided into labelled and labelled free techniques. Many reagents that are enriched with stable isotopes to introduce mass tags of interest for protein quantification involve labelling proteins with reagents (Gygi et al., 1999) but there are also techniques which are label free.

Label free technique is to determine amount of protein in two or more biological samples, but it does not use a stable isotope that basically binds and label the proteins like other protein quantification methods. This technique has the advantage of having no limit number of samples or experimental conditions that can be compared, however, they rely on the performance of the liquid chromatography system or the mass spectrometer to accurately identify the peptide and its quantity. Methods for protein quantification in cell culture systems have been developed, for example stable isotope labelling with amino acids in cell culture (SILAC) (Ong et al., 2002). This method utilises combinations of isotope labelled arginine and lysine to give rise to three different masses that can be detected within a mass spectrometry instrument. This SILAC method is for the incorporation of stable isotope-labelled amino acids into a cellular protein pool and relies on the ‘light’ or ‘heavy’ form of amino acid into the proteins (Lanucara and Eyers, 2011). Every sample that used this method is labelled before any kind of treatment occurs at protein level to minimise errors associated with processing samples within the work flow. For example, gingival fibroblasts would be labelled prior to challenge with oral pathogens. However, SILAC is limited to three channels compared with the peptide labelling techniques. There are other techniques that can do peptide labelling up to 11 channels which allows for comparison of more samples, experimental conditions or replicates of individual conditions within one experiment, which may reduce variability. These techniques include tandem mass tags (TMT), isobaric tags for relative and absolute quantitation (iTRAQ) and isotope-coded affinity tag (ICAT). In TMT, the protein samples are labelled separately with different isobaric mass tags and are replicates of individual conditions within one

experiment and then, pooled into one sample to run on the mass spectrometer. Only ions picked for MS/MS fragmentation are quantified.

To aid with protein identification there are also enrichment strategies available. Antibodies of specific chemistries can be used to isolate proteins of interest. Glycoprotein enrichment is one example using column/resin enrichment (Zhu et al., 2017), whereas phosphopeptides might be isolated by chemical means.

1.14 Project aims

In this research it was hypothesized that modulation of glutathione would alter the ability of neutrophils to chemotax. Thus, the overall aim of the work was to further understand the role of redox balance in the aberrant chemotactic phenotype observed in neutrophils, particularly from periodontitis patients. This will be answered by addressing the following objectives:

i. **To assess glutathione modulating compounds on altering glutathione level in chemotactic behaviour of neutrophil cells using functional neutrophil assays.**

ii. **To optimise neutrophil preparation and separation for proteomics.**

iii. **To assess protein glutathionylation of haemoglobin using glutathione model protein in Orbitrap-based mass spectrometry.**

iv. **To further understand the role of redox balance in neutrophils from periodontitis patients.**

CHAPTER 2 – GENERAL MATERIALS AND METHODS

CHAPTER 2

GENERAL MATERIALS AND METHODS

2.1 Study volunteer donors

2.1.1 Selection of healthy volunteers

All volunteers for blood sample donations were obtained from staff and students recruited from The School of Dentistry. All participants were non-smokers and were not taking any medication. Ethical approval was obtained from the Birmingham Dental Hospital and University of Birmingham. Reference for the ethical approval is 14/SW/1148.

2.1.1 Periodontitis study – volunteer selection

Periodontitis patients were recruited from the Periodontology clinic within the Birmingham Dental Hospital. Gender and age matched healthy controls were recruited as stated in 2.1.1. Ethical approval for the study was approved (Reference: 14/SW/1148) and all 4 volunteers provided written informed consent. Exclusion criteria for both patient and control subjects included pregnancy, smoking and use of vitamin supplements.

2.2 Neutrophil isolation

Neutrophils were isolated from whole blood collected by venepuncture. The method used was based on that of Matthews et al., 2007. Venous blood samples were collected in lithium heparin vacutainers (Greiner, Bio-One, Kremsmunster, Austria); the amount of blood collected was approximately 24ml and did not exceed maximum of 30ml.

2.2.1 Reagents for neutrophil isolation

2.2.1.1 Percoll gradients

Percoll (1.13g/ml, 8 ml) (GE Healthcare, Buckinghamshire, United Kingdom) was used to make up two densities of 1.079g/ml and 1.098g/ml as shown in table 2.1. The 1.098g/ml Percoll density (8 ml) was layered under 1.079g/ml density (8 ml) in a centrifuge tube. These solutions were stored at 4°C prior to use. Sodium chloride (NaCl) (Sigma Aldrich, Dorset, United Kingdom) at a concentration of 1.5M was used as a component for the Percoll gradient. About 3.5ml NaCl was mixed with distilled water and Percoll to form the gradients.

Component	**1.079g/ml density**	**1.0987g/ml density**
Percoll	19.708ml	24.823ml
Water	11.792ml	6.677ml
NaCl (1.5M)	3.5ml	3.5ml

Table 2.1: Composition of Percoll gradients for neutrophil isolation

2.2.1.2 Lysis buffer

Lysis buffer was made by adding ammonium chloride (NH_4Cl) (8.3g; Sigma, A9434) (Sigma Aldrich), potassium bicarbonate (KHCO3) (1g; Sigma, P9144) (Sigma Aldrich), Disodium ethylenediaminetetraacetic acid dihydrate (Na_2 EDTA $2H_2O$) (0.04g; Sigma, E5134) (Sigma Aldrich) and bovine serum albumin (2.5g; BSA; Sigma, A4530) (Sigma Aldrich) sequentially to 1 litre of distilled water and stored 4°C prior to use for about 1 month. This solution was made up once a month.

2.2.1.3 Phosphate buffered saline (PBS)

PBS was made by adding 7.75g sodium chloride (NaCl) (Sigma Aldrich), 0.2g potassium phosphate monobasic (KH_2PO_4) (Sigma Aldrich) and 1.5g potassium phosphate dibasic (K_2HPO_4) (Sigma Aldrich) to a 1 litre distilled water. The solution was then autoclaved and stored at 4°C prior to use.

2.2.1.4 Glucose supplemented phosphate buffered saline (gPBS)

gPBS was made by adding up 1.8g glucose (Sigma-Aldrich), 0.15g calcium chloride ($CaCl_2$) (Sigma-Aldrich) and 1.5ml magnesium chloride ($MgCl_2$) (Sigma-Aldrich) to 1 litre of PBS. The salts were mixed and dissolved before adding the next one and the solution was stored to 4°C prior to use for about 1 week.

2.3 Neutrophil isolation method

Whole blood (8ml) was layered at the top of the Percoll gradients (methods section 2.2.1.1). The tubes were then centrifuged for 8 minutes at 150g, then followed by 10 minutes at 1200g. After centrifugation, five layers formed that consist of plasma at the top, followed by monocyte and lymphocyte layer, Percoll layer and red blood cell layer as shown in Figure 2.1.

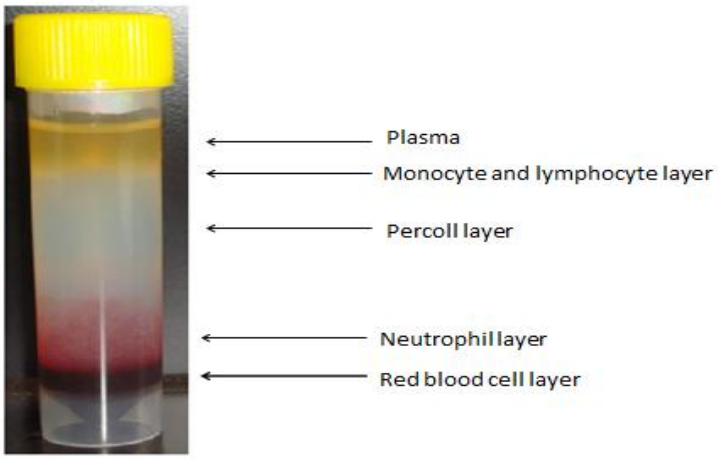

Figure 2.1 : Layers of blood components in Percoll after density centrifugation showing a distinct neutrophil layer from other leukocytes.

The neutrophil layer sat above the red blood cell layer. By using a Pasteur pipette (Appleton Woods, Birmingham, United Kingdom), plasma, monocyte, lymphocyte and Percoll layers was removed by manual aspiration. The neutrophil layer above red blood cell layer was then removed by gentle aspiration using a Pasteur pipette and was added to 50ml centrifuge tube (Sigma-Aldrich) containing lysis buffer (30ml) (methods section 2.2.1.2). The tube was then inverted several times and left at room temperature for 10 minutes to allow for erythrocyte lysis. After that, the cells were centrifuged at 350g for 6 minutes. The supernatant was discarded, and the cell pellet was resuspended in lysis buffer (4ml), incubated for 5 min at room temperature as before, prior to re-centrifugation. The supernatant was removed, and the cell pellet was suspended in PBS (4ml) and centrifuged again to remove any remaining lysis buffer. The supernatant was removed, and cells were suspended in PBS (3ml). The neutrophil cells were counted using a haemocytometer (Neubaeur, Reichart, Hausser Scientific, Horsham, United Kingdom) (methods section 2.4.1) and automated Luna cell counter (methods section 2.4.2). Neutrophils were then resuspended at concentration needed and used immediately in experiments.

2.4 Neutrophil viability using trypan blue and Luna cell counter

2.4.1 Trypan Blue

The cells were counted using a haemocytometer (Neubaeur, Reichart, Hausser Scientific) as shown in figure 2.2. The viability of the cells was checked using trypan blue dye exclusion (Sigma-Aldrich). Cells were mixed with trypan blue at a ratio of 1:1 and this mixture was added to the haemocytometer. Cell count and cell viability was visualized using a light microscope (Leitz Laborluxs, Ontario, Canada). Cells confirmed visually as blue were counted as dead cells. The small squares in red were counted. Each square has volume: 0.2 x 0.2 (width) x 0.1 (depth) = 0.004mm^3. The number of cells per ml was calculated as shown above (Figure 2.2).

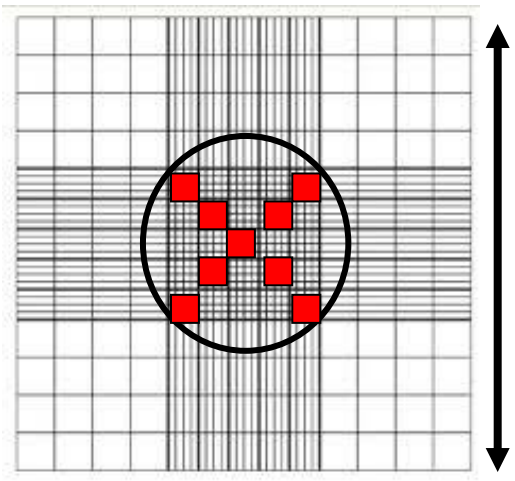

Calculation of number of cells per ml :

- Cell count /9 x 25 = no. of cells in the entire grid.
- No. of cells in the grid x 10^4 = no. of cells per ml.

Figure 2.2 : **Haemocytometer**. Cells observed in the 9 small squares highlighted in red were used in the calculation of cell concentration.

2.4.2 Luna automated cell counter

Neutrophil cells were also counted using Luna automated cell counter (Logos Biosystems, East Sussex, United Kingdom). This Luna cell counter produced total, live and dead cell counts. For each cell count, the live cells were identified with green circles and the dead cells were identified with red circles.

Luna reusable slides were used for cell counting. Sample (10µl) was mixed with trypan blue stain (10µl 0.4%). This mixture was put into the Luna counting slides and the slide was inserted Into the Luna counter instrument until a click sound was heard. The focus knob on the slide of the instrument used to adjust focus on the cells. Cells that are live had dark edges and bright surface while cells that are dead had a dark blue colour. Results was then viewed and saved.

2.5 Boyden chamber: QCM chemotaxis 3µm 96-well cell migration assay

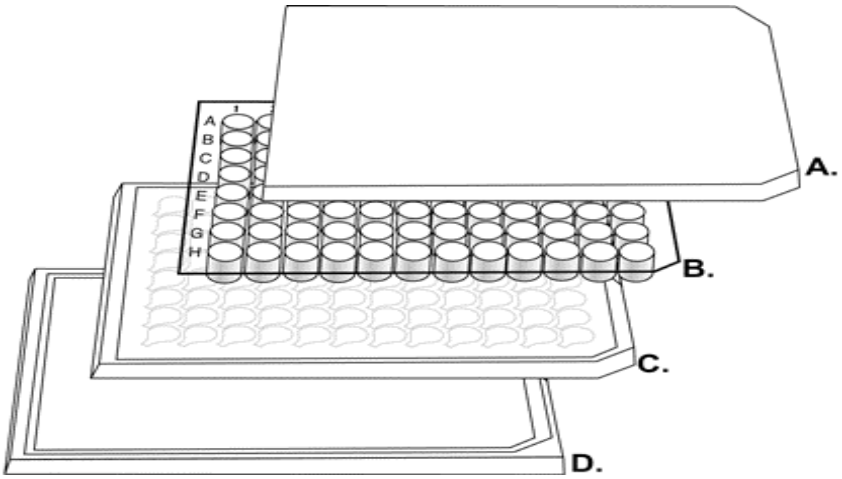

Figure 2.3: QCM chemotaxis assay (3µm). The letter label represents; A; lid, B; cell migration chamber plate, C; 96-well feeder tray, D; base. The cell migration chamber plate was used for cells and the 96-well feeder tray was used for chemoattractant. (Image from manufacturer's instructions, Merck Milipore, Hertfordshire, United Kingdom).

QCM chemotaxis assay (Merck Milipore, Hertfordshire, United Kingdom) is a Boyden chamber for high throughput chemotaxis assay. The method was based on manufacturer's protocol and the manufacturer provided all solutions described. For this assay, fMLP and IL8 chemoattractant (150µl, concentration as described in results) in gBPS was added to the wells of the feeder tray (figure 2.4, label C) in the lower chamber. In the upper chamber, cells (2×10^4 or 2×10^5) were places in 100µl RPMI. Plate was incubated for 1 hour at 37°C in a carbon dioxide (CO_2) incubator that has 4-6% CO_2.

After incubation, the migration chamber plate was removed from the plate assembly and non-migrated cells were gently discarded from the top side of the insert by flipping out the remaining cell suspension. This migration chamber plate was then placed onto a new 96-well feeder tray (second feeder tray) containing prewarmed Cell Detachment Solution (150µl) in the wells. These plates were incubated for 30 minutes at 37°C. During incubation, the migration chamber plate was gently tilted back and forth several times so that cells were completely dislodged from underside.

From the first feeder tray, 75µl of the solution (cells that migrated through the membrane and into the chemoattractant in the lower chamber) was transferred to a new 96-well black plate. Then, 75µl of the detachment solution from the second feeder tray (cells that migrated through the membrane and detached from the membrane by detachment buffer) was transferred to the same well in the 96-well black plate.

The Dye Solution was prepared of CyQuant GR Dye and Lysis Buffer. The ratio of preparation was as follows: CyQuant GR Dye prepared by manufacturer 1:75 was diluted with 4X Lysis Buffer (For example, 4µl dye in 300µl of 4X Lysis Buffer). Lysis Buffer/Dye Solution (50µl) was added to each well in the black 96-well plate containing 150µl of the migratory cells' solution. This plate was incubated for 15 minutes at room temperature and then read with plate reader (Infinite 200 PRO, Tecan Life Sciences, Mannedorf, Switzerland) for fluorescence at 480/520nm.

2.6 GSH-Glo assay (Promega Corporation, Southampton, United Kingdom)

2.6.1 GSH-Glo reagent (2X concentration)

The reagents that are already contained in the assay kit were used to make up the GSH-Glo reagent (2X concentration):, Luciferin-NT substrate and Glutathione S-Transferase were diluted 1:50 in GSH-Glo Reaction Buffer. The GSH-Glo reagent 2X was prepared immediately prior to use.

2.6.2 Luciferin detection reagent

The contents of a bottle of reconstitution buffer with esterase that was provided in the assay kit was transferred to the amber bottle of lyophilized luciferin detection reagent that was also in the assay kit. The solution was mixed by inversion until the substrate was dissolved.

2.6.3 Method for GSH-Glo assay

GSH-Glo assay used to measure the glutathione level in neutrophil cells. Neutrophil cells were in PBS at concentration of 1×10^5. In a 96-well plate, cells were dispensed at 50µl per well. Then, 50µl of prepared GSH-Glo reagent 2X was added per well. Plate was mixed briefly on a rocker (Stuart Gyro-rocker SSL3, Sigma-Aldrich, Dorset, United Kingdom) and incubated at room temperature for 30 minutes. Then the prepared luciferin detection reagent was added at 100µl per well to the 96-well plate. The plate was then mixed briefly on a rocker (Stuart Gyro-rocker SSL3, Sigma-Aldrich) and incubated at room temperature for 15 minutes. The luminescence was then measured using a luminometer (Berthold Technologies, Herts, United Kingdom).

2.7 GSH/GSSG-Glo assay

GSH/GSSG-Glo assay was purchased from Promega Corporation used to measure total glutathione and oxidized glutathione (GSH:GSSH) in neutrophil cells.

2.7.1 Total glutathione lysis reagent

The volume for this reagent was 25µl per well in a 96-well plate. The reagents used was 1µl Luciferin-NT, 10µl passive lysis buffer and 14µl water. This reagent was prepared approximately 30 minutes before use.

2.7.2 Oxidized glutathione lysis reagent

The volume for this reagent was 25µl per well in a 96-well plate. The reagents used was 1µl Luciferin-NT, 0.5µl 25mM N-ethylmaleimide (NEM), 10µl 5X passive lysis buffer and 13.5µl water. The reagent was prepared approximately 30 minutes before use.

2.7.3 Luciferin generation reagent component

The volume for this luciferin generation reagent (100mM) was 50µl per well in a 96-well plate. The reagents used were 1.25µl DTT, 3µl glutathione-S-transferase and 45.75µl glutathione reaction buffer.

2.7.4 Luciferin detection reagent

The contents of a bottle of reconstitution buffer with esterase that was provided in the assay kit was transferred to the amber bottle of lyophilized luciferin detection reagent that was also in the assay kit. The solution was mixed by inversion until the substrate was dissolved.

2.7.5 Method for GSH/GSSG-Glo assay

GSH/GSSG-Glo assay used to measure the total glutathione and oxidized glutathione level in neutrophil cells. Neutrophil cells were in PBS at concentration of 1×10^5. In a 96-well plate, cells were dispensed at 20µl per well. Then, 25µl of prepared total glutathione lysis reagent or oxidized glutathione lysis reagent was added per well. Plate was mixed briefly on a rocker (Stuart Gyro-rocker SSL3, Sigma-Aldrich) for 5

minutes and 50µl of luciferin generation reagent was added per well. Then, the plate was incubated at room temperature for 30 minutes. Then the prepared luciferin detection reagent was added at 100µl per well to the 96-well plate. The plate was then mixed briefly on a rocker (Stuart Gyro-rocker SSL3, Sigma-Aldrich) and incubated at room temperature for 15 minutes. The luminescence was then measured using a luminometer (Berthold Technologies).

2.8 Preparation of whole cell protein extracts

Neutrophil cells were prepared for protein extracts to determine protein contents. After neutrophil isolation from whole blood, cells were lysed with lysis buffer (10% sodium dodecyl sulphate (SDS) in 100mM triethylammonium bicarbonate (TEAB) (ThermoFisher Scientific, Paisley, United Kingdom). Cells were stored at -80°C until used for proteomics experiments. When it was ready, sample viscosity was reduced by shearing deoxyribonucleic acid (DNA) using a microtipsonicator Soniprep 150 (MSE (UK) Ltd, London, United Kingdom) on ice for 10 seconds. Then, lysate was centrifuged at 16,000 xg for 10 minutes at 4°C. The supernatant was then carefully separated and transferred into a new tube. Protein concentration of the supernatant was determined using the BCA Protein Assay (ThermoFisher Scientific). In this study, 100µg of protein were harvested per condition.

2.9 Protein determination using bicinchoninic acid (BCA) assay

All protein measurements were made using the bicinchoninic acid assay (Smith et al., 1985, purchased from Thermo Fisher Scientific), unless otherwise stated.

Bicinchoninic acid reagent solution (Reagent A): containing bicinchoninic acid, sodium carbonate, sodium tartrate and sodium bicarbonate in sodium hydroxide (0.1M, pH11.25) (Sigma)

Reagent B: Copper (II) sulphate pentahydrate solution: 4% (w/v) solution (Sigma).

Protein standard: BSA (1.0 mg/ml) in sodium chloride (0.15M), sodium azide (0.05%) (Sigma).

The standards were prepared using diluted albumin (BSA) (ThermoFisher Scientific). The contents of one Albumin Standard (BSA) ampule was diluted into several clean vials, using the same diluents as the samples. A set of diluted standards was prepared such as the table 2.2:

Vial	Volume of Diluent (µl)	Volume and Source of BSA (µl)	Final BSA Concentration (µg/mL)
A	0	300 of stock	2000
B	125	375 of stock	1500
C	325	325 of stock	1000
D	175	175 of vial B dilution	750
E	325	325 of vial C dilution	500
F	325	325 of vial E dilution	250
G	325	325 of vial F dilution	125
H	400	100 of vial G dilution	25
I	400	0	0 = Blank

Table 2.2: Preparation of Diluted Albumin (BSA) Standards

Then, BCA working reagent (WR) was prepared. In preparation of this reagent, the following formula was used to determine the total volume of WR required:

(# standards + # unknowns) x (# replicates) x (volume of WR per sample) = total volume WR required

WR was prepared by mixing BCA Reagent A (BCA solution) (ThermoFisher Scientific) with BCA Reagent B (Copper II Sulphate Pentahydrate 4% solution) (ThermoFisher Scientific). The ratio was 50 parts of BCA Reagent A with 1 part of BCA Reagent B (50:1), Reagent A:B).

Standards and samples (10µl) were pipetted in duplicate into separate wells of a 96 well plate (Starlab, Milton Keynes, United Kingdom), WR (200µl) was added to each well and plate was mixed thoroughly on a plate shaker for 30 seconds. Plate was then covered and incubated at 37°C for 30 minutes. After that, plate was cooled to room

temperature and absorbance was measured at 570nm in the plate reader (Infinite 200 PRO, Tecan Life Sciences, Mannedorf, Switzerland). Protein concentration was determined through reference to a standard curve.

2.10 Protein digestion in solution.

After protein was determined, 100µg was transferred into a new tube and adjusted to a final volume of 100µl with 100mM TEAB (Thermo Fisher Scientific). 5µl of 100mM tris(2-carboxyethyl) phosphine hydrochloride (TCEP) (Sigma-Aldrich) was added and the sample was incubated at 55°C for 1 hour. Iodoacetamide (9mg) (Sigma-Aldrich) dissolved in TEAB (132ul, 100mM) to make up 375mM iodoacetamide. This solution was protected from light. Then, 5µl of this solution was added to the protein solution and it was incubated for 30 minutes protected from light at room temperature. After that, dithiothreitol (DTT, 5µl, 230mM) (Sigma-Aldrich) was added to quench any excess iodoacetamide and was incubated for 10-15 minutes at room temperature.

For protein digestion, trypsin was used. Before usage, Trypsin Gold Storage Solution (Promega Corporation) (20µl) was added to the bottom of the trypsin glass vial containing 20µg and incubated for 5 minutes. Then, trypsin (2.5µl) was added to the reduced and alkylated protein (100µg). The sample was then digested overnight at 37°C. The next day, sample was dried in a Speed Vac (Thermo Fisher Scientific).

2.11 Macrotrap desalting

Macrotrap desalting was used to desalt protein samples. Firstly, the trap was cleaned 5-10 times using (100µl) of 90% Acetonitrile (ACN), 10% water (H_20) and 0.1% Trifluoroacetic acid (TFA). Then, it was equilibrated 5-10 times using (100µl) of 2% ACN, 98% H_20 and 0.1% TFA. The sample was then loaded with (100µl) of 2% ACN and 0.1% TFA. Salts were removed from the sample using (100µl) of 2% ACN, 98% H_20 and 0.1% TFA. Next, the sample was eluted using (100µl) of 90% ACN, 10% H_2O and 0.1% TFA.

2.12 MicroBCA assay

After digestion, MicroBCA assay was done to determine peptide concentration by a modified bicinchoninic acid assay. This method was based on Krishan et al., 2009. The digested proteins were resuspended in (100µl) of 7.2% Trifluoroacetic acid (TFA) (Sigma-Aldrich). Then, it was centrifuged at 10,000 xg for 20 minutes. The supernatant was taken and diluted 1 in 10 in 0.1M sodium hydroxide (NaOH) (Sigma-Aldrich) with 1% sodium dodecyl sulphate (SDS) (Sigma-Aldrich). Using an Eppendorf thermomixer compact (Sigma-Aldrich), it was heated at 95°C for 5 minutes. Then, it was cooled down to room temperature. After that, (10µl) of the sample was transferred into a microplate well (Starlab, Milton Keynes, United Kingdom) and BSA assay was done as described in 2.9.

2.13 Desalting using ZipTips

For mass spectrometry, residual salts were removed from the extracted peptides using ZipTips (Merck Milipore). This method was done as described by the manufacturer. In this method, TFA (Sigma-Aldrich) was added to sample until 0.1% TFA was achieved. ZipTip was wetted with Acetonitrile (ACN) (Sigma-Aldrich) (10µl) and then equilibrated with TFA (10µl, 0.1% v/v). The 10µl sample was loaded, aspirated and dispensed 7-10 times for maximum binding. The waste was retained. After that, the tip was washed with 0.1% TFA (10µl) (Sigma-Aldrich), aspirated and dispensed twice. Then, to remove all peptides, 10µl 0.1% Formic Acid (Sigma-Aldrich)/ 50% ACN (Sigma-Aldrich) was taken to elute, aspirated and dispensed 10 times. This sample was kept as desalted sample. Then, it was spun in vacuum centrifuge SpeedVac (ThermoFisher Scientific) and stored at -20 or -80°C.

2.14 Western blot

Western blot was used to detect specific actin and glutathionylated proteins in the neutrophils.

2.14.1 Tris-buffered saline (TBS)

For 1L of TBS, 8g sodium chloride (NaCl) (Sigma-Aldrich), 0.2g potassium chloride (KCl) (Sigma-Aldrich) and, 3g Tris base (Sigma-Aldrich) was dissolved in distilled water and adjusted to pH 7.5.

2.14.2 Tris buffered saline with Tween (TBST) for washes

To make up TBST, Tween 20 (500µl, Sigma-Aldrich) was added per litre of TBS.

2.14.3 Antibodies used in western blot

No.	Antibody	Concentration	Manufacturer
1.	Anti-actin	1:5000 dilution	Thermo Fisher Scientific
2.	Anti-glutathione (Anti-PSSG)	1:5000 dilution	Thermo Fisher Scientific
3.	Secondary mouse antibody	1:10,000 dilution	Thermo Fisher Scientific

Table 2.3: Antibodies and concentrations used in western blot.

2.15 Protocol for western blot

Mini-Protean TGX precast gels from Bio-Rad, Hertfordshire, United Kingdom with gel composition of 12% acrylamide were used. Before usage, the comb was removed by pulling it upward in one smooth motion. At the bottom of the gel cassette, the sealing green tape was removed by pulling it gently.

Electrophoresis tank (Bio-Rad) were used. Two gel cassettes were put into it facing each other (front to front). Then, running buffer was added to the outer part and then added to the inner part of tank till overflowing. Protein ladder (ThermoFisher Scientific) 4µl was loaded and sample (20µl) were loaded in separate wells. The tank lid was put on (black top on black) and (red top on red). Then, the tank was run at about 200V for approximately 40 minutes until the dye stain was approaching the bottom of the gel.

2.15.1 Running buffer (10x concentration)

Tris (30.3.g, Sigma-Aldrich) and glycine (144g, Sigma-Aldrich) were dissolved in 900ml distilled water. Then, 10g of sodium dodecyl sulphate (SDS) (Sigma-Aldrich) was added and dissolved. The solution pH was adjusted to 8.3 and made up to 1L.

2.15.2 Sample preparation

Protein samples (20µg) were prepared by mixing 1:1 with Laemlli buffer (Sigma-Aldrich) that consists 20% glycerol, 0.004% bromophenol blue and 0.125M Tris (Sigma-Aldrich). The resulting solution was heated to 95°C for 5min before separation by sodium dodecyl sulphate polyacrylamide gel electrophoresis (SDS-PAGE).

2.15.3 Coomassie Blue Staining

Instant Protein Stain (Expedeon, Cambridge, United Kingdom) was used for gel staining. Instant Protein Stain is a ready to use Coomassie protein stain for polyacrylamide gels. Gels were incubated in 100ml staining solution for 1 hour. Then the staining solution was removed, and the background was removed with water (2 x 100ml) for 1 hour.

2.15.4 Membrane transfer

For membrane transfer, nitrocellulose and transfer blot packs from Bio-Rad were used. The transfer runs at 25V, 2.5mA for 10 minutes.

2.16 Strip Western blot membranes

The western blot membrane was submerged in sodium hydroxide (0.4M) (Sigma-Aldrich) on a rocker (Stuart Gyro-rocker SSL3, Sigma-Aldrich) for 15 minutes. The solution was discarded and replaced with TBS and put on the rocker for 10 minutes. This was repeated twice. Bovine serum albumin (BSA) (Sigma-Aldrich) 3% in TBS was prepared. The membrane was blocked with the BSA solution on a rocker (Stuart Gyro-rocker SSL3, Sigma-Aldrich) for one hour. Then, antibody 1:5000 (Thermo Fisher Scientific) was prepared, hence, the blot was put in the antibody overnight in the cold room (4°C). The blot was put in a black plate (Sigma-Aldrich) and washed with tris buffered saline with Tween (TBST) (Sigma-Aldrich) three times for 10 minutes each time. Then, the blot was incubated in anti-mouse secondary antibody labelled with infra-red label 800CW or 680RD (red or green dyes respectively) at 1:10,000 dilution (Thermo Fisher Scientific) for 1 hour. Then, the blot was washed with TBST three times for 10 minutes each time. Then, the membrane blot was scanned using the Odyssey Licor scanner (Odyssey System, Wakefield, United States).

2.17 Tryptic digestion for gels

2.17.1 Ambic

Ammonium bicarbonate (100mg) (Sigma-Aldrich) was dissolved in distilled water (50ml).

2.17.2 Ambic:ACN

Ammonium bicarbonate (100mg) (Sigma-Aldrich) was dissolved in distilled water (25ml) and acetonitrile (25ml) (Sigma-Aldrich).

2.17.3 ACN:formic acid

Acetonitrile (50ml) (Sigma-Aldrich) was mixed with formic acid (5ml) (Sigma-Aldrich) and distilled water (45ml).

2.17.4 Trypsin

Trypsin (sequencing grade 12.5ng/µl from Promega Corporation).

2.18 Protocol for tryptic digestion of gels

Samples were separated by SDS-PAGE on ready gels (Bio-Rad) (methods section 2.14) and the gels were stained with Instant Protein Stain Coomassie Blue (Expedeon, Cambridge, United Kingdom). Bands of interest were excised in a flow hood to prevent keratin contamination.

Each gel sliced were diced into small pieces (~1mm^2) and placed in a 500µl Eppendorf tube (ThermoFisher Scientific). ACN (100µl) (Sigma-Aldrich) was added and the tube was vortexed for 10 minutes. The supernatant was removed and transferred to a separate tube to be discarded. This dehydration and extraction of Coomassie stain was repeated 3 or 4 times. The pieces were then dried completely in a Speed Vac (ThermoFisher Scientific). The gel volume was estimated (in µl) and trypsin (Promega Corporation) solution was added to cover the gel pieces. The mixture was then vortexed for 10 minutes before incubating at 4°C for 30 minutes. The tube was briefly centrifuged, to sediment the gel pieces, before sealing with Parafilm (Sigma-Aldrich), to prevent evaporation, and incubated at 37°C overnight.

To extract the peptides from the gel pieces, the tube was briefly vortexed and centrifuged. Liquid was removed to a fresh tube. Peptides were extracted by addition of 0.1% TFA in 60% acetonitrile of a volume to cover the gel pieces, 30min at 30°C. The liquid was removed to the same fresh tube and the procedure was repeated. The total liquid removed in the fresh tube was then dried by vacuum centrifuge before desalting (methods section 2.13).

2.19 Mass spectrometry

All mass spectrometry for proteomics was carried out at School of Biosciences, University of Birmingham with assistance from Dr Sabah Pasha (postdoctoral fellow) and Dr Jinglei Yu (mass spectrometry officer).

After protein samples digested as in methods section 2.10 and desalted through steps in methods section 2.12, peptides were loaded on to a 150 mm Acclaim PepMap100 C18 column (ThermoFisher Scientific) in formic acid (0.1% v/v) (Sigma-Aldrich). Peptides were separated over a linear gradient from 3.2% to 44% mobile phase B (acetonitrile with formic acid (0.1% v/v) with a flow rate of 350 nL/min. The column was then washed with 90% mobile phase B before re-equilibrating at 3.2% mobile phase B. The column oven was heated to 35°C. The LC system was coupled to an Advion TriVersa NanoMate (Advion) which infused the peptides directly into an LTQ-Orbitrap Elite ETD (ThermoFisher Scientific).

The mass spectrometer performed a full FT-MS scan (m/z 380-1800) and subsequent CID MS/MS scans of the 7 most abundant ions above an absolute signal intensity threshold of 5000 counts. Full scan mass spectra were recorded at a resolution of 60,000 at m/z 400 and anterior cingulate gyrus (ACG) target of $1x10^6$ (maximum injection time 1s). Precursor ions were fragmented in CID MS/MS with a normalized collision energy of 35% and an activation Q of 0.25. ACG target for CID MS/MS was $1x10^5$ (maximum injection time 50 ms). The width of the precursor isolation window was 2 m/z and only multiply-charged precursor ions were selected for MS/MS. Spectra were acquired for 56 minutes. A full Fourier-transform mass spectrometry (FT-MS) scan (m/z 380-1800) was performed with subsequent higher-energy collisional dissociation (HCD) MS/MS scans of the 7 most abundant ions that passed a minimum signal requirement of 5000 counts. The full FT-MS scans were recorded at 120,000 resolution and ACG target of $1x10^6$ (maximum injection time 1 s). Precursor ions were fragmented in HCD MS/MS with a normalized collision energy of 38% and an activation time of 0.1. ACG target for HCD MS/MS was $1x10^5$ (maximum injection time 50 ms). The width of the precursor isolation window was 2 m/z and only multiply-charged precursor ions were selected for MS/MS. FT first mass value was reduced to 120 m/z to account for tandem mass tags (TMT) reporter ions.

2.20 Proteome discoverer software

The data were analysed using Proteome Discoverer (version 1.4 and 2.1 Thermo Fisher Scientific). Data from each SCX and reverse phase column (C18) set were analysed together and each replicate searched independently. The database used was from Uniprot (Human database) (European Bioinformatics Institute, Cambridge, United Kingdom). The data were searched with the following settings: trypsin as the enzyme with a maximum of two missed cleavages, 10 ppm mass accuracy for the precursor ion, fragment ion mass tolerance was set at 0.8 Da, carbamidomethylation of cysteine and isobaric tags for relative and absolute quantitation (iTRAQ) addition to the N-terminus and lysine residues were set as fixed modifications, and phosphorylation of serine, threonine and tyrosine was set as a variable modification as was oxidation of methionine and TMT addition to lysine. The search results from each of the technical replicates were combined and proteins which were identified with two or more unique peptides were classed as identified. Only unique peptides were used for protein quantification (performed in Proteome Discoverer) and protein grouping was employed (only proteins which contained unique peptides were used).

2.21 Software used in study

Various software was used in this study. Below are the software used.

2.21.1 Graph Pad Prism (GraphPad Software, San Diego, United States)

This software was used to do data analysis, graphs and statistics, for example, Kolmogorov-Smirnov test to determine if the data fits a Gaussian distribution and One Way ANOVA with Tukey's multiple comparison test for significant difference confirmation ($p < 0.0001$).

2.21.2 Proteome Discoverer (ThermoFisher Scientific)

This software was used to identify and quantify protein samples and for analysis of TMT labelled samples. Search engine used was SEQUEST.

2.21.3 Protein-Prospector (University of California, San Francisco, United States)

The Protein-Prospector software was used to in silico digest haemoglobin alpha and beta chain, with and without glutathione modification, to generate peak lists for identification of the proteins.

2.21.4 UniProt (European Bioinformatics Institute)

The Uniprot software provides a database for protein and its functional information.

2.21.5 Xcalibur (ThermoFisher Scientific)

All mass spectrum was put through the Xcalibur to identify the proteins in the neutrophil samples. For glutathione model protein, the mass spectra were deconvoluted using the Xtract function in Xcalibur to obtain the monoisotopic masses.

CHAPTER 3 – Functional assays of neutrophils

CHAPTER 3

Functional assays of neutrophils

3.1 Introduction

Neutrophil function is vital to proper execution of the innate immune system. These cells are first to arrive at a site of infection and carry out three functions: recruitment, response and resolution. Measurement of neutrophil chemotaxis has been done by a wide variety of methods including video microscopy (Muinonen-Martin et al 2010), movement of cells across membranes (Gomez-Lopez et al., 2011) and movement of cells under agarose (Chethana et al., 2012). Recruitment of neutrophils relies on chemotaxis of the cells to the location required. In periodontitis Roberts et al (2015) demonstrated that neutrophils were slower and had less directionality than neutrophils from donors without periodontitis. Previously in our lab, chemotaxis of peripheral blood neutrophils has been determined by video microscopy using the Insall chamber (Roberts thesis 2016). The Insall chamber was developed for the study of *Dictyostelium discoideum* (Muinonen-Martin et al., 2010) and can record many details of the migrating organisms or cells being studied. This approach generates a large amount of information about the migrating cells as each cell is visualised across time and information can be gained about the direction of motion, the distance travelled and even the morphology of the cells. The method is time consuming, with each observation taking at least 20min. Therefore, it is slow and does not lend itself to measuring multiple conditions in parallel. At present in our laboratories the rate limiting factor is the accessibility to only one microscope that can record videos.

Previous research had also demonstrated that the window of opportunity for the neutrophils was limited to 4h before their integrity was compromised in terms of ability to chemotax (Roberts thesis 2016). In this work it was desired to challenge isolated human primary neutrophils with a range of stimuli that might modulate intracellular glutathione (GSH). For this a higher throughput technique would be required for assessing chemotaxis. Thus, available Boyden chamber style assays were evaluated. Three different assays were tested for ease of use and in comparison, with results

from the Insall chamber. It was vital to develop another higher throughput chemotactic technique to study multiple conditions of neutrophils.

Additionally, neutrophil intracellular glutathione (GSH) has also been shown to be of importance to the functionality of neutrophils in their multiple abilities; a decrease in intracellular GSH was found in neutrophils isolated from periodontitis patients (Dias et al 2013). Thus, a key aim of this chapter was to determine if manipulation of intracellular GSH directly changed chemotactic properties of neutrophils isolated from healthy donors. Figure 3.1 shows compounds that intervene in the production of glutathione which was adapted from Harlan et al., (1984) study. The red labels points to inhibitors used to inhibit glutathione levels in glutathione redox cycle, thus manipulate the glutathione levels. The rationale of using these inhibitors is to see whether there are any effects on neutrophils chemotaxis after the glutathione levels were manipulated. In the diagram, cellular glutathione can be depleted by inhibition of glutathione reductase by carmustine (BCNU). Reduced glutathione can also be depleted by formation of a thioester conjugate with 1-chloro-2,4-dinitrobenzene (CDNB) which is catalysed by endogenous glutathione-s-transferase. Buthioninesulfoximine (BSO) is a selective inhibitor of γ-glutamyl-cysteine synthetase and may inhibit glutathione biosynthesis (Alton, 1983). N-acetylcysteine (NAC) is an acetylated cysteine residue and causes increase of GSH level by providing a cysteine precursor. NAC has the ability to minimize negative effects thought to be associated with oxidative stress as it may additionally scavenge reactive oxygen species itself.

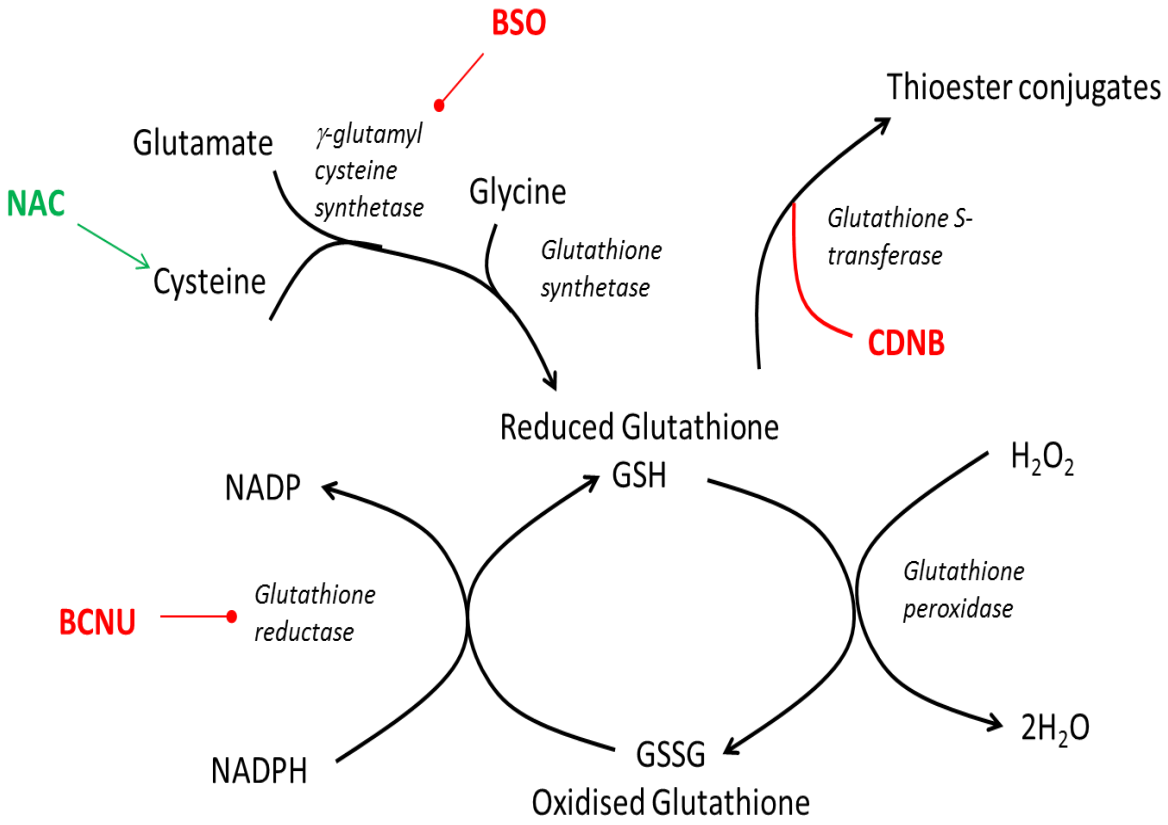

Figure 3.1: Pharmacologic modification of the glutathione redox cycle *in vitro*. Adapted from Harlan et al., 1984. Abbreviations BCNU: carmustine or bis-chloroethylnitrosourea; CDNB: 1-chloro2,4-dinitrobenzene; BSO: buthioninesulfoximine; NAC: N-acetyl cysteine.

3.2 Materials and methods

3.2.1 Real-Time Glo

For neutrophil viability, Real Time Glo assay (Promega Corporation) was used. The method used for determination of time course for neutrophil experiment was that of the manufacturer's protocol.

Prior to starting the assay, MT cell viability substrate, NanoLuc enzyme and cell culture medium was equilibrated to 37°C. The neutrophil cells were plated at various cell densities ($1 \times 10^2 - 1 \times 10^5$) in a white walled 96 well plate. For making the 2X RealTime-Glo reagent MT cell viability substrate (2 µl) and NanoLuc enzyme (2 µl) were added to prewarmed cell culture medium (996 µl) and vortexed to mix.

An equal volume (40µl) of the prepared 2X Real Time-Glo reagent was added to the cells (40µ). Cells were incubated in a cell culture incubator at 37°C and 5% carbon dioxide (CO_2). The luminescence of the sample was measured for 12 hours using a Tristar multimode reader from Berthold Technologies.

3.2.2 Insall chamber

The Insall chamber (Epigem Ltd, Redcar, UK) (figure 3.2) method was based on Muinonen-Martin et al., 2010. The Insall chamber was washed three times with Roswell Park Memorial Institute Medium (RPMI) (Sigma-Aldrich) prior to use. After the last wash a large droplet of RPMI was left on the chamber. Glass coverslips (22 mm) were submerged in 0.2M acid hydrochloric (HCl) (Sigma-Aldrich) in a Petri dish for 15 minutes. Then, the coverslips were washed twice with reverse osmosis water. The coverslips were left to dry on filter paper before use. The coverslips were coated in bovine serum albumin (BSA, 7.5% in PBS, 400µl) (Sigma-Aldrich), ensuring an even coat was formed. Any excess was aspirated from the surface. Immediately. neutrophil cells (1 x 106 /ml, 400ul), suspended in RPMI (containing BSA 1.5ul/ml 7.5%), were added to the coverslip. The coverslip was left at room temperature for 20 minutes for the cells to adhere.

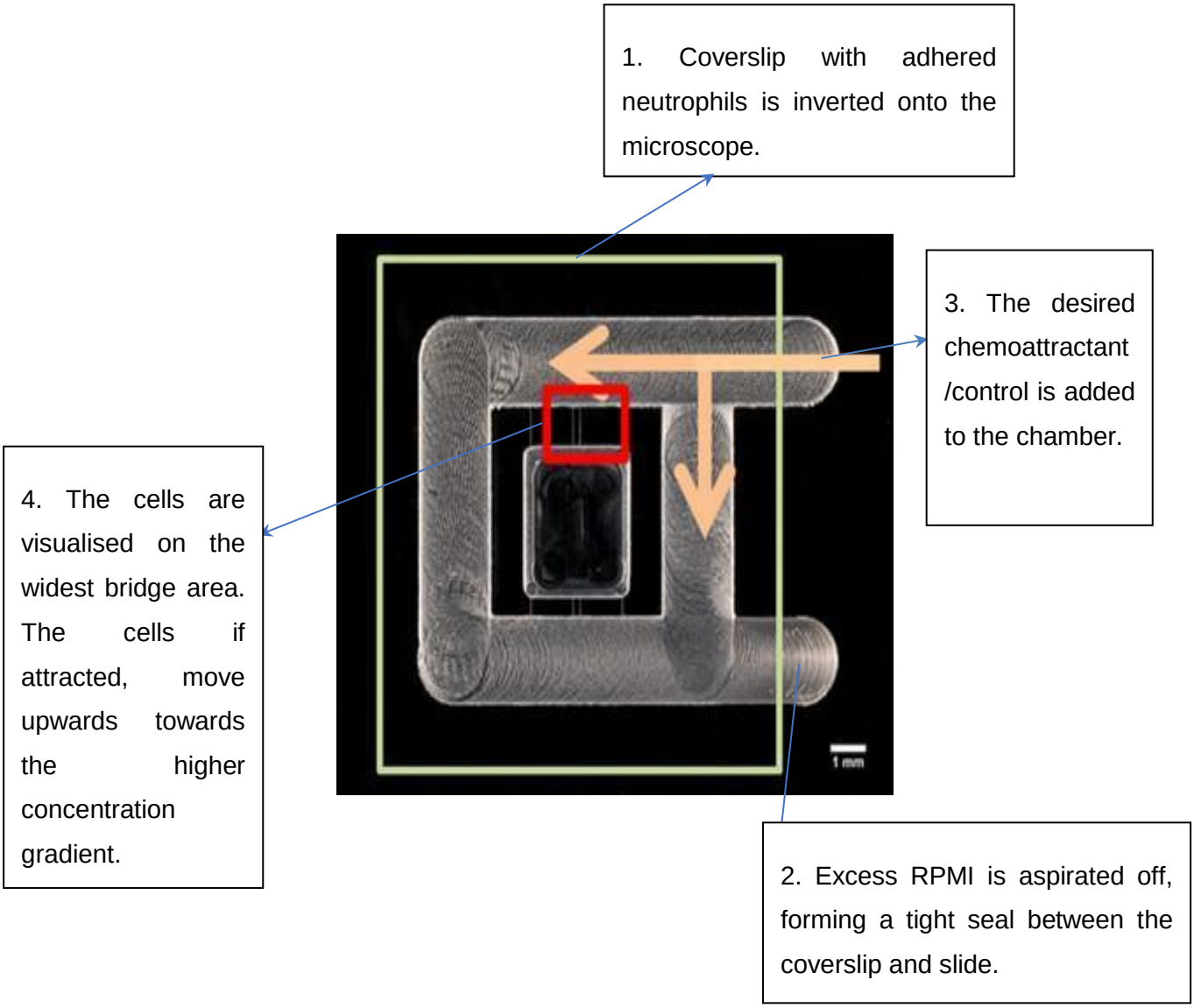

Figure 3.2: Insall chamber for direct visual of chemotaxis on video micrography.

After incubation the coverslip, was inverted over the chamber ensuring the pipette loading bays are exposed. A filter paper was used to aspirate any excess fluid from the chamber. Chemoattractant (80µl) was loaded onto the chamber via the loading bays. The chamber was then visualised immediately using the Zeiss Primovert microscope at x20 magnification. The software used for collecting images using the 'movie' tab was Q Imaging Retiga 2000R camera. An image was captured every 30 seconds for 20 minutes.

For analysing the videos, Manual tracking Plugin software and Image J software (Rasband, W.S., ImageJ, U.S. National Institutes of Health, Bethesda, Maryland, USA) was used. For the videos, there were 20 slides altogether and a reference point was put on the top left of the image. Tracking points were added for the cells that had directional movement towards the chemoattractant. Usually, 15 cells were chosen as previously determined by Roberts et al., (HM Roberts thesis 2016 entitled neutrophil function in chronic inflammatory disease states) and the data points were exported to an Excel table. The images were also saved as an animated graphics interchange format (GIF) file.

The exported data were analysed using an established method provided by Muinonen-Martin et al., 2010. From the spreadsheet, a spider diagram was made to see the measurement of cells movement towards the chemoattractant. Measurement of velocity, speed and chemotactic index was also obtained from the spreadsheet. Velocity is the µm/minutes cells move towards the chemoattractant where positive measurement shows a movement towards the chemoattractant, meanwhile, negative measurement shows a movement away from the chemoattractant. Average speed of a cell in any direction over the time course is known as cell speed (Roberts et al., 2015). Chemotactic index is measure of the accuracy of chemotaxis that was calculated by taking the cosine of the angle between a line directly up the gradient and one that connects a cell's start point to its end point. A value of 1 is directly up the gradient. The average of velocity, speed and chemotactic index was used in Graph Pad Prism (GraphPad software, San Diego, United States of America (USA)) software for statistical analysis.

3.2.3 ChemoTx chamber (Neuroprobe)

ChemoTx Chamber (Neuro Probe, Warwick, United Kingdom) is an example of a single use Boyden Chamber assay. The manufacturer provided a membrane in a metal frame for ease of handling with selectively coated hydrophobic masks around each of the test sites (figure 3.3). The method was based on manufacturer's protocol. Neutrophils (1×10^5 per ml) were suspended in RPMI. The lower chamber of this assay was filled with chemoattractant in gPBS (308µl) per well. The membrane filter was placed above the lower chamber and neutrophils (50µl) were pipetted onto the individual hydrophobic masked test areas. This plate A was incubated for 90 minutes at 37°C.

A second plate (Plate B) was prepared with cell detachment solution (308µl, 0.1uM Versene) per well and then, prewarmed to 37°C. After 90min liquid from the top of the membrane filter was removed and washed once with gPBS (110µl). The filter was removed and placed onto the second plate. Then, it was incubated for 30minutes at 37°C. gPBS (100µl) from each of the lower chamber (plates A and B) was transferred into a black fluorescence plate with clear bottom. The number of cells was measured using Cyquant dye (Thermo Fisher, Loughborough, United Kingdom): the preparation of the solution was as follows: 24µl stock and 120µl suppressor into 5.8ml gPBS. Amount of 50µl CyQuant NF (2x) solution was added to each well. The plate was incubated for 30 minutes at 37°C. Fluorescence readings were taken at 485/535nm from bottom of the plate.

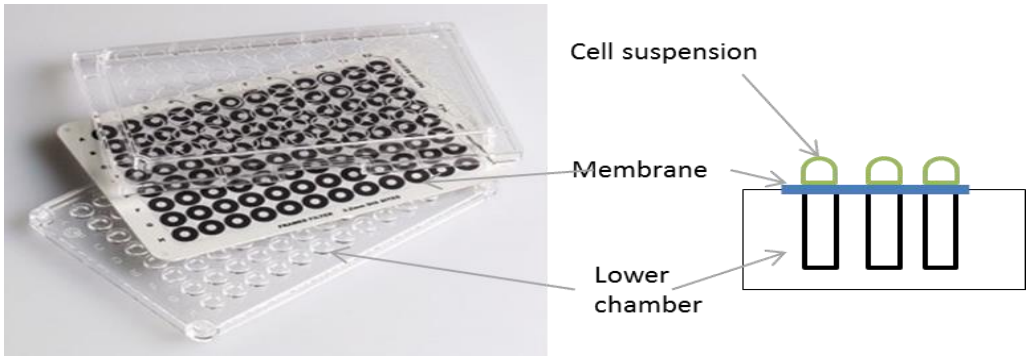

Figure 3.3: ChemoTx Chemotaxis Chamber from Neuro Probe. The metal mounted filter serves as filter and upper chamber onto which drops of cell suspension are placed.

3.2.4 Forty-eight (48) Micro Chemotaxis Chamber (Neuroprobe)

The next Boyden type chamber tried was the Micro chemotaxis chamber, also from Neuroprobe (figure 3.4). This reusable chamber used replaceable polycarbonate track-etch (PCTE) membranes (Neuroprobe) onto which neutrophils became attached following chemotaxis. The bottom well or chamber was filled with chemoattractant in gPBS (25µl) per well. The PCTE membrane filter was placed above the lower chamber and neutrophils (50ul, various concentrations) were pipetted into the top or upper chamber. This plate was incubated for 60 minutes at 37°C. The neutrophils were stained with Giemsa stain (Sigma-Aldrich). About 20µl of stain were put into the wells. Then, the number of neutrophils was then counted using a light microscope.

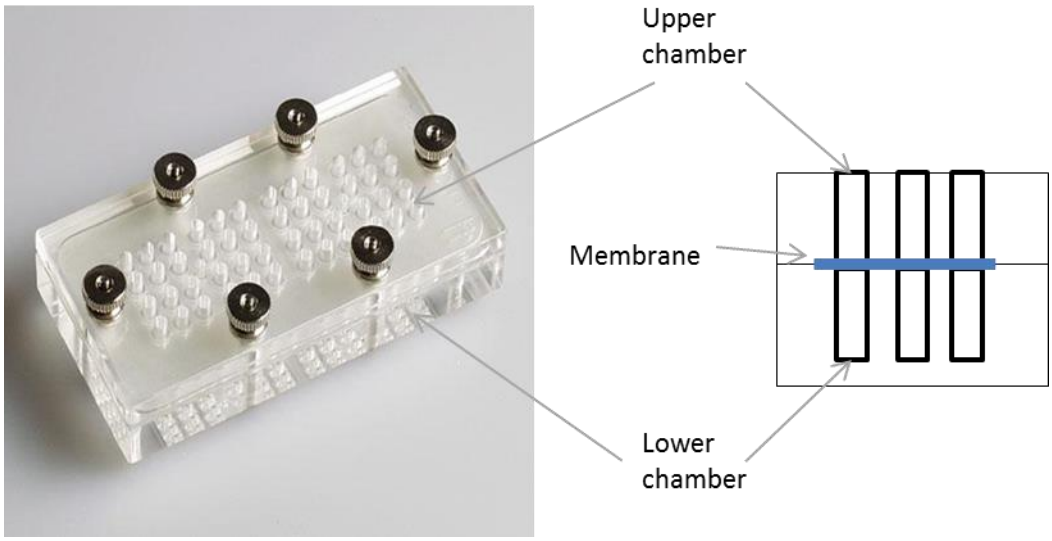

Figure 3.4: Micro Chemotaxis Chamber from Neuro Probe. The upper chamber was used for cells and the lower chamber was used for chemoattractant, between the two chambers a membrane was sandwiched for the neutrophils to traverse.

3.3 Results

3.3.1 Neutrophil cell viability

Neutrophils were routinely isolated from whole blood from healthy volunteers (methods section 2.2). In the first experiments the length of time that the cells could sustain viability outside the body was measured. It was necessary to understand the length of time that neutrophils could remain viable so that extended experiments examining the manipulation of intracellular GSH could be performed before the cells became compromised.

In the first experiments the novel Real-Time Glo (RT Glo, Promega corporation) assay was used. Real-Time Glo was used to record neutrophil cell viability in the same sample well continuously whilst inside the luminometer. This assay is adenosine triphosphate (ATP)-independent and able to identify any changes in cell viability very quickly. Isolated neutrophils were plated in RPMI medium or glucose supplemented PBS (gPBS) in a 96-well plate. The plate was then incubated in a luminometer and continuously monitored for 12 hours. The results (figure 3.5) demonstrate that neutrophils in either RPMI or gPBS lost viability after 4-5h and showed rapid decline after this time. Addition of 4-(2-hydroxyethyl)-1-piperazineethanesulfonic acid (HEPES) to maintain pH diminished this effect. Further addition of foetal bovine serum (FBS) in either RPMI or gPBS appeared to increase the viability of the cells. This, in other cell types, may indicate a growth of the cells but it was unlikely neutrophils. At the end of the 12h experiment it was observed that the liquid evaporated. This factor could have changed the mechanism of the assay. In an attempt to mitigate this effect, the experiment was repeated but with an adhesive cover with RPMI as this showed the most change over the 12h incubation. At the same time the effect of phenol red was also explored, by using a non-phenol red containing medium to compare to the RPMI originally used. Figure 3.6 shows that while the inclusion of phenol red did not alter the response of the cells in the Real Time Glo viability experiment, the restriction of evaporation by use of an adhesive lid prevented the cell death and the apparent increase in cell viability over 12h. Overall these experiments indicated that either RPMI or gPBS could be used to maintain neutrophil viability over the course of subsequent

experiments. Subsequent experiments used a simple Trypan blue exclusion count to verify neutrophil viability as the fine granularity of these experiments was not needed.

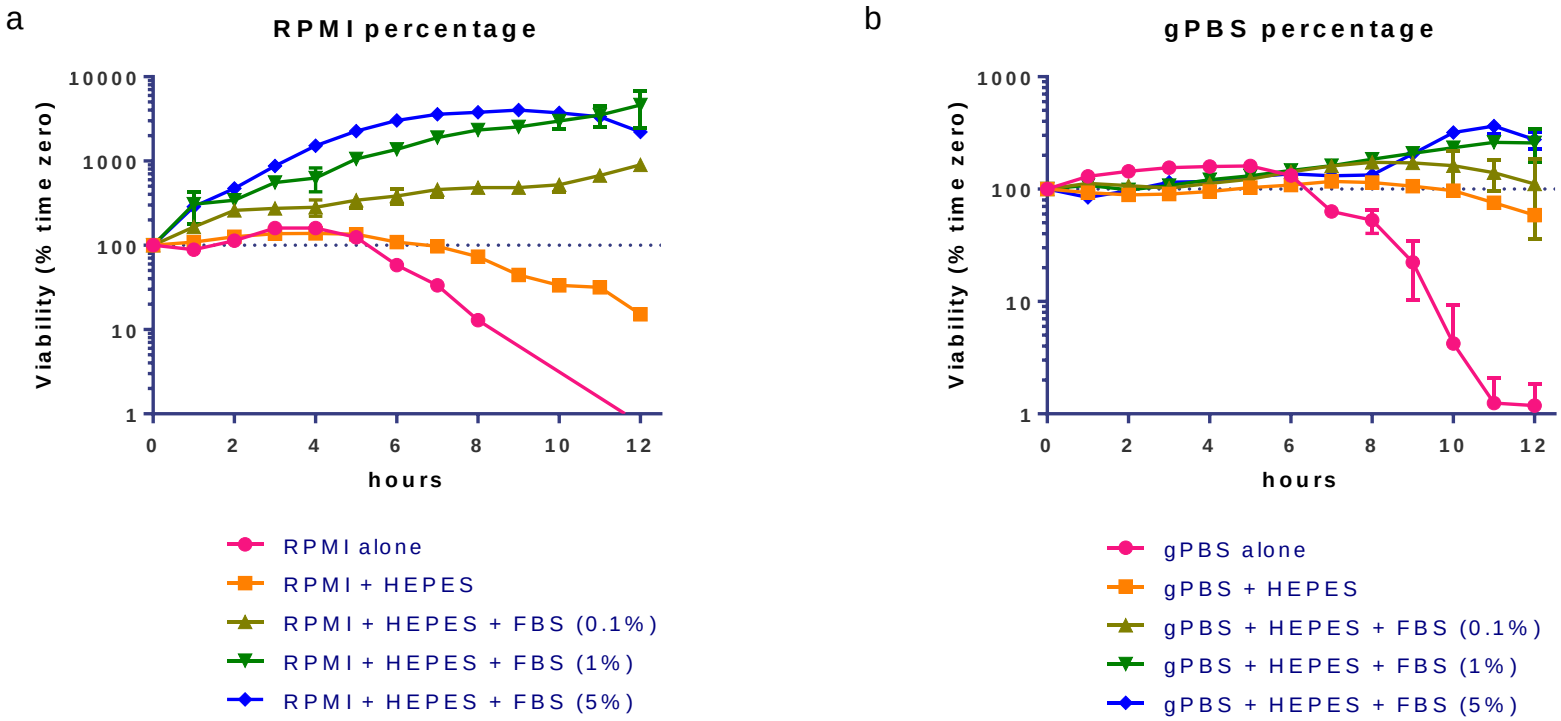

Figure 3.5: Cell viability of neutrophil cells (1 x 10^5) over 12h in either (a) RPMI (with phenol red) or (b) gPBS supplemented with HEPES and or FBS (0.1-10%). Data represented at percentage of time zero viability (mean +/- SD). Viability was measured using Real Time Glo.

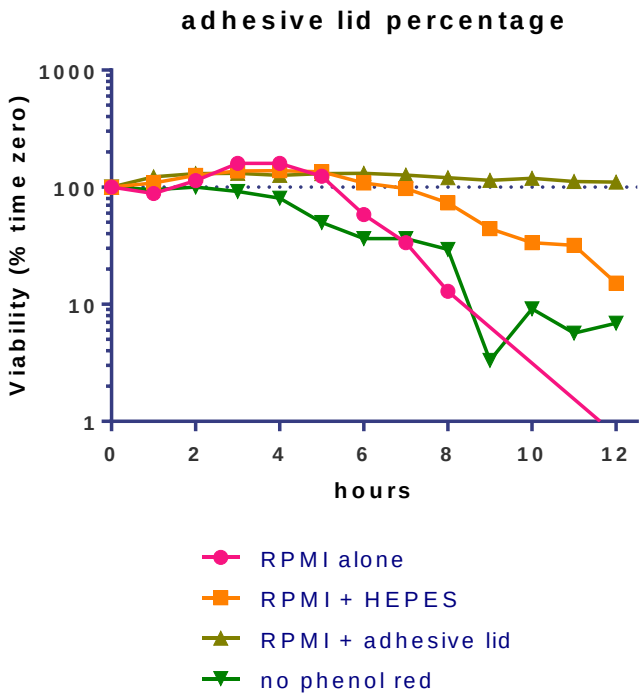

Figure 3.6: Cell viability of neutrophil cells (1 x 10^5) over 12h in RPMI (with or without phenol red) or RPMI (with phenol red) supplemented with HEPES. The experiment was either conducted with or without an adhesive lid to prevent evaporation. Data represented at percentage of time zero viability (mean +/- SD). Viability was measured using Real Time Glo.

3.3.2 Neutrophil cell chemotaxis

There are many ways to measure neutrophil chemotaxis. The purpose of this work was to assess a high throughput chemotaxis assay for the chemotactic ability of neutrophils. In this section, four different methods were used to measure chemotaxis: via video microscopy and the Insall chamber; and via three semi-high through put Boyden chamber methods.

3.3.2.1 Insall chamber analysis of chemotaxis

The Insall Chamber is a direct visualization chamber and can be used to look at neutrophils' chemotactic behaviour in video micrography. Figure 3.7 movement of all tracked cells in a spider diagram format, the cells act in their normal behaviour where they move randomly in one place: their path length is short and not in any particular direction. As for interleukin-8 (IL8) and N-formylmethionine-leucyl-phenylalanine (fMLP) chemoattractant, the neutrophils moved in a directional manner towards the chemoattractant. Neutrophils migrating towards fMLP chemoattractant had faster movement and stronger migration towards the chemoattractant, in comparison to IL8, that is they travelled further, faster. This is quantified by measurement of cell speed (average speed of a cell in any direction over the time course), velocity (average speed of a cell in its most prominent direction over the time course) and chemotactic index (directional accuracy of chemotaxis measurement, calculated as a change in the angle of a cell along the Y axis according to the cosine plot) as shown in figures 3.8. Statistical analysis by one-way ANOVA demonstrated that there was a significance difference for IL8 and fMLP compared to RPMI in terms of speed, velocity and chemotactic index. Whilst this assay provides the most information about the movement of the neutrophils it was the most laborious and difficult to examine a large number of conditions. It is gold standard but not for high throughput.

RPMI IL8 fMLP

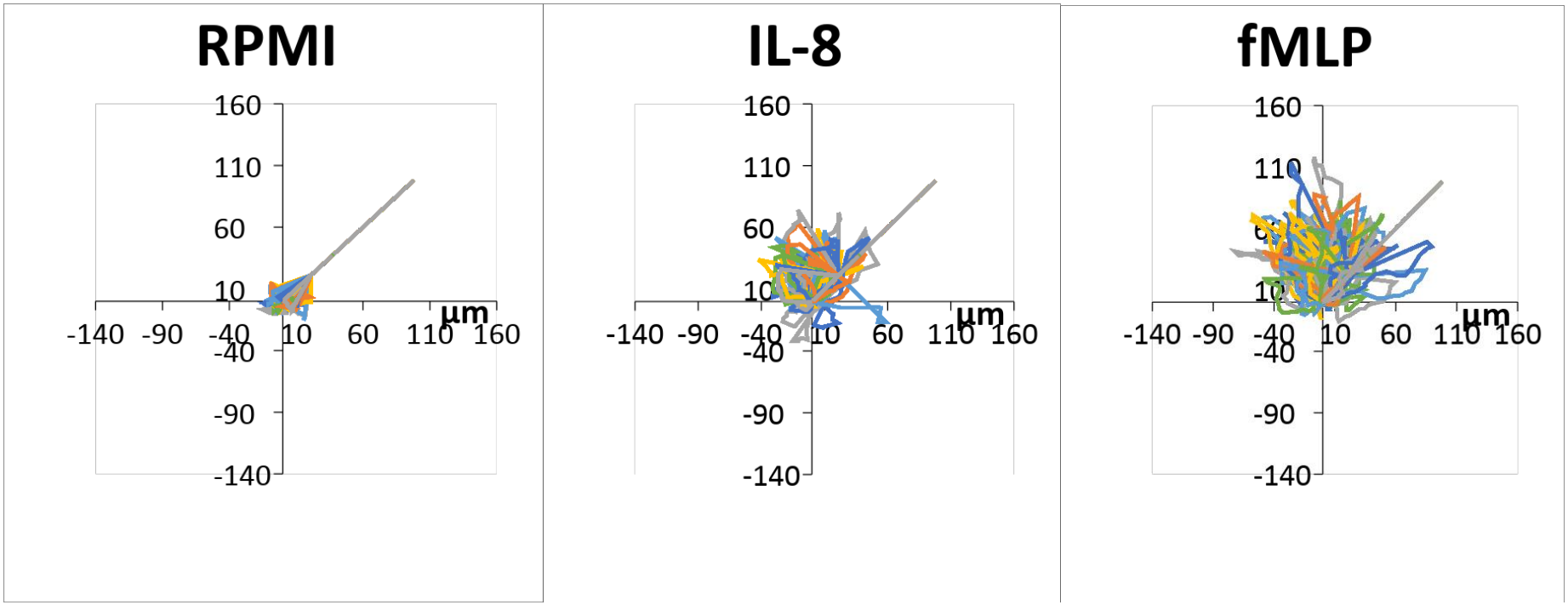

Figure 3.7: Spider diagram of chemotaxis directional movement from Insall Chamber: RPMI (control), IL8 (200ng/ml) and fMLP (10nM) (chemoattractant).

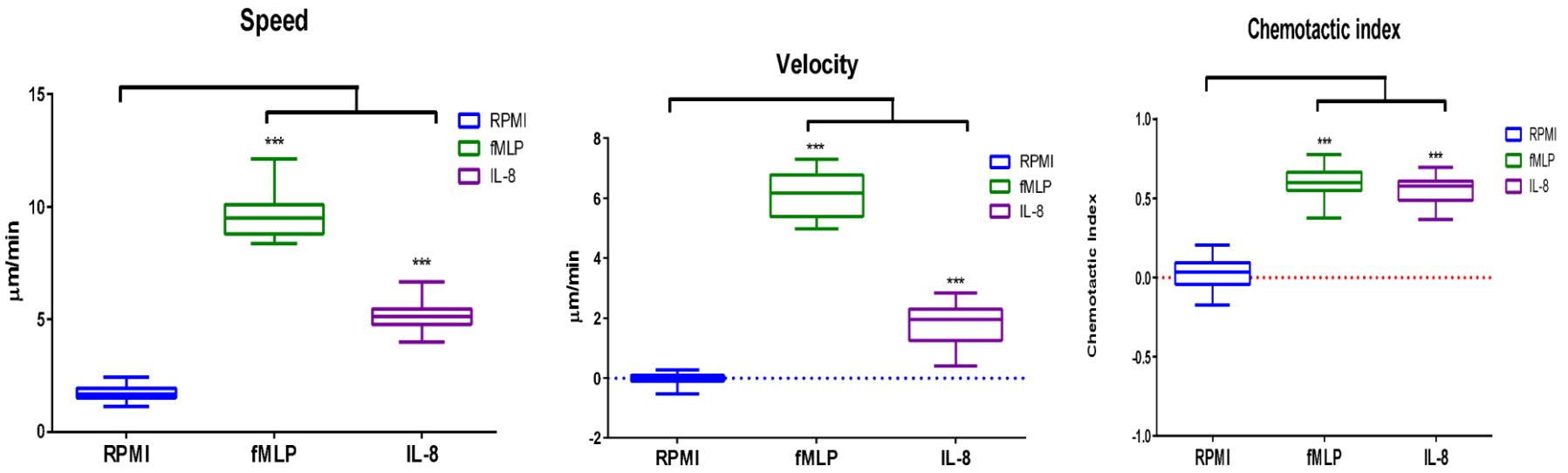

Figure 3.8: Box and whiskers graph of average speed, velocity and chemotactic index of neutrophils isolated from healthy blood volunteers (n=5). Central line represents the median, lower and upper bounds of boxes represent the 25th and 75th percentile respectively, and whiskers represent furthest reaches of the data. Statistical analysis: One-way ANOVA with Tukey's post-test. *** indicates significance difference compared to RPMI ($p<0.001$).

3.3.2.2 ChemoTx chemotaxis chamber

The first Boyden chamber tried was the ChemoTx chemotaxis chamber from Neuroprobe. This device was a made from a metal mounted filter placed above a 96 well plate. Each experimental test area was defined by hydrophobic masks to prevent cross contamination of different areas above different wells. After chemotaxis cells were counted in both the chemoattractant well beneath as well as after dislodging any cells from the membrane itself. It was found that the membrane was extremely fragile and could easily be rupture by a pipette tip. This made it extremely difficult to handle. Additionally, any movement of the filter, for example in tapping the bench to place the plate, could cause the droplet of cells in the hydrophobic area to be dislodged and flow into adjacent areas. For these reasons this chamber was not taken further for experimentation.

3.3.2.3 Micro Chemotaxis chamber

The second Boyden style chamber sued was the Micro chemotaxis chamber, also from Neuropore. This chamber had the advantage of being reusable. However, in contrast to the other chambers, it was recommended to visually count the number of transmigrated neutrophils on the underside of the membrane after use. To do this neutrophil were placed in the upper chamber and allowed to move towards the chemoattractant for 90min. Following this time, the membrane was removed, and cells were visualised by staining. An attempt was then made to count the cells using a light microscope. Figure 3.9 shows a typical membrane before and after use. Whilst the neutrophils are identifiable it was neither particularly high through put nor easy to differentiate between them and the pores in the membrane. As with the ChemoTx membrane the membrane was fragile and easily broken. Thus, this device was not taken further for evaluation.

a b

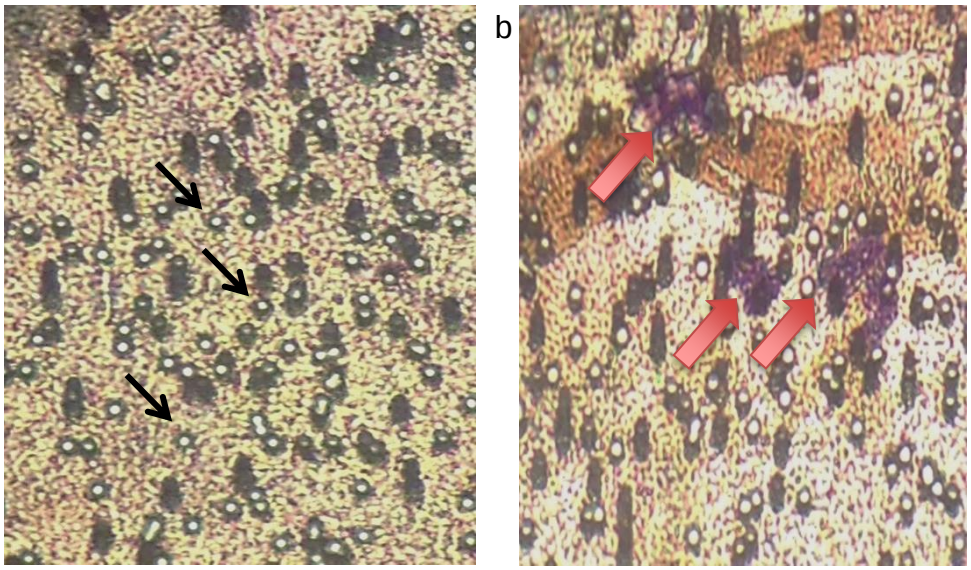

Figure 3.9: Photographs of the poly carbonate track etched (PCTE) membrane. a. shows the membrane before use, the black arrows highlight the pores; b. shows after use, the neutrophils stained purple are highlighted with red arrows.

3.3.2.4 QCM chemotaxis 3µm 96-well cell migration assay (Merck Millipore)

After finding that the ChemoTx Chamber and 48 Well Micro Chemotaxis Chamber do not work well, the QCM chemotaxis 3µm 96-well cell migration assay from Merck Millipore was tested. It was costly however it was robust, and the manufacturer's protocol gave quantifiable results. Neutrophil cells were plated in an upper chamber with attached membrane. This was then placed above a lower chemoattractant containing chamber. Cells migrating directly into the lower chamber plus cells dislodged from the lower side of the membrane were counted by fluorescent detection in a fluorimeter, after incorporation of Cyquant dye. Cyquant dye exhibits strong fluorescence when bound to DNA. Neutrophils isolated from healthy donors were used in this assay to determine if they resulting data showed similar patterns to that found with the Insall chamber. Figure 3.10 shows that neutrophils in this assay migrated towards fMLP and IL8 in a similar manner to that observed by video microscopy, that is that more cells accumulated beyond the membrane in response to fMLP than IL8 but that both chemoattractants cause greater accumulation of cells beyond the membrane compared to PBS. This suggests that the cells were migrating in the direction of the chemoattractants rather than either sedimenting or randomly moving through the membrane.

Due to the ease of use and the results appearing equivalent to the laboratory gold standard, Insall chamber chemotaxis, the QCM cell migration assay was used in subsequent chemotaxis analyses.

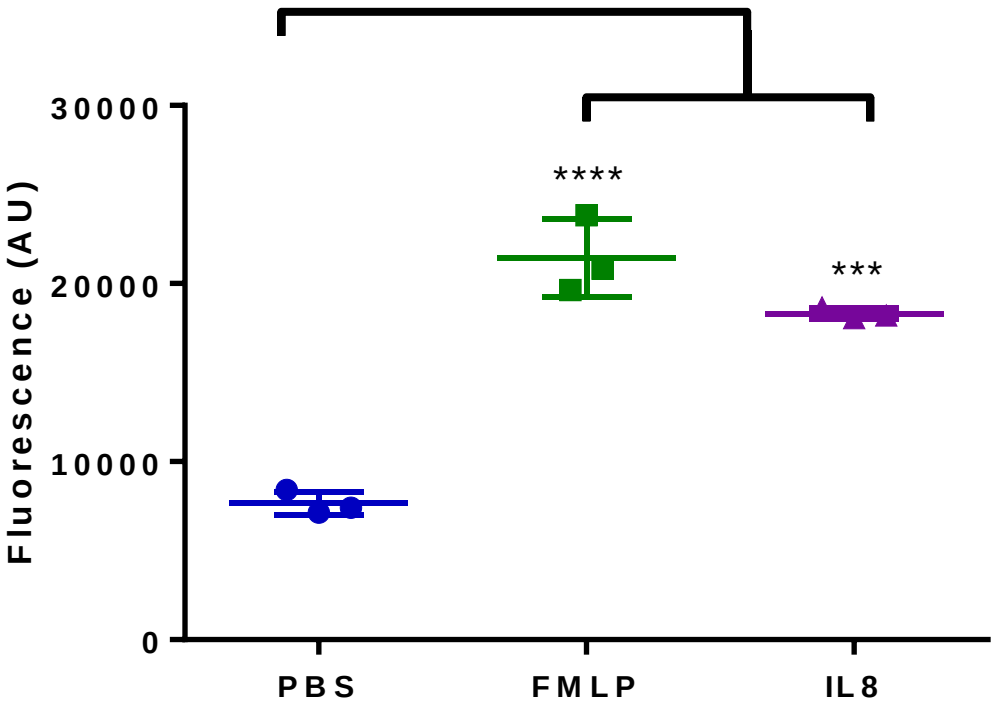

Figure 3.10: Chemotaxis of neutrophil cells towards chemoattractants fMLP (1µM) and IL8 (1µM) as assessed by the QCM chemotaxis 3µm 96-well cell migration assay. n= 3 healthy donors. Central line represents the median, lower and upper bounds of boxes represent the 25th and 75th percentile respectively, and whiskers represent furthest reaches of the data. Statistical analysis: One-way ANOVA with Tukey's post-test. **** $p<0.0001$, *** $p<0.001$ when compared to PBS.

3.3.3 Neutrophil cell glutathione

For neutrophil cell intracellular reduced and oxidised glutathione, the GSH and GSH/GSSG Glo assays were used from Promega (UK). The ratio between reduced and oxidised forms of glutathione was approximately 10:1 as expected in healthy neutrophils (figure 3.11). The assay was straight forward, and no further assays were tested for the measurement of reduced and oxidised glutathione.

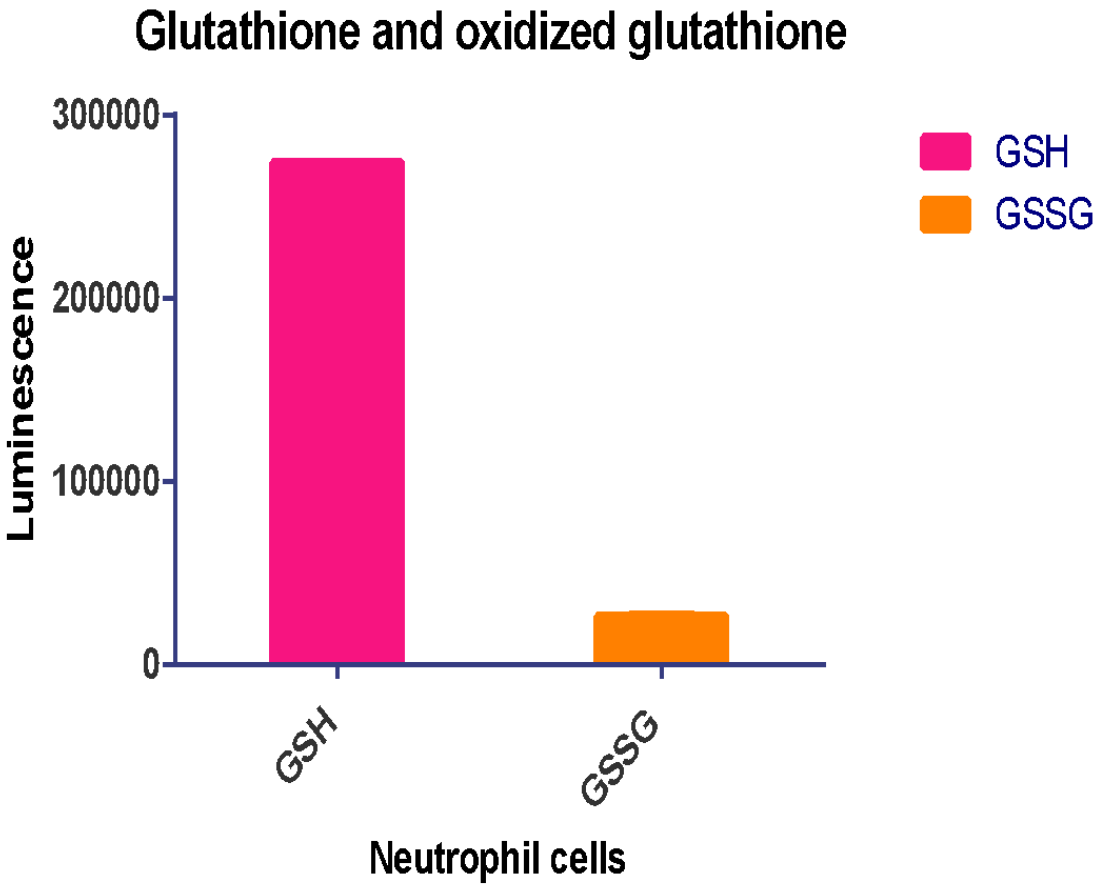

Figure 3.11: Standard graph of glutathione (GSH) and oxidised glutathione (GSSG) from healthy donors using GSH/GSSG-Glo assay. n=3

3.3.4 Effect of manipulation of intracellular glutathione on neutrophil chemotaxis

On completion of a selection of semi high throughput assays for assessment of neutrophil chemotaxis and glutathione measurement the main aim of this chapter was explored. Neutrophils were isolated from healthy volunteers and the intracellular glutathione content was altered by using glutathione modulating compounds which were BSO, BCNU and CDNB. The effect of these on chemotaxis was measured by using the QCM cell migration assay.

For neutrophils with glutathione modulating compounds, over the course of the experiment, cell viability, as measured by trypan blue exclusion, gradually declined across all treatments (figure 3.12). Additionally, no change to viability was found to be caused by the glutathione modulating compounds themselves. Therefore, the compounds do not affect the viability of neutrophils when compared to the vehicle control.

For the glutathione modulating compounds, it was found that CDNB, a depleter of glutathione through thioester conjugation, and BCNU, an inhibitor of glutathione reductase as well as BSO, an inhibitor of rate limiting gamma-glutathione cysteine synthetase all decreased both neutrophil intracellular gluthathione compared to PBS (figure 3.13) and chemotaxis relative to PBS treated cells responding to both fMLP and IL8 in figure 3.14. However, NAC did not appear to have an effect on glutathione levels but did appear to decrease the amount of chemotaxing cells.

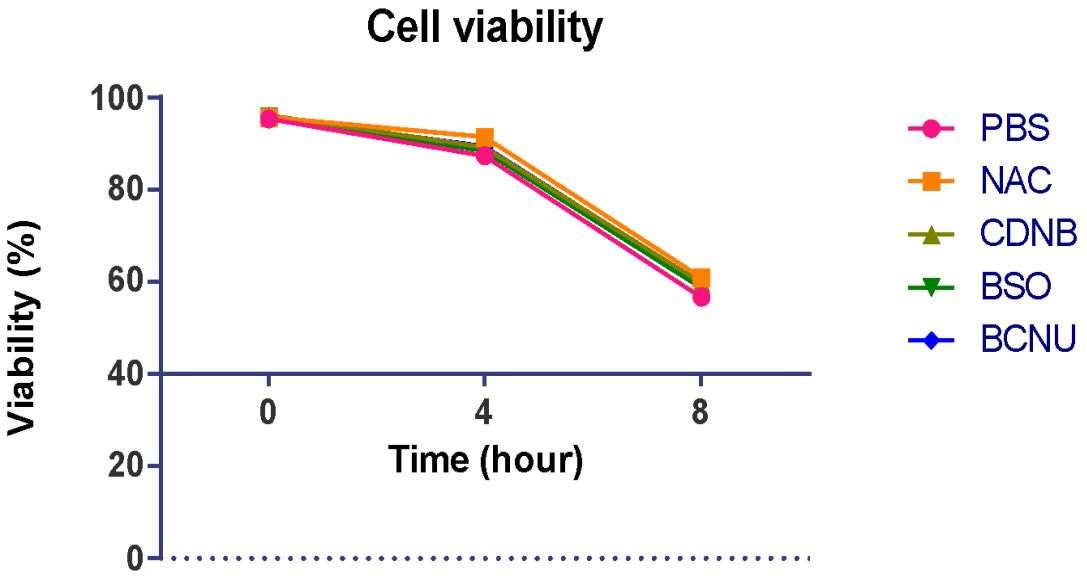

Figure 3.12: Neutrophil cell viability change with glutathione modulating compounds (GSH) compounds. Isolated neutrophils were incubated with BSO (10µM), NAC (5mM), BCNU (5µM) or CDNB (10µM) for 4 or 8h prior to determination of cell viability by trypan blue exclusion. n=4, mean and standard deviation shown.

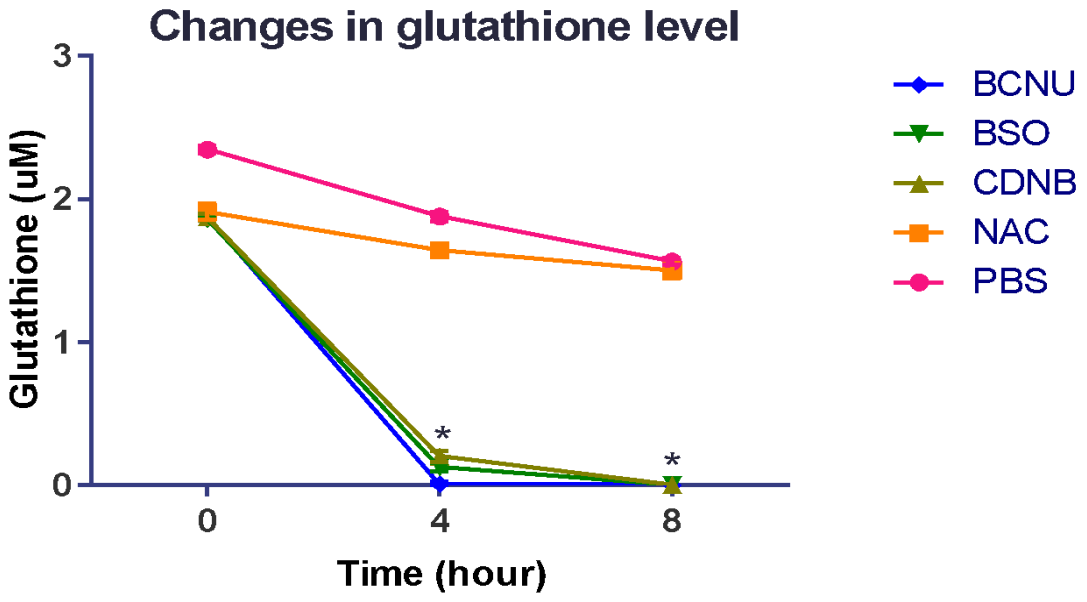

Figure 3.13: Changes in glutathione (GSH) levels of neutrophil cells with glutathione modulating compounds: BSO (10µM), NAC (5mM), BCNU (5µM) and CDNB (10µM) from GSH-Glo glutathione assay. * $p<0.0001$, comparisons are to PBS treatment for each time point. n=4, mean and standard deviation shown.

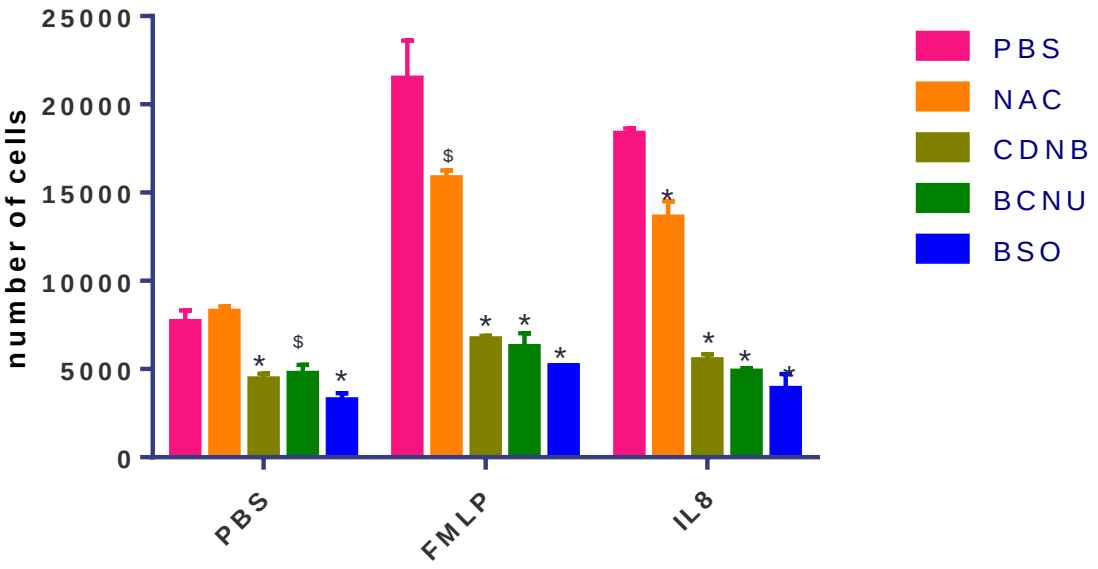

Figure 3.14: Neutrophil cell chemotaxis with glutathione modulating compounds (GSH) compounds. Isolated neutrophils were incubated with BSO (10µM), NAC (5mM), BCNU (5µM) or CDNB (10µM) for 4 h prior to distribution in to 96 well QCM migration assay plate. Cells $1x10^5$ per ml were then allowed to respond to chemoattractants FMLP (1uM) or IL-8 (1uM) for a further 4h before measurement of the number of cells that had migrated. Data are represented as mean +/- standard deviation (n= 4 donors). Significance was measured by One-way ANOVA with Tukey's post-test * $p<0.0001$, $ $p<0.001$ (comparisons are to PBS treatment for each chemoattractant). See section 2.4.2 for methods.

3.4 Discussion

The ultimate aim of the work presented in this chapter was to be able to modulate the intracellular glutathione of neutrophils isolated from healthy donors. To do this the neutrophils would need to be exposed to compounds that could alter the intracellular glutathione. This first incubation would take 4h and then the setup of the chemotaxis would take up to another 4h. Thus, it was vital to understand if neutrophils could survive for this length of time. A new assay was tested as it could monitor in real time the viability of neutrophils over a long period of time. This assay, Real Time Glo from Promega, was set up with a number of conditions. The assay mechanism is based upon the provision of a proprietary luciferase reagent that is cell permeant. This reagent enters viably cells where it is reduced and can then diffuse out of the cell again. The reduced version is then a substrate for extracellular luciferase which catalyses the production of light which can be detected by a luminometer.

Once the initial teething issues of evaporation were sorted out it was possible to assess the use of different additives to either a rich medium such as RPMI or minimal medium such as gPBS could aid in neutrophil viability. It was found that RPMI alone would sustain the cells if evaporation was limited. Various concentrations of foetal bovine serum (FBS) were added to the cell culture medium because FBS can enhance length of survival and contains a high content of growth promoting factors. Additionally, HEPES was added as a buffering agent as the incubation was without carbon dioxide (CO_2). Thus, in subsequent experiments the cells were maintained in RPMI during incubation. Additionally, subsequent assays used Trypan blue exclusion for analysis of cell viability as this was quicker and cheaper long term.

The first chemotaxis assay tested was the ChemoTx chemotaxis chamber from Neuroprobe. This assay has been successfully utilised by, for example, Williams et al., (2017) and Simard (2009). However, here this membrane was found to be very fragile and difficult to handle, it was not even possible to generate any robust data. The second assay tested was the Micro chemotaxis chamber, also from Neuroprobe. This was a reusable chamber that had wells into which neutrophil suspension could be pipetted. This made for a much more stable system, though the membrane was still fragile. This system was developed in 1980 (Falk et al., 1980) and has been used

previously for neutrophil migration studies (Barber et al., 1999). The tricky aspect with this assay was the visualisation of the neutrophils on the membrane. The membrane contained many track etched pores which were easier to visualise then the migrated neutrophils themselves. Whist either of these two approaches might have benefited from further fine tuning, the availability of third chamber was tested at the same time to isolate a more robust assay. This final assay was the QCM assay from Merck Millipore, which had also been previously reported for use with chicken heterophils (Larson 2008). This assay incorporated the robust nature of the wells above the membrane and an integrated membrane to the upper wells. This made for much easier handling. Additionally, the manufacturer's protocol suggested the use of a DNA binding fluorescent dye that allowed for rapid quantitation of the migrating cells. Comparison of migration of human neutrophils towards fMLP or IL8 demonstrated similar patterns to those seen in the Insall chamber. Thus, this assay was chosen for subsequent analysis of neutrophil chemotaxis.

In this study, one of the aims was to perturb the redox balance with glutathione modulating compounds to alter the glutathione level and determine if this perturbed the chemotactic ability of neutrophils. In a study by Harlan et al. (1984), the glutathione redox cycle was perturbed at several points using BCNU, CDNB and BSO. Therefore, the same glutathione modulating compounds used in this study with the addition of NAC as a method to potentially increase glutathione concentrations as well.

Across the length of the experiment the treatment of the neutrophils did not appear to alter cell viability as measured by trypan blue exclusion. The use of this reagent not only was rapid and in expensive but also allowed for analysis without the complication of trying to understand the interaction of the modulating compounds with the enzyme systems in the RT Glo assay.

The compounds altered the glutathione level: BCNU, CDNB or BSO decreased the glutathione level, meanwhile, NAC maintained the glutathione level. NAC delivers cysteine to the cells, but also work as an antioxidant itself. The maintenance of cell viability when intracellular GSH appeared to plummet is of interest. Decreased of GSH is an early event of cell death progression (Henze et al., 2000, Franco and Cidlowski 2009, Chiang et al., 2011). GSH depletion occurs before rupture of plasma membrane or cellular fragmentation in apoptosis (Franco and Cidlowski 2012).

Finally, it was possible to assess the effect of altering intracellular glutathione concentration on neutrophil migration or chemotaxis. Previously this could be inferred from the analysis by Dias et al., (2013) and of Roberts et al., (2015) who separately measured each activity on neutrophils isolated from patients with periodontitis. Data presented here (figure 3.13 and 3.14) demonstrates that a decrease in glutathione causes a decrease in chemotaxis in neutrophils isolated form health donors. Chemotaxis is a highly regulated and complex set of events that involve the detection of a chemoattractant, mobilisation of the intracellular cytoskeleton and the movement of the whole cell through interaction with the extracellular matrix. One key player in the cytoskeleton is the protein actin which forms rod like structures to propel forward the cell body. It exists in two states: either free actin so called G-actin or globular actin or actin in a filament structure so called F-actin or filamentous actin. It has previously been reported that changes to G-actin, such as protein glutathionylation, can prevent it from forming F-actin (Dalle-Donne et al., 2003; Lassing et al., 2007; Shelton et al., 2005; Wang et al., 2001). Protein glutathionylation is a post translational modification that occurs within cells to protect thiol active cysteines. Their formation may be reverted at the expense of glutathione. The decrease in glutathione within the neutrophils may have prevented this. Alternatively, chemotaxis requires the production of limited quantities of hydrogen peroxide (Ball et al., 2017) which also need to be controlled by redox regulation and buffering by glutathione. Decreases in available glutathione may prevent many cellular processes including chemotaxis. Interestingly hydrogen peroxide may also serve as a chemoattractant (Klyubin et al., 1996, Yoo et al., 2011). In the results of the NAC it was seen that this compound also decreased the amount of chemotaxis. It may be that the antioxidant nature of this compound decreased any extracellular hydrogen peroxide preventing key signalling events at the leading edge and decreased the chemotactic abilities of the neutrophils.

3.5 Conclusion

When the redox balance was perturbed with glutathione modulating compounds, the glutathione antioxidant was decreased as well as the chemotactic ability of neutrophils decreased in healthy volunteers. It can be concluded that BCNU, CDNB or BSO decreased intracellular glutathione in primary neutrophils. BCNU, CDNB or BSO decreased chemotaxis of primary neutrophils towards fMLP and IL8 chemoattractants.

CHAPTER 4 – Optimisation of neutrophil sample preparation and separation for proteomics and detection of glutathionylated proteins

CHAPTER 4

Optimisation of neutrophil sample preparation and separation for proteomics and detection of glutathionylated proteins

4.1 Introduction

To maximise the output from mass spectrometry based proteomics it is important to decrease sample complexity as it flows into the mass spectrometer. This improves the value of peptide identification in the mass spectrometer: this is due to the selection of the top 10-20 peptides in each ion packet isolated for fragmentation. If more than this number of peptides is present, then the lower abundance peptides will not be fragmented and hence not identified later in the work flow. By using two dimensional techniques, such as two dimensional chromatography, an increase the number of peptides and ultimately proteins has been demonstrated (eg Batth et al 2014). Similarly, by targeting or isolating peptides with a desired characteristic, eg post translational modification, then the identification of these peptides can also be improved. The data presented in this chapter explores the identification of the best methods to isolate proteins from neutrophils and to separate them by two dimensional chromatography, and additionally to isolate glutathionylated proteins for identification.

For the development of two dimensional chromatography two different methods were compared in the first dimension: strong cation exchange chromatography (SCX), which had been established in the laboratory for a long time; and high pH reverse phase chromatography (C18) which was developed in the lab following a publication by another group at the beginning of these studies (Batth et al., 2014). One potential advantage of the C18 column was that the buffers used might decrease the amount of sample clean up required, and hence decrease sample loss in multiple stages. For both the second dimension was the C18 reverse phase column attached to the mass spectrometer. For the detection of glutathionylated proteins an antibody based detection via Western blotting was developed.

Proteomics information can provide proteins that are expressed from neutrophils in either healthy people or periodontitis patients. Use of proteomic methods allows for various approach to understand and explore the role proteins play in neutrophil cells. Neutrophil primary granules can be found in granulocytes which contain myeloperoxidase, acid hydrolases and defensins. Myeloperoxidase (MPO) is a microbial enzyme which produces hyperchlorous acid from hydrogen peroxide and chloride ions (Hughes et al., 2003). Proteolytic and bactericidal proteins are stored by azurophilic granules (Borregaard et al., 1993). The shape of these granules is described as spherical or football shaped. Secretory vesicles are rich in receptors. Many neutrophil functions are regulated such as adhesion, phagocytosis, killing of bacteria and interaction with endothelial cells during exocytosis of cytoplasmic granules from early activation to the destruction of phagocytosed microorganisms.

4.2 Materials and methods

An overview of the workflows used in this chapter are shown in figure 4.1. In HPLC, strong cation exchange column (SCX) and High-pH reverse phase column (C18) were used. The SCX column separates peptides from negative to positive charge ions. Meanwhile, the C18 column separates peptides from hydrophilic to hydrophobic phase. Liquid chromatography-tandem mass spectrometry (LC-MS/MS) was used to identify a total protein profile from neutrophil cells.

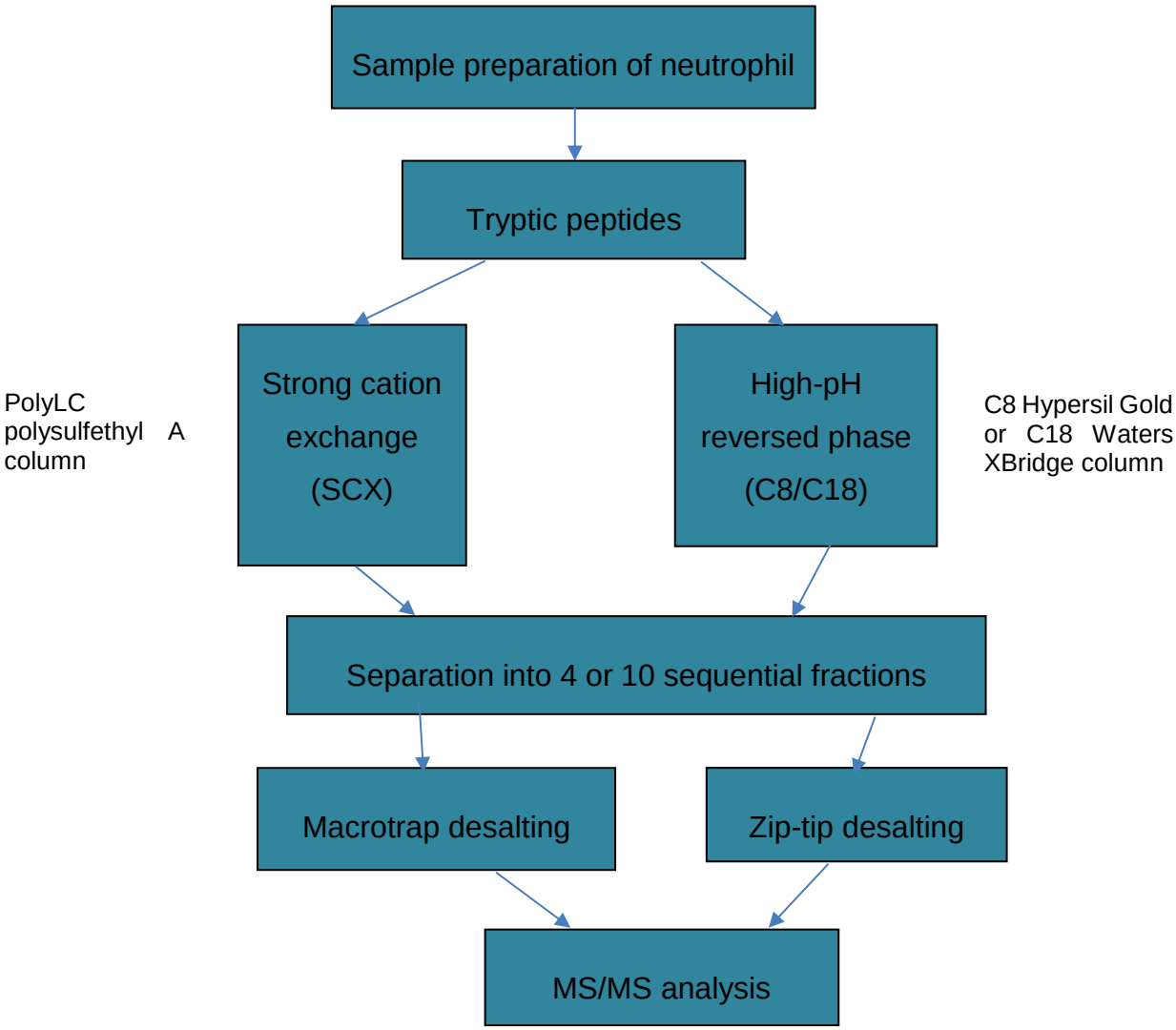

Figure 4.1: Proteomics workflow for detection of whole proteins and glutathionylated proteins in neutrophil cells.

4.2.1 Neutrophil lysis buffer

Various of neutrophil lysis buffer were used to lyse cells which are;

1. 10% SDS with 100 mM TEAB with protease inhibitor (protease mini, Roche)

2. Radioimmunoprecipitation assay buffer (RIPA buffer) with protease inhibitor (protease mini, Roche)

3. M-PER mammalian protein extraction reagent (M-PER buffer) with protease inhibitor (protease mini, Roche)

4. Laemlli buffer

Isolated neutrophils (1 x 10^5 cell per ml) were lysed in any of the buffers described above. For buffers 1-3 the cell suspension was then sonicated (10s, 5Hz) on ice. Any cell debris was pellet by centrifugation (1min, 4000g). Protein content was measured and 20µg was then prepared with Laemlli buffer. For samples prepared directly in Laemlli buffer isolated neutrophils (1 x 10^5 cells) were lysed directly in Laemlli buffer. Samples in Laemlli buffer were heated at 95°C for 5min.

20µl prepared neutrophil protein (from methods 1-4) was loaded onto a 12% sodium dodecyl sulphate polyacrylamide gel electrophoresis (SDS-PAGE) gel (Bio-Rad) and electrophoresed at 150V for approximately 90min until the dye front reached the bottom of the gel. . Then, Coomassie blue protein stain (refer methods section 2.15.3) was used to stain the proteins and allow bands to be viewed directly in the gel.

4.2.2 Strong Cation Exchange (SCX) column fractionation

The method was based on Batth et al 2014. Briefly:

The SCX chromatography was done on a polysulfethyl A column (100 mm ×2.1 mm, 5 µm particle size. PolyLC, Columbia, MD) with a javelin guard cartridge (10 mm × 2.1 mm, 5 µm particle size, 200 Åpore size. PolyLC, Columbia, MD). Two mobile phase buffers (A and B) were prepared. Buffer A: potassium dihydrogen orthophosphate (10 mM, pH 3) salt was dissolved in water and 20% ACN added. For buffer B: potassium

dihydrogen orthophosphate (10 mM) and potassium chloride (500 mM, pH 3) was dissolved in water and 20% ACN was added. The flow rate was set at 0.2ml/minutes to accommodate pressure for the system below 20MPa. Gradient for liquid chromatography ran from 0 % mobile phase B for 15min, 0-70% B over 65min, 70-100% B over 20min. The column was washed and re-equilibrated in buffer A over 10min.

4.2.3 High pH Reverse Phase (HpH) Fractionation

In this study, HpH was done on either a XBridge Shield RP18 (5µm particle size, 2.1 mm internal diameter x 100 mm long column, Waters, UK) or a Hypersil Gold C8 column (5µm particle size, 2.1 mm internal diameter x 50 mm long column, Thermo Fisher, UK) on the ETTAN LC system, a HPLC operating system at 500 mL/min for peptide separation. 100µl of sample was injected on to the column in each experiment. For experiments, buffer A consisted of 1000mL of water added with 10mM ammonium hydroxide and buffer B consisted of 90% acetonitrile in with 10mM ammonium hydroxide. Both buffers were adjusted to pH 10 with ammonium hydroxide. All of the peptide fractions were collected using a collector (fraction collector F9-R) at 2 min intervals. Samples were loaded onto the column at 500 mL/min for 2min after the fractionation gradient commenced as follows: 1% to 25% B in 50 min, 60% B in 4 min, and ramped to 70% B in 2 min. At this point, fraction collection was halted, and the gradient was held at 70% B for 5 min before being ramped back to 1% B, during which time the column was washed and re-equilibrated. The number of fractions that were concatenated was set to 10 fractions and 4 fractions throughout the experiment. Prior to concatenation, ammonium hydroxide was evaporated in a Speed Vacuum operating at 45°C.

Column storage

All columns were washed and equilibrated into 100 % acetonitrile and were stored at 2-4°C.

4.3 Results

4.3.1 Lysis of neutrophil cell

In previous studies, various methods have been used to lyse cells: here four methods were compared. The lysis buffers used were: 10% SDS with 100 mM TEAB with protease inhibitor; radioimmunoprecipitation assay buffer (RIPA buffer) with protease inhibitor; M-PER mammalian protein extraction reagent (M-PER buffer) with protease inhibitor; and Laemlli buffer without protease inhibitor (reference methods section 4.2.1). From the Coomassie protein stain in figure 4.2, neutrophil cells in all three lysis buffers showed a ladder of protein bands between predominantly between 70 kDa to 40 kDa. Meanwhile, the proteins prepared directly in Laemlli buffer appear to show a different pattern: the predominant bands between 70-40kDa are absent and there appear to be a larger quantity of low molecular weight protein bands; there appear to be more higher molecular weight bands.

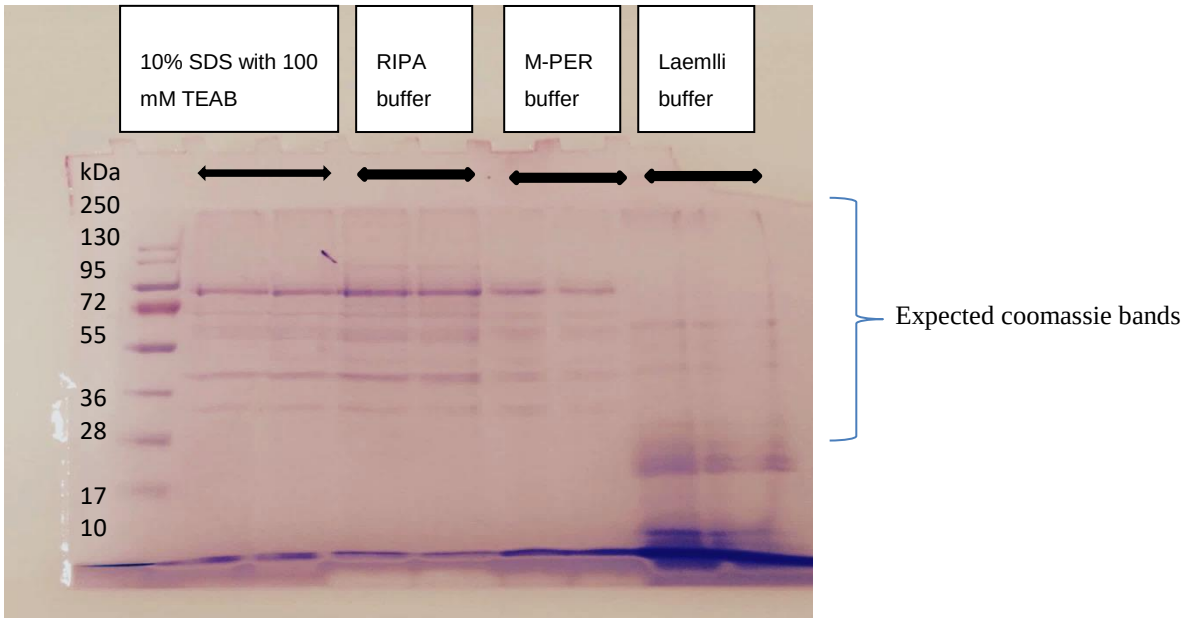

Figure 4.2: Representative SDS-PAGE gel of coomassie blue protein stain for neutrophil cells in four different lysis buffer: 10% SDS with 100 mM TEAB with protease inhibitor, RIPA buffer with protease inhibitor, M-PER buffer with protease inhibitor and Laemlli buffer without protease inhibitor. (see general methodology section 2.15 for western blot protocol).

4.3.2 High performance liquid chromatography (HPLC)

To start with investigating the efficacy of the different types of chromatography that could be used a BSA digest was prepared as this was rapid, inexpensive and did not require donation of neutrophils. Although a relatively simple mixture, in comparison to a digest prepared from a complex mixture of proteins, this was able to show a range of results for the three columns. Representative chromatograms from the separation of BSA digests on the three columns are shown in figure 4.3, 4.4 and 4.5. Table 4.1 shows the number of proteins detected for digested neutrophil extracts without fractionation and after separation by SCX of HpH reverse phase columns.

	Neutrophil without fractionation	Number of fractions	SCX	C8 Hypersil	C18 Waters XBridge
Number of protein fractions	120+/-18 (n=3)	4	86+/-13 (n=3)	44+/-4 (n=3)	183 +/- 20(n=3)
Number of protein fractions		10	244+/-55 (n=3)	200+/-115 (n=3)	484 +/- 25(n=3)

Table 4.1: Number of proteins detected from a digest prepared from neutrophil cell extracts either without fractionation or with fractionation by three chromatography set ups. Total numbers of proteins identified by using either 4 or 10 concatenated fractions form these separations are also shown. Number of proteins detected by mass spectrometry after separation by SCX, C8 and C18 columns shown as mean +/- SD.

A

B

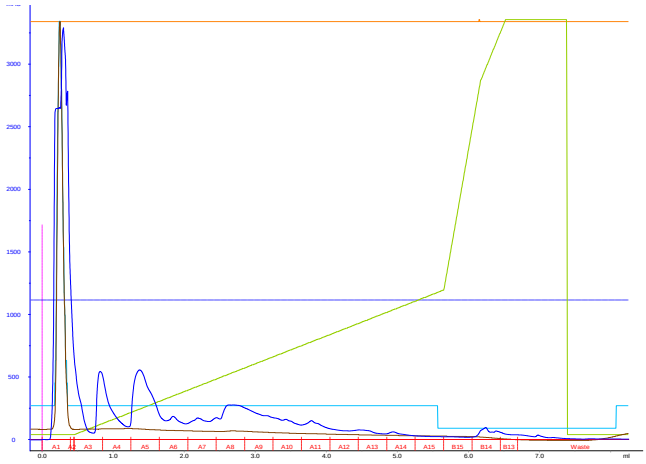

C

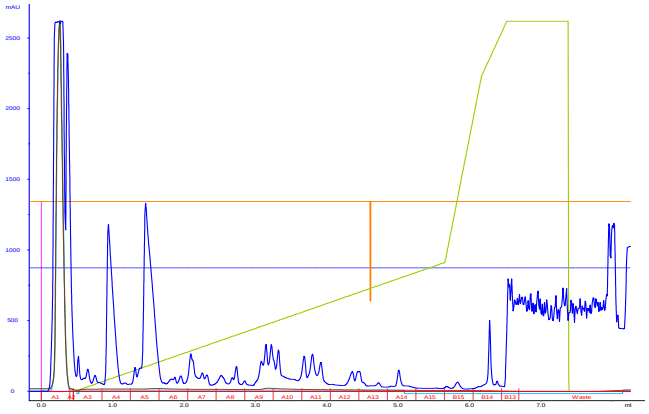

Figure 4.3: Representative separation of digested BSA on A, strong cation exchange (SCX) polyLC polysulfethyl column, B High-pH reverse phase (C8) Hypersil Gold column and C High-pH reverse phase (C18) Waters XBridge column. 22 fractions were collected from each separation. Pink represents injection, continuous blue line shows peptide profile, green line shows gradient B concentration.

4.3.3 Coverage and peptide spectrum matches (PSM's) in neutrophil separations

The data obtained from the separation of neutrophil digests was examined for protein coverage and numbers of peptide spectral matches (PSMs) to ascertain further information about the proteins detected. Coverage is the percentage of the protein sequence covered by identified peptides. Proteins coverage depends on factors such as protein size and abundance. The number of PSMs is the total number of identified peptide spectra matched for the protein and included multiple identifications of the same peptide sequence so gives a qualitative indication of the abundance of the protein.

Coverage of proteins extracted from neutrophil cells and separated by either SCX or C18 HpH reverse phase in the first dimension are shown in figure 4.4. Percentage of protein coverage for neutrophil cells on both columns are similar in terms of coverage. A higher coverage may be of use when trying to gain deeper insights into the proteome for not merely detection of proteins but analysis of isoforms or splice variants. As the latter was not a major focus of this thesis the coverage was adequate for the aims presented here.

The number of PSMs per protein discovered in digested neutrophil extracts, separated by either SCX or C18 HpH reverse phase in the first dimension, are shown in figure 4.5. It can be seen that the number of PSMs detected per protein increases with greater fractions and with the use of the HpH reverse phase strategy.

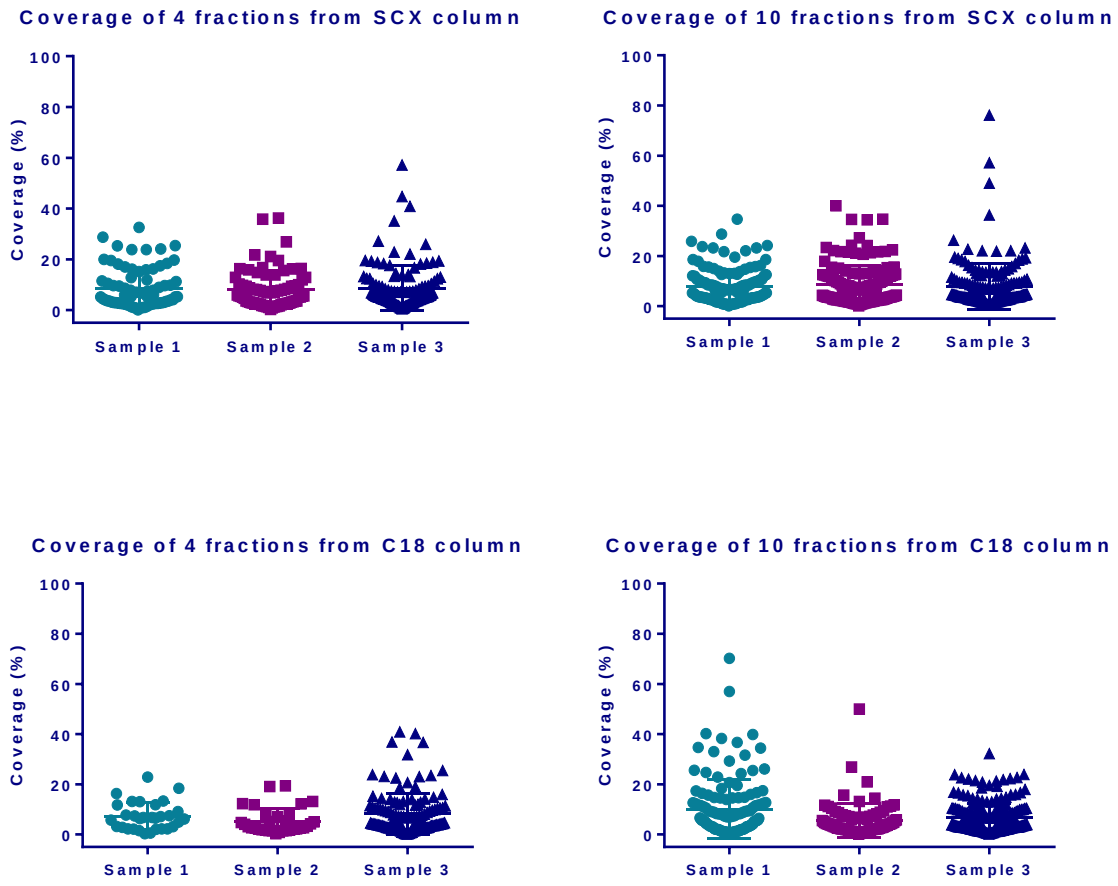

Figure 4.4: Protein coverage of fractions collected after separation of neutrophil samples separated by either SCX or HpH C18 column in the first dimension. n=3 neutrophil donors.

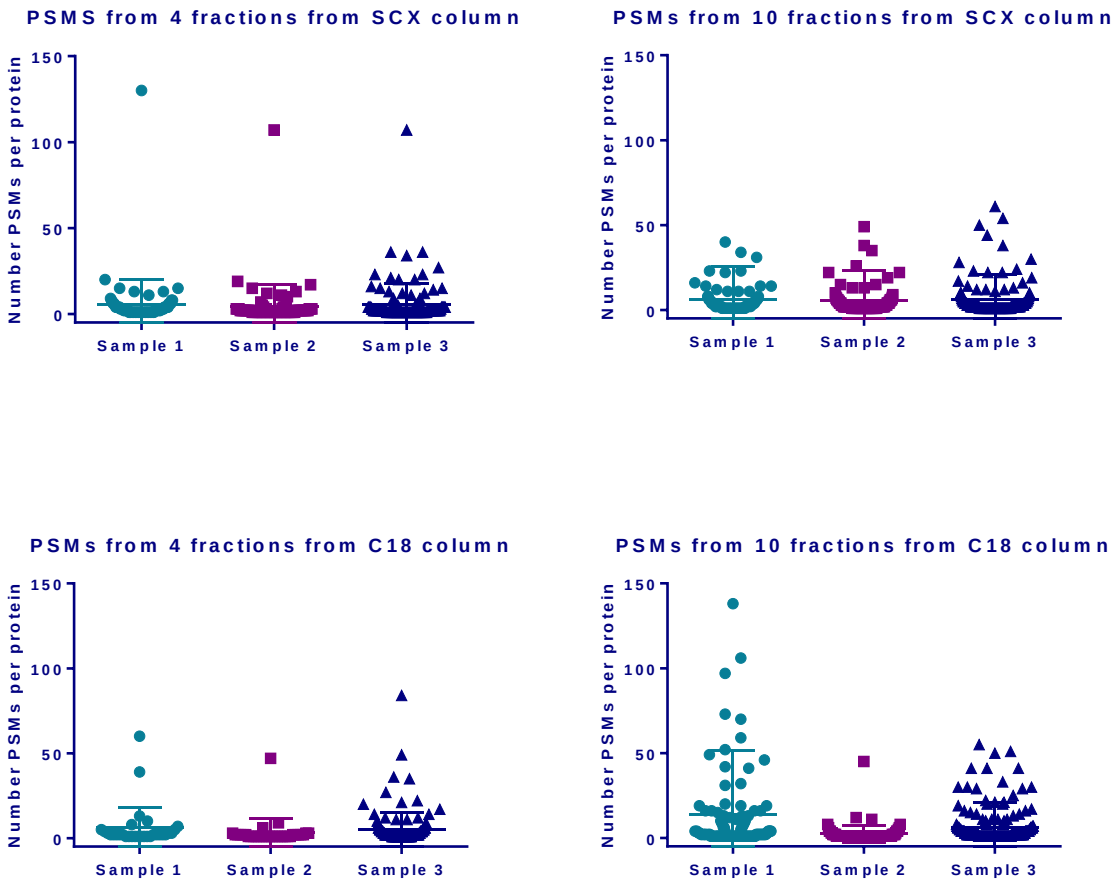

Figure 4.5: Number of PSMs detected per protein from detected in fractions collected after separation of neutrophil samples separated by either SCX or HpH C18 column in the first dimension. n=3 neutrophil donors.

4.3.4 Protein class in neutrophil separations

Exploration of the proteins detected revealed proteins expected to be of neutrophil or cellular origin eg actin, but also proteins indicative of the matrix from which they were isolated: blood. The most abundant contaminating protein was haemoglobin. Whilst red blood cells are lysed on purpose during the neutrophil isolation procedure to allow for their removal haemoglobin was a persistent contaminant. Its presence however can be excluded by filtering and identification as a contaminant in Proteome Discoverer. However, if present in high quantities it would decrease the opportunity to detect less abundant proteins. Thus, cell washing was done meticulously during neutrophil isolation.

The detected proteins by either chromatography method were analysed by bioinformatics tool Panther to understand if there was any difference in the protein function, or class. The analysis, shown in figure 4.6, demonstrated that it appeared that similar protein classes were returned for either separation type, suggesting that similar proteins were being detected. The Venn diagram in figure 4.7 analysed by bioinformatics tool Venny 2.1 shown that there are similar proteins detected in both chromatography method. (For the list of proteins detected by SCX and C18, refer to appendix 8.1 and 8.2)

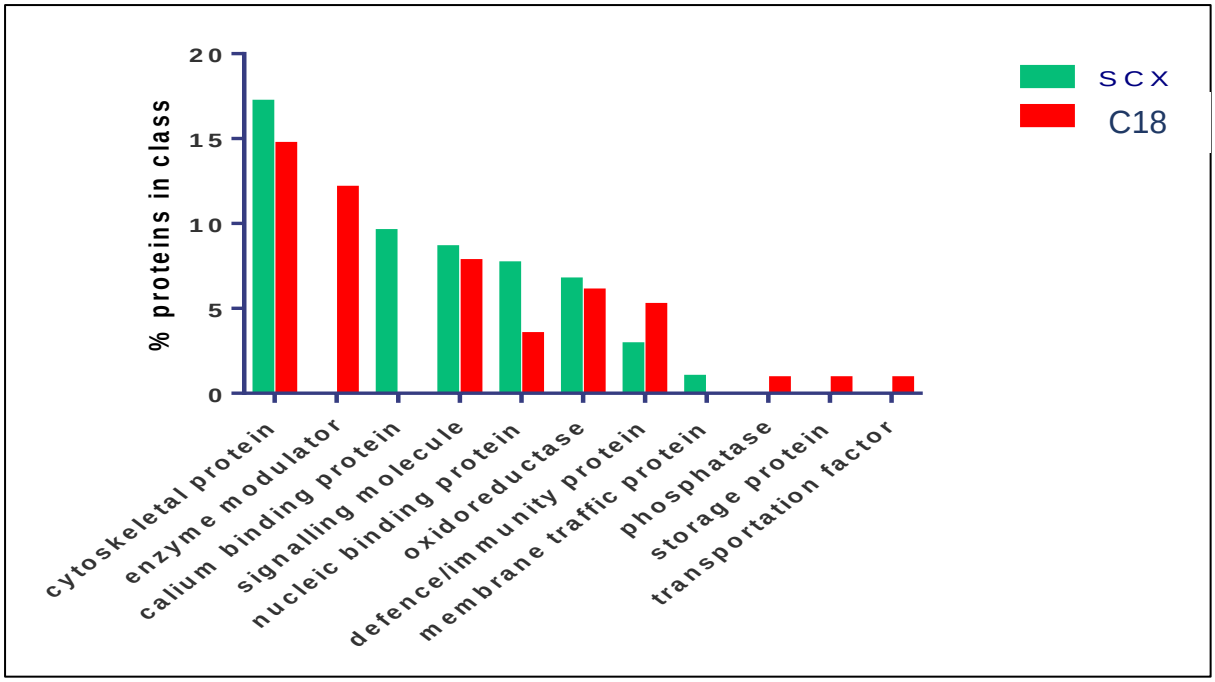

Figure 4.6: Percentage of proteins binned into different protein classes by Panther for neutrophil cell protein extracts separated by either SCX or HpH C18 chromatography.

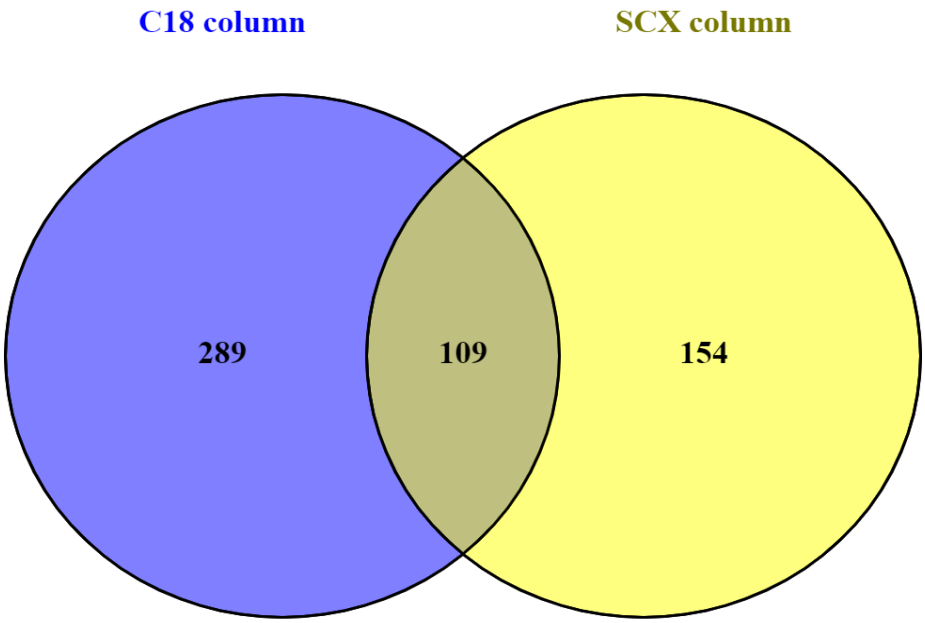

Figure 4.7: Numbers of similar proteins detected by Venny 2.1 for neutrophil cell protein extracts separated by either SCX or HpH C18 chromatography.

4.3.5 Detection of glutathionylated proteins via Western blotting

To stimulate the chemotactic phenotype of neutrophils, cells were stimulated with fMLP (10nM) or IL8 (200ng/ml) for up to 60min. Examination of Coomassie stained gels of stimulated cells (figure 4.8) showed that there was a remarkable difference in the protein profile between FMLP and IL8 stimulated cells. The approximately 72kDa highly abundant proteins was excised from the gels and trypsin digested. Analysis by LC-MS/MS identified the protein as myeloperoxidase (MPO). MPO is a primary or azurophilic granule protein. Primary granules are exocytosed rapidly in response to stimuli and from these results the strength of fMLP stimulation is re-iterated.

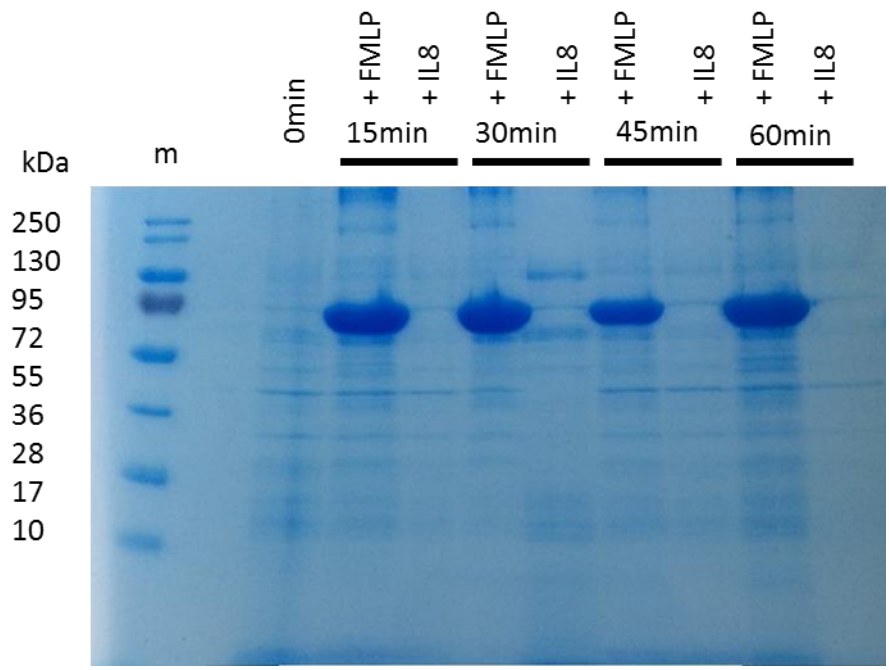

Figure 4.8: Coomassie stained SDS-PAGE gel showing separation of neutrophil extracts. Cells were stimulated with either IL8 or fMLP for up to 60min. ‘m’ represents the molecular weight markers. (see general methodology section 2.15.3 for Coomassie blue staining protocol).

In preliminary experiments to detect glutathionylated proteins or actin neutrophil extracts from three separate donors were used with an antibody against glutathionylated proteins (PSSG) and then the same membranes were stripped and reprobed with an antibody against actin. The output of these experiments is seen in figure 4.9. In two of the donors glutathionylated proteins are visible as a small number of bands from high to low molecular weight but with a larger number in the low end. Neutrophil extracts from one donor did not reveal any glutathionylated proteins. All three donors, however, showed very similar quantities of actin.

Next neutrophil cells were stimulated with either fMLP or IL8 and the same proteins detected. Figure 4.10 shows that for both proteins the stimulation appears to make little difference to the pattern of proteins detected.

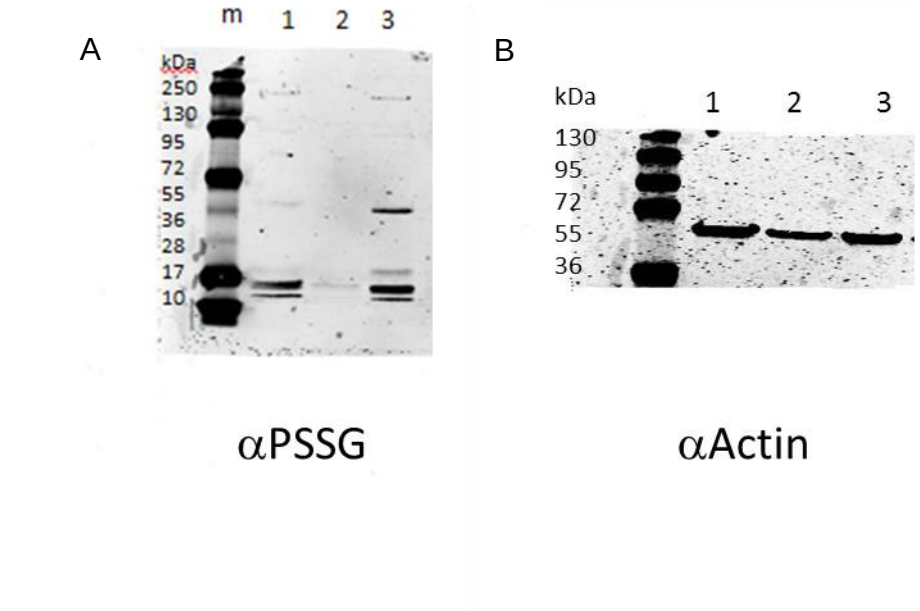

Figure 4.9: Western blots of neutrophil extracts from three different healthy donors (label 1,2 & 3). Proteins of interest were detected by A. anti-glutathionylated (PSSG) antibody or B anti-actin antibody. 'm' represents the molecular weight markers. Representative of n=3 experiments. (see general methodology section 2.15 for western blot protocol).

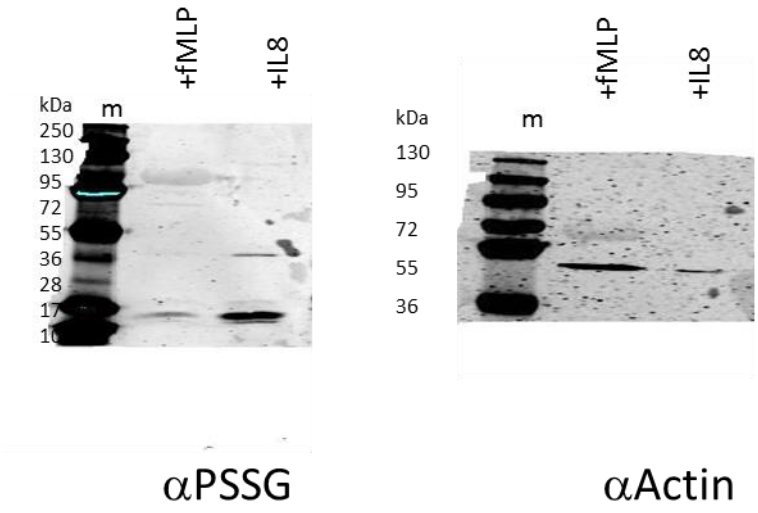

Figure 4.10: Western blots of neutrophil extracts. Cells were stimulated with either IL8 or FMLP for 60min. Proteins of interest were detected by A. anti-glutathionylated (PSSG) antibody or B anti-actin antibody. 'm' represents the molecular weight markers. (see general methodology section 2.15 for western blot protocol).

4.4 Discussion

In this chapter methods were developed and refined in our laboratories for the optimisation of neutrophil sample preparation and separation for proteomics and detection of glutathionylated proteins. First an off-line high-pH reverse-phase fractionation was developed using off-line basic reverse-phase fractionation technique from a publication by Batth et al (2014). Batth et al (2014) had developed their protocol for in-depth phosphoproteome studies which detected multiphosphorylated peptides.

For lysis of neutrophil cells, protein inhibitors were used to stop the action of a broad range of proteases that could degrade proteins present in the neutrophil samples. Neutrophils contain a large amount of proteases and it is vital to keep proteins intact to allow for identification of peptides later in the proteomics work flow and to allow for comparison by SDS-PAGE. No protease inhibitors were added to the Laemlli buffer because this buffer denatures proteins rapidly preventing protease activity anyway.

Once cells had been lysed and homogenised the extracted proteins were separated by SDS-PAGE. The gels were stained with Coomasie blue and compared visually. The reason for these lower molecular weight proteins was not investigated further but could be due to more efficient lysis of granules containing lower molecular weight species or possibly degraded proteins, though this is unlikely due to the processing of the cells to proteins rapidly in a denaturing solution The higher molecular weight species could the release of membrane-bound proteins by this method, that are perhaps not as abundant in the other preparations. Since the interest of this study was to look at which proteins are glutathionylated in the cytosol of neutrophils, it was concluded to continue the use of 10% SDS with 100 mM TEAB with protease inhibitor as the lysis buffer for neutrophil cells as this was the simplest buffer that could generate potentially the best preparation of cytosolic proteins.

High performance liquid chromatography (HPLC) was used to fractionate samples before submitting for mass spectrometry analysis. In this research, three columns were used: strong cation exchange column (SCX) and two high-pH reverse phase column (C8 and C18). The SCX column separates peptides based on their charge whereas the HpH reverse phase used peptide hydrophobicity as the separating factor. For the SCX column, digested protein sample was injected onto the HPLC and the

peptide mixture interacted with the negatively charged polysulfethyl functional groups on the polymer beads. Peptides with a negative charge will move faster and elute earlier from the column in comparison to the positively charged peptides that elute later. The high-pH reverse phase column separates peptides based on hydrophobic interactions. This has been shown to be more efficient in fractionation compared to that of charge-based separations like SCX (Batth et al., 2014).

Of all three column types it was immediately apparent that the Hypersil Gold C8 column showed much less separation of the peptides in comparison to both the SCX and Waters XBridge columns may be because this matrix is more commonly used to separated proteins rather than peptides. Additionally, the Waters XBridge column showed very good resolution of the peptides, by returning to the base line, and seemed to limit a large number of peptides coming through very rapidly in the initially wash, where negatively charged peptides do not bind appear to the SCX column. Thus, the Waters XBridge column was selected for the main work in this thesis. This was pleasing as it out performed the established method in our laboratory. All the methods seemed to produce similar results in terms of the protein classes detected.

To verify that this was the correct choice digested neutrophil lysates were also separated by the three columns and fraction collected. The fractions were then concatenated and pooled to either 4 or 10 fractions for analysis by mass spectrometry. From table 4.1, the highest quantity of proteins was detected using the C18 Waters XBridge column compared to the C8 Hypersil Gold and SCX column. This confirmed the choice of using the Waters XBridge column in further studies.

In a study by Rørvig et al (2013) a larger number of proteins were detected than presented here. However, these authors were looking to study all the granule proteins within neutrophils. They used a nitrogen cavitation technique to effectively breakdown all the granule membranes after subcellular fractionation. This was not a technique available nor was the release of all the granule proteins desired as this may have clouded the results of the chemotactic machinery found in the cytosol.

Proteins extracted from neutrophils were separated by SDS-PAGE and the proteins transferred to nitrocellulose membranes by electroblotting. The membranes were then probed for proteins of interest by using antibodies, in the process overall known as

Western blotting. Of particular interest in this study was the detection of glutathionylated proteins in general and actin specifically. The latter was of interest because of the discovery by Sakai et al (2012) that demonstrated that glutathionylated actin prevented efficient chemotaxis of neutrophils.

Actin is an abundant protein in cytoskeleton of neutrophils and used during cell movement (Kuhns et al., 2019). Actin is the protein that would be of interest to see in this study. Thus, it was readily detected by western blotting. Glutathionylated proteins appeared to be more elusive and were not consistently detected in neutrophils extracts from different donors. An attempt was made to purify glutathionylated proteins using the BioGEE system. BioGEE utilises a biotinylated glutathione ethyl ester that can be introduced in to cells during a pre-incubation with cells, or during culturing in longer lived cells. The biotin conjugate can then be purified by use of streptavidin beads to pull down proteins with biotinylated glutathione covalently attached. A method was reported by Brenan et al., (2006) who demonstrated low concentrations of glutathionylated proteins from neutrophils. Further optimisation may be required, or many more neutrophils cells need to be used as input to these experiments. An alternative might also be to use the 'redox array' technology to identify glutathionylated protein irrespective of its relative abundance (Mullen et al., 2015). This technique was developed to work with secreted proteins rather than cytosolic ones and can detect proteins 100x lower in concentration than those found by mass spectrometry. However, an antibody array is also part of the set up meaning that this is a targeted approach rather than a discovery based approach.

4.5 Conclusion

Work presented here supports the choice of using HpH reverse phase chromatography for increasing the numbers of proteins detected in neutrophil cell extracts. Detection of glutathionylated proteins by western blotting was possible but may be inconsistent in detection or the quantity of glutathionylation between neutrophil donors may be inconsistent. Detection of actin however was consistent by western blotting. The discrepancy in glutathionylated protein detection may be due to low concentrations that even purification methods did not improve.

CHAPTER 5 – Detection of protein glutathionylation in model protein haemoglobin

CHAPTER 5

Detection of protein glutathionylation in model protein haemoglobin

5.1 Introduction

In this thesis, one of the aims was to detect protein glutathionylation. Therefore, a model glutathionylated protein was examined first to establish if current instrumentation available could identify this modification. The protein used was human haemoglobin (Thermo Fisher Scientific, Paisley, United Kingdom) as previously described by (Regazzoni et al., 2009). Mass spectrometry was used as a platform to characterise the modified and unmodified forms of the protein. Two methods were used: direct infusion mass spectrometry and LC-MS/MS. Through direct infusion, samples were injected directly into the instrument and thus, everything in the sample was detected simultaneously. Through the LC-MS/MS method, sample first went through reverse phased column (C18) and then, through Orbitrap-based mass spectrometer, allowing for a separation of proteoforms or peptides. Proteoforms are the narrowest view of a particular protein which means that it is the same protein but in different proteoforms, for example modified and unmodified haemoglobin may be thought of as different proteoforms.

Glutathionylation is a process to protect protein thiols from irreversible oxidation and also to prevent loss of GSH under oxidative stress. Previous study mentioned that significant redox disturbances occur in neutrophils of periodontitis patients associated with deregulation of anti-inflammatory transcription factor Nrf2 pathway producing neutrophil hyperactivity (Dias et al., 2013). There are studies that have shown linkage of cigarette smoking and nicotine toxicity to glutathione depletion in periodontal tissues (Chapple and Matthews., 2007). There are also studies that reported areca nut alkaloid, arecoline-induced thiol depletion in periodontal ligament fibroblasts may make them more vulnerable to the effects of nicotine (Jr et al., 2007) and periodontal ligament fibroblast glutathione levels were decreased in a dose-dependent means by cigarette smoke (Chang et al., 2003).

5.2 Materials and methods

5.2.1 Direct infusion analysis:

A 10µL sample of 10mM haemoglobin solution in 0.1% formic acid was introduced to the mass spectrometer at a gas pressure of 0.3 pound-force per square inch (PSI) and 1.8 kV. The aqueous solution was injected directly into the mass spectrometry equipped with a TriVersa Nanomate chip-based electrospray device (Advion, Ithaca, New York), the electrospray ionization (ESI) source. The optimized parameters were as follows: gas pressure 0.3 psi, a tip voltage of 1.55 kV for direct infusion electrospray and a capillary temperature of 250 °C. Each analysis required about 5 minutes. Mass spectra were acquired by scanning over the 100-1000 m/z range. Xcalibur Analyst internal software (v2.0.7, Thermo Fisher Scientific) was used for instrumentation control and data acquisition.

5.2.2 Haemoglobin glutathionylation

Method for haemoglobin glutathionylation was adapted from a study done by Woodi et al. (2009). For preparation of glutathionyl haemoglobin, commercial haemoglobin (Thermo Fisher Scientific) was used with large excess of oxidized glutathione (GSSG) (Thermo Fisher Scientific) at a concentration of 67 mM in 0.5 M ammonium bicarbonate buffer (pH 8) for 12 hours at 37°C. A sephadex G-10 column (GE Healthcare, Buckinghamshire, United Kingdom) was used to remove any excess glutathione and buffer salts before mass spectrometry analysis following the manufacturer's instructions.

5.3 Results

5.3.1 Haemoglobin mass list

To accurately identify glutathionylated proteoforms, Protein Prospector (http://prospector.ucsf.edu/prospector/mshome.htm) was used to generate lists of mass to charge ratio for proteins. The original source of the human haemoglobin protein sequences were UniProt (accession numbers: haemoglobin alpha P69905 and haemoglobin beta P68871).The resulting mass lists are shown in table 5.1 and were used to identify the haemoglobin proteins and glutathionylation modification of haemoglobin beta.

From the results (figure 5.1, 5.2, 5.3 and 5.4), protein glutathionylation was observed in haemoglobin through direct infusion using whole protein and in LC-MS/MS using whole protein and digested protein. Glutathionylation was observed in beta subunit of haemoglobin only, maybe because of an accessible cysteine residue indicated by a mass increment of 305 Da. A previous study by Woodi et al (2009) suggested a mass increment of 305 Da for glutathionylation because addition of one glutathione molecule was observed in the beta chain of haemoglobin only.

Haemoglobin	Hbα	Hbβ	HbSG β
Uniprot reported mass (average)	15248.93	15989.30	NA
M	15125.92	15866.28	16171.30
M+H	15126.93	15867.29	16172.31
(M+2H)/2	7563.97	7934.15	8086.66
(M+3H)/3	5042.98	5289.77	5391.44
(M+4H)/4	3782.49	3967.58	4043.83
(M+5H)/5	3026.19	3174.26	3235.27
(M+6H)/6	**2521.99**	**2645.39**	**2696.22**
(M+7H)/7	**2161.85**	**2267.62**	**2311.19**
(M+8H)/8	**1891.75**	**1984.29**	**2022.42**
(M+9H)/9	**1681.67**	**1763.93**	**1797.82**
(M+10H)/10	**1513.60**	**1587.64**	**1618.14**
(M+11H)11	**1376.09**	**1443.40**	**1471.13**
(M+12H)/12	**1261.50**	**1323.20**	**1348.62**
(M+13H)/13	**1164.54**	**1221.49**	**1244.95**
(M+14H)/14	**1081.43**	**1134.31**	**1156.10**
(M+15H)/15	**1009.40**	**1058.76**	**1079.09**
(M+16H)/16	**946.38**	**992.65**	**1011.71**
(M+17H)/17	890.77	934.32	952.26
(M+18H)/18	841.34	882.47	899.41
(M+19H)/19	797.11	836.08	852.13
(M+20H)/20	757.30	794.32	809.57
(M+21H)/21	721.29	756.55	771.07
(M+22H)/22	688.55	722.20	736.07
(M+23H)/23	658.66	690.85	704.11
(M+24H)/24	631.25	662.10	674.81
(M+25H)/25	606.04	635.66	647.86
(M+26H)/26	582.77	611.25	622.98

Table 5.1: Haemoglobin mass list used to search for haemoglobin glutathionylation detected by mass spectrometry. These data were generated using in silico digestion by Protein Prosepctor. ‘M’ refers to mass of the proteoform, meanwhile ‘M+xH/x’ refers to mass with x proton charges and subsequent mass to charge ratio. Bold text indicates mass to charge ratio that were detected during mass spectrometry experiments. NA = not available

5.3.2 Direct infusion method

In this study, direct infusion electrospray ionization mass spectrometry (ESI-MS) was used to identify protein glutathionylation in haemoglobin. Haemoglobin samples with and without incubation with GSSG were injected directly into the mass spectrometer. By using direct infusion, all proteins present were observed at the same time. In the haemoglobin sample, the masses of haemoglobin were detected according to the mass list in table 5.1 and a representative mass spectrum is shown in figure 5.1. This was also the same for glutathionylated haemoglobin (figure 5.2) where the glutathionylated protein masses were detected in the β subunit. Tandem mass spectra of intact proteins can be complex, therefore spectral deconvolution was used to group all mass to charge ratios, or isotopomer envelopes, together to examine the entire mass of the protein subunits. Deconvolution takes into account of mass to charge ratio and converts it to one species. The deconvoluted mass spectra of unmodified haemoglobin for the alpha subunit was centred at 15125 Da and the haemoglobin beta subunit at 15866 Da. Modified haemoglobin beta subunit centred at 16171 Da confirming a mass shift of 305 Da suggesting that the subunit was glutathionylated as previously reported by Woodi et al., (2009).

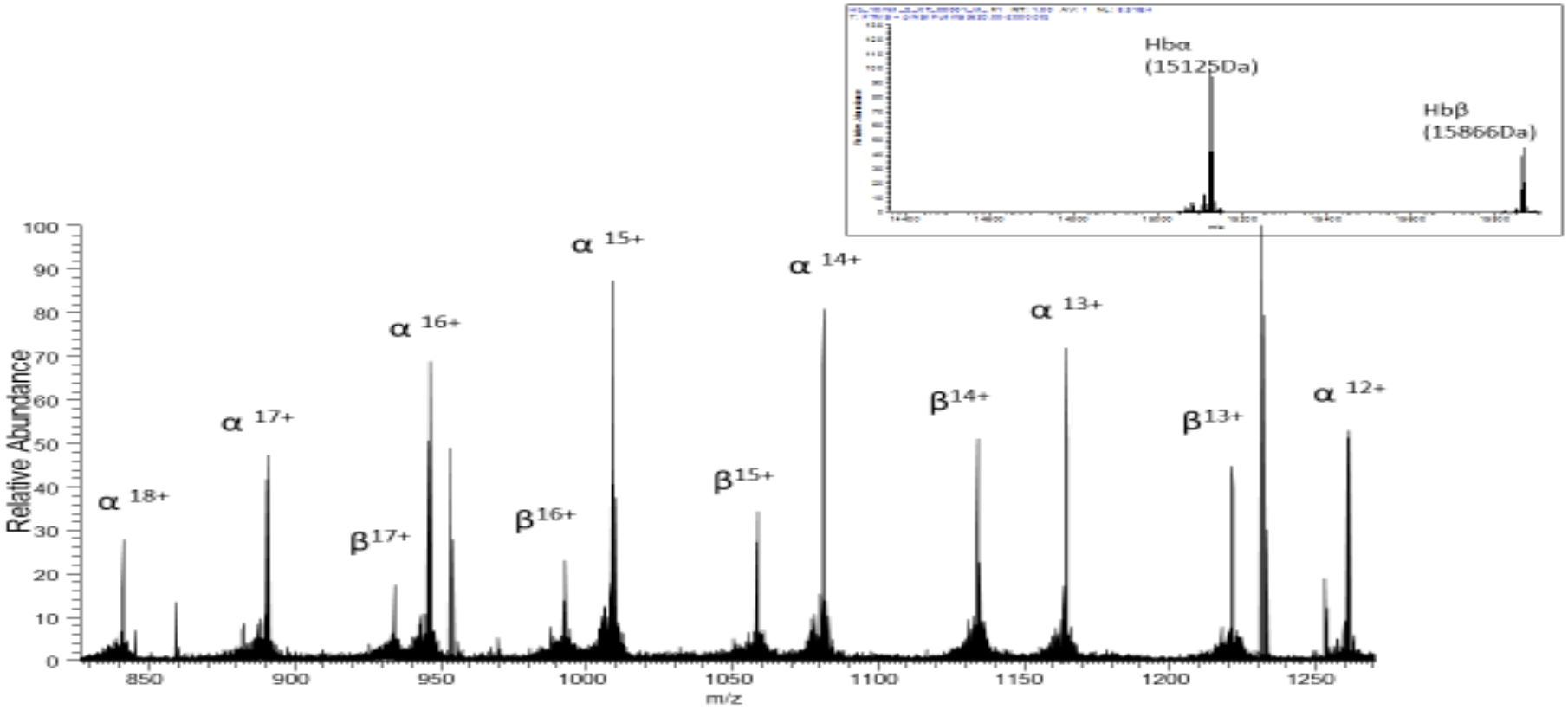

Figure 5.1: Mass spectrum of whole haemoglobin protein generated by direct infusion mass spectrometry. The top panel depicts deconvoluted peaks for alpha and beta subunits with masses of 15125 Da and 15866 Da respectively. The bottom panel depicts the mass spectra of haemoglobin along with the charge distribution for alpha and beta subunits of Hb.

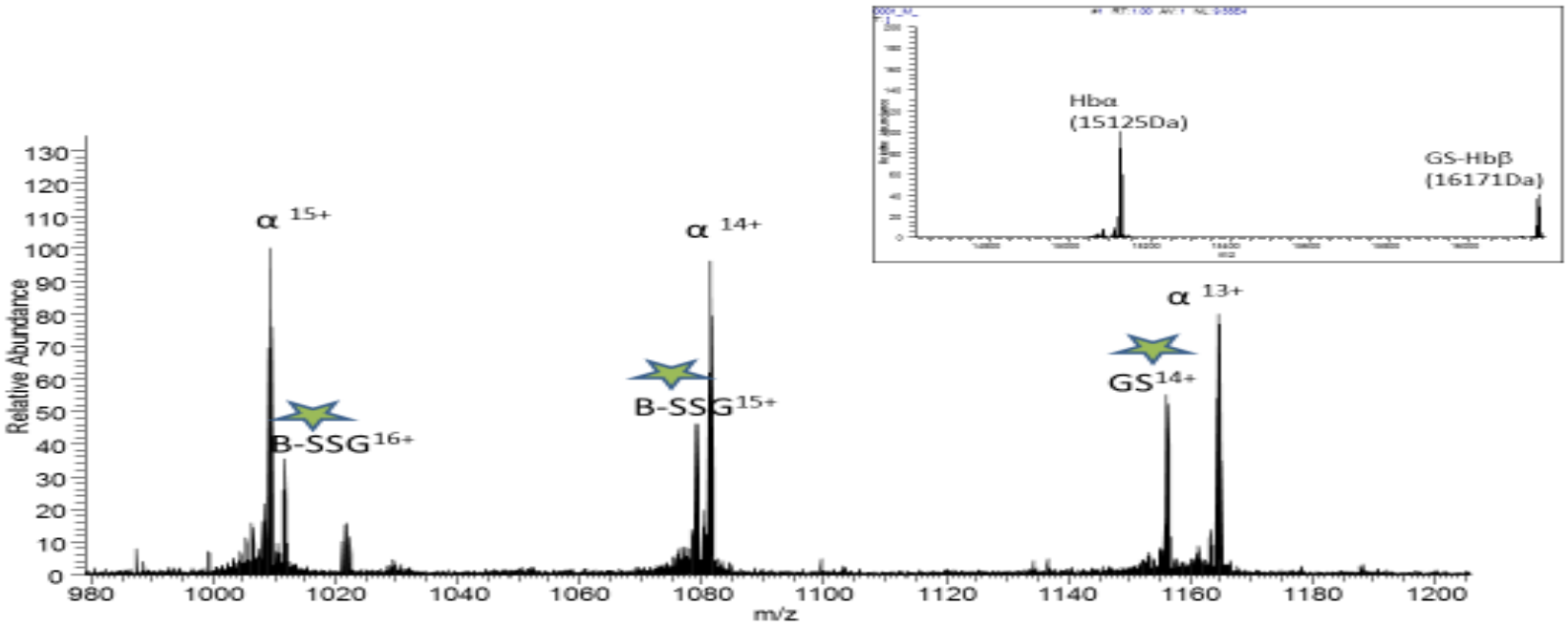

Figure 5.2: Mass spectrum of whole glutathionylated haemoglobin protein by direct infusion mass spectrometry showing alpha and glutathionylated beta peaks of masses 15125 Da and 16171 Da respectively in the top panel. The bottom panel depicts the mass spectra of haemoglobin along with the charge distribution for alpha and glutathionylated beta subunits of Hb.

5.3.3 Liquid Chromatography – tandem Mass Spectrometry (LC-MS/MS) analysis of Hb and modified Hb.

Native and glutathionylated haemoglobin samples were separated by HPLC (reverse phase C18) coupled to Orbitrap-based mass spectrometry. Haemoglobin was diluted 50-fold before it was analysed by LC-MS/MS for intact haemoglobin α and β chain. The alpha and beta chains eluted at different retention times allowing for separation of the overlapping spectra previously seen by direct infusion MS (figures 5.3 and 5.4). Also, as seen with direct infusion MS, glutathionylation was observed on the beta chain. The deconvoluted spectra again showed masses of 15125 Da, 15866 Da and 16171 Da for the alpha, beta and glutathionylated beta chains respectively. In figure 5.3, different isoforms of haemoglobin can also be seen (unannotated peaks by the beta chain). It is suggested that this could be delta haemoglobin.

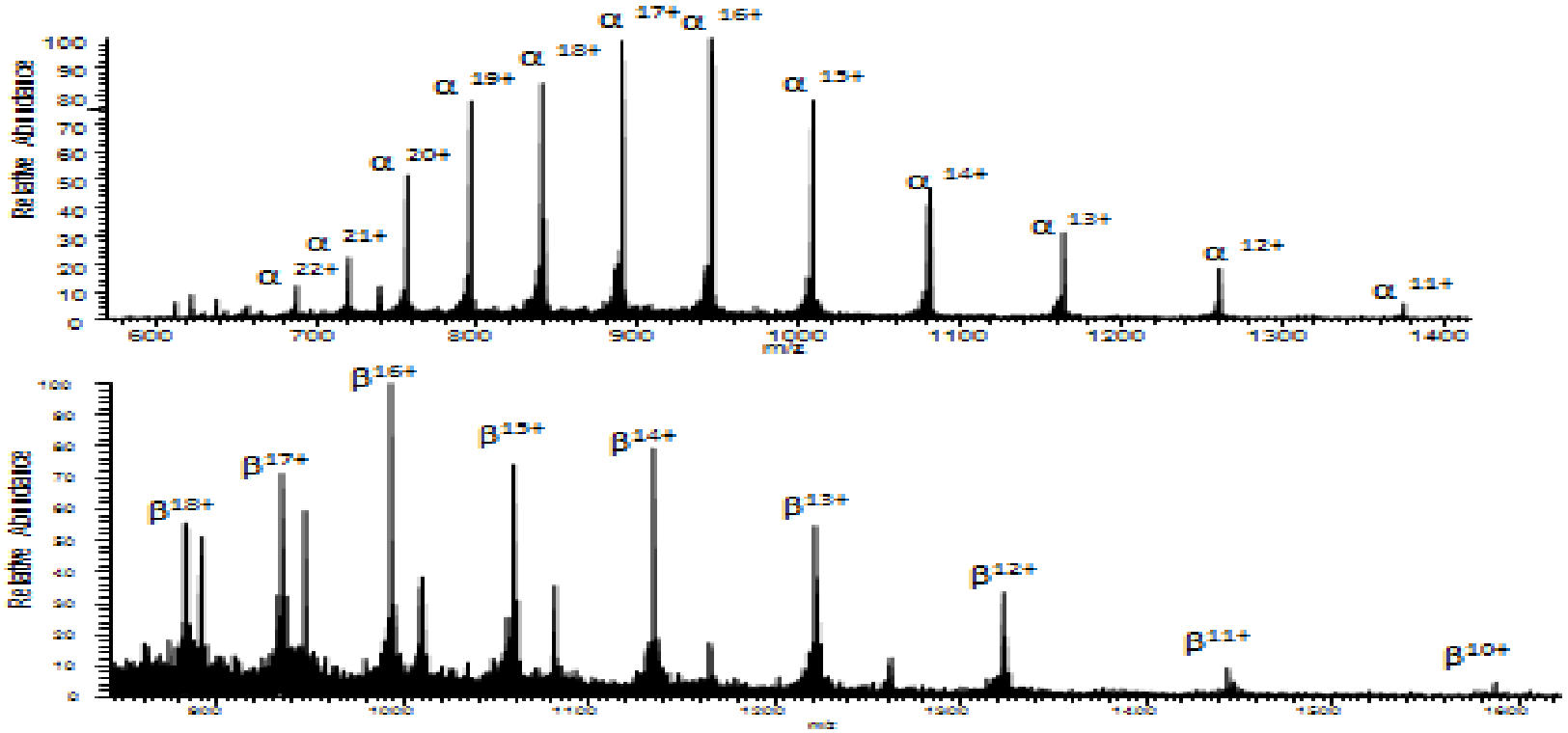

Figure 5.3: Mass spectrum haemoglobin analysed by LC-MS/MS. The upper panel depicts mass spectra of haemoglobin along with the charge distribution for alpha subunits of Hb. Meanwhile, the lower panel depicts mass spectra of haemoglobin along with the charge distribution for beta subunits of Hb.

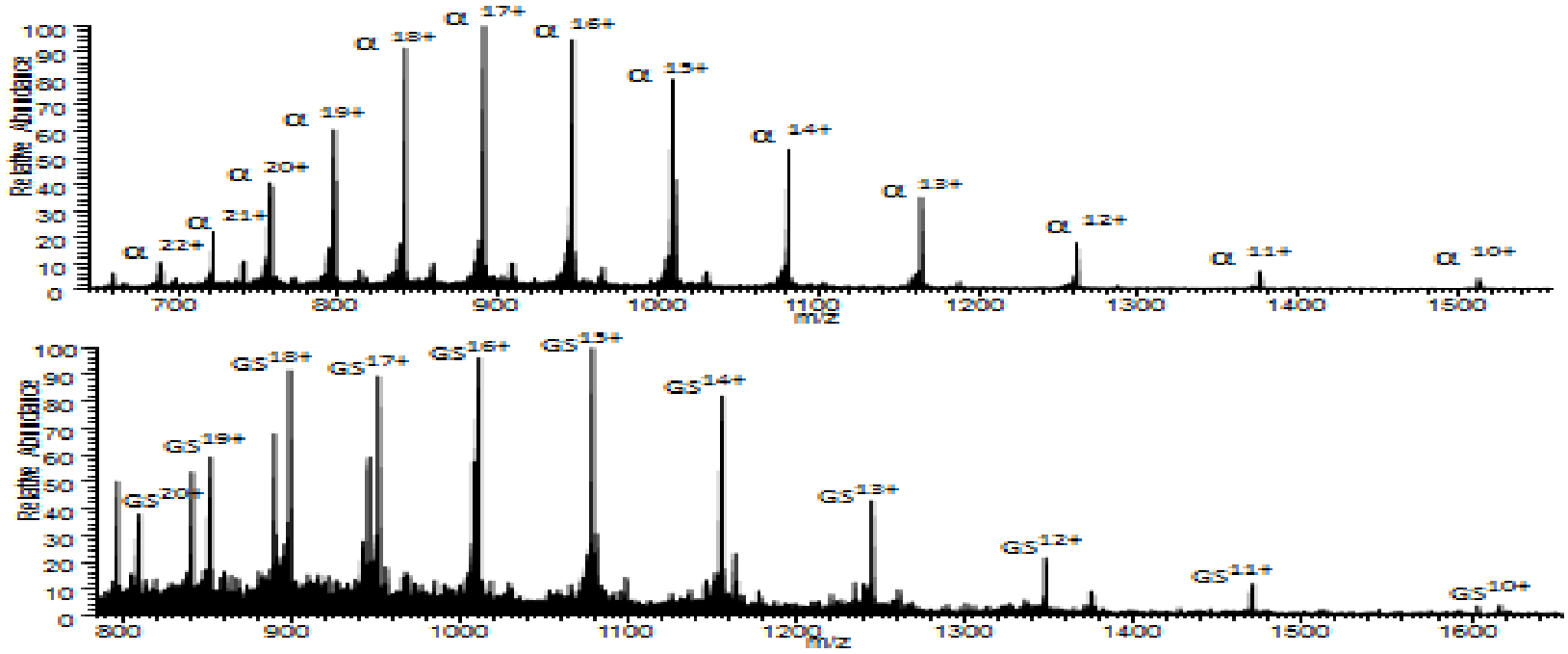

Figure 5.4: Mass spectrum of glutathionylated haemoglobin analysed by LC-MS/MS. The upper panel depicts mass spectra of haemoglobin along with the charge distribution for alpha subunits of Hb. Meanwhile, the lower panel depicts mass spectra of haemoglobin along with the charge distribution for beta subunits of Hb modified by glutathionylation.

5.3.4 Haemoglobin digested samples and LC-MS/MS method

Haemoglobin and glutathionylated haemoglobin samples were digested with trypsin overnight. These samples were then desalted using Ziptips to purify and concentrate the samples. Following this, they were analysed by mass spectrometry using LC-MS/MS. Haemoglobin was found with a coverage of 80% Hb and 96% Hb-SSG when compared to the human database. About 80% of PSMs came from Hb and any remainder may be small quantities of contaminants in the Hb purchased (tables 5.2 and 5.3). For the Hb-SSG, about 91% of PSMs came from Hb and the other remainder could be contaminants in the Hb purchased. Digested Hb beta analysed by LC-MS/MS also yielded identification of modified peptides (figure 5.5).

Human Hemoglobin subunit beta:

MVHLTPEEKSAVTALWGKVNVDEVGGEALGRLLVVYPWTQRFFESFGDLSTPDAV

MGNPKVKAHGKKVLGAFSDGLAHLDNLKGTFATLSELHCDKLHVDPENFRLLGNVL

VCVLAHHFGKEFTPPVQAAYQKVVAGVANALAHKYH

Peptides:

GTFATLSELHcDK (4 PSMs)

VLGAFSDGLAHLDnLKGTFATLSELHcDK (4 PSMs)

GTFATLSELHcDKLHVDPENFR (1 PSM)

LLGNVLVcVLAHHFGK (5 PSMs)

LLGnVLVcVLAHHFGK (4 PSMs)

Figure 5.5: Sequence of human Hb beta (accession P68871) showing the location of glutathionylated cysteine (green) and the individual peptides identified below. c denotes modified cysteine and n denotes deamidated asparagine. Number of PSMs identified are also indicated, total PSMs identified for Hb-beta peptides was 307.

Accession	Description	PSMs
P68871	Haemoglobin subunit beta	209
P02042	Haemoglobin subunit delta	108
P69905	Haemoglobin subunit alpha	99
P00915	Carbonic anhydrase 1	65
P69891	Haemoglobin subunit gamma-1	43
P69892	Haemoglobin subunit gamma-2	43
P00918	Carbonic anhydrase 2	14
P02768	Serum albumin	11
P30041	Peroxiredoxin-6	6
P0CG48	Polyubiquitin-C	3

Table 5.2: Protein profiling of digested haemoglobin with trypsin. The table shows the protein accession number, protein description and number of PSMs.

Accession	Description	PSMs
P68871	Haemoglobin subunit beta	437
P69905	Haemoglobin subunit alpha	353
P02042	Haemoglobin subunit delta	82
P00915	Carbonic anhydrase 1	35
P69892	Haemoglobin subunit gamma-2	29
P00918	Carbonic anhydrase 2	17
P30041	Peroxiredoxin-6	8
P60174	Triosephosphate isomerase	4

Table 5.3: Protein profiling of digested glutathionylated haemoglobin with trypsin. The table shows the protein accession number, protein description and number of PSMs.

5.4 Discussion

In this chapter, methods were established to demonstrate that protein glutathionylation could be detected by instruments available. The haemoglobin sample preparation method published by Woodi et al., (2009) and Regazzoni et al (2009) was followed but different mass spectrometry instrument used. In this study, various methods of mass spectrometry were tested, for example direct infusion and LC-MS/MS methods of intact protein and LC-MS/MS of digested protein, to identify the modification. In Woodi et al., (2009) study, haemoglobin was used to look for glutathionylation using single quadrupole mass spectrometry, whereas here the orbitrap mass spectrometer was used. In Regazzoni et al., (2009) study, the mass spectrometry used was LTQ-Orbitrap Hybrid mass spectrometer that used a linear ion trap for fragmentation, whereas here used LTQ-Orbitrap Elite ETD mass spectrometer that used the electron-transfer dissociation (ETD) ion trap mass analyser for fragmentation.

Glutathionylation is a posttranslational modification of protein cysteine residues by the addition of glutathione. Glutathionylation is often involved in protection of protein cysteines from irreversible oxidation and also in protein regulation (Cooper et al., 2011, Zhiyou & Liang-Jun 2013, Liang-Jun 2014). This modification alters protein mass charge, structure, function and prevents degradation due thiol over oxidation. Formation of protein glutathionylation involves the formation of a mixed disulphide between a free thiol group on a protein and molecule of GSH, It can occur through oxidation of a protein thiol group in response to reactive oxygen species (ROS) and reaction with GSH. A study by Regazzoni et al., (2009) indicated that glutathionylated haemoglobin as biomarker of oxidative stress through its ability of GSSG to form into Hb-SSG. In this study, glutathionylation of intact haemoglobin could be observed using the direct infusion and LC-MS/MS methods. This study was similar to Regazzoni et al., (2009) study that used mass spectrometry method of direct infusion and digested haemoglobin samples, thus, was able to look at haemoglobin glutathionylation. The modification could only be observed at the beta-chain with an absence of modification on the alpha-chain. This was similar to the Woodi et al., (2009) and Regazzoni et al., (2009) study that observed the modification only in the beta-chain due to the addition of one glutathione molecule.

Incidentally, during this study it was the first time haemoglobin intact protein sample directly analysed by technique reversed-phase liquid chromatography tandem mass spectrometry (LC-MS/MS). Particularly, if the objective is identification, intact proteins of $\leq$ 30kDa can be analysed intact through LC-MS/MS or otherwise protein digestion is necessary (Udeshi et al., 2008). Human haemoglobin is a protein of 64.5kDa consists of two α-chains and two β-chains that are noncovalent associated (Perutz et al., 1960). Detection of intact haemoglobin by mass spectrometry is challenging because of its noncovalent association of the 4 Hb subunits (Peng et al., 2005). Previous study developed technique nano electrospray ionization tandem mass spectrometry (nanoESI MS/MS) for detection of intact haemoglobin protein interaction with platinum drug (oxaliplatin) (Peng et al., 2005). Another previous study did a liquid chromatography (LC) separation of blood samples intact protein using reverse-phase (RP) chromatography as a first step, then the fractions collected that were of interest was digested with trypsin for mass spectrometry analysis by top-down and bottom-up technique for protein separation as a second step allowing identification of Hb sequences as well as glutathione modification using this approach (Huttenhain & Hess 2010).

It was demonstrated that the instruments in the laboratory could pick up glutathionylation using intact preparations of haemoglobin. This would be beneficial in the future to use this model protein to look for glutathionylation modification using the mass spectrometer instrument available in the laboratory.

5.5 Conclusion

Glutathionylation modification could be observed in haemoglobin samples through direct infusion mass spectrometry and LC-MS/MS methods in LTQ-Orbitrap Elite ETD mass spectrometer (ThermoFisher Scientific, Paisley, United Kingdom).

CHAPTER 6 – Assessment of neutrophils role in periodontitis patients

CHAPTER 6

Assessment of neutrophils role in periodontitis patients

6.1 Introduction

In this chapter, a clinical study is described that was set up to investigate the role of periodontitis on alterations to peripheral blood neutrophils: periodontitis patients were compared to healthy controls and also before and after periodontal therapy. In this study, neutrophils were isolated from whole blood to assess glutathionylated proteins, neutrophil chemotaxis and further understand redox balance of neutrophils.

Neutrophils are important for periodontal health because: they can respond to inflammatory mediators and enter the periodontal tissues towards chemoattractant signals produced by bacteria in the gingiva (Scott and Krauss, 2011); they are able to mount an antimicrobial attack on dental plaque via reactive oxygen species (ROS) and other species; they are able to phagocytize bacteria and thereby remove them; they have neutrophil extracellular traps (NETs). Findings from (Bhansali et al., 2013) have shown that neutrophils from localized aggressive periodontitis (LAP) patients failed to generate the products of the respiratory burst. This is because elevated superoxide generation in LAP neutrophils is associated with increase in diacylglycerol and reduced levels of diacylglycerol kinase in LAP patients. LAP patients usually exhibit abnormal neutrophil functions to a variety of environment and host stimuli (Bhansali et al., 2013). The hyperactivity and reactivity of blood neutrophils from periodontitis patients is a constitutive characteristic of the host in relation to the elaboration of priming agents into plasma (Bhansali et al., 2013) and (Dias et al., 2013).

There was aberrant chemotaxis in periodontitis patients compared to healthy people. (Roberts et al., 2015). Following periodontal treatment, it was found out that speed reduced in response to both chemoattractants meanwhile velocity and accuracy were normalized for Interleukin-8 which is a weak chemoattractant and remained significantly reduced for fMLP (Roberts et al., 2015). Another study was done using Boyden Chamber reported impairment of neutrophil movement in chronic periodontitis relative to control subjects (Prakash and Kumar, 2012). The study also showed that chemotactic response altered in neutrophils after periodontal treatment suggested that periodontal treatment does have an effect although it was at a lesser degree.

Tandem mass tag (TMT) is quantitative proteomics. There are labelled isobaric tags for peptide identification and quantification. Each neutrophil sample gets a different TMT tag. This quantitative proteomics can give information on identification and number of peptides in the neutrophil sample. In the mass spectrometry, measurement of peptides fragment and tags were done which give relative quantification that measure relative to how much there is of a different part of sample. There are other ways to measure quantitative proteomics such as label-free technique and SILAC. Label-free technique was not done in this experiment as it is more expensive to use label-free than labelled tags as how the mass spectrometry service was set up in the laboratory. SILAC was not done also because its purpose is for growing cells in incorporate amino acid in proteins as it introduces heavy and light form of amino acid in proteins in the cell culture. Neutrophils are not growing cells; therefore, it is not suitable to use SILAC as quantitative proteomics.

6.2 Materials and methods

6.2.1 Study participants

Periodontitis patients (n=4) were recruited from periodontitis new patient clinics at the University of Birmingham's School of Dentistry and Birmingham Dental Hospital. Age (+/- 5 years) and gender matched healthy controls (n=4) were recruited from staff of the University of Birmingham's School of Dentistry. Volunteers gave written informed consent and medical history including age, gender, ethnicity and smoking status at recruitment. They donated approximately 25ml blood for this study from which neutrophils were isolated as described in general methodology section 2.2. Periodontitis patients made one donation before non-surgical treatment began and one two months post treatment. Healthy volunteers gave one donation only. Periodontitis patients underwent standard non-surgical periodontal treatment of 5 treatments for 5 weeks as one treatment per week, carried out by one hygienist. Thereafter they were given 2 months for healing and were then called back for post treatment review. Out of the 4 patients recruited only 2 patients that came back for the post treatment visit at the 2 month review despite recall letters being sent. The cause was not known. The patient flow diagram is shown in Figure 6.1. Measurements that were recorded in this clinical study were percentage of sites of bleeding on probing (% bleeding) and presence of plaque percentage (plaque index (PI) %). Periodontal disease was classified as severe periodontitis are based on Page et al (2012) case definitions (severe periodontitis: $\geq$ 2 interproximal sites with PPD $\geq$ 5mm). Controls were not examined for periodontal health, merely asked for their latest classification by their general dental practitioner. Thus, they may have had some level of gingivitis.

The recruitment of periodontal patients was based on inclusion and exclusion criteria. The inclusion criteria were patients with periodontitis defined as having 2 or more sites with PPD of 5-9mm, loss of attachment and bleeding on probing. The exclusion criteria were patients lacking capacity to consent, smokers and those with other chronic inflammatory conditions such as diabetes, arthritis and chronic kidney disease.

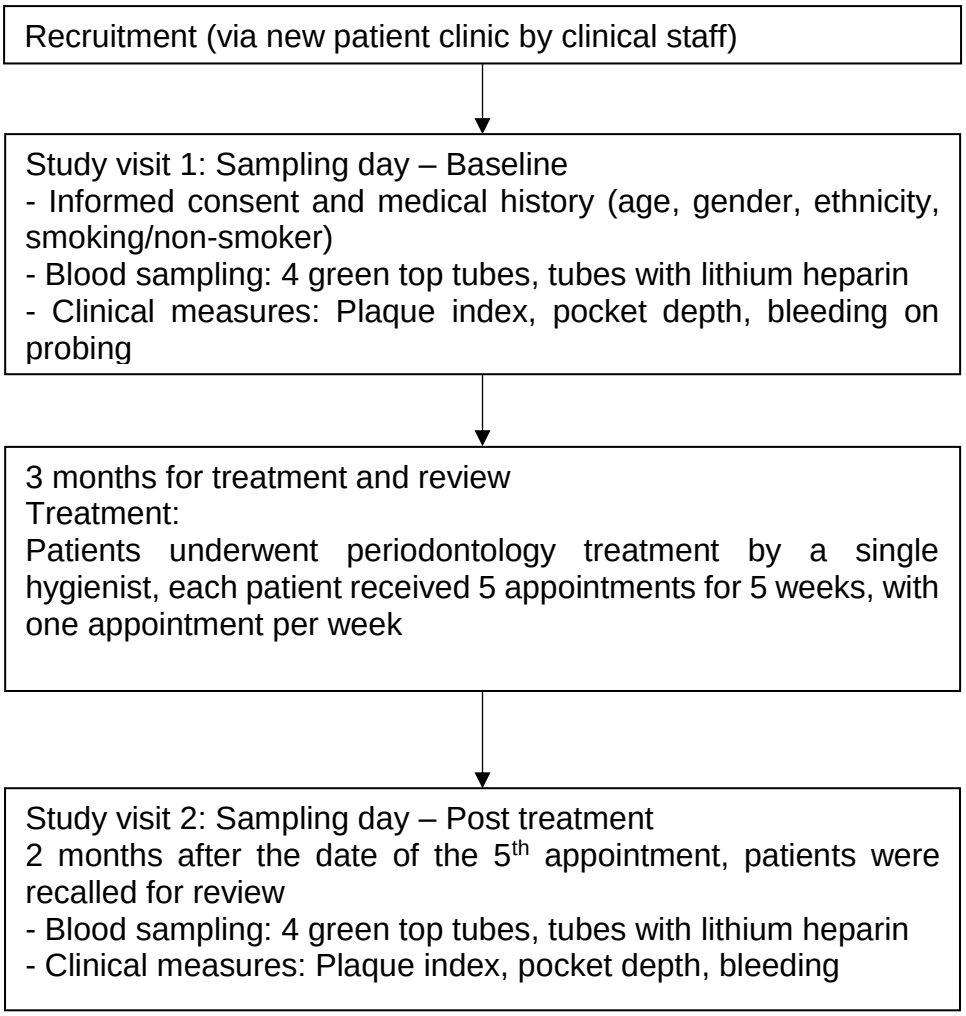

Figure 6.1: Clinical study workflow for periodontitis patients.

6.2.2 Quantitative Proteomics

For detection of all protein including potentially glutathionylated proteins, neutrophils were lysed with lysis buffer and protease inhibitor (section 4.3.1) and then stored at -20°C until all samples had been prepared. Protein content of each preparation was measured by BCA assay (section 2.9).

Extracted proteins (100µg) isolated from neutrophil samples were reduced, alkylated and digested overnight (as described in section 2.10). The TMT Label Reagents (Thermo Fisher Scientific) from the kit was equilibrated to room temperature before use. Anhydrous acetonitrile (4µl) was added to each tube containing individual TMT labels (0.8mg). The reagent was vortexed for 5 minutes to allow it to dissolve. Then, the tube was briefly centrifuged.

Then, one of the TMT label reagent (41µl) was added to one peptide preparation to create ten differently labelled peptide preparations. The reactions were incubated for 1 hour at room temperature. To quench the reaction, hydroxylamine (8µl, 5% in 100mM TEAB) was added to the reactions and they were incubated for 15 minutes at room temperature. All labelled samples were combined and dried by vacuum centrifugation. The sample was then cleaned up using macrotrap desalting method (method section 2.11). After this, the samples were sent to be analysed through the mass spectrometry (Q Exactive HF hybrid quadrupole-Orbitrap mass spectrometer, Thermo Scientific) for peptide identification. The work flow is shown in figure 6.2.

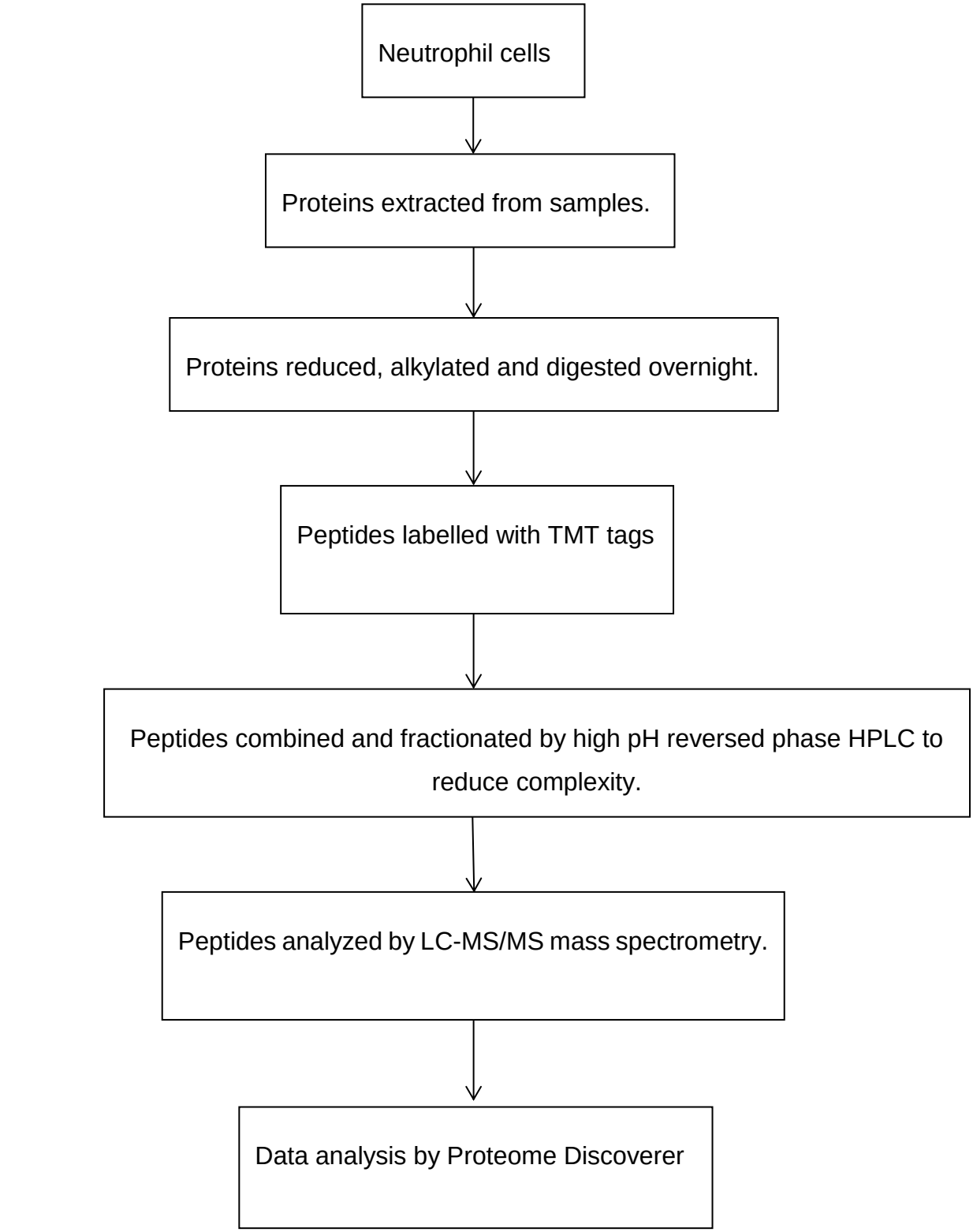

Figure 6.2: Work flow for preparation of TMT labelled peptides and their analysis.

6.3 Results

6.3.1 Clinical study outcomes of treatment

Four volunteers were enrolled into this study with severe periodontitis. Four healthy controls were then recruited as gender and age-matched (+/- 5 years) for comparison. Periodontitis patients received standard non-surgical periodontal therapy for 2 months. Out of the 4 patients recruited, only 2 patients that came back for review and post treatment sampling. The cause was not known, and efforts were made to recall them, to no avail. Figure 6.3 shows an approximate consolidated standards of reporting trials (CONSORT) diagram for the patient pathway with numbers at each stage.

The demographic profiles of the patients and controls are shown in table 6.1. From the change in baseline, it can be seen that, there were improvements in percentage of bleeding site, clinical attachment loss (CAL), mean periodontal pocket depth (PPD) and of teeth with PPD> 4mm for periodontitis patients returning after treatment. These data indicate the treatment for patients N002 and N005, who returned for the review visit, was successful. It can be seen in table 6.2 that there is more clinical attachment loss (CAL) than periodontal pocket depth (PPD) which means patients had some recession as well. For local bleeding, the percentage of bleeding on probing (BOP) should be less than 30%, otherwise if it is $\geq$ 30%, is considered as general BOP (Lang et al., 1986). In table 6.2, patient N001, N002, N003 and N005 have percentage of bleeding more than 10% at recruitment, before treatment, but after treatment for patients N002 and N005 the percentage of bleeding on probing improved and was then at less than 10%. Patient N002 had more percentage plaque surfaces after treatment compared to before treatment, it could be speculated that this may be due to consumption of plaque inducing foods prior to that day of sampling or a relapse to poor cleaning practises. One of the limitations of this clinical study is that patient N004 withdraw consent and patient N001 and N003 did not return for clinical evaluation post treatment.

	Control group	Periodontitis group
Number	4	4
Mean age (range)	40.5 +/- 4.5 years old	40.75 +/- 2.5 years old
Gender (% female)	50%	50%

Table 6.1: Demographic profile of periodontal patients and control in clinical study.

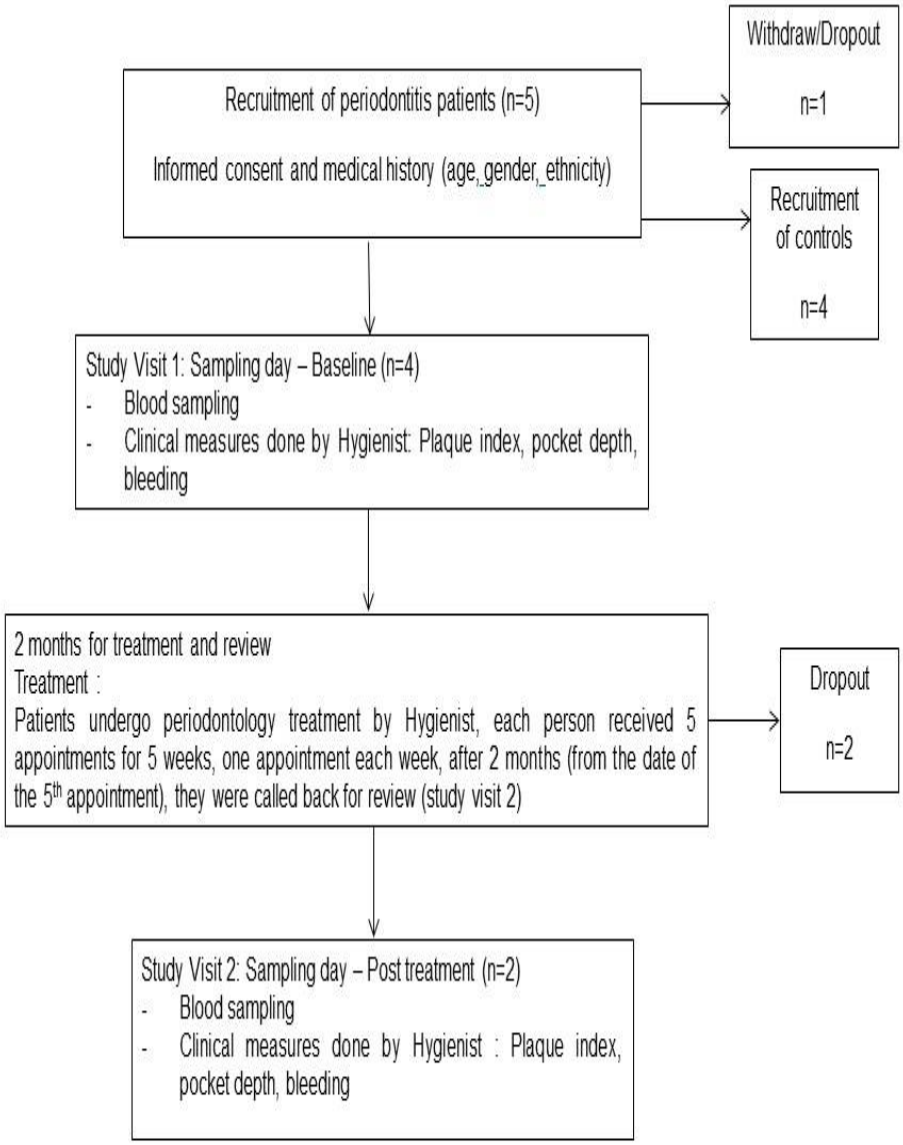

Figure 6.3: CONSORT diagram representing the flow of the clinical study starting from recruitment of periodontitis patients until exit from the study after follow up review following treatment. This diagram also indicates the number of periodontitis patients at each phase and measurements taken.

Table 6.2: The table represents the periodontal profile of the patients before V1 periodontal treatment (pre-treatment); V2 after periodontal treatment (post-treatment); PPD-, periodontal pocket depth; CAL-, clinical attachment loss.

ID patient	N001		N002		N003		N005	
Visit	V1	V2	V1	V2	V1	V2	V1	V2
Number of teeth	31	-	28	28	31	-	29	29
Percentage bleeding	21.0	-	11.3	8.6	27.2	-	13.8	8.0
Percentage plaque surfaces	46.8	-	0.9	20.5	20.2	-	39.7	31.9
PPD Mean +/- SD (range)	2.6 +/- 1.8 (0-8)	-	3.0 +/- 2.8 (0-14)	2.7 +/- 2.4 (0-12)	4.0 +/- 2.5 (1-9)	-	2.0 +/- 1.5 (0-8)	1.8 +/- 1.8 (0-10)
Teeth>4mm	15	-	16	15	24	-	10	9
CAL Mean +/- SD	2.6 +/- 1.8	-	3.1 +/- 2.8	2.8 +/- 2.4	4.0 +/- 2.5	-	2.7 +/- 2.4	2.5 +/- 2.8
% sites1-2mm	59.1	-	57.1	61.3	41.9	-	62.1	55.7
% sites3-4mm	23.1	-	9.1	12.9	18.8	-	14.5	15.6
% sites >4mm	15.1	-	22.6	16.1	39.2	-	15.6	0.0

6.3.2 Neutrophil cell viability

To verify the viability of neutrophils isolated from periodontitis patients pre and post treatment and healthy controls cell viability determined by trypan blue exclusion assay using the automated Luna cell counter (as described in section 2.4.2). Figure 6.4 represents the cell viability for periodontitis patients before and after treatment and control at time point of 0 and 4 hours. Neutrophil cells were at least 87% viable with the majority at 95%. The cells are still viable after 4 hours and suitable for experimentation.

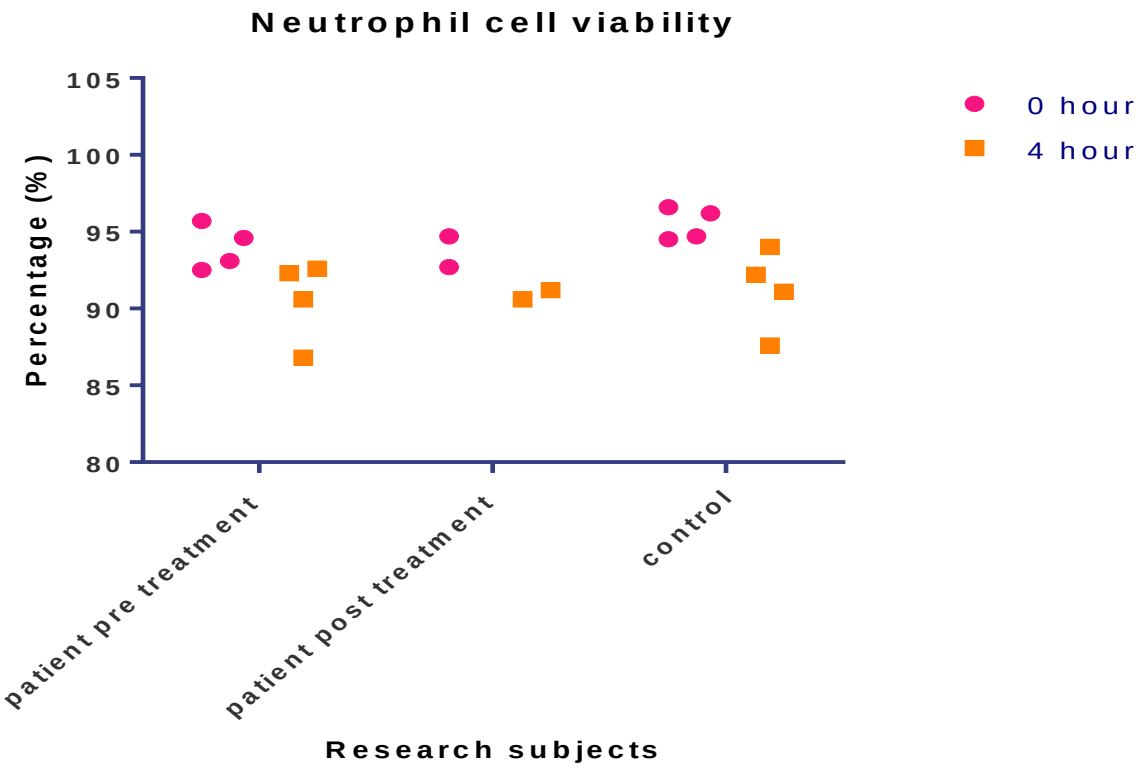

Figure 6.4: Neutrophil cell viability for periodontitis patients before and after periodontal treatment and healthy controls at 0, after isolation and after four hours. Cell viability was measured by trypan blue exclusion assay (section 2.4.2) using the automated Luna cell counter.

6.3.3 Chemotaxis of neutrophil cells

Chemotactic ability of the neutrophil cells was measured from periodontitis patients and controls and results are shown in figure 6.5. The controls had higher chemotactic ability compared to the pre-treatment patients. It is also shown in figures 6.5 and 6.6 that after periodontal treatment, two review patients had improvement in their chemotactic ability towards the chemoattractant fMLP. However, these changes were small, and the movement of the neutrophils does not reach the same level as control donors. Looking at the effect of IL8 shows that there is not as simple a relationship with a variable effect of treatment of neutrophil movement towards IL8. While the pre and post results could not be examined statistically due to too few remaining in the study the comparison between pre-treatment chemotaxis and healthy controls showed a non-significant trend for increased chemotaxis in the control donor neutrophils.

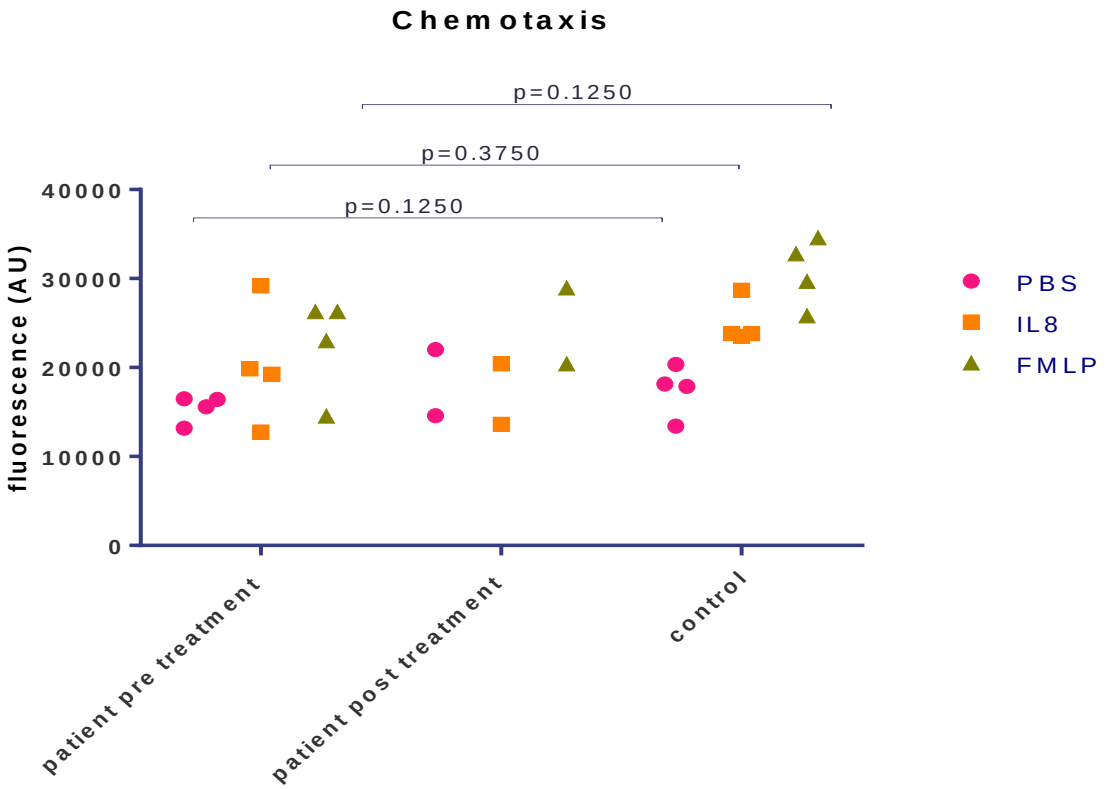

Figure 6.5: Periodontitis patient pre-treatment and post-treatment as well as clinical study control chemotactic ability of neutrophil cells in Phosphate buffered saline (PBS), Interleukin 8 (IL8) and N-Formylmethionine-leucyl-phenylalanine (fMLP) chemoattractants. Statistical analysis: Wilcoxon paired test.

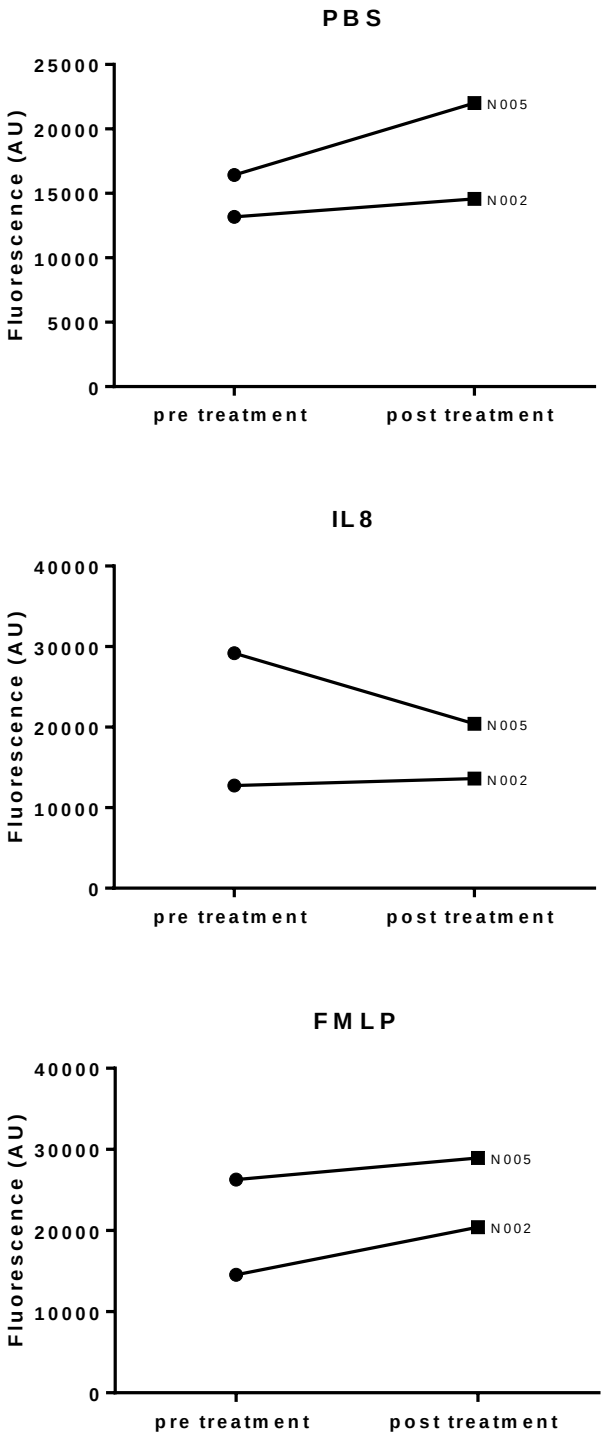

Figure 6.6: Direction of change for patients N002 and N005 for chemotactic ability of neutrophil cells towards Phosphate buffered saline (PBS), Interleukin 8 (IL8) and N-Formylmethionine-leucyl-phenylalanine (fMLP) chemoattractants.

6.3.4 Measurement of total glutathione (GSH) and oxidized glutathione (GSSG)

The amount of glutathione was measured as well as the ratio of total glutathione/oxidized glutathione in periodontitis patients (pre- and post- treatment) and controls. Figure 6.7 shows the amount of total glutathione and oxidized glutathione. The control donors had a higher quantity of glutathione compared to periodontitis patient's pre-treatment. However, one patient post-treatment nearly had the same amount of glutathione with the matched control. Figure 6.8 shows that there was no significant difference between GSH/GSSG ratio of control and pre-treatment periodontitis patients.

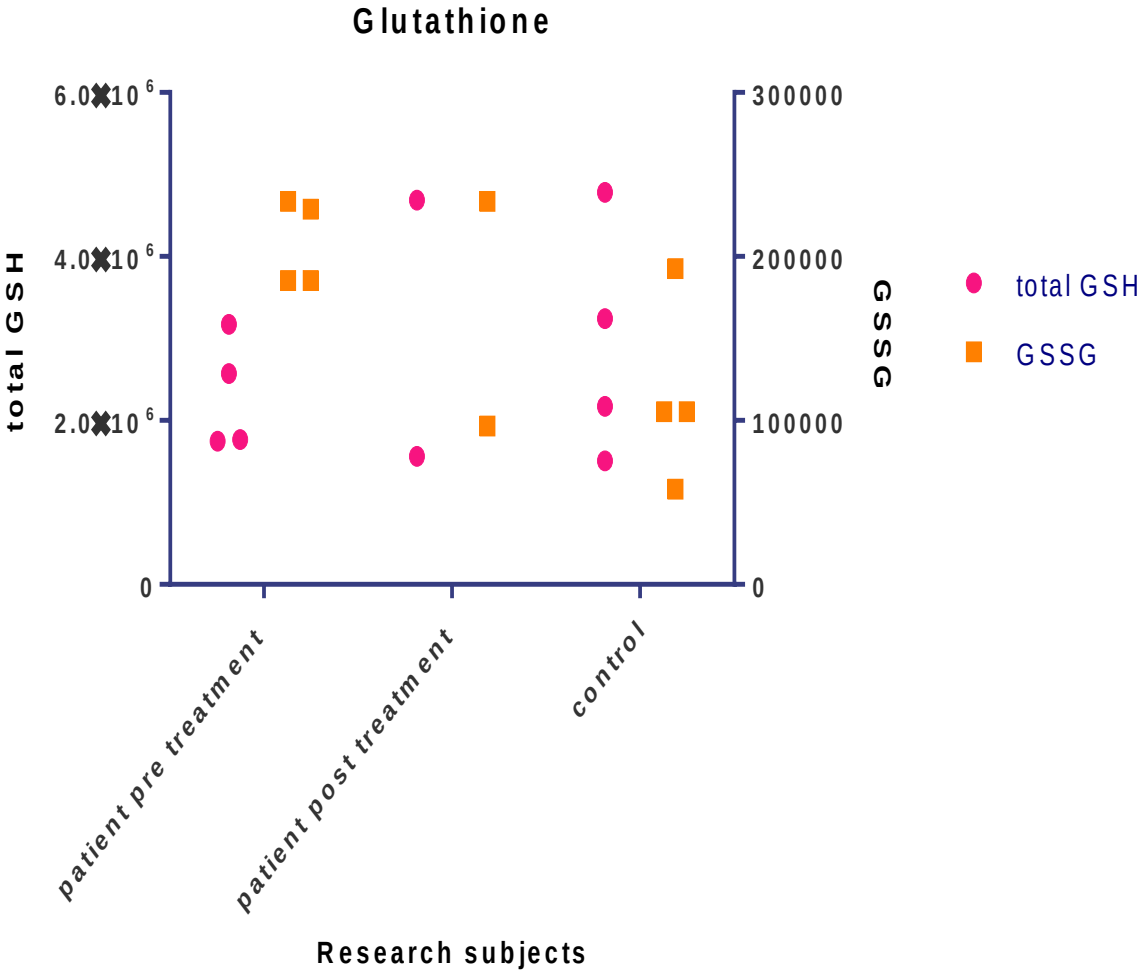

Figure 6.7: Control and periodontitis patient pre-treatment and post-treatment total glutathione (GSH) and oxidized glutathione (GSSG). GSH and GSSG were measured by respective Glo assays (section 2.7).

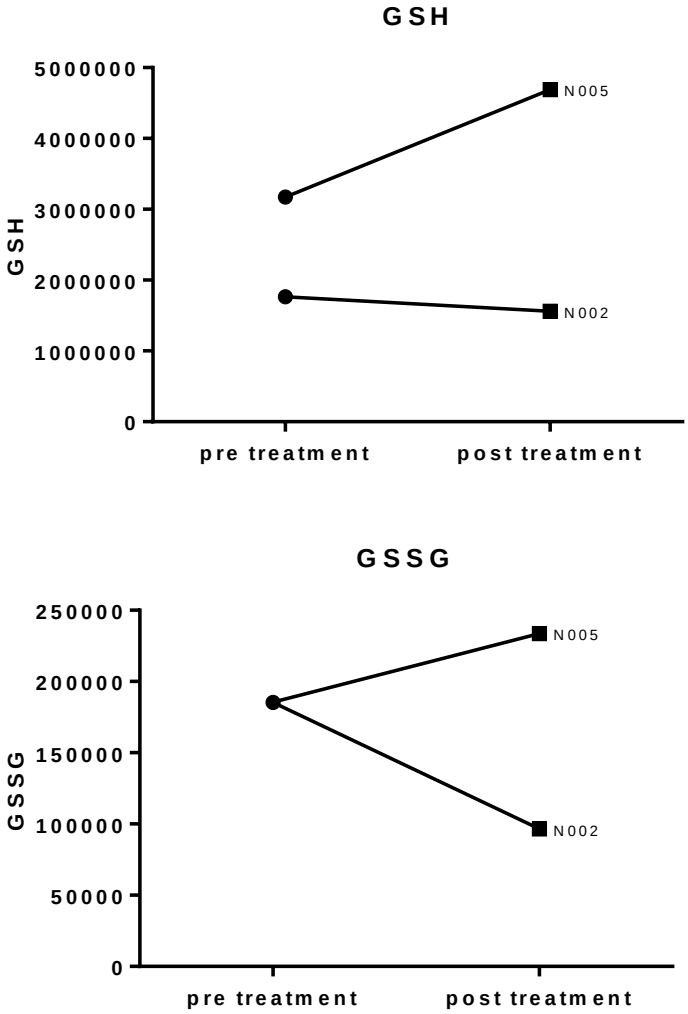

Figure 6.8: Periodontitis patient pre-treatment and post-treatment total glutathione (GSH) and oxidized glutathione (GSSG) showing change after treatment. GSH and GSSG were measured by respective Glo assays (section 2.7).

6.3.5 Detection of glutathionylated proteins

This part of the study aimed to detect glutathionylated proteins in the controls and periodontitis patients by use of quantitative proteomics based mass spectrometry using tandem mass tag (TMT) labels and western blotting for glutathionylated proteins.

Neutrophil cell extracts were reduced, alkylated and digested with trypsin overnight. The resulting peptides from each extract were then labelled with individual TMT reagents and mixed together. This pooled sample was the fractionated by high pH reverse phase HPLC in 10 fractions and the new Q Exactive mass spectrometer as it was much more sensitive, and more information could be gained by using it. Each fraction was analysed in triplicate technical repeats. Use of the principal component analysis (PCA) tool within Proteome Discoverer (v2.2) illustrated that the triplicate repeats clustered together (figure 6.9). It appears that the post treatment samples cluster more closely together than the pre-treatment samples, however this is a small sample set to draw conclusions from.

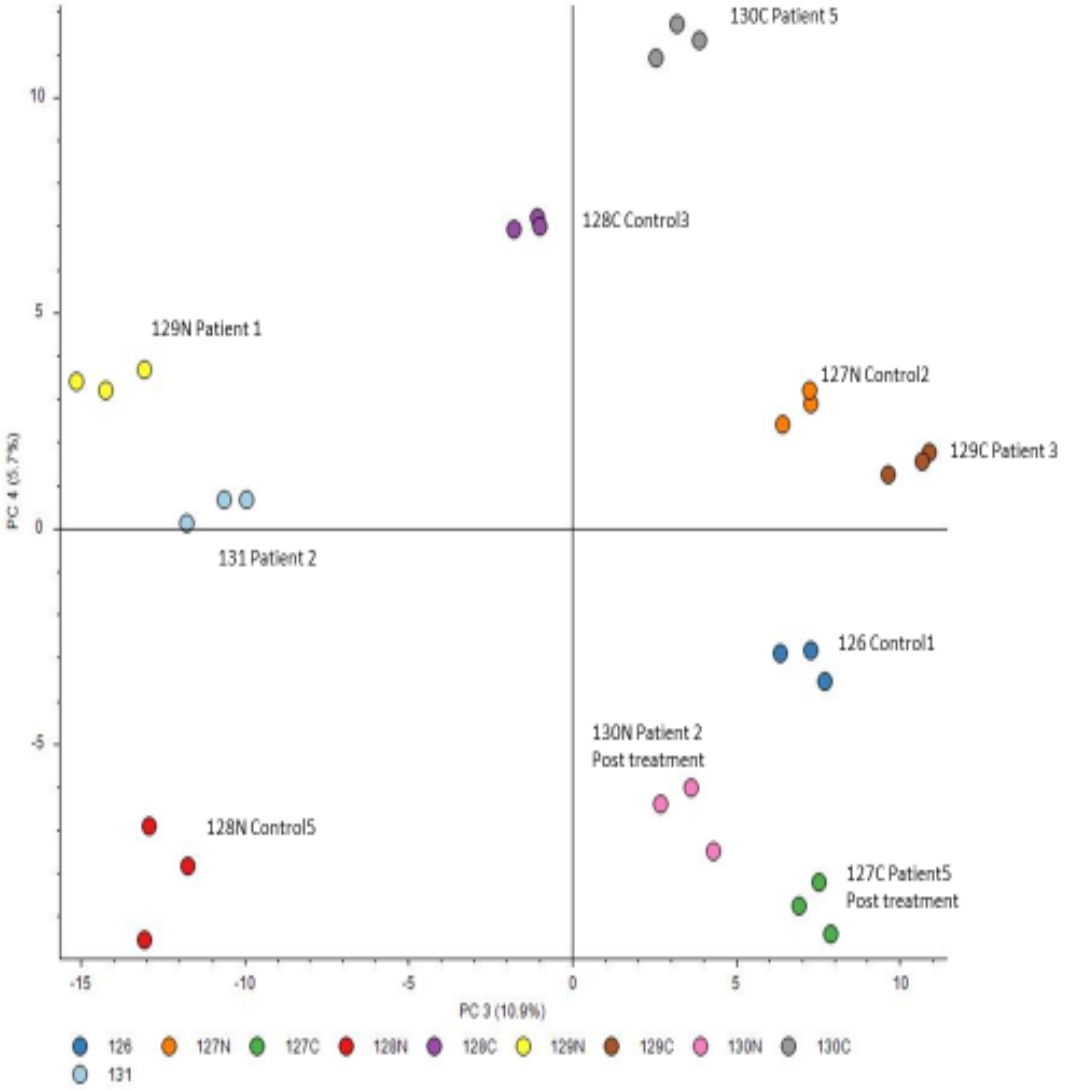

Figure 6.9: Principle component analysis (PCA) of data from the proteomic analysis of extracted neutrophil samples from periodontal patients (pre and post treatment) and controls. Graph was drawn in Proteome Discoverer (version 2.2). Each sample is represented by a different colour as denoted at the bottom of the graph. The label used for each sample is also indicated.

Using all the data the clustering of the different samples was also explored and visualised using hierarchical clustering (using maximum distance and average linkage) with the online R based tool ClustVis. Figure 6.10 shows the generated heatmap. To create this representation, mean averages were determined for all proteins from all control samples and the ratio of these proteins to all the control and patients' samples was determined. These were then compared. It can be seen that the majority of the proteins show a relatively pale colour highlighting that most proteins do not change greatly in abundance between the different samples. In patients 1 and 2 there are darker colours (particularly at the top of the columns) indicating that there were greater changes between these proteins and the average control value. These have been identified as haemoglobins. Examining the pattern of clustering it can be seen that the different types of samples, i.e. control or patient pre-treatment or patient post treatment, appear to cluster together with the exception of control 5. This perhaps indicates similarities in the underlying protein profile of these different neutrophil conditions.

Figure 6.10: Heatmap showing ratio to mean of all controls for all samples from periodontal patients (pre and post treatment) and controls. No scaling was applied to rows. Both rows and columns are clustered using maximum distance and average linkage. 495 rows, 10 columns. Heatmap was generated by using ClustVis R based online tool. Colours show fold change for individual proteins in comparison to the mean value calculated from the controls for the same protein. Tx denotes post treatment samples.

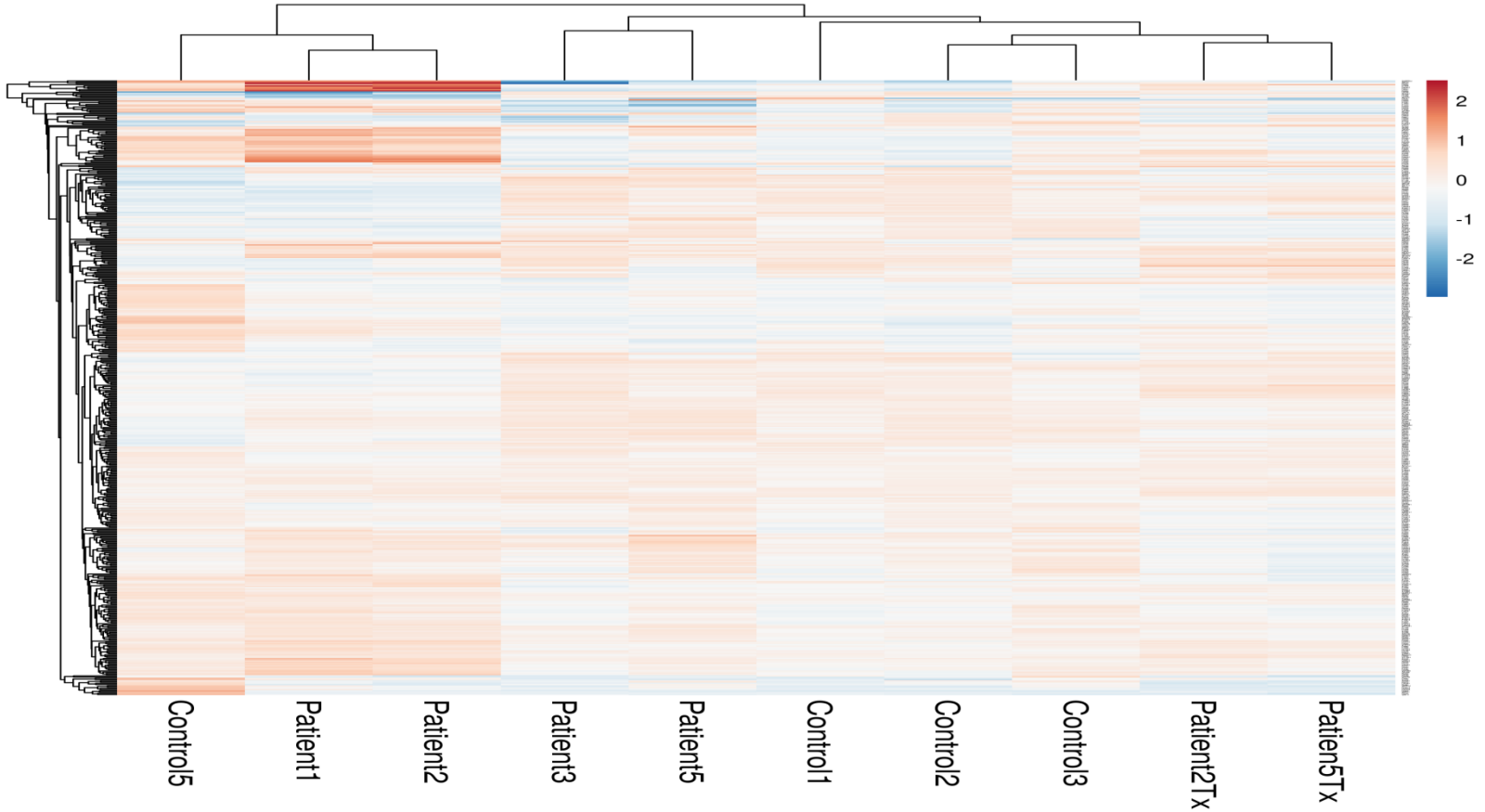

To explore the TMT data, volcano plots were drawn (figure 6.11) for individual pairs of patients and controls, patients before and after therapy and for an overall change between health and periodontitis (figure 6.12). Many proteins did not change. Following generally accepted rules a 2 fold cut off and p value of less than 0.05 was used to identify proteins of potential interest. The colours on the volcano plots highlight proteins with significant and twofold change. The proteins highlighted by the individual volcano plots in figure 6.11 are detailed in appendix 8.5 and 8.6. The proteins highlighted in the overall volcano plot in figure 6.12 are discussed further later and are listed in appendix 8.3.

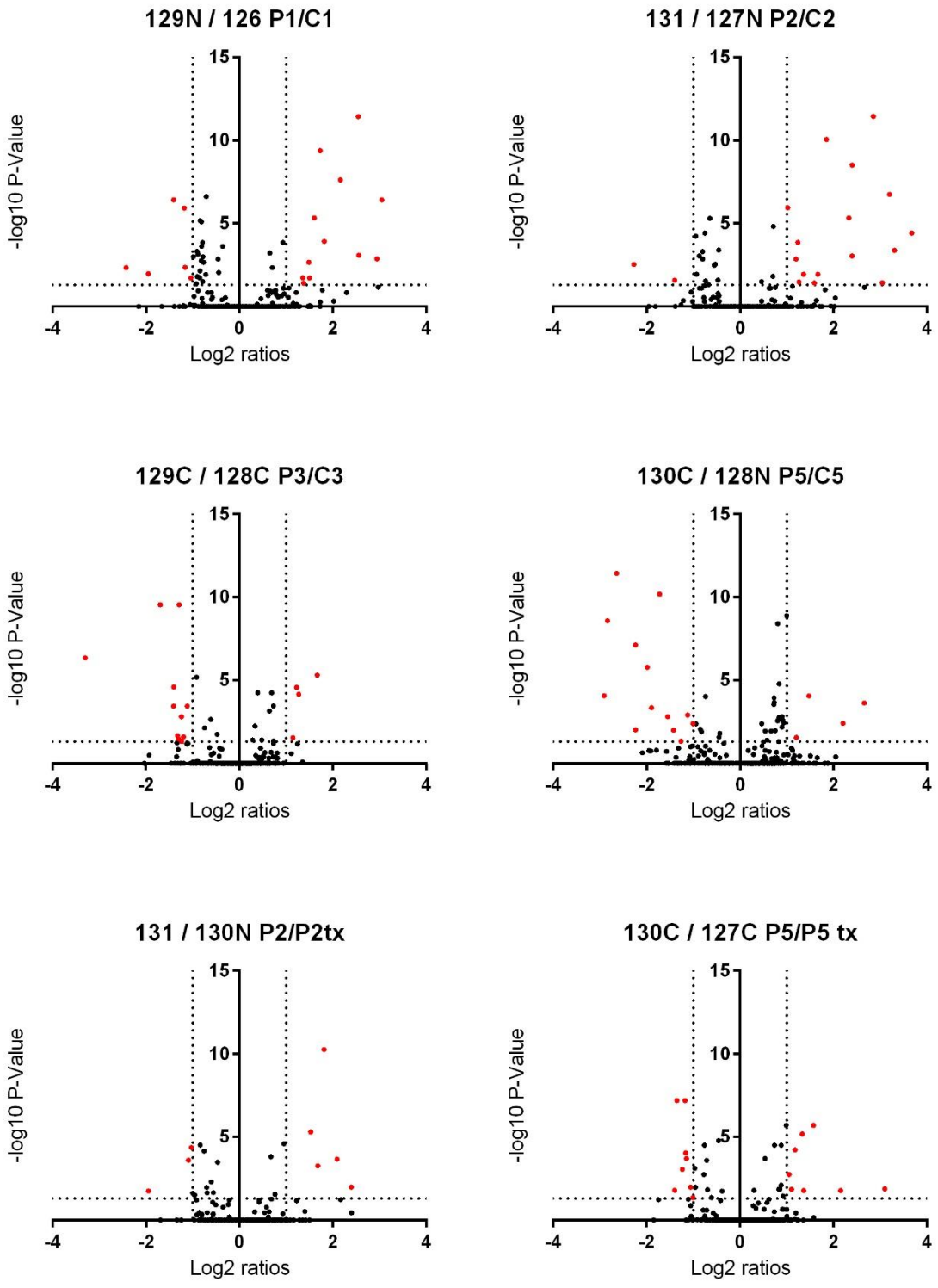

Figure 6.11: Volcano plots of individual periodontal patients versus controls. Red dots represent data where both greater than two fold and less than 0.05 significance are found. C represents controls and P periodontitis patients. Tx represents samples from periodontitis patients after treatment.

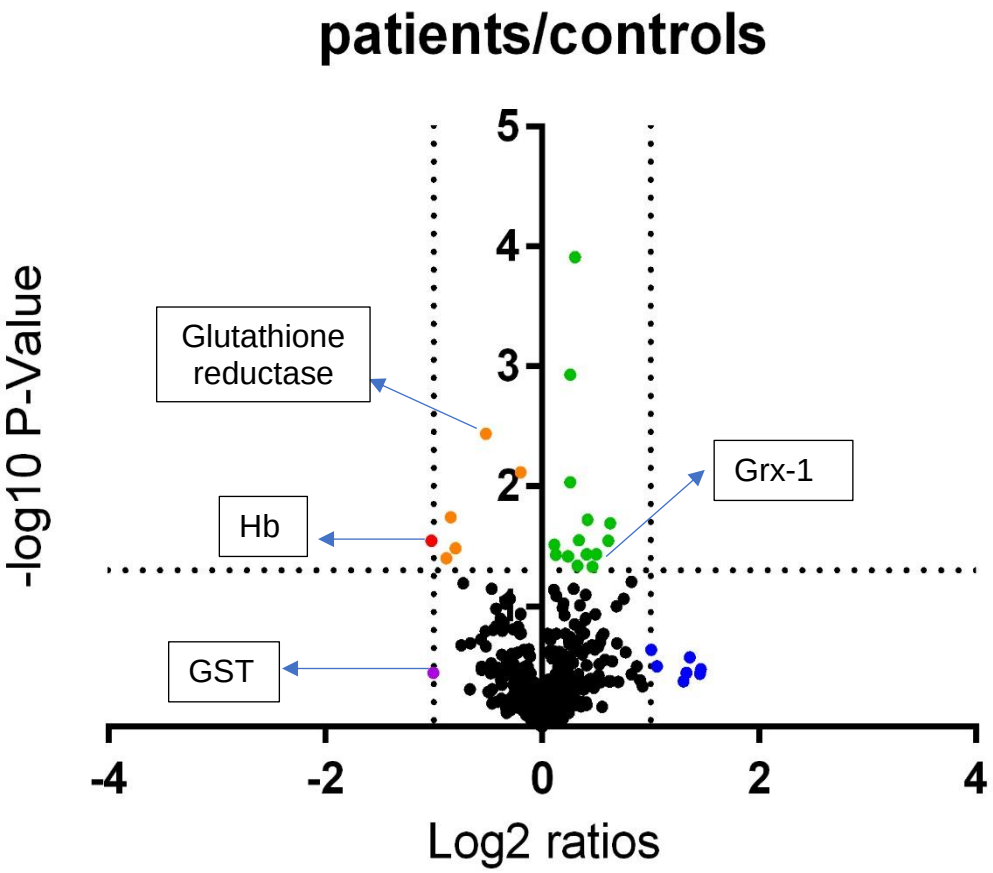

Figure 6.12: Volcano plot of all periodontal patients versus controls. Mean changes between age and gender matched pairs were calculated and assessed. The colours represent changes that are either more than 2 fold changed (blue and violet) or have significance less than 0.05 (orange or green) or that are both greater than two fold and less than 0.05 (red).

6.3.6 Western blotting for PSSG and actin

For detection of total glutathionylated proteins (PSSG) and actin protein, each sample was separated by SDS-PAGE, electroblotted on to membranes, which were then probed for these antigens. Patient samples and matched controls were run on the same gels to aid comparison. Figure 6.13 shows the scans of the membranes. In the images visible bands can been seen for glutathionylated protein and actin in some lanes. Due to the different quantities of actin detected it suggests that even though similar quantities of protein were added to each well there was unequal loading. The quantity of actin was then used to normalise the amount of PSSG detected. Figure 6.14 shows that there appears to be more PSSG in the patient samples than controls, however this difference did not reach statistical significance and there are no data for one control and neither of the post treatment patient samples.

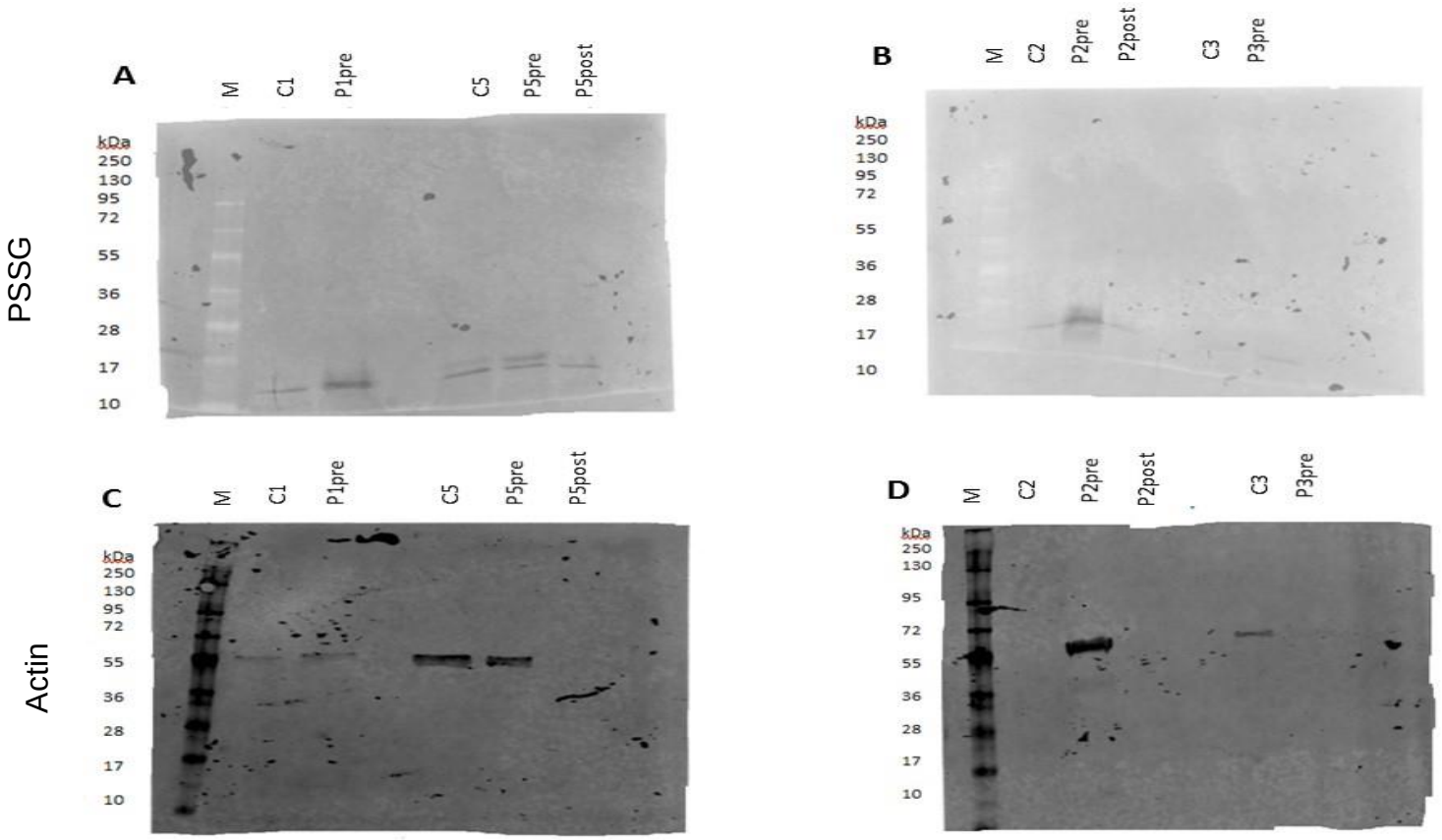

Figure 6.13: Western blots of PSSG and actin protein detected in patient and control neutrophil extracts. Figure A; Blot of PSSG, B; Blot of PSSG, C; Blot of actin and D; Blot of actin. The symbol for the lanes on the blot represents: M; molecular weight protein ladder, C; control, P; patient, pre; pre-treatment phase and post; post-treatment phase.

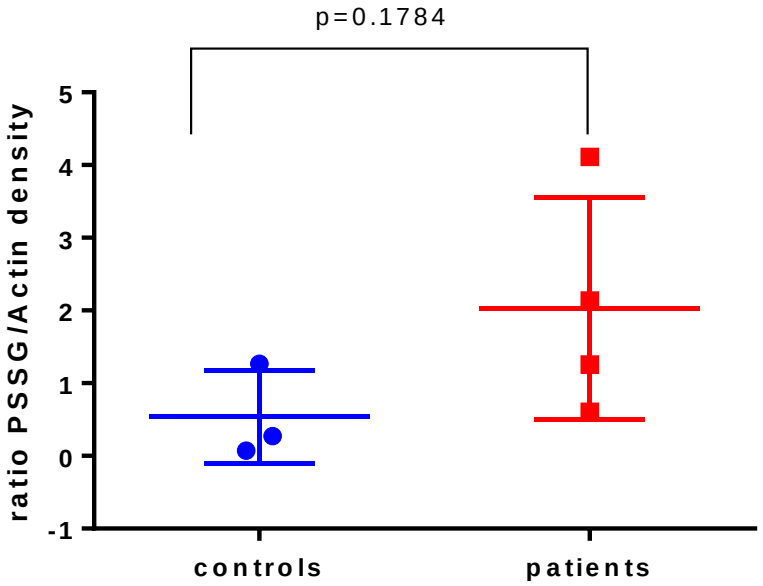

Figure 6.14: Densitometry analysis of the quantity of PSSG and Actin detected by Western blotting in control samples and patient samples pretreatment. Software Gel Analyzer was used to measure the darkness and volume of the bands found in figure 6.13. Middle bar represents the mean and the outer bars represent the standard deviation. Bands were not detected in sample C2 or in either of the post treatment patient samples. Data was analysed by Student's T Test.

6.4 Discussion

In this chapter, a pilot clinical study was done to examine the effect of periodontal therapy on neutrophil function and proteome, which were compared to age and gender matched control (ie non-periodontitis) donors. Various clinical measures were used to determine the periodontal status of the patient donors. A single dental clinician completed the periodontal disease diagnosis and a single dental hygienist provided therapy and monitored the periodontal condition of the four clinical subjects. A full mouth examination was conducted on mesial and medio buccal sites per tooth on the maxilla and mandible. Probing pocket depth (PPD, mm) and bleeding on probing (BOP, dichotomous absence or presence) were done using a dental probe and charted. For the definition of BOP, if the accumulated percentage of bleeding was less than 30%, it was defined as local bleeding. However, if the percentage was 30% or higher, it can be considered as general BOP (Lang et al., 1986). For examination of each individual's oral hygiene, presence of plaque at each tooth was recorded to determine the percentage of plaque surface. Table 6.2 shows that the two patients (N002 and N005) who came for pre-treatment and post-treatment visits had improvements in percentage BOP, PPD and CAL. Therefore, suggesting that the non-surgical periodontal treatment was successful for these two patients.

In this pilot clinical study, 5 patients were recruited, one patient withdrew leaving 4 patients at the start of the study; two patients completed the second recall visit. Using the data in chapter 6, a power calculation was done to determine the sample study. If the data in figure 6.14 was taken and expected that there is a difference between the controls and patients for statistical significance, the power calculation determines that it is expected to be 6 people (n=6) in this study sample. Therefore, if this study was to be done in the future, about 12 people need to be recruited accounting for any dropouts as well. As for this study, the dropout rates were quite high as the aim was for 5 people from clinic that is the pragmatic number for a small study. Unfortunately, some people did not come back.

From each donor, neutrophils were isolated and the viability of these cells was determined at time of isolation and 4h later. These experiments illustrated (figure 6.4) that the cells had comparable viability both at time of isolation and after the duration of the experiments used for both patient and healthy donors.

The first experiment to compare neutrophil properties between patients and healthy controls and between pre and post treatment of patients was neutrophil chemotaxis (figure 6.5). The number of donors was small and this may have impacted on the level of statistical significance reached when comparing the patients pre-treatment to healthy controls, however there was a trend towards there being fewer neutrophils migrated in patient isolations than controls suggesting that they were slower. This is in agreement with video microscopy analysis of neutrophil isolated from periodontitis patients using the Insall chamber in our laboratory (Roberts et al., 2015) and also similar, though less high throughput, Boyden chamber analysis of neutrophil movement by Kumar and Prakash, 2012). It is not possible to draw out conclusions from the two patients who returned after treatment as the numbers were very small and there was variability in response to the different chemoattractants (figure 6.6): improvements were seen for PBS and fMLP but one patient had decreased chemotaxis to IL8 whilst thither remained unchanged. Previously Roberts et al (2015) had found that there was a persistent reduction in speed (movement in any direction) though an improvement in velocity (movement towards the chemoattractant) for IL8 in periodontal disease patients compared to controls even after therapy. The Boyden chamber cannot give this level of information about movement but gives a more rapid answer that could be used to gain insight in greater numbers of patients more rapidly.

Next the intracellular total and oxidised glutathione levels were measured in isolated neutrophils. Previous studies have demonstrated that GSH is lower in periodontitis patients compared to controls (Dias et al., 2013, Bains & Bains 2015). Data in figure 6.7 suggests that the donors used in this study may also follow this trend however there is a large amount of variability between the donors and no significant difference were detected. Trends post-treatment were also variable (for figure 6.8) and there

appear to be no other studies that have attempted to measure this. Changes in glutathione in gingival crevicular fluid do show changes towards a more reducing environment after periodontal therapy however (Grant et al., 2010).

One of the main aims of this thesis was to explore if there was a change in glutathione status within neutrophils from periodontitis patients and if this was associated with changes in their chemotaxis. Glutathione may adduct reactive cysteines and thereby protect them from oxidation. To explore the potential for this cell lysates were created and the protein composition and glutathionylation status of the identified proteins was explored by quantitative mass spectrometry. In the first instance protein content was explored: visualisation of this can be seen in figure 6.10 as a heat map. This visualisation and clustering demonstrated some heterogeneity of the samples but generally clustered patient neutrophil profiles or control neutrophil protein profiles together.

Volcano plots were used to explore the data either as individuals (figure 6.11) or as the mean comparing pretreatment with controls (figure 6.12). The latter revealed a number of proteins of interest that were consistently altered between the donors. Three proteins that are part of the glutathione cycle were identified: glutaredoxin-1 (Grx-1) was increased significantly in a small quantity; GST was decreased over 2 fold but non-significantly, suggesting that less GSH was leaving the cell; and glutathione reductase was significantly decreased but less than 2 fold, perhaps indicating that the GSH cycle was perturbed and more GSSG may be present in the neutrophil cell. Future work could be to increase the amount of data in the volcano plot via an increased number of patients and to increase number of proteins for detection through greater off line separation.

Haemoglobin was identified as being significantly and over 2 fold decreased. In the neutrophil isolation procedure, erythrocytes ware lysed. However, there may be still a small contamination of red blood cells in the neutrophils, which may be caused by handling techniques during the isolation procedure.

Other proteins of interest that were highlighted (refer to appendix 8.3), either because they showed the most significant change in the analysis included glutathione reductase; DNA-apurinic or apyrimidinic site lyase; Cdc42; glycogen phosphorylase; Alcohol dehydrogenase class-3; or highest fold change was eosinophil peroxidase. These are discussed below.

In the glutathione redox cycle, oxidation of reduced glutathione by hydrogen peroxide is catalysed by glutathione peroxidase. It is then reconverted by glutathione reductase to form reduced glutathione. Therefore, glutathione reductase is important in the production of glutathione itself as the glutathione regeneration is catalysed by glutathione reductase. In neutrophils, glutathione reductase plays an important role in regulation of the respiratory burst and cell signalling. Glutathione reductase was significantly but slightly decreased ($p=0.004$, fold change 0.69; appendix 8.3). Decreases in this enzyme may contribute to the neutrophil status observed in periodontitis.

DNA-apurinic or apyrimidinic site lyase was altered in expression: mild decrease at fold change 0.87, $p=0.007$. DNA-apurinic or apyrimidinic site lyase plays a role to repair oxidative damage to DNA bases as it is a DNA repair enzyme. From the action of DNA glycosylases, this enzyme catalyses the excision of ribose residues at apurinic and apyrimidinic DNA sites. In neutrophils, it plays a role in repair of oxidative DNA damage. This is important as previous studies have shown that periodontitis patients have excess production of reactive oxygen species (ROS) (Dahiya et al., 2013) and this enzyme could help to repair the neutrophils DNA damage. DNA-apurinic or apyrimidinic site lyase deficient cells have been shown to have increased ROS, which is a hallmark of periodontal neutrophil phenotype and thus this may be a novel mechanism in these cells requiring further study.

Cell division control protein 42 homolog, or Cdc42, regulates signalling pathways that control diverse cellular functions including cell morphology, migration, endocytosis, and cell cycle progression. Cdc42 is also involved in regulating actin cytoskeleton and

processes that are dependent on actin cytoskeleton, such as phagocytosis, cell migration and chemotaxis. In actin cytoskeleton, Cdc42 regulates membrane receptors in the signal transduction pathway to form filopodia. Filopodia are membrane protrusions that extend from the plasma membrane in migratory cells that contain actin filaments and are able to function as sensory probes into the cellular surroundings. In neutrophils, Cdc42 are also involved in chemotaxis: an increase in Cdc42 activity can stimulate migration speed, such as seen in neutrophils isolated from knockout mice (Szczur et al., 2006).

Glycogen is accumulated in the liver and glycogen phosphorylase is one that plays an important role in carbohydrate metabolism. In this study, glycogen phosphorylase was found to be mildly but significantly increased (1.2 fold change, p=0.009). This protein catalyses the reaction initiating glycogen degradation, to generate glucose-1-phosphate the main source of glucose in the neutrophil. This suggests energy requirement in neutrophils in circulation in periodontitis patients.

Alcohol dehydrogenase class-3 (ADH3) catalyses the oxidation of long-chain primary alcohols by oxidation of glutathione. ADH3 acts as an S-hydroxymethyl glutathione dehydrogenase and as a glutathione-dependent formaldehyde dehydrogenase it can detoxify formaldehyde. Every cell in the human body produces formaldehyde and it is metabolized quickly to prevent accumulation. The reaction occurs at the expense of glutathione and therefore could be a source of glutathione loss within neutrophils. The change is ADH3 was fold change 1.23, p=0.0001.

Eosinophil peroxidase was increased by 2.57 fold change (p=0.23). It is found in the primary granules in innate immune cells in humans, including neutrophils. This enzyme catalyses the peroxidase reaction and shares some similarities with myeloperoxidase, wherein its products can disrupt bacterial cell walls. Eosinophil peroxidase is also found in eosinophils, which are the most common, but of low abundance, contaminant in neutrophil isolations. Previous studies (Thomas et al., 2015) have investigated the transcriptomic contribution of eosinophils to density

centrifugation isolated neutrophils and found that the portion of eosinophil transcripts is very low. Although eosinophils were not quantified in these studies previous experience within the lab from examining cytospins suggests eosinophil contamination to be low (Roberts et al., 2016).

Taken together there is a picture of altered glutathione regulation through changes of proteins recycling glutathione within neutrophils of periodontitis patients. Unfortunately, it was not possible to identify any glutathionylated protein targets, one of the desired aims of the study. This is most likely due to low abundance that was then diluted further by addition of the TMT tags for quantitation. Future studies could make use of iodo-TMT tags that could isolate glutathionylated proteins only. This approach has been used by a small number of groups (for example Pan et al., 2014). There are a number of controlled steps required to ensure that glutathionylated proteins are isolated instead of other cysteine modifications or oxidations.

6.5 Conclusion

In periodontitis patients prior to treatment, glutathione quantity was decreased and chemotactic ability was impaired compared to controls. The two review periodontitis patients showed improvement in clinical measures and also showed a slight (non-significant) increase in chemotaxis and increment of ratio GSH:GSSG. The redox balance in periodontitis patients was perturbed and appeared to affect the glutathione antioxidant and chemotactic ability of neutrophils. On top of this the glutathione enzyme systems also appeared to be perturbed within these neutrophils, perhaps giving some hints to mechanisms of the decrease in glutathione.

CHAPTER 7 – GENERAL DISCUSSION

CHAPTER 7

GENERAL DISCUSSION

Neutrophil cells are important leucocytes however can cause bystander damage to host tissues through ROS production. In normal cellular function glutathione is used to protect intracellular mechanisms from ROS mediated damage, and to maintain cellular homeostasis for example chemotaxis (Sakai et al., 2012). However, in periodontitis patients, neutrophils have lower intracellular glutathione level (Dias et al., 2013) and display aberrant chemotactic behaviour (Roberts et al., 2015). Therefore, this thesis comprises methods developed for exploring neutrophil function; particularly by exploration of neutrophils healthy volunteers and periodontitis patients to look at modulation of glutathione, the ability of neutrophils to chemotax and changes to the proteome. Biological experiments to assess and optimize functional assays of neutrophils for chemotaxis were made and measurement of intracellular glutathione. Proteomics workflows were produced for detection of glutathionylated proteins from neutrophils. Finally, a clinical study was done to look at these aspects in periodontitis patients.

The first novel finding of the work presented here was that manipulation of intracellular glutathione did result in changes in chemotaxis as hypothesised. This is in agreement with Sakai et al (2012) and provides a mechanistic view of changes in periodontitis patients, where our group and others have previously demonstrated decreases in chemotaxis. A summary of the results is shown in figure 7.1. Inflammatory reactions in periodontal tissues causes oxidative stress induces hydrogen peroxide (H_20_2) product. (Kiyoshima et al., 2012). For chemotaxis, hydrogen peroxide (H_20_2) is a second messenger that is produced at the leading edge of chemotaxis cells (Lennicke et al., 2015). Motile cells generate H_20_2 and initiate cofilin activity oxidation at protrusion (Cameron et al., 2015). Aquaporin helps H_20_2 accumulates into the cells as

it is inside the membrane can allow H_20 to pass through and activates protein tyrosine phosphatase thus activates the migration pathway (Tamma et al., 2018). Leucocyte migration at Fish's eyes in T-cells undergoes chemokinesis as it goes in any direction of chemotaxis (Deng & Huttenlocher 2012).

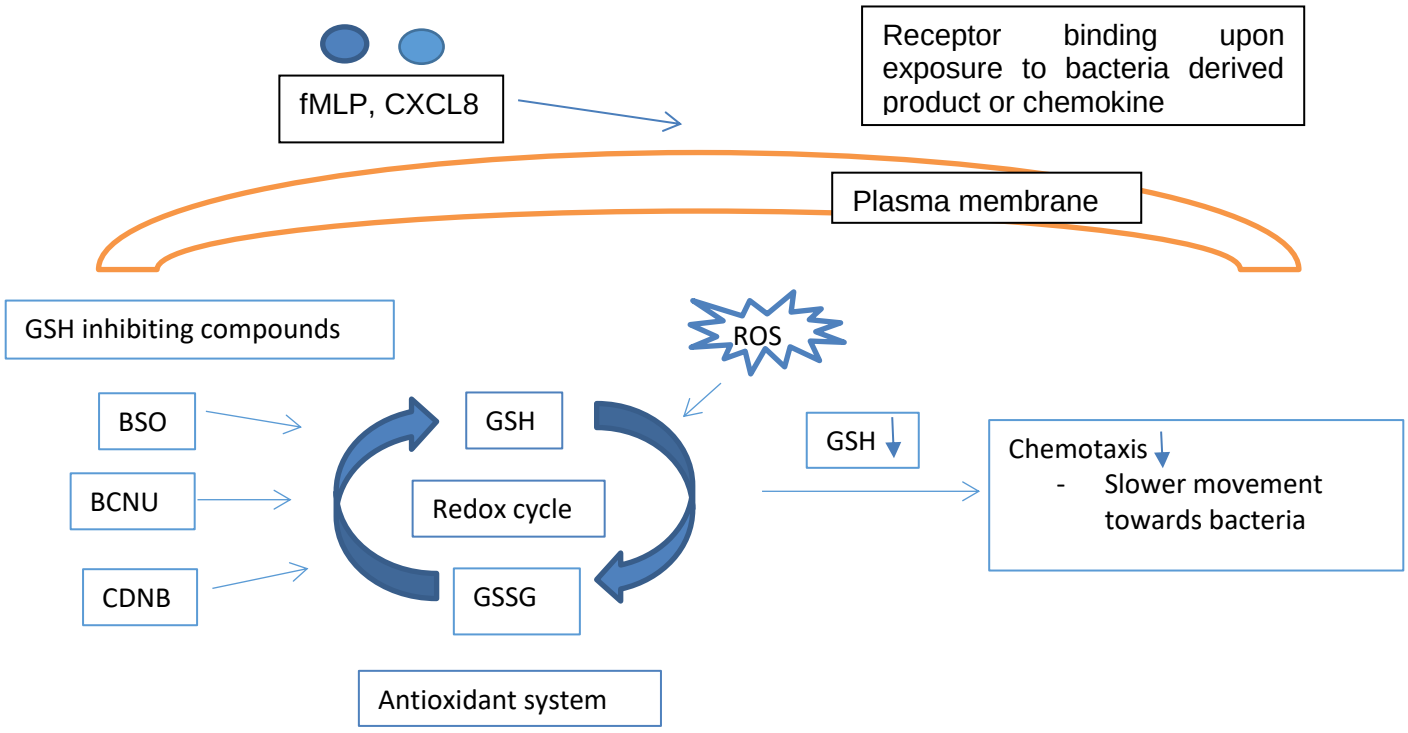

Figure 7.1: Glutathione depleting compounds decrease neutrophil chemotaxis.

The second novel aspect of this work was the establishment of the High-pH reverse phase methodology for two dimensional chromatography in our laboratories. At the commencement of these studies this method had just been published (Batth et al., 2014) and it allowed an increase in protein detection. Therefore, in this study, 2D off line HPLC-MS/MS technique was evaluated and implemented that increased the number of proteins discovered. When a new instrument arrived in the laboratory which

was the Q Exactive mass spectrometer (Thermo Fisher), more proteins were discovered as the system was much more sensitive and more information was obtained.

Advances in laboratory mass spectrometry capabilities by this thesis also encompassed detection of glutathionylated proteins and peptides. The results presented herein describe direct infusion ESI-MS and liquid chromatography-mass spectrometry LC-MS/MS can recognize protein glutathionylation in haemoglobin samples. Haemoglobin was used in this study as a model protein to test the system and glutathionylation was successfully detected at the whole protein and peptide level for the b chain as previously described. However, when using the neutrophil digested sample, it was not possible to find the modification. This may have been to do with low abundance or sample complexity (Chandramouli et al., 2009). Enrichment of glutathionylated peptides may be of interest. There are several ways to extract glutathionylated proteins such as BioGee and redox array technology (Mullen et al., 2015). Whilst the Bio-GEE technique was piloted in these studies it was never successful.

Finally, a clinical study utilized the methods developed and allowed for in depth analysis of the neutrophil proteome from periodontitis patients. This appears to be the first time that quantitative proteomics has been used to examine the neutrophil proteome of periodontitis patients. It could be seen that there was difference between patients and controls: and for one of the patients that underwent periodontal therapy, the change in the proteome after treatment made the overall protein profile more similar to neutrophils from healthy donors. Future work could involve analysis for proteins that were discovered from neutrophils in periodontitis patients, whether the proteins are involved in any activity from signalling or antimicrobial activity.

7.1 Major limitations

7.1.1 Recruitment of patients

In this study, only 5 patients were recruited, and 1 patient withdrew during the 1st sampling visit. The limitation of the study is on the number of periodontitis patients recruited within the limited time period of the PhD study. However, in the future, this study could be expanded to recruit more patients for the sampling to obtain a larger data.

In this pilot clinical study, 5 patients were recruited, one patient withdrew leaving 4 patients at the start of the study; two patients completed the second recall visit. Using the data in chapter 6, a power calculation was done to determine the sample study. If the data in figure 6.14 was taken and expected that there is a difference between the controls and patients for statistical significance, the power calculation determines that it is expected to be 6 people (n=6) in this study sample. Therefore, if this study was to be done in the future, about 12 people needs to be recruited including criteria for any dropout rates. As for this study, the dropout rates were quite high as the aim was for 5 people from clinic that is the pragmatic number for a small study. Unfortunately, some people did not come back.

7.1.2 Glutathionylated proteins

Glutathionylated proteins could not be identified in periodontitis patients, therefore various things need to be changed and new discoveries in the future. It is recommended to do N, N-biotinyl glutathione disulphide (bio-GEE) to study protein S-glutathionylation to detect glutathionylated proteins in proteomics. This treatment of cells mimics protein S-glutathionylation and allows for purification using streptavidin-agarose.

7.1.3 High performance liquid chromatography (HPLC)

The HPLC that was used in this study was damaged, therefore new HPLC equipment was bought by the laboratory, however, it did not work in the same way, in that peptides could not be detected. Hence, for future recommendation, a replicate procedure of the High-pH reverse phase HPLC could be coupled offline to the Q Exactive mass spectrometer. Q Exactive mass spectrometer is the newest mass spectrometer equipment in the laboratory and is much faster, has increased sensitivity, increased resolution and less ion loss. Hence, Q Exactive mass spectrometer was much better compared to the Orbitrap mass spectrometer as it detected increased number of proteins.

7.2 Recommendations for future research

The results outlined in this thesis point to glutathionylated proteins in neutrophil cells, which could improve neutrophil chemotactic behaviour and redox balance with periodontal treatment. However, this study had a limitation in the numbers of periodontal patients recruited. Therefore, it is recommended to do a similar study to recruit more patients for the sampling. A better technique could also be developed for detecting glutathionylated proteins in proteomics such as N, N-biotinyl glutathione disulphide (bio-GEE) to study protein S-glutathionylation. Further analysis could be done on the proteins that were discovered in the heatmap to pick up any proteins and looked at individual proteins. Therefore, by understanding the role of redox balance in neutrophils to the inflammation, more strategies could be applied to perturb the redox balance, or any other strategies could be identifying to prevent the progression of periodontitis.

REFERENCES

Al-Rasheed A. Elevation of white blood cells and platelet counts in patients having chronic periodontitis. Vol. 24, Saudi Dental Journal. 2012. p. 17–21.

Alton M. Selective Modification of Glutathione Metabolism. Vol. 220, Science. 1983. p. 472–7.

André, M, Le Caer JP, Greco C, Planchon S, El Newer W, Boucheix C, Rubinstein E, Chamot-Rooke J, Le Naour F. Proteomic analysis of the tetraspanin web using LC-ESI-MS / MS and MALDI-FTICR-MS'. 2006. pp. 1437–1449.

Andrew N, Insall RH. Chemotaxis in shallow gradients is mediated independently of PtdIns 3-kinase by biased choices between random protrusions. Vol. 9, Nature Cell Biology. 2007. p. 193–200.

Appenzeller-Herzog C. Glutathione- and non-glutathione-based oxidant control in the endoplasmic reticulum. Vol. 124, Journal of Cell Science. 2011. p. 847–55.

Asmat, U., Abad, K. and Ismail, K. Diabetes mellitus and oxidative stress-A concise review. Vol. 24, Saudi Pharmaceutical Journal. 2016. p. 547–53.

Babior BM, Curnutte JT, McMurrich BJ. The particulate superoxide-forming system from human neutrophils. Vol. 58, J.Clin.Invest. 1976. p. 989–96.

Bains R, Bains V. The antioxidant master glutathione and periodontal health. Vol. 12, Dental Research Journal. 2015. p. 389.

Ball JA, Vlisidou I, Blunt MD, Wood W, Ward SG. Hydrogen Peroxide Triggers a Dual Signaling Axis To Selectively Suppress Activated Human T Lymphocyte Migration. J Immunol. 2017;198(9):3679–89.

Banerjee S, Mazumdar S. Electrospray Ionization Mass Spectrometry: A Technique to Access the Information beyond the Molecular Weight of the Analyte. Vol. 2012, International Journal of Analytical Chemistry. 2012. p. 1–40.

Barber MR, Pantschenko AG, Hinckley LS, Yang TJ. Inducible and constitutive in vitro neutrophil chemokine expression by mammary epithelial and myoepithelial cells. Clin Diagn Lab Immunol. 1999;6(6):791–8.

Batth TS, Francavilla C, Olsen J V. Off-line high-pH reversed-phase fractionation for in-depth phosphoproteomics. Vol. 13, Journal of Proteome Research. 2014. p. 6176–86.

Beckman KB, Ames BN. The free radical theory of aging matures. Vol. 78, Physiological reviews. 1998. p. 547–81.

Bertolotto M, Contini P, Ottonello L, Pende A, Dallegri F, Montecucco F. Neutrophil migration towards C5a and CXCL8 is prevented by non-steroidal anti-inflammatory drugs via inhibition of different pathways. Vol. 171, British Journal of Pharmacology. 2014. p. 3376–93.

Bingham CO, Moni M. Periodontal disease and rheumatoid arthritis: The evidence accumulates for complex pathobiologic interactions. Vol. 25, Current Opinion in Rheumatology. 2013. p. 345–53.

Birben E, Sahiner UM, Sackesen C, Erzurum S, Kalayci O. Oxidative stress and antioxidant defense. Vol. 5, World Allergy Organization Journal. 2012. p. 9–19.

Bishop CR, Rothstein G, Ashenbrucker HE, Athens JW. Leukokinetic Studies. Vol. 50, Journal of Clinical Investigation. 2008. p. 1678–89.

Borges I, Machado Moreira EA, Filho DW, De Oliveira TB, Da Silva MBS, Fröde TS. Proinflammatory and oxidative stress markers in patients with periodontal disease. Mediators Inflamm. 2007;2007.

Borregaard N, Cowland JB. Granules of the human neutrophilic polymorphonuclear leukocyte. Vol. 89, Blood. 1997. p. 3503–21.

Borregaard N, Lollike K, Kjeldsen L, Sengeløv H, Bastholm L, Nielsen MH, et al. Human neutrophil granules and secretory vesicles. Vol. 51, European Journal of Haematology. 1993. p. 187–98.

Brennan JP, Miller JI, Fuller W, Wait R, Begum S, Dunn MJ, Eaton P. The utility of N, N-biotinyl glutathione disulfide in the study of protein S-glutathiolation. Mol Cell Proteomics. 2006. Vol 5:215–225.

Brodbelt, J. S. Ion Activation Methods for Peptides and Proteins. Analytical Chemistry, 2016. pp. 30–51.

Bryant, RE, Des Prez RM, Rogers DE. Studies on human leukocyte motility. Journal of experimental medicine, 1966 pp. 483–499.

Cai Z, Yan L-J. Protein Oxidative Modifications: Beneficial Roles in Disease and Health. J Biochem Pharmacol Res. 2013;1(1):15–26.

Cameron JM, Gabrielsen M, Chim YH, Munro J, McGhee EJ, Sumpton D, et al. Polarized cell motility induces hydrogen peroxide to inhibit cofilin via cysteine oxidation. Vol. 25, Current Biology. 2015. p. 1520–5.

Cañas B, Lopez-Ferrer D, Ramos-Fernandez A, Camafeita E, Calvo E. Mass spectrometry technologies for proteomics. Briefings in Functional Genomics and Proteomics, 4(4), 2006. pp. 295–320.

Cartwright, G., Athens, J. and Wintrobe, M. The kinetics of granulopoiesis in normal man. Blood. 1964. pp. 780–803.

Chandramouli K, Qian P-Y. Proteomics: Challenges, Techniques and Possibilities to Overcome Biological Sample Complexity. Vol. 1, Human Genomics and Proteomics. 2009.

Chang YC. Hseih YS, Lii CK, Huang FM, Tai KW, Chou MY. Induction of c-fos expression by nicotine in human periodontal ligament fibroblasts is related to cellular thiol levels. Journal of Periodontal Research. 2003. pp. 44–50.

Chapple IL, Brock G, Eftimiadi C, Matthews JB. Glutathione in gingival crevicular fluid and its relation to local antioxidant capacity in periodontal health and disease. Mol Pathol. 2002. pp. 367–373.

Chapple ILC, and Matthews JB. The role of reactive oxygen and antioxidant species in periodontal tissue destruction. Periodontology 2000. 2007. pp. 160–232.

Chen HC. Boyden Chamber Assay. Cell Migration. Vol. 294, 2005. pp. 015–022.

Chethana K, Padma R, Suragimath G, Anil M, Jagadish Pai B, Walvekar A. A study to assess and compare the peripheral blood neutrophil chemotaxis in smokers and non smokers with healthy periodontium, gingivitis, and chronic periodontitis. Vol. 16, Journal of Indian Society of Periodontology. 2012. p. 54.

Chiang H Sen, Maric M. Lysosomal thiol reductase negatively regulates autophagy by altering glutathione synthesis and oxidation. Free Radic Biol Med. 2011;51(3):688–99.

Cooper AJ, Pinto JT, Callery PS. Reversible and irreversible protein glutathionylation: biological and clinical aspects. Expert Opin Drug Metab Toxicol. 2011;7(7):891–910.

Cooper CE, Vollaard NBJ, Choueiri T, Wilson MT. Exercise, free radicals and oxidative stress. Biochemical Society transactions. 2002. pp. 280–5.

Cooper PR, Palmer LJ, Chapple ILC. Neutrophil extracellular traps as a new paradigm in innate immunity: friend or foe?. Periodontology 2000. 2013. pp. 165–197.

D’Aiuto F, Parkar M, Andreou G, Suvan J, Brett PM, Ready D, Tonetti MS. Periodontitis and systemic inflammation: control of the local infection is associated with a reduction in serum inflammatory markers. J Dent.Res. 2004. pp. 156–160.

Dahiya P, Bhardwaj R, Chaudhary K, Kamal R, Gupta R, Kaur S. Reactive oxygen species in periodontitis. J Indian Soc Periodontol. 2013;17(4):411.

Dahlgren C, Karlsson A. Respiratory burst in human neutrophils. Journal of Immunological Methods. 1999. pp. 3–14.

Dale DC, Boxer L, Liles WC. The phagocytes - neutrophils and monocytes. Blood. Vol. 112(4), 2008. pp. 935–946.

Dalle-Donne I, Giustarini D, Rossi R, Colombo R, Milzani A. Reversible S-glutathionylation of Cys374 regulates actin filament formation by inducing structural changes in the actin molecule. Free Radic Biol Med. 2003;34(1):23–32.

de Pablo P, Chapple ILC, Buckley CD, Dietrich T. Periodontitis in systemic rheumatic diseases. Nat Rev Rheumatol. 2009;5(4):218–24.

Deng Q, Huttenlocher A. Leukocyte migration from a fish eye's view. Vol. 125, Journal of Cell Science. 2012. p. 3949–56.

Dias IHK, Chapple ILC, Milward M, Grant MM, Hill E, Brown J, et al. Sulforaphane Restores Cellular Glutathione Levels and Reduces Chronic Periodontitis Neutrophil Hyperactivity In Vitro. PLoS One. 2013;8(6).

Dias IHK, Matthews JB, Chapple ILC, Wright HJ, Dunston CR, Griffiths HR. Activation of the neutrophil respiratory burst by plasma from periodontitis patients is mediated by pro-inflammatory cytokines. J Clin Periodontol. 2011;38(1):1–7.

Dickinson BC, Chang Christopher J. Chemistry and biology of reactive oxygen species in signaling or stress responses. Nat Chem Biol. 2012. pp. 504–511.

Doroshenko T, Chaly Y, Savitskiy V, Maslakova O, Portyanko A, Gorudko I. Phagocytosing neutrophils down-regulate the expression of chemokine receptors CXCR1 and CXCR2. Blood. 2002;100(7):2668–71.

Dro W. Aging-related changes in the thiol / disulfide redox state : implications for the use of thiol antioxidants q. 2002. pp. 1331–1343.

Epstein FH, Weiss SJ. Tissue Destruction by Neutrophils. New England Journal of Medicine. 1989. pp. 365–376.

Falick AM, Shackleton CHL, Green BN, Witkowska HE. Tandem mass spectrometry in the clinical analysis of variant hemoglobins. Rapid Commun Mass Spectrom. 1990;4(10):396–400.

Falk W, Goodwin RH, Leonard EJ. A 48-well micro chemotaxis assembly for rapid and accurate measurement of leukocyte migration. J Immunol Methods. 1980;33(3):239–47.

Faurschou M, Borregaard N. Neutrophil granules and secretory vesicles in inflammation. Microbes and Infection. 2003. pp. 1317–1327.

Feng D, Nagy JA, Pyne K, Dvorak HF, Dvorak AM. Neutrophils emigrate from venules by a transendothelial cell pathway in response to FMLP. J Exp Med. 1998;187(6):903–15.

Filippi MD. Mechanism of Diapedesis: Importance of the Transcellular Route. Advances in Immunology. 2016. pp. 25–53.

Fisher-Wellman K, Bloomer RJ. Acute exercise and oxidative stress: a 30 year history. Dyn Med. 2009. p. 1.

Forman HJ, Zhang H, Rinna A. Glutathione: Overview of its protective roles, measurement, and biosynthesis. Molecular Aspects of Medicine. 2009. pp. 1–12.

Fowler EB, Breault LG, Cuenin MF. Periodontal disease and its association with systemic disease. Vol. 166. Mil Med. 2001. p. 85–9.

Franco R, Cidlowski JA. Apoptosis and glutathione: Beyond an antioxidant. Vol. 16, Cell Death and Differentiation. 2009. p. 1303–14.

Gamonal J, Acevedo A, Bascones A, Jorge O, Silva A. Characterization of cellular infiltrate, detection of chemokine receptor CCR5 and interleukin-8 and RANTES chemokines in adult periodontitis. J Periodontal Res. 2001;36(3):194–203.

Gomez-Lopez N, Vadillo-Ortega F, Estrada-Gutierrez G. Combined Boyden-flow cytometry assay improves quantification and provides phenotypification of leukocyte chemotaxis. PLoS One. 2011;6(12).

Grant MM, Brock GR, Matthews JB, Chapple ILC. Crevicular fluid glutathione levels in periodontitis and the effect of non-surgical therapy. J Clin Periodontol. 2010;37(1):17–23.

Grant MM, Creese AJ, Barr G, Ling MR, Scott AE, Matthews JB, et al. Proteomic analysis of a noninvasive human model of acute inflammation and its resolution: The twenty-one day gingivitis model. J Proteome Res. 2010;9(9):4732–44.

Graves DT, Cochran D. The contribution of interleukin-1 and tumor necrosis factor to periodontal tissue destruction. J Periodontol. 2003;74(3):391–401.

Griffith OW. Mechanism of action, metabolism, and toxicity of buthionine sulfoximine and its higher homologs, potent inhibitors of glutathione synthesis. J Biol Chem. 1982;257(22):13704–12.

Gygi SP, Rist B, Gerber SA, Turecek F, Gelb MH, Aebersold R. Quantitative analysis of complex protein mixtures using isotope-coded affinity tags. Vol. 17, Nature Biotechnology. 1999. p. 994–9.

Haag AM. Mass analyzers and mass spectrometers. In: Advances in Experimental Medicine and Biology. 2016. p. 157–69.

Hajishengallis E, Hajishengallis G. Neutrophil homeostasis and periodontal health in children and adults. Vol. 93, Journal of Dental Research. 2014. p. 231–7.

Hale J. Advantageous uses of mass spectrometry for the quantification of proteins. Int J Proteomics. 2013;doi: 10.1155/2013/219452.

Harlan JM, Levine JD, Callahan KS, Schwartz BR, Harker LA. Glutathione redox cycle protects cultured endothelial cells against lysis by extracellularly generated hydrogen peroxide. J Clin Invest. 1984;73(3):706–13.

Hasturk H, Kantarci A. Activation and resolution of periodontal inflammation and its systemic impact. Periodontol 2000. 2015;69(1):255–73.

Hatzelmann A, Schatz M, Ullrich V. Involvement of glutathione peroxidase activity in the stimulation of 5-lipoxygenase activity by glutathione-depleting agents in human polymorphonuclear leukocytes. Eur J Biochem. 1989;180(3):527–33.

Hauser NJ, Han H, McLuckey SA, Basile F. Electron transfer dissociation of peptides generated by microwave D-cleavage digestion of proteins. J Proteome Res. 2008;7(5):1867–72.

Hentze H, Gantner F, Kolb SA, Wendel A. Depletion of hepatic glutathione prevents death receptor-dependent apoptotic and necrotic liver injury in mice. Am J Pathol. 2000;156(6):2045–56.

Hirschfeld J, Chapple ILC, White PC, Milward MR, Cooper PR,. Modulation of Neutrophil Extracellular Trap and Reactive Oxygen Species Release by Periodontal Bacteria. Infect Immun. 2017;85(12):1–14.

Ho CS, Lam CWK, Chan MHM, Cheung RCK, Law LK, Lit LCW, et al. Electrospray ionisation mass spectrometry: principles and clinical applications. Clin Biochem Rev. 2003;24(1):3–12.

Hughes R, Andrew PW, Kilvington S. Enhanced killing of Acanthamoeba cysts with a plant peroxidase-hydrogen peroxide-halide antimicrobial system. Appl Environ Microbiol. 2003;69(5):2563–7.

Hüttenhain R, Hess S. A combined top-down and bottom-up MS approach for the characterization of hemoglobin variants in Rhesus monkeys. Proteomics. 2010;10(20):3657–68.

Hwang C, Sinskey AJ, Lodish HF. Oxidized redox state of glutathione in the endoplasmic reticulum. Science (80-). 1992;257(5076):1496–502.

Janetopoulos C, Firtel RA. Directional sensing during chemotaxis. Vol. 582, FEBS Letters. 2008. p. 2075–85.

Johansson T, Lindberg S, Åstot C. Novel glutathione conjugates of phenyl isocyanate identi fi ed by ultra-performance liquid chromatography / electrospray ionization mass spectrometry and nuclear magnetic resonance. 2014. pp. 68–79.

Jones DP, Park Y, Gletsu-Miller N, Liang Y, Yu T, Accardi CJ, et al. Dietary sulfur amino acid effects on fasting plasma cysteine/cystine redox potential in humans. Nutrition. 2011;27(2):199–205.

Kaplan MJ, Radic M. Neutrophil Extracellular Traps: Double-Edged Swords of Innate Immunity. J Immunol. 2012;189(6):2689–95.

Kaplowitz N, Tak YA, Ookhtens M. The Regulation of Hepatic Glutathione. Annual Review of Pharmacology and Toxicology. 1985. pp. 715–744.

Kehrer JP. The effect of bcnu (carmustine) on tissue glutathione reductase activity. Toxicol Lett. 1983;17(1–2):63–8.

Kim MS, Pandey A. Electron transfer dissociation mass spectrometry in proteomics. Vol. 12, Proteomics. 2012. p. 530–42.

Kiyoshima T, Enoki N, Kobayashi I, Sakai T, Nagata K, Wada H, et al. Oxidative stress caused by a low concentration of hydrogen peroxide induces senescence-like changes in mouse gingival fibroblasts. Vol. 30, International Journal of Molecular Medicine. 2012. p. 1007–12.

Klebanoff SJ. Myeloperoxidase-halide-hydrogen peroxide antibacterial system. J Bacteriol. 1968;95(6):2131–8.

Klyubin IV, Ksenia M, Kirpichnikova I. Hydrogen peroxide-induced chemotaxis of mouse peritoneal neutrophils. Eur J Cell Biol. 1996;70:3

Kolaczkowska E, Kubes P. Neutrophil recruitment and function in health and inflammation. Nat Rev Immunol. 2013;13(3):159–75.

Kuhns DB, Fink DL, Choi U, Sweeney C, Lau K, Priel DL, et al. Regular Article Cytoskeletal abnormalities and neutrophil dysfunction in WDR1 de fi ciency. 2019;128(17):2135–44.

Kumar J, Teoh SL, Das S, Mahakknaukrauh P. Oxidative stress in oral diseases: Understanding its relation with other systemic diseases. Vol. 8, Frontiers in Physiology. 2017.

Kumar RS, Prakash S. Impaired neutrophil and monocyte chemotaxis in chronic and aggressive periodontitis and effects of periodontal therapy. Indian J Dent Res. 2012;23(1):69–74.

Lang NP, Joss A, Orsanic T, Gusberti FA, Siegrist BE. Bleeding on probing. A predictor for the progression of periodontal disease? J Clin Periodontal. 1986;(July):590-6.

Lanucara F, Eyers CE. Mass spectrometric-based quantitative proteomics using SILAC. In: Methods in Enzymology. 2011. p. 133–50.

Larson CL, Shah DH, Dhillon AS, Call DR, Ahn S, Haldorson GJ, et al. Campylobacter jejuni invade chicken LMH cells inefficiently and stimulate differential expression of the chicken CXCLi1 and CXCLi2 cytokines. Microbiology. 2008;154(12):3835–47.

Lassing I, Schmitzberger F, Björnstedt M, Holmgren A, Nordlund P, Schutt CE, et al. Molecular and Structural Basis for Redox Regulation of β-Actin. J Mol Biol. 2007;370(2):331–48.

Lennicke C, Rahn J, Lichtenfels R, Wessjohann LA, Seliger B. Hydrogen peroxide - Production, fate and role in redox signaling of tumor cells. Vol. 13, Cell Communication and Signaling. 2015.

Ley K, Laudanna C, Cybulsky MI, Nourshargh S. Getting to the site of inflammation: The leukocyte adhesion cascade updated. Vol. 7, Nature Reviews Immunology. 2007. p. 678–89.

Li MX, Shan JL, Wang D, He Y, Zhou Q, Xia L, Zeng LL, Li ZP, Wang G, Yang ZZ. Human apurinic/apyrimidinic endonuclease 1 translocalizes to mitochondria after photodynamic therapy and protects cells from apoptosis. Cancer Sci;2012. 103(5):882-8.

Ling MR, Chapple ILC, Matthews JB. Neutrophil superoxide release and plasma C-reactive protein levels pre- and post-periodontal therapy. J Clin Periodontol. 2016;43(8):652–8.

Loos G, Schepdael A Van, Cabooter D. Quantitative mass spectrometry methods for pharmaceutical analysis. 2016;

Lushchak VI. Glutathione Homeostasis and Functions: Potential Targets for Medical Interventions. Journal of Amino Acids. 2012. pp. 1–26.

Manda A, Pruchniak MP, Araźna M, Demkow UA. Neutrophil extracellular traps in physiology and pathology. Vol. 39, Central European Journal of Immunology. 2014. p. 116–21.

Masella R, Di Benedetto R, Varì R, Filesi C, Giovannini C. Novel mechanisms of natural antioxidant compounds in biological systems: Involvement of glutathione and glutathione-related enzymes. Vol. 16, Journal of Nutritional Biochemistry. 2005. p. 577–86.

Mates J, Gomez C, Castro I. Antioxidant enzymes and human diseases. Clin Biochem. 1999;32(8):595–603.

Matthews JB, Wright HJ, Roberts A, Cooper PR, Chapple ILC. Hyperactivity and reactivity of peripheral blood neutrophils in chronic periodontitis. Clin Exp Immunol. 2007;147(2):255–64.

Matthews JB, Wright HJ, Roberts A, Ling-Mountford N, Cooper PR, Chapple ILC. Neutrophil hyper-responsiveness in periodontitis. J Dent Res. 2007;86(8):718–22.

McCall MR, Frei B. Can antioxidant vitamins maternally reduce oxidative damage in humans?'. Free Radical Biol. Med. 1999. pp. 1034–1053.

Meredith MJ, Reed DJ. Status of the mitochondrial pool of glutathione in the isolated hepatocyte. Journal of Biological Chemistry. 1982. pp. 3747–3753.

Mergenhagen SE, Tempel TR, Snyderman R. Immunologic Reactions and Periodontal Inflammation. Journal of Dental Research. 1970. pp. 256–261.

Monk PN, Scola AM, Madala P, Fairlie DP. Function, structure and therapeutic potential of complement C5a receptors. Vol. 152, British Journal of Pharmacology. 2007. p. 429–48.

Muinonen-Martin AJ, Knecht DA, Veltman DM, Thomason PA, Kalna G, Insall RH. Measuring chemotaxis using direct visualization microscope chambers. Vol. 1046, Methods in Molecular Biology. 2013. p. 307–21.

Muinonen-Martin AJ, Veltman DM, Kalna G, Insall RH. An improved chamber for direct visualisation of chemotaxis. Vol. 5, PLoS ONE. 2010.

Mullen L, Vaudry D, Chan P, Ghezzi P, Bottazzi B, Seavill M, Hammouz R. Development of ‘Redox Arrays’ for identifying novel glutathionylated proteins in the secretome. Vol. 5, Scientific Reports. 2015. p. 14630.

Muller D. 2018 Rheumatoid Arthritis. Integrative Medicine. 2018. p. 493–500.e1.

Muller WA. Getting Leukocytes to the Site of Inflammation. Vol. 50, Veterinary Pathology. 2013. p. 7–22.

Nazir MA. Prevalence of periodontal disease, its association with systemic diseases and prevention. Vol. 11, International journal of health sciences. 2017. p. 72–80.

Nicu EA, Van Der Velden U, Nieuwland R, Everts V, Loos BG. Elevated platelet and leukocyte response to oral bacteria in periodontitis. Vol. 7, Journal of Thrombosis and Haemostasis. 2009. p. 162–70.

Niethammer P, Grabher C, Look AT, Mitchison TJ. A tissue-scale gradient of hydrogen peroxide mediates rapid wound detection in zebrafish. Vol. 459, Nature. 2009. p. 996–9.

Ohyama H, Nakasho K, Yamanegi K, Noiri Y, Kuhara A, Kato-Kogoe N, et al. An unusual autopsy case of pyogenic liver abscess caused by periodontal bacteria. Vol. 62. Jpn Infect Dis. 2009. p. 381–3.

Ong S-E, Blagoev B, Kratchmarova I, Kristensen DB, Steen H, Pandey A. Stable isotope labeling by amino acids in cell culture, SILAC, as a simple and accurate approach to expression proteomics. Vol. 1, Molecular & cellular proteomics : MCP. 2002. p. 376–86.

Ookhtens M, Kaplowitz N. Role of the liver in interorgan homeostasis of glutathione and cyst(e)ine. Vol. 18, Seminars in Liver Disease. 1998. p. 313–29.

Page RC, Eke PI, Wei L, Thornton-Evans G, Genco RJ. Update of the Case Definitions for Population-Based Surveillance of Periodontitis. J Periodontol. 2012;(December):1–8.

Pan K-T, Chen Y-Y, Pu T-H, Chao Y-S, Yang C-Y, Bomgarden RD, et al. Mass Spectrometry-Based Quantitative Proteomics for Dissecting Multiplexed Redox Cysteine Modifications in Nitric Oxide-Protected Cardiomyocyte Under Hypoxia. Vol. 20, Antioxidants & Redox Signaling. 2013. p. 1365–81.

Peng J, Mandal R, Sawyer M, Li XF. Characterization of intact hemoglobin and oxaliplatin interaction by nanoelectrospray ionization tandem mass spectrometry. Clin Chem. 2005;51(12):2274–81.

Perutz MF, Rossmann MG. Cullis AF. Muirhead H, Will G, North AC. The structure of haemoglobin. A three dimensional Fourier synthesis at 5.5 A resolution, obtained by X-ray analysis. Nature Vol 85. 1960. p. 416.

Potempa J, Mydel P, Koziel J. The case for periodontitis in the pathogenesis of rheumatoid arthritis. Vol. 13, Nature Reviews Rheumatology. 2017. p. 606–20.

Rahman K. Studies on free radicals, antioxidants, and co-factors. Clin Interv Aging. 2007;2(2):219–36.

Regazzoni L, Panusa A, Yeum KJ, Carini M, Aldini G. Hemoglobin glutathionylation can occur through cysteine sulfenic acid intermediate: Electrospray ionization LTQ-Orbitrap hybrid mass spectrometry studies. J Chromatogr B Anal Technol Biomed Life Sci. 2009;877(28):3456–61.

Roberts H. Neutrophil function in chronic inflammatory disease states. Doctoral thesis. University of Birmingham. 2016.

Roberts H, White P, Dias I, McKaig S, Veeramachaneni R, Thakker N, et al. Characterization of neutrophil function in Papillon-Lefèvre syndrome. Vol. 100, Journal of Leukocyte Biology. 2016. p. 433–44.

Roberts HM, Ling MR, Insall R, Kalna G, Spengler J, Grant MM, et al. Impaired neutrophil directional chemotactic accuracy in chronic periodontitis patients. J Clin Periodontol. 2015;42(1):1–11.

Rørvig S, Østergaard O, Heegaard NHH, Borregaard N. Proteome profiling of human neutrophil granule subsets, secretory vesicles, and cell membrane: correlation with transcriptome profiling of neutrophil precursors. J Leukoc Biol. 2013;94(4):711–21.

Sadik CD, Kim ND, Luster AD. Neutrophils cascading their way to inflammation. Vol. 32, Trends in Immunology. 2011. p. 452–60.

Sakai J, Li J, Subramanian KK, Mondal S, Bajrami B, Hattori H, et al. Reactive Oxygen Species-Induced Actin Glutathionylation Controls Actin Dynamics in Neutrophils. Immunity. 2012;37(6):1037–49.

Samanta AK, Oppenheim JJ, Matsushima K. Interleukin 8 (monocyte-derived neutrophil chemotactic factor) dynamically regulates its own receptor expression on human neutrophils. J Biol Chem. 1990;265(1):183–9.

Scheiermann C, Frenette PS, Hidalgo A. Regulation of leucocyte homeostasis in the circulation. Cardiovasc Res. 2015;107(3):340–51.

Schieber M, Chandel NS. ROS function in redox signaling and oxidative stress. Vol. 24, Current Biology. 2014.

Schmidt EP, Lee WL, Zemans RL, Yamashita C, Downey GP. On, Around, and Through: Neutrophil-Endothelial Interactions in Innate Immunity. Physiology. 2011;26(5):334–47.

Schumacher C, Clark-Lewis I, Baggiolini M, Moser B. High- and low-affinity binding of GRO alpha and neutrophil-activating peptide 2 to interleukin 8 receptors on human neutrophils. Proc Natl Acad Sci. 2006;89(21):10542–6.

Scott DA, Krauss JL. Neutrophils in periodontal inflammation. In: Periodontal Disease. 2011. p. 56–83.

Shao D, Oka S, Brady CD, Haendeler J,Eaton P, Sadoshima J. Redox modification of cell signaling in the cardiovascular system. J Mol Cell Cardiol. 2012;52(3):550–8.

Shelton MD, Chock PB, Mieyal JJ. Glutaredoxin: Role in Reversible Protein S - Glutathionylation and Regulation of Redox Signal Transduction and Protein Translocation. Antioxid Redox Signal. 2005;7(3–4):348–66.

Sherratt PJ, Hayes JD. *9* Glutathione S-transferases, Enzyme Systems that Metabolise Drugs and Other Xenobiotics. Edited by Costas Ioannides. 2002.

Simard P, Galarneau H, Marois S, Rusu D, Hoemann CD, Poubelle PE, et al. Neutrophils exhibit distinct phenotypes toward chitosans with different degrees of deacetylation: Implications for cartilage repair. Arthritis Res Ther. 2009;11(3).

Singh R, Ali I, Sharma B, Aboul-Enein HY, Singh P. Separation of biological proteins by liquid chromatography. Vol. 18, Saudi Pharmaceutical Journal. 2011. p. 59–73.

Smith PK, Hermanson GT, Gartner FH, Frovenzano MD, Fujimoto EK, Goeke NM, et al. Measurement of Protein Using Bicinchoninic Acid. Anal Biochem. 1985;150:76–85.

Stabel TJ, Fedorka-Cray PJ, Gray JT. Neutrophil phagocytosis following inoculation of Salmonella choleraesuis into swine. Vet Res Commun. 2002;26(2):103–9.

Summers SA, Tilakaratne WM, Fortune F, Ashman N. Renal Disease and the Mouth. Vol. 120, American Journal of Medicine. 2007. p. 568–73.

Szczur K, Xu H, Atkinson S, Zheng Y, Filippi MD. Rho GTPase CDC42 regulates directionality and random movement via distinct MAPK pathways in neutrophils. Blood. 2006;108(13):4205–13.

Tamma G, Valenti G, Grossini E, Donnini S, Marino A, Marinelli RA, et al. Aquaporin Membrane Channels in Oxidative Stress, Cell Signaling, and Aging: Recent Advances and Research Trends. Vol. 2018, Oxidative Medicine and Cellular Longevity. 2018. p. 1–14.

Taylor GW. Bidirectional interrelationships between diabetes and periodontal diseases: An epidemiologic perspective. Vol. 6. Ann Periodontol. 2001. p. 99–12.

Thomas HB, Moots RJ, Edwards SW, Wright HL. Whose gene is it anyway? the effect of preparation purity on neutrophil transcriptome studies. Vol. 10, PLoS ONE. 2015.

Udeshi ND, Compton PD, Shabanowitz J, Hunt DF, Rose KL. Methods for analyzing peptides and proteins on a chromatographic timescale by electron-transfer dissociation mass spectrometry. Nat Protoc. 2008;3(11):1709–17.

Van Dyke TE, Horoszewicz HU, Cianciola LJ, Genco RJ. Neutrophil chemotaxis dysfunction in human periodontitis. Infect Immun. 1980;27(1):124–32.

Van Dyke TE. The etiology and pathogenesis of periodontitis revisited. Journal of applied oral science : revista FOB. 2007. p. 7757.

Vogiatzi G, Tousoulis D, Christodoulos S. The Role of Oxidative Stress in Atherosclerosis oxidative stress and Atherosclerosis. Hell J Cardiol. 2009;50:402–9.

Wahid A, Chaudhry S, Ehsan A, Butt S, Khan AA. Bidirectional relationship between chronic kidney disease & periodontal disease. Pakistan J Med Sci. 2013;29(1):211–5.

Wang J, Boja ES, Tan W, Tekle E, Fales HM, English S, et al. Reversible Glutathionylation Regulates Actin Polymerization in A431 Cells. J Biol Chem. 2001;276(51):47763–6.

Weyrich AS, Elstad MR, McEver RP, McIntyre TM, Moore KL, Morrissey JH, et al. Activated platelets signal chemokine synthesis by human monocytes. J Clin Invest. 1996;97(6):1525–34.

Williams AE, José RJ, Mercer PF, Brealey D, Parekh D, Thickett DR, et al. Evidence for chemokine synergy during neutrophil migration in ARDS. Thorax. 2017;72(1):66–73.

Woodi M, Mondal AK, Padmanabhan B, Rajagopalan KP. Analysis of protein posttranslational modifications by mass spectrometry: With special reference to haemoglobin. Indian J Clin Biochem. 2009;24(1):23–9.

Yan L-J. Protein Redox Modification as a Cellular Defense Mechanism against Tissue Ischemic Injury. Oxid Med Cell Longev. 2014;2014:1–12.

Yoo SK, Starnes TW, Deng Q, Huttenlocher A. Lyn is a redox sensor that mediates leukocyte wound attraction in vivo. Nature. 2011;480(7375):109–12.

Zeviani WM, Ferreira DFDPD, Muniz JA, Wada CY, Vitor J, Esalq T, et al. Cardiovascular disease parameters in periodontitis. J Periodontol. 2009;80(3):1–5.

Zhu R, Zacharias L, Wooding KM, Peng W, Mechref Y. Glycoprotein Enrichment Analytical Techniques: Advantages and Disadvantages. In: Methods in Enzymology. 2017. p. 397–429.

Zubarev RA, Makarov A. Orbitrap Mass Spectrometry. Anal Chem. 2013;85(11):5288–96.

CHAPTER 8 – APPENDICES

Appendix 8.1: List of proteins from all fractions pooled from high-pH reverse phase (C18) Waters Bridge column and analysed by mass spectrometry (LC-MS/MS). n=3

Protein ID	Gene name	Description of gene
P06702	S100A9	Protein S100A9
P05109	S100A8	Protein S100A8
P07737	PFN1	Profilin1
P62937	PPIA	Peptidylprolyl cistrans isomerase A
P60660	MYL6	Myosin light polypeptide 6
P69905	HBA1	Hemoglobin subunit alpha
P60709	ACTB	Actin, cytoplasmic 1 Actin
P04083	ANXA1	Annexin A1
P61626	LYZ	Lysozyme C
P12429	ANXA3	Annexin A3
P02788	LTF	Lactotransferrin
P02768	ALB	Serum albumin
P08311	CTSG	Cathepsin G
P05164	MPO	Myeloperoxidase
P06733	ENO1	Alphaenolase
P47756	CAPZB	Factincapping protein subunit beta
P04040	CAT	Catalase
P08107	HSPA1A	Heat shock 70 kDa protein 1A/1B
P14618	PKM	Pyruvate kinase PKM

P26038	MSN	Moesin
P14780	MMP9	Matrix metalloproteinase9
Q9Y490	TLN1	Talin1
P21333	FLNA	FilaminA
P80511	S100A12	Protein S100A12
P59665	DEFA1	Neutrophil defensin 1
P02042	HBD	Hemoglobin subunit delta
P04075	ALDOA	Fructosebisphosphate aldolase A
P60174	TPI1	Triosephosphate isomerase
P0C0S5	H2AFZ	Histone H2A.Z
P32119	PRDX2	Peroxiredoxin2
P16401	HIST1H1B	Histone H1.5
P08670	VIM	Vimentin
P06396	GSN	Gelsolin
P35579	MYH9	Myosin9
P68871	HBB	Hemoglobin subunit beta
Q9HD89	RETN	Resistin
P62805	HIST1H4A	Histone H4
O60814	HIST1H2BK	Histone H2B type 1K
P31949	S100A11	Protein S100A11
P04406	GAPDH	Glyceraldehyde3phosphate dehydrogenase
P12724	RNASE3	Eosinophil cationic protein
P16403	HIST1H1C	Histone H1.2
P24158	PRTN3	Myeloblastin
P13645	KRT10	Keratin, type I cytoskeletal 10

P04264	KRT1	Keratin, type II cytoskeletal 1
P06744	GPI	Glucose6phosphate isomerase
P11488	GNAT1	Guanine nucleotidebinding protein G(t) subunit alpha1
P52209	PGD	6phosphogluconate dehydrogenase, decarboxylating
K4DIE0	NUMA1	Nuclear mitotic apparatus protein 1 (Fragment)
P12814	ACTN1	Alphaactinin1
P07996	THBS1	Thrombospondin1
H0YL80	TPM1	Tropomyosin alpha1 chain (Fragment)
H0YFX9	H2AFJ	Histone H2A (Fragment)
G3V1N2	HBA2	HCG1745306, isoform CRA_a
P23528	CFL1	Cofilin1
H3BUH7	ALDOA	Fructosebisphosphate aldolase A (Fragment)
P02775	PPBP	Platelet basic protein
P14174	MIF	Macrophage migration inhibitory factor
Q9Y536	PPIAL4A	Peptidylprolyl cistrans isomerase Alike 4A/B/C
P09211	GSTP1	Glutathione Stransferase P
O75594	PGLYRP1	Peptidoglycan recognition protein 1
P49913	CAMP	Cathelicidin antimicrobial peptide
P15153	RAC2	Rasrelated C3 botulinum toxin substrate 2
P19105	MYL12A	Myosin regulatory light chain 12A
Q6NXT2	H3F3C	Histone H3.3C
P20160	AZU1	Azurocidin
P06733-2	ENO1	Isoform MBP1 of Alphaenolase
B0YJC5	VIM	Vimentin
P00558	PGK1	Phosphoglycerate kinase 1

P11142	HSPA8	Heat shock cognate 71 kDa protein
P37837	TALDO1	Transaldolase
P29401	TKT	Transketolase
P11215	ITGAM	Integrin alphaM
Q9UM07	PADI4	Proteinarginine deiminase type4
P08514	ITGA2B	Integrin alphaIIb
Q9NU22	MDN1	Midasin
D6RCN3	ANXA5	Annexin A5
P62328	TMSB4X	Thymosin beta4
C9JTX5	ACTB	Actin, cytoplasmic 1 (Fragment)
K7EJ44	PFN1	Profilin 1, isoform CRA_b
F5H2R5	ARHGDIB	Rho GDPdissociation inhibitor 2 (Fragment)
J3KS60	ARHGDIA	Rho GDPdissociation inhibitor 1
H0YLF3	B2M	Beta2microglobulin form pI 5.3 (Fragment)
D6RFM2	TPM3	Tropomyosin alpha3 chain
C9JTV5	ARPC2	Actinrelated protein 2/3 complex subunit 2 (Fragment)
P26447	S100A4	Protein S100A4
H7C1S1	NCF1	Neutrophil cytosol factor 1 (Fragment)
P80723	BASP1	Brain acid soluble protein 1
O60361	NME2P1	Putative nucleoside diphosphate kinase
P10153	RNASE2	Nonsecretory ribonuclease
O95626	ANP32D	Acidic leucinerich nuclear phosphoprotein 32 family member D
B1AK87	CAPZB	Capping protein (Actin filament) muscle Zline, beta, isoform CRA_a
P26583	HMGB2	High mobility group protein B2
P02763	ORM1	Alpha1acid glycoprotein 1

Q5T3N1	ANXA1	Annexin (Fragment)
B2RPK0	HMGB1P1	Putative high mobility group protein B1like 1
P52565	ARHGDIA	Rho GDPdissociation inhibitor 1
P01036	CST4	CystatinS
P08133	ANXA6	Annexin A6
Q96KK5	HIST1H2AH	Histone H2A type 1H
H3BT25	PKM	Pyruvate kinase PKM (Fragment)
P01037	CST1	CystatinSN
Q06830	PRDX1	Peroxiredoxin1
P15531	NME1	Nucleoside diphosphate kinase A
P23284	PPIB	Peptidylprolyl cistrans isomerase B
Q13231	CHIT1	Chitotriosidase1
P00738	HP	Haptoglobin
P67936	TPM4	Tropomyosin alpha4 chain
C9JKM9	XPO1	Exportin1 (Fragment)
C9J0S5	LTF	Kaliocin1 (Fragment)
P18669	PGAM1	Phosphoglycerate mutase 1
P30101	PDIA3	Protein disulfideisomerase A3
P52566	ARHGDIB	Rho GDPdissociation inhibitor 2
O75015	FCGR3B	Low affinity immunoglobulin gamma Fc region receptor IIIB
P50395-2	GDI2	Isoform 2 of Rab GDP dissociation inhibitor beta
C9J155	NCF1	Neutrophil cytosol factor 1 (Fragment)
P23381	WARS	TryptophantRNA ligase, cytoplasmic
O15143	ARPC1B	Actinrelated protein 2/3 complex subunit 1B
O15144	ARPC2	Actinrelated protein 2/3 complex subunit 2

O00299	CLIC1	Chloride intracellular channel protein 1
U3KPS2	PRTN3	Myeloblastin
P17213	BPI	Bactericidal permeabilityincreasing protein
P09525	ANXA4	Annexin A4
O14745	SLC9A3R1	Na(+)/H(+) exchange regulatory cofactor NHERF1
Q15942	ZYX	Zyxin
P63104	YWHAZ	1433 protein zeta/delta
P00338	LDHA	Llactate dehydrogenase A chain
Q8WUT4	LRRN4	Leucinerich repeat neuronal protein 4
P19878-2	NCF2	Isoform 2 of Neutrophil cytosol factor 2
P48595	SERPINB10	Serpin B10
P50552	VASP	Vasodilatorstimulated phosphoprotein
P07900	HSP90AA1	Heat shock protein HSP 90alpha
P26641	EEF1G	Elongation factor 1gamma
P11413	G6PD	Glucose6phosphate 1dehydrogenase
P30520	ADSS	Adenylosuccinate synthetase isozyme 2
P13796	LCP1	Plastin2
P07237	P4HB	Protein disulfideisomerase
P40121	CAPG	Macrophagecapping protein
C9JKR2	ALB	Albumin, isoform CRA_k
P47755	CAPZA2	Factincapping protein subunit alpha2
P08238	HSP90AB1	Heat shock protein HSP 90beta
O43707	ACTN4	Alphaactinin4
F8VSC5	SCYL2	SCY1like protein 2 (Fragment)
Q13586	STIM1	Stromal interaction molecule 1

P68104	EF1A1	Elongation factor 1-alpha 1
P51589	CYP2J2	Cytochrome P450 2J2
Q5HY54	FLNA	FilaminA
C9K0F3	TPST1	Proteintyrosine sulfotransferase 1 (Fragment)
D6R904	TPM3	Tropomyosin alpha3 chain
E9PMP4	CCDC67	Deuterosome protein 1
F5H0N6	OLR1	Oxidized low-density lipoprotein receptor 1, soluble form (Fragment)
E5RGE1	YWHAZ	1433 protein zeta/delta (Fragment)
F8WBC0	RAP1B	Rasrelated protein Rap1b (Fragment)
E9PGV1	GSTM2	Glutathione Stransferase Mu 2
F8WEE7	F8WEE7	SEC14-like protein 2
E5RG49	ATP6V1H	Vtype proton ATPase subunit H (Fragment)
H0YK21	ZFAND6	AN1type zinc finger protein 6 (Fragment)
B0AZS9	BNIP3L	BCL2/adenovirus E1B 19 kDa protein-interacting protein 3-like
D6RJB2	APBB3	Amyloid beta A4 precursor proteinbinding family B member 3
F6XY72	NME1NME2	Nucleoside diphosphate kinase
H3BT58	COTL1	Coactosinlike protein
Q4VY20	YWHAB	1433 protein beta/alpha (Fragment)
Q5T123	SH3BGRL3	SH3 domainbinding glutamic acidrichlike protein 3
E9PLV4	PHF21A	PHD finger protein 21A (Fragment)
Q96T52	IMMP2L	Mitochondrial inner membrane protease subunit 2
R4GN98	S100A6	Protein S100-A6 (Fragment)
P80723-2	BASP1	Isoform 2 of Brain acid soluble protein 1
K7EQF2	PLCD3	1-phosphatidylinositol 4,5-bisphosphate phosphodiesterase delta-3 (Fragment)
A2A2D0	STMN1	Stathmin (Fragment)

B1AH77	RAC2	Ras-related C3 botulinum toxin substrate 2
Q9NP64	ZCCHC17	Nucleolar protein of 40 kDa
F5H4M0	VPS37B	Vacuolar protein sortingassociated protein 37B (Fragment)
P25815	S100P	Protein S100P
Q499Y3	2 SV	Putative uncharacterized protein C10orf88like
H0YAH8	TGFBI	Transforming growth factorbetainduced protein igh3 (Fragment)
P49842-4	STK19	Isoform 4 of Serine/threonineprotein kinase 19
Q96MC5-2	C16orf45	Isoform 2 of Uncharacterized protein C16orf45
D6RCA8	ANXA3	Annexin (Fragment)
Q9UHG0-2	DCDC2	Isoform 2 of Doublecortin domaincontaining protein 2
P06748-3	NPM1	Isoform 3 of Nucleophosmin
J3QSA3	UBB	Ubiquitin (Fragment)
M0R2W4	STAP2	Signaltransducing adaptor protein 2 (Fragment)
Q6ZSX4	EPB41L2	Band 4.1like protein 2
P68431	HIST1H3A	Histone H3.1
Q86Y82	STX12	Syntaxin12
K7ERT7	VAT1	Synaptic vesicle membrane protein VAT-1 homolog (Fragment)
M0QY96	HNRNPM	Heterogeneous nuclear ribonucleoprotein M (Fragment)
G3V1A4	CFL1	Cofilin 1 (Nonmuscle), isoform CRA_a
J3QRP4	CNDP2	Cytosolic nonspecific dipeptidase
H3BU13	PKM	Pyruvate kinase PKM (Fragment)
J3KMY5	NPC2	Epididymal secretory protein E1
K7EMV3	H3F3B	Histone H3

H0YA76	CNOT6L	CCR4NOT transcription complex subunit 6like (Fragment)
B1APY9	ELAVL4	ELAVlike protein 4
C9IZ41	ZYX	Zyxin (Fragment)
F8VUA8	C14orf79	Uncharacterized protein C14orf79
K7ESA3	K7ESA3	Synaptic vesicle membrane protein VAT-1 homolog (Fragment)
Q9H299	SH3BGRL3	SH3 domainbinding glutamic acidrichlike protein 3
P62158	CALM1	Calmodulin
P08579	SNRPB2	U2 small nuclear ribonucleoprotein B''
V9GYJ7	GDI2	Rab GDP dissociation inhibitor beta (Fragment)
O60884	DNAJA2	DnaJ homolog subfamily A member 2
Q5T7C4	HMGB1	High mobility group protein B1
E9PF05	SUMF1	Sulfatasemodifying factor 1
E9PJB2	C11orf73	Protein Hikeshi
Q7Z6M3-2	0	Isoform 2 of Allergin-1
F5H450	FZD10	Frizzled10
K7ELW0	PARK7	Protein DJ1
P01877	IGHA2	Ig alpha2 chain C region
P16949	STMN1	Stathmin
C9J386	H2AFV	Histone H2A
P04080	CSTB	CystatinB
H7BZJ3	H7BZJ3	Thioredoxin (Fragment)
K7EQR1	UBN1	Ubinuclein1 (Fragment)
K7EM16	VASP	Vasodilator-stimulated phosphoprotein (Fragment)
K7ENA0	GPI	Glucose6phosphate isomerase (Fragment)

H0YKH0	TLE3	Transducinlike enhancer protein 3
P02774-2	GC	Isoform 2 of Vitamin Dbinding protein
Q13316-2	DMP1	Isoform 2 of Dentin matrix acidic phosphoprotein 1
B4DXJ9	PSMA6	Proteasome (Prosome, macropain) subunit, alpha type, 6, isoform CRA_a
O15400-2	STX7	Isoform 2 of Syntaxin7
H0Y7A0	EMILIN1	EMILIN1 (Fragment)
M0R042	TUBB4A	Tubulin beta4A chain (Fragment)
B0YJC4	VIM	Vimentin
Q5JVS8	VIM	Vimentin (Fragment)
B7Z4N8	USP14	Ubiquitin carboxylterminal hydrolase
F5GXH2	LDHA	Llactate dehydrogenase A chain (Fragment)
P60174-4	TPI1	Isoform 4 of Triosephosphate isomerase
Q86VE9-3	SERINC5	Isoform 3 of Serine incorporator 5
Q9H098	FAM107B	Protein FAM107B
P80188	LCN2	Neutrophil gelatinase-associated lipocalin
Q15428	SF3A2	Splicing factor 3A subunit 2
E9PHT9	ANXA5	Annexin
O43439-2	CBFA2T2	Isoform 2 of Protein CBFA2T2
M0R149	PRAM1	PMLRARAregulated adapter molecule 1 (Fragment)
K7EJH8	ACTN4	Alpha-actinin-4 (Fragment)
Q9BTT0	ANP32E	Acidic leucine-rich nuclear phosphoprotein 32 family member E
P37802	TAGLN2	Transgelin2
H0YF68	TAOK3	Serine/threonineprotein kinase TAO3 (Fragment)
Q5JRS1	UBA1	Ubiquitin-like modifier-activating enzyme 1 (Fragment)
C9JUG7	CAPZA2	F-actin-capping protein subunit alpha-2

G3V4U0	FBLN5	Fibulin-5
Q92930	RAB8B	Ras-related protein Rab-8B
A8K8G0	HDGF	Hepatomaderived growth factor
G3V2W4	ACTN1	Alphaactinin1 (Fragment)
D6RG15	TWF2	Twinfilin2
P31946	YWHAB	1433 protein beta/alpha
Q04917	YWHAH	1433 protein eta
P10412	HIST1H1E	Histone H1.4
Q5VU63	TPM3	Tropomyosin alpha3 chain
F8W835	PRPH	Peripherin (Fragment)
C9JBC2	HDAC7	Histone deacetylase 7 (Fragment)
P51858	HDGF	Hepatoma-derived growth factor
Q14002-2	CEACAM7	Isoform 2b of Carcinoembryonic antigenrelated cell adhesion molecule 7
P09417	QDPR	Dihydropteridine reductase
K7EMN2	PGD	6phosphogluconate dehydrogenase, decarboxylating (Fragment)
A8MYZ5	IQCF6	IQ domaincontaining protein F6
Q5T8M8	ACTA1	Actin, alpha skeletal muscle
Q9NUQ9	FAM49B	Protein FAM49B
P15259	PGAM2	Phosphoglycerate mutase 2
H0Y9Z7	H0Y9Z7	Kinesin-like protein KIF13A (Fragment)
Q8WVY7	UBLCP1	Ubiquitinlike domaincontaining CTD phosphatase 1
P54108	CRISP3	Cysteinerich secretory protein 3
P30044	PRDX5	Peroxiredoxin5, mitochondrial
P40925	MDH1	Malate dehydrogenase, cytoplasmic
P62491	RAB11A	Rasrelated protein Rab11A

P28676	GCA	Grancalcin
P04350	TUBB4A	Tubulin beta4A chain
Q99536	VAT1	Synaptic vesicle membrane protein VAT1 homolog
B4DDF9	ANXA4	Annexin
Q9Y4D8-3	HECTD4	Isoform 3 of Probable E3 ubiquitinprotein ligase HECTD4
Q9Y266	NUDC	Nuclear migration protein nudC
P17066	HSPA6	Heat shock 70 kDa protein 6
P22626-2	HNRNPA2B1	Isoform A2 of Heterogeneous nuclear ribonucleoproteins A2/B1
Q5T2D2	TREML2	Tremlike transcript 2 protein
Q86X10-4	RALGAPB	Isoform 4 of Ral GTPaseactivating protein subunit beta
P22626	HNRNPA2B1	Heterogeneous nuclear ribonucleoproteins A2/B1
H0YHL7	CORO1C	Coronin-1C (Fragment)
B7Z817	DHCR24	Delta(24)sterol reductase
P23526-2	AHCY	Isoform 2 of Adenosylhomocysteinase
V9GYF0	V9GYF0	Rho guanine nucleotide exchange factor 2 (Fragment)
Q8IX06	REXO1L1P	Putative exonuclease GOR
F8WDB9	CAP2	Adenylyl cyclaseassociated protein
P02675	FGB	Fibrinogen beta chain
H3BS21	HP	Haptoglobin (Fragment)
B1AKP8	MTOR	Serine/threonine-protein kinase mTOR
E9PEI0	CDCA2	Cell division cycleassociated protein 2
Q5SVZ7	ZMYM1	Zinc finger MYM-type protein 1 (Fragment)
P23381-2	WARS	Isoform 2 of TryptophantRNA ligase, cytoplasmic
D6RA82	ANXA3	Annexin

C9JB56	ARHGAP25	Rho GTPaseactivating protein 25
P08246	ELANE	Neutrophil elastase
P46020-3	PHKA1	Isoform 3 of Phosphorylase b kinase regulatory subunit alpha, skeletal muscle isoform
P78417	GSTO1	Glutathione Stransferase omega1
Q7L0X0	TRIL	TLR4 interactor with leucine rich repeats
Q8TCJ2	STT3B	Dolichyldiphosphooligosaccharideprotein glycosyltransferase subunit STT3B
K7EQ48	GPI	Glucose6phosphate isomerase
Q9Y2J2-3	EPB41L3	Isoform C of Band 4.1-like protein 3
Q9ULH4	LRFN2	Leucine-rich repeat and fibronectin type-III domain-containing protein 2
B4DKG1	NAB1	NGFIAbinding protein 1
F2Z393	TALDO1	Transaldolase
Q9NYL9	TMOD3	Tropomodulin3
B4E2V5	STOM	Erythrocyte band 7 integral membrane protein
P0C874	SPATA31D3	Putative spermatogenesisassociated protein 31D3
P98168	ZXDA	Zinc finger Xlinked protein ZXDA
O43488	AKR7A2	Aflatoxin B1 aldehyde reductase member 2
Q8N7B1	HORMAD2	HORMA domaincontaining protein 2
O95718-3	ESRRB	Isoform 3 of Steroid hormone receptor ERR2
H7C144	ACTN4	Alpha-actinin-4 (Fragment)
E9PN89	HSPA8	Heat shock cognate 71 kDa protein (Fragment)
P18206-3	VCL	Isoform 3 of Vinculin
F5H3K3	F5H3K3	Spermatogenesis-associated protein 2
O95025	SEMA3D	Semaphorin3D
P50395	GDI2	Rab GDP dissociation inhibitor beta
F5H4R1	MAP3K4	Mitogenactivated protein kinase kinase kinase 4

Q96JG8-4	MAGED4	Isoform 4 of Melanoma-associated antigen D4
P43246	MSH2	DNA mismatch repair protein Msh2
K7EM23	K7EM23	Uncharacterized protein C17orf66
P13688-3	CEACAM1	Isoform 3 of Carcinoembryonic antigen-related cell adhesion molecule 1
P61160	ACTR2	Actinrelated protein 2
D6REY1	CHIT1	Chitotriosidase-1
P11021	HSPA5	78 kDa glucoseregulated protein
J3QLC9	HP	Haptoglobin (Fragment)
Q4VNC0	ATP13A5	Probable cation-transporting ATPase 13A5
P02788-2	LTF	Isoform DeltaLf of Lactotransferrin
H0YI72	ANKS1B	Ankyrin repeat and sterile alpha motif domaincontaining protein 1B (Fragment)
P03905	MT-ND4	NADH-ubiquinone oxidoreductase chain 4
P31997	CEACAM8	Carcinoembryonic antigenrelated cell adhesion molecule 8
P35527	KRT9	Keratin, type I cytoskeletal 9
Q8WUH2	TGFBRAP1	Transforming growth factorbeta receptorassociated protein 1
Q9UJU6	DBNL	Drebrin-like protein
B7WPN9	ATP13A4	Probable cationtransporting ATPase 13A4
Q96P15	SERPINB11	Serpin B11
Q9NQH7-3	XPNPEP3	Isoform 3 of Probable XaaPro aminopeptidase 3
Q13591	SEMA5A	Semaphorin5A
Q58FF3	HSP90B2P	Putative endoplasminlike protein
Q9UBW7	ZMYM2	Zinc finger MYM-type protein 2
A8MVU1	NCF1C	Putative neutrophil cytosol factor 1C
Q16696	CYP2A13	Cytochrome P450 2A13

P43246-2	MSH2	Isoform 2 of DNA mismatch repair protein Msh2
Q9HDC9	APMAP	Adipocyte plasma membraneassociated protein
P31146	CORO1A	Coronin1A
Q01518	CAP1	Adenylyl cyclaseassociated protein 1
V9GZ37		Heat shock 70 kDa protein 1A/1B
P00739	HPR	Haptoglobinrelated protein
B4E022	TKT	Transketolase
E7EVW7	HCLS1	Hematopoietic lineage cellspecific protein
O95171	SCEL	Sciellin
Q5H9M0	MUM1L1	PWWP domaincontaining protein MUM1L1
Q01518-2	CAP1	Isoform 2 of Adenylyl cyclaseassociated protein 1
O15042-3	U2SURP	Isoform 3 of U2 snRNPassociated SURP motifcontaining protein
P04839	CYBB	Cytochrome b245 heavy chain
P61158	ACTR3	Actinrelated protein 3
G5EA52	PDIA3	Protein disulfide isomerase family A, member 3, isoform CRA_b
Q15070	OXA1L	Mitochondrial inner membrane protein OXA1L
Q9HAW4-2	CLSPN	Isoform 2 of Claspin
Q9Y2Q0	ATP8A1	Probable phospholipidtransporting ATPase IA
J3KP11	CACNA1E	Voltagedependent Rtype calcium channel subunit alpha1E
Q52LW3	ARHGAP29	Rho GTPaseactivating protein 29
Q8TF30	WHAMM	WASP homologassociated protein with actin, membranes and microtubules
H7C022	WDR60	WD repeatcontaining protein 60 (Fragment)
O75083	WDR1	WD repeatcontaining protein 1
F8W6C1	SPTBN1	Spectrin beta chain, non-erythrocytic 1 (Fragment)

Q8N3C0	ASCC3	Activating signal cointegrator 1 complex subunit 3
H9KV75	ACTN1	Alphaactinin1
E9PDY4	CR1	Complement receptor type 1
Q05655	PRKCD	Protein kinase C delta type
P35609	ACTN2	Alphaactinin2
Q8NDG6	TDRD9	Putative ATP-dependent RNA helicase TDRD9
P19021	PAM	Peptidylglycine alphaamidating monooxygenase
Q5T2X4	CEP350	Centrosomeassociated protein 350 (Fragment)
Q9NQH7	XPNPEP3	Probable Xaa-Pro aminopeptidase 3
Q99715-4	COL12A1	Isoform 4 of Collagen alpha1(XII) chain
A8MYE6	ITGB2	Integrin beta
Q1MSJ5-1	CSPP1	Isoform 1 of Centrosome and spindle poleassociated protein 1
Q9P2E3-2	ZNFX1	Isoform 2 of NFX1-type zinc finger-containing protein 1
Q06203	PPAT	Amidophosphoribosyltransferase
F5H228	TRIO	Triple functional domain protein
P08514-3	0	Isoform 3 of Integrin alpha-IIb
Q01082-3	0	Isoform 2 of Spectrin beta chain, non-erythrocytic 1
Q9P2N6	KANSL3	KAT8 regulatory NSL complex subunit 3
O60486	PLXNC1	PlexinC1
Q9UHB6	LIMA1	LIM domain and actinbinding protein 1
Q9Y4B4	RAD54L2	Helicase ARIP4
Q8N655	C10orf12	Uncharacterized protein C10orf12
Q5TCU6	TLN1	Talin-1
Q6WKZ4	RAB11FIP1	Rab11 familyinteracting protein 1

Q05707-3	COL14A1	Isoform 3 of Collagen alpha1(XIV) chain
Q9BYW2	SETD2	Histone-lysine N-methyltransferase SETD2
P16157	ANK1	Ankyrin1
O75339	CILP	Cartilage intermediate layer protein 1
E9PBV1	NWD1	NACHT and WD repeat domaincontaining protein 1
Q9P273	TENM3	Teneurin3
P11277	SPTB	Spectrin beta chain, erythrocytic
Q9BY89	KIAA1671	Uncharacterized protein KIAA1671
Q01082	SPTBN1	Spectrin beta chain, nonerythrocytic 1
P53804	TTC3	E3 ubiquitinprotein ligase TTC3
Q5VT06	CEP350	Centrosome-associated protein 350

Appendix 8.2: List of protein for all fractions pooled from strong cation exchange (SCX) column and analyzed through mass spectrometry (LC-MS/MS).

Protein ID	Gene name	Description of gene
A0M8Q6	IGLC7	Ig lambda-7 chain C region
A6NEQ6	COL9A1	Collagen alpha-1(IX) chain
A8K2U0	A2ML1	Alpha-2-macroglobulin-like protein 1
P62937	PPIA	Peptidylprolyl cistrans isomerase A
P60660	MYL6	Myosin light polypeptide 6
P69905	HBA1	Hemoglobin subunit alpha
P60709	ACTB	Actin, cytoplasmic 1 Actin
P04083	ANXA1	Annexin A1
P61626	LYZ	Lysozyme C
P12429	ANXA3	Annexin A3
P02788	LTF	Lactotransferrin
P02768	ALB	Serum albumin
P08311	CTSG	Cathepsin G
P05164	MPO	Myeloperoxidase
P06733	ENO1	Alphaenolase
P47756	CAPZB	Factincapping protein subunit beta
P04040	CAT	Catalase
P08107	HSPA1A	Heat shock 70 kDa protein 1A/1B

P14618	PKM	Pyruvate kinase PKM
P26038	MSN	Moesin
P14780	MMP9	Matrix metalloproteinase9
Q9Y490	TLN1	Talin1
P21333	FLNA	FilaminA
P80511	S100A12	Protein S100A12
P59665	DEFA1	Neutrophil defensin 1
P02042	HBD	Hemoglobin subunit delta
P04075	ALDOA	Fructosebisphosphate aldolase A
P60174	TPI1	Triosephosphate isomerase
P0C0S5	H2AFZ	Histone H2A.Z
P32119	PRDX2	Peroxiredoxin2
P16401	HIST1H1B	Histone H1.5
P08670	VIM	Vimentin
P06396	GSN	Gelsolin
P35579	MYH9	Myosin9
P68871	HBB	Hemoglobin subunit beta
Q9HD89	RETN	Resistin
P62805	HIST1H4A	Histone H4
O60814	HIST1H2BK	Histone H2B type 1K
P31949	S100A11	Protein S100A11
P04406	GAPDH	Glyceraldehyde3phosphate dehydrogenase
P12724	RNASE3	Eosinophil cationic protein
P16403	HIST1H1C	Histone H1.2
P24158	PRTN3	Myeloblastin

P13645	KRT10	Keratin, type I cytoskeletal 10
P04264	KRT1	Keratin, type II cytoskeletal 1
P06744	GPI	Glucose6phosphate isomerase
P11488	GNAT1	Guanine nucleotidebinding protein G(t) subunit alpha1
P52209	PGD	6phosphogluconate dehydrogenase, decarboxylating
K4DIE0	NUMA1	Nuclear mitotic apparatus protein 1 (Fragment)
P12814	ACTN1	Alphaactinin1
P07996	THBS1	Thrombospondin1
H0YL80	TPM1	Tropomyosin alpha1 chain (Fragment)
H0YFX9	H2AFJ	Histone H2A (Fragment)
G3V1N2	HBA2	HCG1745306, isoform CRA_a
P23528	CFL1	Cofilin1
H3BUH7	ALDOA	Fructosebisphosphate aldolase A (Fragment)
P02775	PPBP	Platelet basic protein
P14174	MIF	Macrophage migration inhibitory factor
Q9Y536	PPIAL4A	Peptidylprolyl cistrans isomerase Alike 4A/B/C
P09211	GSTP1	Glutathione Stransferase P
O75594	PGLYRP1	Peptidoglycan recognition protein 1
P49913	CAMP	Cathelicidin antimicrobial peptide
P15153	RAC2	Rasrelated C3 botulinum toxin substrate 2
P19105	MYL12A	Myosin regulatory light chain 12A
Q6NXT2	H3F3C	Histone H3.3C
P20160	AZU1	Azurocidin
P06733-2	ENO1	Isoform MBP1 of Alphaenolase

B0YJC5	VIM	Vimentin
P00558	PGK1	Phosphoglycerate kinase 1
P11142	HSPA8	Heat shock cognate 71 kDa protein
P37837	TALDO1	Transaldolase
P29401	TKT	Transketolase
P11215	ITGAM	Integrin alphaM
Q9UM07	PADI4	Proteinarginine deiminase type4
P08514	ITGA2B	Integrin alphaIIb
Q9NU22	MDN1	Midasin
D6RCN3	ANXA5	Annexin A5
P62328	TMSB4X	Thymosin beta4
C9JTX5	ACTB	Actin, cytoplasmic 1 (Fragment)
K7EJ44	PFN1	Profilin 1, isoform CRA_b
F5H2R5	ARHGDIB	Rho GDPdissociation inhibitor 2 (Fragment)
J3KS60	ARHGDIA	Rho GDPdissociation inhibitor 1
H0YLF3	B2M	Beta2microglobulin form pI 5.3 (Fragment)
D6RFM2	TPM3	Tropomyosin alpha3 chain
C9JTV5	ARPC2	Actinrelated protein 2/3 complex subunit 2 (Fragment)
P26447	S100A4	Protein S100A4

B1AMJ5	CDK5RAP2	CDK5 regulatory subunit-associated protein 2 (Fragment)
B4DDN2	NEK11	Serine/threonine-protein kinase

B4E0G6	RBM6	RNA-binding protein 6
C9J0S5	LTF	Kaliocin-1 (Fragment)
C9JUH3	CCM2	Malcavernin
D6RCA8	ANXA3	Annexin (Fragment)
E5RGE1	YWHAZ	14-3-3 protein zeta/delta (Fragment)
E9PEA7	STAC	SH3 and cysteine-rich domain-containing protein
E9PJX3	DCST1	DC-STAMP domain-containing protein 1
F5H228	TRIO	Triple functional domain protein
F5H7B0	SKIV2L	Helicase SKI2W
F8VS53	SOCS2	Suppressor of cytokine-signaling 2
F8VSC5	SCYL2	SCY1-like protein 2 (Fragment)
F8VV57	KRT5	Keratin, type II cytoskeletal 5 (Fragment)
F8VY05	CCDC38	Coiled-coil domain-containing protein 38 (Fragment)
F8W1C8	ZNF606	Zinc finger protein 606 (Fragment)
F8W6P5	HBB	LVV-hemorphin-7 (Fragment)
F8W9B8	EXOC5	Exocyst complex component 5
F8WBA9	SELENBP1	Selenium-binding protein 1
G3V1N2	HBA2	HCG1745306, isoform CRA_a
G3V3H7	AKAP6	A-kinase anchor protein 6
G8JLD3	ERC1	ELKS/Rab6-interacting/CAST family member 1
H0YBM4	ASAP1	Arf-GAP with SH3 domain, ANK repeat and PH domain-containing protein 1 (Fragment)
H0YJ97	TRIP11	Thyroid receptor-interacting protein 11 (Fragment)
H0YL80	TPM1	Tropomyosin alpha-1 chain (Fragment)
H3BSI0	GOLGA8O	Golgin subfamily A member 8O (Fragment)
H7BXU9	FGFR2	Fibroblast growth factor receptor 2 (Fragment)

H7BZ69	BBS9	Protein PTHB1 (Fragment)
H7BZJ3	PDIA3	Thioredoxin (Fragment)
H7BZJ8	AZGP1	Zinc-alpha-2-glycoprotein (Fragment)
H7C013	ALB	Serum albumin (Fragment)
H7C1M1	PPP2R3A	Serine/threonine-protein phosphatase 2A regulatory subunit B'' subunit alpha (Fragment)
H7C4A0	ANKRD44	Serine/threonine-protein phosphatase 6 regulatory ankyrin repeat subunit B (Fragment)
H7C5G8	RBM28	RNA-binding protein 28 (Fragment)
I3L3P5	P4HB	Protein disulfide-isomerase (Fragment)
I3L428	SMYD4	SET and MYND domain-containing protein 4 (Fragment)
I3L4X5	USP31	Ubiquitin carboxyl-terminal hydrolase 31
I3L520	DNAH2	Dynein heavy chain 2, axonemal (Fragment)
J3KQ37	RGPD8	RANBP2-like and GRIP domain-containing protein 8
J3KRE2	ARHGDIA	Rho GDP-dissociation inhibitor 1
J3QQV3	CEP112	Centrosomal protein of 112 kDa (Fragment)
K7EMD9	KRT13	Keratin, type I cytoskeletal 13 (Fragment)
K7EPY2	TBX4	T-box transcription factor TBX4 (Fragment)
M0QZ61	PIH1D1	PIH1 domain-containing protein 1 (Fragment)
M0R327	ZNF701	Zinc finger protein 701 (Fragment)
O60234	GMFG	Glia maturation factor gamma
O60814	HIST1H2BK	Histone H2B type 1-K
O75594	PGLYRP1	Peptidoglycan recognition protein 1
O94806	PRKD3	Serine/threonine-protein kinase D3
O94885	SASH1	SAM and SH3 domain-containing protein 1
O95104	SCAF4	Splicing factor, arginine/serine-rich 15
O95396	MOCS3	Adenylyltransferase and sulfurtransferase MOCS3

P00558	PGK1	Phosphoglycerate kinase 1
P01034	CST3	Cystatin-C
P01036	CST4	Cystatin-S
P01037	CST1	Cystatin-SN
P01040	CSTA	Cystatin-A
P01591	IGJ	Immunoglobulin J chain
P01620		Ig kappa chain V-III region SIE
P01777		Ig heavy chain V-III region TEI
P01833	PIGR	Polymeric immunoglobulin receptor
P01834	IGKC	Ig kappa chain C region
P01857	IGHG1	Ig gamma-1 chain C region
P01859	IGHG2	Ig gamma-2 chain C region
P01876	IGHA1	Ig alpha-1 chain C region
P01877	IGHA2	Ig alpha-2 chain C region
P02533	KRT14	Keratin, type I cytoskeletal 14
P02538	KRT6A	Keratin, type II cytoskeletal 6A
P02549	SPTA1	Spectrin alpha chain, erythrocytic 1
P02730	SLC4A1	Band 3 anion transport protein
P02766	TTR	Transthyretin
P02768	ALB	Serum albumin
P02775	PPBP	Platelet basic protein
P02787	TF	Serotransferrin
P02788	LTF	Lactotransferrin
P02814	SMR3B	Submaxillary gland androgen-regulated protein 3B
P04075	ALDOA	Fructose-bisphosphate aldolase A

P04080	CSTB	Cystatin-B
P04083	ANXA1	Annexin A1
P04264	KRT1	Keratin, type II cytoskeletal 1
P04406	GAPDH	Glyceraldehyde-3-phosphate dehydrogenase
P04745	AMY1A	Alpha-amylase 1
P05109	S100A8	Protein S100-A8
P05164	MPO	Myeloperoxidase
P05164-2	MPO	Isoform H14 of Myeloperoxidase
P06396	GSN	Gelsolin
P06702	S100A9	Protein S100-A9
P06733	ENO1	Alpha-enolase
P06733-2	ENO1	Isoform MBP-1 of Alpha-enolase
P06870	KLK1	Kallikrein-1
P07237	P4HB	Protein disulfide-isomerase
P07737	PFN1	Profilin-1
P08246	ELANE	Neutrophil elastase
P08311	CTSG	Cathepsin G
P08670	VIM	Vimentin
P08727	KRT19	Keratin, type I cytoskeletal 19
P08729	KRT7	Keratin, type II cytoskeletal 7
P08F94-2	PKHD1	Isoform 2 of Fibrocystin
P09211	GSTP1	Glutathione S-transferase P
P09228	CST2	Cystatin-SA
P0CF51	TRGC1	T-cell receptor gamma chain C region 1
P0CG04	IGLC1	Ig lambda-1 chain C regions

P0CW71	HSMCR30	Putative metaphase chromosome protein 1
P10243-2	MYBL1	Isoform 2 of Myb-related protein A
P10599	TXN	Thioredoxin
P10636	MAPT	Microtubule-associated protein tau
P10636-3	MAPT	Isoform Tau-A of Microtubule-associated protein tau
P10745	RBP3	Retinol-binding protein 3
P11277-3	SPTB	Isoform 3 of Spectrin beta chain, erythrocytic
P12273	PIP	Prolactin-inducible protein
P12429	ANXA3	Annexin A3
P13645	KRT10	Keratin, type I cytoskeletal 10
P13796	LCP1	Plastin-2
P13804	ETFA	Electron transfer flavoprotein subunit alpha, mitochondrial
P14780	MMP9	Matrix metalloproteinase-9
P14923	JUP	Junction plakoglobin
P15259	PGAM2	Phosphoglycerate mutase 2
P15924	DSP	Desmoplakin
P16403	HIST1H1C	Histone H1.2
P20061	TCN1	Transcobalamin-1
P21333	FLNA	Filamin-A
P22079	LPO	Lactoperoxidase
P23280	CA6	Carbonic anhydrase 6
P25311	AZGP1	Zinc-alpha-2-glycoprotein
P26038	MSN	Moesin
P27348	YWHAQ	14-3-3 protein theta
P30740	SERPINB1	Leukocyte elastase inhibitor

P31025	LCN1	Lipocalin-1
P32119	PRDX2	Peroxiredoxin-2
P35527	KRT9	Keratin, type I cytoskeletal 9
P35579	MYH9	Myosin-9
P35908	KRT2	Keratin, type II cytoskeletal 2 epidermal
P36873	PPP1CC	Serine/threonine-protein phosphatase PP1-gamma catalytic subunit
P37837	TALDO1	Transaldolase
P46020	PHKA1	Phosphorylase b kinase regulatory subunit alpha, skeletal muscle isoform
P48147	PREP	Prolyl endopeptidase
P49639	HOXA1	Homeobox protein Hox-A1
P52565	ARHGDIA	Rho GDP-dissociation inhibitor 1
P52566	ARHGDIB	Rho GDP-dissociation inhibitor 2
P59665	DEFA1	Neutrophil defensin 1
P60709	ACTB	Actin, cytoplasmic 1
P61626	LYZ	Lysozyme C
P61647	ST8SIA6	Alpha-2,8-sialyltransferase 8F
P62805	HIST1H4A	Histone H4
P62937	PPIA	Peptidyl-prolyl cis-trans isomerase A
P68871	HBB	Hemoglobin subunit beta
P69905	HBA1	Hemoglobin subunit alpha
Q02040	AKAP17A	A-kinase anchor protein 17A
Q05707	COL14A1	Collagen alpha-1(XIV) chain
Q05707-3	COL14A1	Isoform 3 of Collagen alpha-1(XIV) chain
Q14166	TTLL12	Tubulin--tyrosine ligase-like protein 12
Q14207	NPAT	Protein NPAT

Q14993	COL19A1	Collagen alpha-1(XIX) chain
Q15059-2	BRD3	Isoform 2 of Bromodomain-containing protein 3
Q15078	CDK5R1	Cyclin-dependent kinase 5 activator 1
Q15477	SKIV2L	Helicase SKI2W
Q16549	PCSK7	Proprotein convertase subtilisin/kexin type 7
Q2TBE0	CWF19L2	CWF19-like protein 2
Q3BBV0	NBPF1	Neuroblastoma breakpoint family member 1
Q4G112	HSF5	Heat shock factor protein 5
Q4KWH8-2	PLCH1	Isoform 2 of 1-phosphatidylinositol 4,5-bisphosphate phosphodiesterase eta-1
Q5T085	AMY1B	Alpha-amylase 1 (Fragment)
Q5T7V8	GORAB	RAB6-interacting golgin
Q5T8M8	ACTA1	Actin, alpha skeletal muscle
Q5TAQ9	DCAF8	DDB1- and CUL4-associated factor 8
Q5VT06	CEP350	Centrosome-associated protein 350
Q5XKE5	KRT79	Keratin, type II cytoskeletal 79
Q6NXT2	H3F3C	Histone H3.3C
Q6P5S2	C6orf58	UPF0762 protein C6orf58
Q6S8J7-2	POTEA	Isoform 2 of POTE ankyrin domain family member A
Q6ZU67	BEND4	BEN domain-containing protein 4
Q7Z3D6	C14orf159	UPF0317 protein C14orf159, mitochondrial
Q7Z3Z0	KRT25	Keratin, type I cytoskeletal 25
Q7Z4W1	DCXR	L-xylulose reductase
Q7Z794	KRT77	Keratin, type II cytoskeletal 1b
Q86TG7-2	PEG10	Isoform RF1 of Retrotransposon-derived protein PEG10
Q8N2H3	PYROXD2	Pyridine nucleotide-disulfide oxidoreductase domain-containing protein 2

Q8N302	AGGF1	Angiogenic factor with G patch and FHA domains 1
Q8N427	NME8	Thioredoxin domain-containing protein 3
Q8N4F0	BPIFB2	BPI fold-containing family B member 2
Q8NGN5	OR10G8	Olfactory receptor 10G8
Q8TAL5	C9orf43	Uncharacterized protein C9orf43
Q8TAX7	MUC7	Mucin-7
Q8WZ55	BSND	Barttin
Q96DA0	ZG16B	Zymogen granule protein 16 homolog B
Q96DR5	BPIFA2	BPI fold-containing family A member 2
Q96EK7-2	FAM120B	Isoform 2 of Constitutive coactivator of peroxisome proliferator-activated receptor gamma
Q96EU7	C1GALT1C1	C1GALT1-specific chaperone 1
Q96JM2	ZNF462	Zinc finger protein 462
Q96P15	SERPINB11	Serpin B11
Q99798	ACO2	Aconitate hydratase, mitochondrial
Q99848	EBNA1BP2	Probable rRNA-processing protein EBP2
Q9BQS8	FYCO1	FYVE and coiled-coil domain-containing protein 1
Q9C029-1	TRIM7	Isoform 4 of Tripartite motif-containing protein 7
Q9H094-5	NBPF3	Isoform 5 of Neuroblastoma breakpoint family member 3
Q9H3U1-2	UNC45A	Isoform 2 of Protein unc-45 homolog A
Q9H4B7	TUBB1	Tubulin beta-1 chain
Q9H694-2	BICC1	Isoform 2 of Protein bicaudal C homolog 1
Q9HC58	SLC24A3	Sodium/potassium/calcium exchanger 3
Q9HC84	MUC5B	Mucin-5B
Q9NU22	MDN1	Midasin

Q9P1Z3	HCN3	Potassium/sodium hyperpolarization-activated cyclic nucleotide-gated channel 3
Q9P2D1	CHD7	Chromodomain-helicase-DNA-binding protein 7
Q9UBN4-6	TRPC4	Isoform Zeta of Short transient receptor potential channel 4
Q9UGM3	DMBT1	Deleted in malignant brain tumors 1 protein
Q9UNS1-2	TIMELESS	Isoform 2 of Protein timeless homolog
Q9Y2Q0	ATP8A1 P	Probable phospholipid-transporting ATPase IA
Q9Y2Q0-2	ATP8A1	Isoform 2 of Probable phospholipid-transporting ATPase IA
Q9Y2Z9	COQ6	Ubiquinone biosynthesis monooxygenase COQ6
Q9Y3B3	TMED7	Transmembrane emp24 domain-containing protein 7
Q9Y6M7-5	SLC4A7	Isoform 5 of Sodium bicarbonate cotransporter 3
Q9Y6W5	WASF2	Wiskott-Aldrich syndrome protein family member 2
R4GN98	S100A6	Protein S100-A6 (Fragment)
U5GXS2	MPP7	MAGUK p55 subfamily member 7 (Fragment)

Appendix 8.3: Accession number, description of protein and log mean of periodontal patients.

Accession	Description	LOG2 fold change	Log10 p-value
P68871	Haemoglobin subunit beta	-1.02	1.55
P28161	Glutathione S-transferase Mu 2	-1.00	0.45
P00915	carbonic anhydrase 1	-0.88	1.40
P02042	Haemoglobin subunit delta	-0.84	1.74
P69905	Haemoglobin subunit alpha	-0.79	1.49
P00390	Glutathione reductase, mitochondrial	-0.52	2.44
P27695	DNA-(apurinic or apyrimidinic site) lyase	-0.20	2.12
P07339	Cathepsin D	0.11	1.52
Q07960	rho GTPase-activating protein 1	0.13	1.43
P35754	Glutaredoxin-1	0.24	1.42
Q9P2E9-1	Ribosome-binding protein 1	0.24	1.42
P60953	Cell division control protein 42 homolog	0.26	2.93
P06737-1	Glycogen phosphorylase, liver form	0.26	2.03
P11766	alcohol dehydrogenase class-3	0.30	3.91
P43490	nicotinamide phosphoribosyltransferase	0.33	1.34
P40227-1	T-complex protein 1 subunit zeta	0.34	1.55
P28838	cytosol aminopeptidase	0.41	1.44
Q14697-2	Isoform 2 of Neutral alpha-glucosidase AB	0.42	1.72

P28676	Grancalcin	0.46	1.33
Q01432-4	Isoform 2 of AMP deaminase 3	0.50	1.43
O75915	PRA1 family protein 3	0.61	1.55
Q9UJ70-2	Isoform 2 of N-acetyl-D-glucosamine kinase	0.63	1.69
P60842	Eukaryotic initiation factor 4A-I	1.01	0.64
P05164-3	Isoform H7 of Myeloperoxidase	1.06	0.50
Q6FI13	Histone H2A type 2-A	1.30	0.38
P08311	Cathepsin G	1.33	0.45
P11678	Eosinophil peroxidase	1.36	0.58
P23527	Histone H2B type 1-O	1.45	0.44
P62805	histone H4	1.46	0.48
P51858	hepatoma-derived growth factor	-0.75	0.68
P02769	Serum albumin	-0.73	1.20
P54819	Adenylate kinase 2, mitochondrial	-0.66	0.31
Q3SZR3	Alpha-1-acid glycoprotein	-0.66	0.69
P02768-1	Serum albumin	-0.56	0.73
P62140	Serine/threonine-protein phosphatase PP1-beta catalytic subunit	-0.56	0.48
P20810-6	Isoform 6 of Calpastatin	-0.56	0.50
P32119	Peroxiredoxin-2	-0.52	0.79
Q28194	Thrombospondin-1 (Fragment)	-0.52	0.67
P16402	Histone H1.3	-0.50	0.29
Q96HE7	ERO1-like protein alpha	-0.49	0.28
P14678-3	Isoform SM-B1 of Small nuclear ribonucleoprotein-associated proteins B and B'	-0.47	0.45

P54108-3	Isoform 3 of Cysteine-rich secretory protein 3	-0.47	0.53
P61981	14-3-3 protein gamma	-0.47	1.15
P10412	Histone H1.4	-0.46	0.20
O75015	Low affinity immunoglobulin gamma Fc region receptor III-B	-0.46	0.31
P16104	Histone H2AX	-0.45	0.81
P40121	Macrophage-capping protein	-0.43	0.83
P42166	Lamina-associated polypeptide 2, isoform alpha	-0.42	0.98
Q96E17	ras-related protein Rab-3C	-0.42	0.20
P32320	cytidine deaminase	-0.41	0.49
P04264	Keratin, type II cytoskeletal 1	-0.39	0.90
O75368	SH3 domain-binding glutamic acid-rich-like protein	-0.39	0.47
P31150	Rab GDP dissociation inhibitor alpha	-0.38	0.39
P11166	Solute carrier family 2, facilitated glucose transporter member 1	-0.38	0.23
P02763	Alpha-1-acid glycoprotein 1	-0.37	0.35
P23526-1	Adenosylhomocysteinase	-0.37	0.60
P08637	Low affinity immunoglobulin gamma Fc region receptor III-A	-0.37	0.81
P07910-1	Heterogeneous nuclear ribonucleoproteins C1/C2	-0.37	0.80
O00232-1	26s proteasome non-atpase regulatory subunit 12	-0.36	0.87
P50990	T-complex protein 1 subunit theta	-0.35	0.42
Q9Y2Y8	proteoglycan 3	-0.35	0.22
P36957	Dihydrolipoyllysine-residue succinyltransferase component of 2-oxoglutarate dehydrogenase complex, mitochondrial	-0.34	0.18
P25787	Proteasome subunit alpha type-2	-0.34	1.02
P62158	Calmodulin	-0.33	0.14

P00488	Coagulation factor XIII A chain	-0.33	0.18
P41218	Myeloid cell nuclear differentiation antigen	-0.33	0.49
P04179	Superoxide dismutase	-0.33	0.43
P05204	Non-histone chromosomal protein HMG-17	-0.33	0.11
P13645	Keratin, type I cytoskeletal 10	-0.33	0.55
Q5JTV8-3	Isoform 3 of Torsin-1A-interacting protein 1	-0.31	0.51
Q01518-1	adenylyl cyclase-associated protein 1	-0.31	0.20
Q92688	Acidic leucine-rich nuclear phosphoprotein 32 family member B	-0.30	0.45
Q14739	Lamin-B receptor	-0.30	0.14
P00918	Carbonic anhydrase 2	-0.29	1.06
P61077-3	Isoform 3 of Ubiquitin-conjugating enzyme E2 D3	-0.28	0.24
Q9Y2S6	Translation machinery-associated protein 7	-0.28	0.60
Q9HBI1-2	Isoform 2 of Beta-parvin	-0.28	0.22
P27348	14-3-3 protein theta	-0.28	0.16
Q15942	Zyxin	-0.28	0.43
P0DOX5	immunoglobulin gamma-1 heavy chain	-0.27	0.19
P49721	proteasome subunit beta type-2	-0.27	0.35
P22061-2	Isoform 2 of Protein-L-isoaspartate(D-aspartate) O-methyltransferase	-0.27	0.53
P62937	peptidyl-prolyl cis-trans isomerase A	-0.26	0.81
Q15257-1	Serine/threonine-protein phosphatase 2A activator	-0.26	0.28
Q9UBW5-1	Bridging integrator 2	-0.26	0.22
P10768	S-formylglutathione hydrolase	-0.25	0.50
P63241-2	Isoform 2 of Eukaryotic translation initiation factor 5A-1	-0.25	0.20
P09429	High mobility group protein B1	-0.24	0.41

P52907	F-actin-capping protein subunit alpha-1	-0.23	0.31
Q15366-2	Isoform 2 of Poly(rC)-binding protein 2	-0.23	0.61
P31146	Coronin-1A	-0.23	0.349
Q9NQR4	Omega-amidase NIT2	-0.22	0.16
P07737	profilin-1	-0.22	0.21
P14317	Hematopoietic lineage cell-specific protein	-0.22	0.47
P61970	nuclear transport factor 2	-0.22	0.83
P16401	Histone H1.5	-0.22	0.16
Q01518-2	Isoform 2 of Adenylyl cyclase-associated protein 1	-0.21	0.23
P49189	4-tnimethylaminobutyraldehyde dehydrogenase	-0.21	0.31
P26583	High mobility group protein B2	-0.20	0.32
P06703	protein S100-A6	-0.20	0.16
Q14847-2	Isoform 2 of LIM and SH3 domain protein 1	-0.20	0.16
Q16698	2,4-dienoyl-CoA reductase, mitochondrial	-0.20	0.77
P80723	Brain acid soluble protein 1	-0.20	0.27
P13798	Acylamino-acid-releasing enzyme	-0.20	0.94
Q9UKM9-1	RNA-binding protein Raly	-0.20	0.94
P08758	annexin A5	-0.20	0.22
P12429	annexin A3	-0.20	0.23
P63313	thymosin beta-10	-0.20	0.78
Q9UL46	proteasome activator complex subunit 2	-0.20	0.26
Q14103	heterogeneous nuclear ribonucleoprotein D0	-0.19	0.42
P13693	Translationally-controlled tumor protein	-0.19	0.39
P24557-3	Isoform 3 of Thromboxane-A synthase	-0.19	0.27

P61626	lysozyme c	-0.19	0.18
Q06830	peroxiredoxin-1	-0.19	0.49
P02775	Platelet basic protein	-0.19	0.33
P20061	Transcobalamin-1	-0.19	0.16
P04083	annexin A1	-0.18	0.15
P55957-2	Isoform 2 of BH3-interacting domain death agonist	-0.18	0.28
O75367-1	Core histone macro-H2A.1	-0.18	0.36
P50502	Hsc70-interacting protein	-0.18	0.20
P11310-2	Isoform 2 of Medium-chain specific acyl-CoA dehydrogenase, mitochondrial	-0.17	0.24
Q05315	galectin-10	-0.17	0.13
Q99497	protein/nucleic acid deglycase DJ-1	-0.17	0.64
P14780	Matrix metalloproteinase-9	-0.17	0.26
Q14019	coactosin-like protein	-0.16	0.14
P30044-1	Peroxiredoxin-5, mitochondrial	-0.15	0.16
P36871-1	Phosphoglucomutase-1	-0.15	0.50
P31949	protein S100-A11	-0.15	0.10
A6NI72	Putative neutrophil cytosol factor 1B	-0.14	0.27
P51991-1	Heterogeneous nuclear ribonucleoprotein A3	-0.14	0.43
P04075-2	Isoform 2 of Fructose-bisphosphate aldolase A	-0.14	0.29
P16403	Histone H1.2	-0.14	0.14
Q9NYL9	tropomodulin-3	-0.13	0.15
Q00839	Heterogeneous nuclear ribonucleoprotein U	-0.13	0.50
P26038	Moesin	-0.13	0.33

O75131	Copine-3	-0.13	0.30
Q9H299	SH3 domain-binding glutamic acid-rich-like protein 3	-0.13	0.22
P40197	Platelet glycoprotein V	-0.12	0.14
Q92522	Histone H1x	-0.12	0.13
P61088	ubiquitin-conjugating enzyme E2 N	-0.12	0.64
P02730	Band 3 anion transport protein	-0.12	0.09
Q9NQC3	Reticulon-4	-0.12	0.18
P11215-2	Isoform 2 of Integrin alpha-M	-0.13	0.16
P13489	Ribonuclease inhibitor	-0.12	0.60
P00491	purine nucleoside phosphorylase	-0.12	0.16
P61916	Epididymal secretory protein E1	-0.11	0.26
O00764-1	Pyridoxal kinase	-0.12	0.15
P04040	catalase	-0.12	0.46
Q15084-2	Isoform 2 of Protein disulfide-isomerase A6	-0.12	0.23
P33241-3	Isoform 3 of Lymphocyte-specific protein 1	-0.12	0.13
P20340-1	Ras-related protein Rab-6A	-0.11	0.22
P22234	multifunctional protein ADE2	-0.11	0.59
P00761	Trypsin OS=Sus scrofa PE=1 SV=1	-0.11	0.20
P54725	UV excision repair protein RAD23 homolog A	-0.11	0.06
P07305	Histone H1.0	-0.10	0.08
P80511	Protein S100-A12	-0.10	0.11
Q1KMD3	heterogeneous nuclear ribonucleoprotein U-like protein 2	-0.10	0.19
P40926	Malate dehydrogenase, mitochondrial	-0.10	0.44
Q9UQ80	proliferation-associated protein 2G4	-0.10	0.11

P30504	HLA class I histocompatibility antigen, Cw-4 alpha chain	-0.10	0.19
P14314	Glucosidase 2 subunit beta	-0.10	0.06
P61604	10 kDa heat shock protein, mitochondrial	-0.09	0.20
P13796	Plastin-2	-0.08	0.07
P78417	Glutathione S-transferase omega-1	-0.08	0.09
P00558	phosphoglycerate kinase 1	-0.08	0.07
P40925-3	Isoform 3 of Malate dehydrogenase, cytoplasmic	-0.08	0.11
P51149	ras-related protein Rab-7a	-0.08	0.11
Q92930	Ras-related protein Rab-8B	-0.08	0.06
P19338	Nucleolin	-0.07	0.07
P80188	Neutrophil gelatinase-associated lipocalin	-0.07	0.08
P37837	Transaldolase	-0.07	0.06
P10599-1	thioredoxin	-0.07	0.10
P23528	Cofilin-1	-0.07	0.07
Q9UM07	Protein-arginine deiminase type-4	-0.07	0.03
Q9Y5Z4-1	Heme-binding protein 2	-0.07	0.37
P50552	Vasodilator-stimulated phosphoprotein	-0.07	0.15
P18669	Phosphoglycerate mutase 1	-0.07	0.13
Q6JBY9	CapZ-interacting protein	-0.07	0.13
P52566	Rho GDP-dissociation inhibitor 2	-0.06	0.08
P09211	Glutathione S-transferase P	-0.06	0.04
P08567	pleckstrin	-0.06	0.08
P63104	14-3-3 protein zeta/delta	-0.06	0.05
P0DMV8	heat shock 70 kDa protein 1A	-0.06	0.13

Q13011	Delta(3,5)-Delta(2,4)-dienoyl-CoA isomerase, mitochondrial	-0.06	0.16
P09917	arachidonate 5-lipoxygenase	-0.06	0.08
P23368-1	NAD-dependent malic enzyme, mitochondrial	-0.06	0.18
P25815	Protein S100-P	-0.05	0.04
P05107	Integrin beta-2	-0.05	0.11
P02788	Lactotransferrin	-0.05	0.05
Q969H8	Myeloid-derived growth factor	-0.05	0.12
P31946	14-3-3 protein beta/alpha	-0.05	0.07
P26641-2	Isoform 2 of Elongation factor 1-gamma	-0.05	0.11
Q9BRA2	Thioredoxin domain-containing protein 17	-0.05	0.05
Q15907	Ras-related protein Rab-11B	-0.05	0.14
P62258-1	14-3-3 protein epsilon	-0.05	0.26
Q00325-1	Phosphate carrier protein, mitochondrial	-0.04	0.07
Q96FJ2	Dynein light chain 2, cytoplasmic	-0.04	0.06
Q9NZN3	EH domain-containing protein 3	-0.04	0.03
Q3ZBD7	Glucose-6-phosphate isomerase OS=Bos taurus GN=GPI PE=2 SV=4	-0.04	0.04
Q12905	Interleukin enhancer-binding factor 2	-0.04	0.13
P05455	Lupus La protein	-0.04	0.05
P55008-1	Allograft inflammatory factor 1	-0.04	0.13
P26599-3	Isoform 3 of Polypyrimidine tract-binding protein 1	-0.04	0.11
Q6P4A8	Phospholipase B-like 1	-0.04	0.04
P22894	Neutrophil collagenase	-0.04	0.03
Q9BRF8-1	Serine/threonine-protein phosphatase CPPED1	-0.03	0.10
P58546	Myotrophin	-0.03	0.03

P07741-1	Adenine phosphoribosyltransferase	-0.03	0.17
P37802-2	Isoform 2 of Transgelin-2	-0.03	0.04
P60900	Proteasome subunit alpha type-6	-0.03	0.06
P06744	glucose-6-phosphate isomerase	-0.03	0.03
Q9HC38	Glyoxalase domain-containing protein 4	-0.03	0.02
P00738	Haptoglobin	-0.03	0.05
P00387-3	Isoform 3 of NADH-cytochrome b5 reductase 3	-0.03	0.30
P04839	Cytochrome b-245 heavy chain	-0.02	0.07
Q99439	Calponin-2	-0.02	0.03
P19878	Neutrophil cytosol factor 2	-0.02	0.06
P30048	Thioredoxin-dependent peroxide reductase, mitochondrial	-0.02	0.03
P05109	Protein S100-A8	-0.02	0.02
P30046	D-dopachrome decarboxylase	-0.02	0.04
Q16881-1	Thioredoxin reductase 1, cytoplasmic	-0.02	0.04
P08133-1	annexin A6	-0.02	0.02
P14866	Heterogeneous nuclear ribonucleoprotein L	-0.02	0.08
Q10588	ADP-ribosyl cyclase/cyclic ADP-ribose hydrolase 2	-0.02	0.04
P45880-1	Isoform 1 of Voltage-dependent anion-selective channel protein 2	-0.02	0.07
P46459	Vesicle-fusing ATPase	-0.01	0.02
Q92882	osteoclast-stimulating factor 1	-0.01	0.03
P68036-3	Isoform 3 of Ubiquitin-conjugating enzyme E2 L3	-0.01	0.01
P26447	Protein S100-A4	-0.01	0.01
P22626	heterogeneous nuclear ribonucleoproteins A2/B1	-0.01	0.01
P50395-1	Rab GDP dissociation inhibitor beta	-0.01	0.04

P47756-2	Isoform 2 of F-actin-capping protein subunit beta	-0.01	0.02
P11142-1	Heat shock cognate 71 kDa protein	-0.01	0.03
P30043	flavin reductase (NADPH)	-0.01	0.02
P11413-2	Isoform Long of Glucose-6-phosphate 1-dehydrogenase	-0.01	0.01
P07996	thrombospondin-1	-0.01	0.01
P29350-4	Isoform 4 of Tyrosine-protein phosphatase non-receptor type 6	-0.01	0.01
P15144	aminopeptidase N	-0.00	0.00
P09525	annexin A4	-0.00	0.00
P09960-1	leukotriene A-4 hydrolase	-0.00	0.00
P07359	Platelet glycoprotein Ib alpha chain	0.00	0.00
O43707	Alpha-actinin-4	0.00	0.00
P02776	Platelet factor 4	0.00	0.00
P54727	UV excision repair protein RAD23 homolog B	0.00	0.01
Q6UX06	Olfactomedin-4	0.00	0.00
P05106	Integrin beta-3	0.01	0.01
P53004	Biliverdin reductase A	0.01	0.03
P62328	Thymosin beta-4	0.01	0.02
P15311	Ezrin	0.01	0.04
P06702	Protein S100-A9	0.02	0.02
O75594	peptidoglycan recognition protein 1	0.02	0.02
P61224-1	Ras-related protein Rap-1b	0.02	0.03
P31948-2	Isoform 2 of Stress-induced-phosphoprotein 1	0.02	0.04
P52209-2	Isoform 2 of 6-phosphogluconate dehydrogenase, decarboxylating	0.02	0.03
P61978-2	Isoform 2 of Heterogeneous nuclear ribonucleoprotein K	0.02	0.03

Q9Y376	Calcium-binding protein 39	0.02	0.02
P49748-3	Isoform 3 of Very long-chain specific acyl-CoA dehydrogenase, mitochondrial	0.02	0.04
Q9ULZ3	apoptosis-associated speck-like protein containing a CARD	0.03	0.02
P23284	peptidyl-prolyl cis-trans isomerase B	0.03	0.04
P30405	Peptidyl-prolyl cis-trans isomerase F, mitochondrial	0.03	0.09
P12814-1	Alpha-actinin-1	0.03	0.07
P15954	Cytochrome c oxidase subunit 7C, mitochondrial	0.03	0.02
P22307-1	Non-specific lipid-transfer protein	0.03	0.26
P04080	Cystatin-B	0.03	0.02
P29401-2	Isoform 2 of Transketolase	0.03	0.02
P60174	Triosephosphate isomerase	0.04	0.05
P24158	Myeloblastin	0.04	0.04
P06733-1	alpha-enolase	0.04	0.04
P17213	Bactericidal permeability-increasing protein	0.04	0.03
P61204	ADP-ribosylation factor 3	0.04	0.03
P50995	annexin A11	0.04	0.23
P30040-1	Endoplasmic reticulum resident protein 29	0.04	0.25
P14550	alcohol dehydrogenase	0.04	0.30
P62136-2	Isoform 2 of Serine/threonine-protein phosphatase PP1-alpha catalytic subunit	0.04	0.33
Q12906-7	Isoform 7 of Interleukin enhancer-binding factor 3	0.05	0.19
P02647	Apolipoprotein A-I	0.05	0.15
P16949-2	Isoform 2 of Stathmin	0.05	0.05
Q13177	Serine/threonine-protein kinase PAK 2	0.05	0.18

P38646	Stress-70 protein, mitochondrial	0.05	0.05
O75390	citrate synthase, mitochondrial	0.05	0.77
P22314	Ubiquitin-like modifier-activating enzyme 1	0.05	0.13
O95336	6-phosphogluconolactonase	0.05	0.08
Q99536	Synaptic vesicle membrane protein VAT-1 homolog	0.06	0.12
P11021	78 kDa glucose-regulated protein	0.06	0.39
O15143	Actin-related protein 2/3 complex subunit 1B	0.06	0.11
O75340	programmed cell death protein 6	0.06	0.07
Q9P1F3	Costars family protein ABRACL	0.06	0.05
Q15833-1	Syntaxin-binding protein 2	0.06	0.12
P02675	Fibrinogen beta chain	0.06	0.06
O00194	ras-related protein rab-27b	0.06	0.03
P30086	phosphatidylethanolamine-binding protein 1	0.06	0.31
Q96QK1	Vacuolar protein sorting-associated protein 35	0.07	0.12
P46976-1	Glycogenin-1	0.07	0.15
O75083	WD repeat-containing protein 1	0.07	0.08
P10720	Platelet factor 4 variant	0.07	0.06
P07108-5	Isoform 5 of Acyl-CoA-binding protein	0.07	0.07
P19367-3	Isoform 3 of Hexokinase-1	0.07	0.12
Q9Y490	Talin-1	0.07	0.13
Q9H4A4	aminopeptidase B	0.07	0.08
P55145	Mesencephalic astrocyte-derived neurotrophic factor	0.08	0.06
P00492	Hypoxanthine-guanine phosphoribosyltransferase	0.08	0.61
P32942	Intercellular adhesion molecule 3	0.08	0.64

Q6XQN6-2	Isoform 2 of Nicotinate phosphoribosyltransferase	0.08	0.72
P06865	Beta-hexosaminidase subunit alpha	0.08	0.23
P67936	Tropomyosin alpha-4 chain	0.08	0.08
P48595	serpin B10	0.08	0.20
P10644	cAMP-dependent protein kinase type I-alpha regulatory subunit	0.08	0.07
P11234-2	Isoform 2 of Ras-related protein Ral-B	0.08	0.06
P12956	X-ray repair cross-complementing protein 6	0.08	0.11
P36222	Chitinase-3-like protein 1	0.08	0.10
P20073-1	Annexin A7	0.08	0.18
P49591	Serine--tRNA ligase, cytoplasmic	0.09	0.09
Q9HDC9	Adipocyte plasma membrane-associated protein	0.09	0.33
P68104	Elongation factor 1-alpha 1	0.09	0.17
Q12913-1	Receptor-type tyrosine-protein phosphatase eta	0.09	0.11
Q04760-1	lactoylglutathione lyase	0.09	0.29
P61158	actin-related protein 3	0.09	0.11
O15511-1	Actin-related protein 2/3 complex subunit 5	0.09	0.57
P31943	Heterogeneous nuclear ribonucleoprotein H	0.09	0.10
Q13561-2	Isoform 2 of Dynactin subunit 2	0.09	0.15
P55786	puromycin-sensitive aminopeptidase	0.10	0.18
P04406	glyceraldehyde-3-phosphate dehydrogenase	0.10	0.08
Q06323	Proteasome activator complex subunit 1	0.10	0.13
P39687	Acidic leucine-rich nuclear phosphoprotein 32 family member A	0.10	0.15
P30041	Peroxiredoxin-6	0.10	0.12
Q9NVA2-2	Isoform 2 of Septin-11	0.10	0.26

P13639	Elongation factor 2	0.10	0.12
O60234	glia maturation factor gamma	0.10	0.12
Q9ULV4-3	Isoform 3 of Coronin-1C	0.10	0.22
P08514-1	integrin alpha-IIb	0.10	0.18
P18206	Vinculin	0.10	0.27
P21333	Filamin-A	0.11	0.19
Q96RU3-1	Formin-binding protein 1	0.11	0.23
Q16851	UTP--glucose-1-phosphate uridylyltransferase	0.11	0.63
P30520	adenylosuccinate synthetase isozyme 2	0.11	0.30
P61106	Ras-related protein Rab-14	0.11	1.14
Q6IBS0	Twinfilin-2	0.11	0.25
P99999	cytochrome c	0.11	0.11
Q15691	Microtubule-associated protein RP/EB family member 1	0.12	0.13
O15144	Actin-related protein 2/3 complex subunit 2	0.12	0.10
P10809	60 kDa heat shock protein, mitochondrial	0.12	0.25
Q96G03	Phosphoglucomutase-2	0.12	0.24
O00151	PDZ and LIM domain protein 1	0.12	0.06
P15153	Ras-related C3 botulinum toxin substrate 2	0.12	0.37
Q9H0U4	ras-related protein Rab-1B	0.12	0.16
P48643	T-complex protein 1 subunit epsilon	0.12	0.19
Q14974	Importin subunit beta-1	0.12	0.28
P04899-1	guanine nucleotide-binding protein G(i) subunit alpha-2	0.13	0.19
P61586	Transforming protein RhoA	0.12	0.43
P16050	arachidonate 15-lipoxygenase	0.12	0.22

Q92820	Gamma-glutamyl hydrolase	0.12	0.24
P06753-2	Isoform 2 of Tropomyosin alpha-3 chain	0.13	0.19
P13224-2	Isoform 2 of Platelet glycoprotein Ib beta chain	0.13	0.15
Q5JWF2-1	Guanine nucleotide-binding protein G(S) subunit alpha isoforms XLas	0.13	0.14
P52565	rho GDP-dissociation inhibitor 1	0.13	1.09
P61020	Ras-related protein Rab-5B	0.13	0.78
P55072	Transitional endoplasmic reticulum ATPase	0.14	0.42
P27105	erythrocyte band 7 integral membrane protein	0.14	0.23
P05089-2	Isoform 2 of Arginase-1	0.14	0.18
P59998-3	Isoform 3 of Actin-related protein 2/3 complex subunit 4	0.15	0.27
Q96C19	EF-hand domain-containing protein D2	0.15	0.50
O00299	chloride intracellular channel protein 1	0.15	0.31
P39019	40S ribosomal protein S19	0.15	0.13
Q7L1Q6-3	Isoform 3 of Basic leucine zipper and W2 domain-containing protein 1	0.15	0.42
P48147	prolyl endopeptidase	0.15	0.39
Q96QH2-2	Isoform 2 of PML-RARA-regulated adapter molecule 1	0.15	0.25
P00505	Aspartate aminotransferase, mitochondrial	0.16	0.31
Q99729-1	Heterogeneous nuclear ribonucleoprotein A/B	0.16	0.20
P04632	Calpain small subunit 1	0.16	0.62
P13716-2	Isoform 2 of Delta-aminolevulinic acid dehydratase	0.16	0.25
Q15365	Poly(RC)-binding protein 1	0.16	0.34
Q13813-2	Isoform 2 of Spectrin alpha chain, non-erythrocytic 1	0.17	0.19
P62826	GTP-binding nuclear protein RAN	0.17	0.46
O14773	Tripeptidyl-peptidase 1	0.17	0.60

P02671-1	Fibrinogen alpha chain	0.17	0.15
P22392-2	Isoform 3 of Nucleoside diphosphate kinase B	0.17	0.49
P07237	Protein disulfide-isomerase	0.18	0.23
P15586	N-acetylglucosamine-6-sulfatase	0.18	0.29
O43488	aflatoxin B1 aldehyde reductase member 2	0.18	0.38
Q8WUM4-2	Isoform 2 of Programmed cell death 6-interacting protein	0.18	0.51
P27797	Calreticulin	0.18	0.32
P51159-1	Ras-related protein Rab-27A	0.18	0.61
P07602-3	Isoform Sap-mu-9 of Prosaposin	0.18	0.36
P29692-2	Isoform 2 of Elongation factor 1-delta	0.19	0.99
P09972	Fructose-bisphosphate aldolase C	0.19	0.33
P62873	Guanine nucleotide-binding protein G(I)/G(S)/G(T) subunit beta-1	0.19	0.13
P37840-1	Alpha-synuclein	0.19	0.11
P04908	histone H2A type 1-B/E	0.19	0.07
P21796	voltage-dependent anion-selective channel protein 1	0.19	0.46
P61160-2	Isoform 2 of Actin-related protein 2	0.19	0.59
P46940	Ras GTPase-activating-like protein IQGAP1	0.20	1.03
Q15080-1	Neutrophil cytosol factor 4	0.20	0.60
P25786-2	Isoform Long of Proteasome subunit alpha type-1	0.20	0.39
Q15404-1	Ras suppressor protein 1	0.20	0.23
O75923-13	Isoform 13 of Dysferlin	0.20	0.22
P08575-1	Receptor-type tyrosine-protein phosphatase C	0.20	0.51
Q13201	Multimerin-1	0.20	0.24
Q9UHD8-1	Septin-9	0.21	0.93

P61026	ras-related protein rab-10	0.21	0.27
Q8IX19	Mast cell-expressed membrane protein 1	0.21	0.32
P16671	Platelet glycoprotein 4	0.21	0.58
Q13185	chromobox protein homolog 3	0.21	0.46
O14950	Myosin regulatory light chain 12B	0.21	0.17
P30740	Leukocyte elastase inhibitor	0.21	0.54
P07195	L-lactate dehydrogenase B chain	0.22	0.18
P31939	bifunctional purine biosynthesis protein purH	0.22	0.50
Q9NUQ9	protein FAM49B	0.22	0.77
O14745	Na(+)/H(+) exchange regulatory cofactor NHE-RF1	0.22	0.14
P16152	Carbonyl reductase	0.22	0.17
P48059-3	Isoform 3 of LIM and senescent cell antigen-like-containing domain protein 1	0.22	0.28
O95810	caveolae-associated protein 2	0.22	0.15
Q14005-1	Pro-interleukin-16	0.23	0.33
P07355-2	Isoform 2 of Annexin A2	0.23	0.39
O75475-1	PC4 and SFRS1-interacting protein	0.24	0.29
P08238	Heat shock protein HSP 90-beta	0.24	0.49
P50570-1	Dynamin-2	0.24	0.45
Q92841	Probable ATP-dependent RNA helicase DDX17	0.24	0.37
P53396-1	ATP-citrate synthase	0.25	0.25
P12724	eosinophil cationic protein	0.25	0.12
Q9ULC4-3	Isoform 3 of Malignant T-cell-amplified sequence 1	0.25	0.71
P00338-3	Isoform 3 of L-lactate dehydrogenase A chain	0.25	0.17

P15121	aldose reductase	0.25	0.35
P19971-2	Isoform 2 of Thymidine phosphorylase	0.25	0.68
P30101	Protein disulfide-isomerase A3	0.25	0.35
P51148-2	Isoform 2 of Ras-related protein Rab-5C	0.26	0.35
P48735	Isocitrate dehydrogenase	0.26	0.55
Q9UII2-1	ATPase inhibitor, mitochondrial	0.26	0.75
P53999	Activated RNA polymerase II transcriptional coactivator p15	0.26	0.33
P18054	Arachidonate 12-lipoxygenase, 12S-type	0.27	0.42
O75874	Isocitrate dehydrogenase	0.27	0.25
P09874	Poly	0.27	0.25
P02679	Fibrinogen gamma chain	0.28	0.22
P07900-2	Isoform 2 of Heat shock protein HSP 90-alpha	0.29	0.71
P14625	Endoplasmin	0.29	0.67
O15145	Actin-related protein 2/3 complex subunit 3	0.29	0.53
Q13838-2	Isoform 2 of Spliceosome RNA helicase DDX39B	0.29	0.27
P17931	Galectin-3	0.29	1.15
Q86UX7	Fermitin family homolog 3	0.29	0.63
Q3ZCW2	Galectin-related protein	0.30	0.28
P06396	Gelsolin	0.30	0.86
P11169	Solute carrier family 2, facilitated glucose transporter member 3	0.30	0.35
P06748	Nucleophosmin	0.32	0.33
P10153	Non-secretory ribonuclease	0.32	0.18
Q8IUE6	Histone H2A type 2-B	0.32	0.20

P00366	Glutamate dehydrogenase 1, mitochondrial OS=Bos taurus GN=GLUD1 PE=1 SV=2	0.33	0.41
P27824-2	Isoform 2 of Calnexin	0.33	0.72
O43447	peptidyl-prolyl cis-trans isomerase H	0.34	0.44
P30085	UMP-CMP kinase	0.35	1.01
O75695	Protein XRP2	0.35	0.81
P84243	histone H3.3	0.36	0.17
P14770	Platelet glycoprotein IX	0.36	0.21
Q05655-2	Isoform 2 of Protein kinase C delta type	0.37	0.79
P28482	mitogen-activated protein kinase 1	0.37	0.63
P59665	Neutrophil defensin 1	0.37	0.35
P62979	Ubiquitin-40S ribosomal protein S27a	0.37	0.60
Q9H4M9	EH domain-containing protein 1	0.38	0.37
O60506	Heterogeneous nuclear ribonucleoprotein Q	0.38	0.33
Q09666-1	Neuroblast differentiation-associated protein AHNAK	0.38	0.31
P14618	Pyruvate kinase PKM	0.39	0.78
P06576	ATP synthase subunit beta, mitochondrial	0.40	0.89
P28070	Proteasome subunit beta type-4	0.40	0.90
Q9NR31	GTP-binding protein SAR1a	0.40	1.10
P53634-1	Dipeptidyl peptidase 1	0.40	0.20
P02656	Apolipoprotein C-III	0.41	0.18
P24534	Elongation factor 1-beta	0.41	0.51
P60709	Actin, cytoplasmic 1	0.41	0.66
P20160	Azurocidin	0.43	0.39

O00160	Unconventional myosin-If	0.45	0.40
P52790	Hexokinase-3	0.46	0.68
P52272	Heterogeneous nuclear ribonucleoprotein M	0.48	0.32
Q15102	Platelet-activating factor acetylhydrolase IB subunit gamma	0.49	0.64
P09651-1	Heterogeneous nuclear ribonucleoprotein A1	0.49	0.94
P68366	Tubulin alpha-4A chain	0.51	0.39
P09382	Galectin-1	0.52	0.66
P20700	Lamin-B1	0.52	0.43
P50225	Sulfotransferase 1A1	0.53	0.52
P0C0S5	Histone H2A.Z	0.53	0.37
P68032	Actin, alpha cardiac muscle 1	0.54	0.70
P49913	cathelicidin antimicrobial peptide	0.55	0.75
Q5QNW6-2	Isoform 2 of Histone H2B type 2-F	0.56	0.16
P43405-1	Tyrosine-protein kinase SYK	0.57	0.77
P68371	Tubulin beta-4B chain	0.58	0.56
P60660	Myosin light polypeptide 6	0.62	0.38
P08246	Neutrophil elastase	0.63	0.38
P68363	Tubulin alpha-1B chain	0.64	0.54
P13010	X-ray repair cross-complementing protein 5	0.69	1.00
P25705-1	ATP synthase subunit alpha, mitochondrial	0.69	0.69
P35579-1	Myosin-9	0.70	0.37
Q01469	Fatty acid-binding protein, epidermal	0.75	1.06
Q13418	Integrin-linked protein kinase	0.77	0.62
P07437	tubulin beta chain	0.82	0.44

Q9H4B7	tubulin beta-1 chain	0.82	1.20
P18124	60S ribosomal protein L7	0.87	0.50
P08670	Vimentin	0.90	0.39
P68431	Histone H3.1	0.93	0.34

Appendix 8.4: Upregulated genes from periodontal patients compared to controls analysed by DAVID bioinformatics tool. Gene ontology is shown.

Gene name	GO Description	Gene symbol	combination detected in
Calmodulin	Calcium ion binding	CALM1	(130C/128N) Patient 5/control 5
Cystatin-B	For cysteine protease inhibitor	CSTB	(130C/128N) Patient 5/control 5
Cathepsin G	For immune response	CTSG	(131/127N) Patient 2/control 2
Eosinophil peroxidase	Peroxidase activity	EPX	(129N/126) Patient 1/control 1 (131/127N) Patient 2/control 2
Coagulation factor XIII A chain	For blood coagulation	F13A1	(131/127N) Patient 2/control 2
Fibrinogen gamma chain	For receptor binding, cell surface receptor signalling pathway	FGG	(130C/127C) Patient 5/patient 5 post treatment
Guanine nucleotide-binding protein	For GTPase activity, protein binding	GNB1	(129C/128C) Patient 3/control 3

G(I)/G(S)/G(T) subunit beta-1			
Histone H2A.Z	DNA binding	H2AFZ	(129N/126) Patient 1/control 1 (131/127N) Patient 2/control 2
Histone H3.3	DNA binding	H3F3A	(129N/126) Patient 1/control 1 (131/127N) Patient 2/control 2
Histone H1.5	DNA binding	HIST1H1B	(131/127N) Patient 2/control 2
Histone H1.4	DNA binding	HIST1H1E	(131/127N) Patient 2/control 2
Histone H2B type 1-O	DNA binding	HIST1H2BO	(129N/126) Patient 1/control 1 (131/127N) Patient 2/control 2 (131/130N) Patient 2/patient 2 post treatment

Histone H4	At the intracellular nuclear chromosome	HIST1H4A	(131/127N) Patient 2/control 2
Histone H2A type 2-A	DNA binding	HIST2H2AA3	(129N/126) Patient 1/control 1 (131/127N) Patient 2/control 2 (131/130N) Patient 2/patient 2 post treatment
Non-histone chromosomal protein HMG-17	For chromatin binding, nucleic acid binding	HMGN2	(131/127N) Patient 2/control 2
Integrin beta-3	Receptor binding	ITGB3	(130C/127C) Patient 5/patient 5 post treatment
L-lactate dehydrogenase B chain	For glycolysis	LDHB	(130C/128N) Patient 5/control 5
Platelet factor 4	Chemokine	PF4	(129N/126) Patient 1/control 1
Pyruvate kinase	For kinase activity in glycolysis	PKM	(130C/127C)

			Patient 5/patient 5 post treatment
Platelet basic protein	Chemokine	PPBP	(130C/127C) Patient 5/patient 5 post treatment
Ras-related protein Rab-27B	For GTPase activity, pyrophisphotase activity, For phagocytosis	RAB27B	(130C/127C) Patient 5/patient 5 post treatment (130C/128N) Patient 5/control 5
Tubulin alpha-1B chain	Nucleotide binding, Structural constituent of cytoskeleton	TUBA1B	(129N/126) Patient 1/control 1 (131/127N) Patient 2/control 2
Tubulin beta-4B chain	Nucleotide binding, Structural constituent of cytoskeleton	TUBB4B	(129N/126) Patient 1/control 1

Appendix 8.5: Down regulated genes from periodontal patients compared to controls analysed by DAVID bioinformatics tool. Gene ontology is shown.

Gene name	GO Description	Gene symbol	combination detected in
Annexin A1	Fatty acid metabolic process	ANXA1	(129N/126) Patient 1/control 1
Bactericidal permeability-increasing protein	For immune system process	BPI	(130C/127C) Patient 5/patient 5 post treatment
Calmodulin	Calcium ion binding, calmodulin binding	CALM1	(129N/126) Patient 1/control 1 (131/127N) Patient 2/control 2 (131/130N) Patient 2/ patient 2 post treatment
Coagulation factor XIII A chain	For cellular protein modification process	F13A1	(130C/127C) Patient 5/patient 5 post treatment (129C/128C) Patient 3 /control 3 (130C/128N) Patient 5/control 5
Histone H3.3	DNA binding	H3F3A	(130C/128N)

			Patient 5/control 5
Histone H1.5	DNA binding	HIST1H1B	(130C/127C) Patient 5/patient 5 post treatment (130C/128N) Patient 5/control 5
Histone H1.3	DNA binding	HIST1H1D	(130C/127C) Patient 5/patient 5 post treatment (129C/128C) Patient 3 /control 3 (130C/128N) Patient 5/control 5
Histone H1.4	DNA binding	HIST1H1E	(130C/127C) Patient 5/patient 5 post treatment (129C/128C) Patient 3 /control 3 (130C/128N) Patient 5/control 5

Histone H2B type 1-O	DNA binding	HIST1H2BO	(129C/128C) Patient 3 /control 3 (130C/128N) Patient 5/control 5
Histone H2A type 2-A	DNA binding	HIST2H2AA3	(130C/128N) Patient 5/control 5
Non-histone chromosomal protein HMG-17	Chromatin binding, nucleic acid binding	HMGN2	(130C/128N) Patient 5/control 5
Neutrophil gelatinase-associated lipocalin	For binding, isomerase activity	LCN2	(130C/127C) Patient 5/patient 5 post treatment
Lactotransferrin	For binding	LTF	(130C/127C) Patient 5/patient 5 post treatment
Platelet factor 4	Chemokine	PF4	(129C/128C) Patient 3 /control 3
Profilin-1	Actin binding	PFN1	(129N/126) Patient 1/control 1 (131/130N) Patient 2/ patient 2 post treatment
Ras-related protein Rab-3C	For GTPase activity	RAB3C	(130C/128N) Patient 5/control 5
Protein S100-A6	Calcium ion binding	S100A6	(129N/126)

			Patient 1/control 1
Protein S100-A8	Calcium ion binding	S100A8	(130C/127C) Patient 5/patient 5 post treatment (131/130N) Patient 2/ patient 2 post treatment
Protein S100-P	Calcium ion binding	S100P	(129N/126) Patient 1/control 1
Band 3 anion transport protein	Transmembrane transporter activity	SLC4A1	(129C/128C) Patient 3 /control 3

Appendix 8.6: Abstract for British Society for Oral and Dental Research Conference, September 2015 (poster presentation)

Title: Neutrophil cell glutathione changes in chemotaxis

Introduction: Chronic periodontitis is an inflammatory disorder affecting the teeth, connective tissues and alveolar bone within the oral cavity. Neutrophils from periodontitis patients have decreased intracellular glutathione. Intracellular glutathione is essential for a number of homeostatic and cellular processes, including chemotaxis and is the main intracellular redox buffer.

Objectives: To analyse the effect of alteration in glutathione levels on chemotactic behaviour of neutrophils

Methods: Neutrophils were isolated from the peripheral blood of healthy volunteers. Real Time Glo was used as a viability assay to determine time course for neutrophil cells experiment. A Boyden type chamber was used to assess neutrophil chemotaxis with and without the pre-incubation of glutathione depletion reagents: BSO, CDNB, BCNU. Chemoattractants used were FMLP and IL8.

Results: CDNB, a deplete of glutathione through thioester conjugation, and BCNU, an inhibitor of glutathione reductase both altered neutrophil chemotaxis relative to control treated cells responding to both FMLP and IL8. However BSO, an inhibitor of rate limiting gamma-glutathione cysteine synthetase, did not appear to have an effect.

Conclusion: Alterations in chemotaxis and intracellular glutathione in periodontits patients are already known separately, this study may begin to help in our understanding the mechanism by which these two factors may be linked.

Authors (First Name Initial Last Name): Nurul-Iman B.S, M. M. Grant

Authors/Institutions: Dentistry, University of Birmingham, Birmingham, United Kingdom, Presenter: Nurul Iman

Presenter (E-mail only): NIB455@bham.ac.uk

Preferred presentation type: Poster

Support Funding Agency/Grant Number: Malaysian Ministry for Higher Education

Appendix 8.7: Abstract for Society for Redox Biology and Medicine Conference, November 2016

The innate immune system is the first line of defence against invading microorganisms, and neutrophils are the most abundant leukocyte and the first to arrive at a site of infection. Periodontitis is a highly prevalent chronic non- communicable disease and in its most severe form is the sixth most prevalent human disease, affecting 11.2% of the world's population. It has been associated various systemic diseases and conditions, such as diabetes. In periodontitis it is known that neutrophils have aberrant chemotactic behaviour (Roberts et al PMID: 25360483), as well as increased reactive oxygen species production whilst resting (hyper activity) and when stimulated (hyper-reactivity) (Matthews et al PMID: 17223966). This combination may lead to enhanced tissue damage in the periodontal lesion. We have also shown that levels of glutathione in the periodontal lesion (Grant et al PMID: 19968740) and within circulating peripheral neutrophils (Dias et al PMID: 23826097) are decreased, demonstrating a loss in redox buffering and capacity. Previous studies have shown the importance of glutathionylation of actin in chemotactic movement of neutrophils (Sakai et al 2012 PMID: 23159440). With the long term aim to examine how diminished glutathione levels in periodontitis effect chemotaxis, we examined the effect of glutathione modulation by buthioninesulfoximine (BSO), N-acetylcysteine (NAC), bis-chloroethylnitrosourea (BCNU) and 1-chloro-2,4-dinitrobenzene (CDNB) on neutrophil intracellular glutathione, viability and chemotaxis towards interleukin 8 and N-formylmethionyl-leucyl-phenylalanine (fMLP). BSO, BCNU and CDNB decreased the chemotaxis and glutathione levels in peripheral neutrophils isolated from healthy donors. Future studies will translate this work into a periodontal cohort and examine protein glutathionylation by mass spectrometry.